APPENDIX A

EXPERIMENTAL DATABASE OF BENDING TESTS

A.1. Introduction

A database of experimental tests is a useful tool to verify the reliability of a theoretical model. As mentioned in Chapter 2, a database of bending tests has been assembled in the current study to compare the existing theoretical models and then highlight their lacks in predicting the failure load.

The collected data are summarized in the following sections of Appendix A.

A.2. Bending test database

A.2.1. Selection criteria for the database

As mentioned in §2.2.4, for the inclusion on the database, beams should accomplish to be conventionally reinforced concrete beams, with rectangular cross-section, externally strengthened by bonded plates, simply supported and tested in a three or four-point bending configuration. Concrete T-beams or beams where the external plate was prestressed before bonding have been excluded from the database. Specimens for which geometry, material properties, failure mode or failure load were not reported, have also been excluded from this database.

The database has been grouped into two sets: the first group contains all beams that only were strengthened by a plate glued on their tension face, and the second includes beams that were also strengthened in shear or that were externally anchored. Only the first group has been analyzed by means of the theoretical formulation presented in §2.3 and in §5.3.

A special distinction has been made between those beams that were preloaded before bonding the external reinforcement. After analyzing the results of precracked beams that belong to the database, an observation is that such a previous load has no significant effect at failure load levels.

A.2.2. Compiled data

Table A.1 to A.34 give details of the compiled beams in terms of geometry, material properties, and loading configuration. Units are specified in each column. Specimens have been organized by following a chronological order related to the year of publication and an alphabetical order for each year.

As shown in column 1, specimens have been named by the first author initial followed by the publication year of the source describing the test and by the specimen name according to this publication. Column 2 points out if external anchorages were affixed on the beam. Column 3 indicates if an initial load was applied previously to the strengthening procedure.

The geometry of the RC beam is given by columns 4 to 9, where b, h, A_s, A_s', A_w, s_w, denote the width and depth of the beam, the internal tensile steel reinforcement area, the internal compressive steel reinforcement area, the shear reinforcement area and the stirrups spacing, respectively.

Material properties of the unstrengthened beam are listed in columns 10 to 14. Concrete properties are given by the mean cylinder compressive strength (f_{cm}), the tensile strength (f_{ctm}) and the modulus of elasticity (E_c). Columns 15 and 16 list the internal steel properties, that is, the yield strength (f_{ym}) and the modulus of elasticity (E_s).

The geometry and mechanical properties of the plates bonded to the tensile face of the reinforced concrete beams are denoted by b_L, t_L, a, E_L, ε_{Lu}, being the plate width, thickness, unplated length, modulus of elasticity and ultimate strain of the bonded plate (columns 17 to 21). The material type of the external plate is given by column 15, named *M*, with the following meaning: "-" control beam, *A* Aramid Fiber Reinforced Polymer (AFRP) laminate, *C* Carbon Fiber Reinforced Polymer (CFRP) laminate, *G* Glass Fiber Reinforced Polymer (GFRP) laminate, *H* Hybrid laminate made from carbon and glass, and *S* steel plate. The fabrication procedure in case of FRP laminates (wet lay-up (*W*) or pultruded (*P*)) is given by column 16, as *F*.

The thickness (t_a) and the shear modulus of the adhesive (G_a) are listed in columns 22 and 23.

Tables A.1 to A.34 also define the load configuration and the failure load, where L, L_{shear}, V_{exp}, M_{exp} represent the beam span, the distance from the support to the load application point, the maximum shear force at failure located at the support, and the maximum bending moment at failure applied on the load application point.

Finally the mode of failure is given by the following nomenclature: *CC* as concrete crushing, *R* as plate rupture, *P* as premature peeling failure in general without distinguishing the initiation point, *PC* when peeling was reported to be initiated near cracks, *PED* when peeling was initiated at the plate end due to a high stress concentration, *PES* when peeling was initiated by a shear crack at the plate end, *S* in case a shear failure was reported, *O* for other modes of failure.

It should be mentioned that the initials *NR* denote all data not clearly reported in the published references.

The last row of Tables A.1 to A.34 gives the reference source of the data shown in each table.

A.2.3. Assumptions for geometry and material properties

In some of the assembled tests, almost all geometrical and material properties were reported except for some missing data. In these cases, if the basic properties, the failure mode and the ultimate load are available, the missing data will be assumed following the criteria described below.

1) The only assumption related to geometry of the unstrengthened section is concrete cover which has been assumed as ten percent of the beam depth minus the stirrup diameter and the radius of the tensile reinforcement, ($0.10\ h$ - ϕ_w - $\phi_s/2$).
2) For concrete properties, in case no split cylinder test was performed to obtain the tensile strength and no information about the modulus of elasticity was available, both values have been calculated by the Spanish Structural Concrete Code (EHE, 1999)
3) When the concrete cube compressive strength was reported instead of the cylinder strength, this value has been assumed as shown in equation (A.1)

$$f_{cm,\,cylinder} = 0.8 f_{cm,\,cube} \tag{A.1}$$

4) For steel properties, when no information was available, yielding strength has been assumed as 500 *MPa* and the modulus of elasticity as 200 *GPa*.
5) Regarding the strengthening material, only the thickness of the sheet was reported in some of the wet lay-up laminates. In this case, and if the number of plies employed on the laminate manufacturing is known, the plate thickness will be calculated as the sheet thickness plus the adhesive between sheets multiplied by the total number of plies, as shown in equation (A.2). The reported value in column 18 of Tables A.1 to A.34 is the plate thickness.

$$t_L = n\left(t_{sheet} + t_{adh,sheets}\right) \tag{A.2}$$

6) The adhesive properties are the most common missing data, especially the thickness which is difficult to control on site. For pultruded plates, the thickness of the adhesive has been assumed to be 2.00 *mm* when it was not reported. For these well-documented tests of the database with pultruded laminates, the mean average for the adhesive thickness is 2.10 *mm*. For wet lay-up laminates, the adhesive thickness has been assumed to be 0.42 *mm* based on measurements performed by Smith and Teng (2002 b).
7) For the adhesive modulus of elasticity, a value of 8500 *MPa* has been assumed according to Smith and Teng (2002 b). The average value for 391 tests well-documented is 5179 *MPa*. By distinguishing the pultruded strengthened beams assembled on the database, the calculated average is slightly lower than the assumed value, 7060 *MPa*. For the 194 tests strengthened by wet lay-up laminates, the average value is 4699 *MPa* which is very similar to the average value for the 101 well-documented steel plated beams (4445 *MPa*).
8) When no information about the ultimate strain is given, this value has been assumed as 10000 $\mu\varepsilon$ for steel plates and 15000 $\mu\varepsilon$ for FRP plates.

All assumptions listed above constitute an approach that does not significantly affect the results of the statistical analysis performed in Chapter 2.

Table A.1. Experimental bending test database (I)

			Geometry of RC beam						Material properties					Plate strengthening							Adhesive		Load configuration				
Specimen (1)	Ext anch (2)	Pr (3)	b mm (4)	h mm (5)	A_s mm^2 (6)	A_s' mm^2 (7)	A_w mm^2 (8)	s_w mm (9)	f_{cm} MPa (10)	f_{ctm} MPa (11)	E_c MPa (12)	f_{ym} MPa (13)	E_s GPa (14)	M (15)	F (16)	b_L mm (17)	t_L mm (18)	a mm (19)	E_L GPa (20)	ε_{Lu} με (21)	t_a mm (22)	G_a MPa (23)	L m (24)	L_{shear} m (25)	V_{uexp} kN (26)	M_{uexp} kNm (27)	Mode (28)
J80 C11			100	150	100	0	NR	NR	73.9	4.9	35670	490	200.0	S	-	80	1.60	50	200.0	10000	1.60	2577	1.10	0.25	NR	NR	NR
J80 C12			100	150	100	0	NR	NR	73.9	4.9	35670	490	200.0	S	-	80	1.60	50	200.0	10000	1.60	2577	1.10	0.36	NR	NR	NR
J82 URB2			100	150	157	101	808	70	52.6	3.8	31848	530	200.0	S	-	80	1.60	50	200.0	1085	2.00	3269	NR	0.75	20.00	15.00	R
J82 URB3			100	150	157	101	808	70	52.6	3.8	31848	530	200.0	S	-	80	1.60	50	200.0	1315	2.00	3269	NR	0.75	27.50	20.63	S
J82 URB4			100	150	157	101	808	70	52.6	3.8	31848	530	200.0	S	-	80	1.60	50	200.0	1090	2.00	3269	NR	0.75	28.80	21.60	P
J82 URB5			100	150	157	101	808	70	52.6	3.8	31848	530	200.0	S	-	80	1.60	50	200.0	1200	2.00	3269	NR	0.75	26.60	19.95	P
J82 ORB2			100	150	804	101	808	70	52.6	3.8	31848	487	200.0	S	-	80	1.60	50	200.0	1090	2.00	3269	NR	0.75	48.80	36.60	P
J88 F31			155	225	942	0	-	-	45.6	3.4	30367	430	200.0	S	-	125	6.00	50	200.0	10000	1.50	108	2.25	0.77	NR	NR	NR
S89 204			155	255	942	0	NR	NR	56.4	4.0	32605	470	200.0	S	-	125	1.60	50	200.0	10000	1.50	769	2.30	0.77	NR	NR	NR
S89 205			155	255	942	0	NR	NR	59.7	4.2	33221	470	200.0	S	-	125	1.60	50	200.0	10000	1.50	769	2.30	0.77	NR	NR	NR
S89 208			155	255	942	0	NR	NR	57.8	4.1	32865	470	200.0	S	-	125	1.60	50	200.0	10000	3.00	769	2.30	0.77	NR	NR	NR
S89 209			155	255	942	0	NR	NR	61.4	4.3	33533	470	200.0	S	-	125	1.60	50	200.0	10000	3.00	769	2.30	0.77	NR	NR	NR
S89 217			155	255	942	0	NR	NR	58.3	4.1	32959	470	200.0	S	-	125	1.60	50	200.0	10000	6.00	808	2.30	0.77	NR	NR	NR
S89 218			155	255	942	0	NR	NR	60.8	4.2	33424	470	200.0	S	-	125	1.60	50	200.0	10000	6.00	808	2.30	0.77	NR	NR	NR
O90 1/1			125	150	402	157	NR	NR	48.0	3.5	30891	444	200.0	S	-	125	1.60	350	200.0	1250	2.00	1654	2.10	NR	NR	9.20	NR
O90 1/2			125	150	402	157	NR	NR	48.0	3.5	30891	444	200.0	S	-	125	1.60	350	200.0	1250	2.00	1654	2.10	NR	NR	9.90	NR
O90 2/1			125	150	402	157	NR	NR	34.0	2.6	27537	444	200.0	S	-	125	1.60	350	200.0	1250	2.00	1654	2.10	NR	NR	12.20	NR
O90 2/2			125	150	402	157	NR	NR	34.0	2.6	27537	444	200.0	S	-	125	1.60	350	200.0	1250	2.00	1654	2.10	NR	NR	11.50	NR
O90 3/1		x	125	150	402	157	NR	NR	28.0	2.2	25811	444	200.0	S	-	125	1.60	350	200.0	1250	2.00	1654	2.10	NR	NR	11.30	NR
O90 3/2		x	125	150	402	157	NR	NR	28.0	2.2	25811	444	200.0	S	-	125	1.60	350	200.0	1250	2.00	1654	2.10	NR	NR	10.80	NR

J80: Jones et al. (1980); J82: Jones et al. (1982) (referenced by Colotti et al., 2004); J88: Jones et al. (1988); S89: Swamy et al. (1989); O90: Oelhers and Moran (1990)

Table A.2. Experimental bending test database (II)

			Geometry of RC beam						Material properties					Plate strengthening								Adhesive		Load configuration				
Specimen (1)	Ext anch (2)	Pr (3)	b mm (4)	h mm (5)	A_s mm^2 (6)	A_s' mm^2 (7)	A_w mm^2 (8)	s_w mm (9)	f_{cm} MPa (10)	f_{ctm} MPa (11)	E_c MPa (12)	f_{ym} MPa (13)	E_s GPa (14)	M (15)	F (16)	b_L mm (17)	t_L mm (18)	a mm (19)	E_L GPa (20)	$\varepsilon_{L,u}$ με (21)	t_a mm (22)	G_a MPa (23)	L m (24)	L_{shear} m (25)	V_{uexp} kN (26)	M_{uexp} kNm (27)	Mode (28)
O90 3/3		x	125	150	402	157	NR	NR	28.0	2.2	25811	444	200.0	S	-	125	1.60	350	200.0	1250	2.00	1654	2.10	NR	NR	12.60	NR
O90 3/4		x	125	150	402	157	NR	NR	28.0	2.2	25811	444	200.0	S	-	125	3.00	350	200.0	1250	2.00	1654	2.10	NR	NR	13.50	NR
O90 4/1		x	125	150	402	157	NR	NR	45.0	3.3	30234	444	200.0	S	-	125	5.00	350	200.0	1250	2.00	1654	2.10	NR	NR	12.60	NR
O90 4/2		x	125	150	402	157	NR	NR	45.0	3.3	30234	444	200.0	S	-	125	5.00	350	200.0	1250	2.00	1654	2.10	NR	NR	14.00	NR
O90 4/3		x	125	150	402	157	NR	NR	44.0	3.3	30008	444	200.0	S	-	125	5.00	350	200.0	1250	2.00	1654	2.10	NR	NR	13.50	NR
O90 4/4		x	125	150	402	157	NR	NR	44.0	3.3	30008	444	200.0	S	-	125	5.00	350	200.0	1250	2.00	1654	2.10	NR	NR	14.40	NR
O90 5/1		x	125	150	402	157	NR	NR	44.0	3.3	30008	444	200.0	S	-	125	5.00	350	200.0	1250	2.00	1654	2.10	NR	NR	11.50	NR
O90 5/2		x	125	150	402	157	NR	NR	44.0	3.3	30008	444	200.0	S	-	125	5.00	350	200.0	1250	2.00	1654	2.10	NR	NR	15.10	NR
O90 5/3		x	125	150	402	157	NR	NR	43.0	3.2	29779	444	200.0	S	-	125	5.00	350	200.0	1250	2.00	1654	2.10	NR	NR	11.50	NR
O90 5/4		x	125	150	402	157	NR	NR	43.0	3.2	29779	444	200.0	S	-	125	5.00	350	200.0	1250	2.00	1654	2.10	NR	NR	9.90	NR
O90 6/1			125	150	402	157	NR	NR	36.0	2.8	28066	444	200.0	S	-	125	5.00	350	200.0	1250	2.00	1654	2.10	NR	NR	16.00	NR
O90 6/2			125	150	402	157	NR	NR	36.0	2.8	28066	444	200.0	S	-	125	5.00	350	200.0	1250	2.00	1654	2.10	NR	NR	12.60	NR
O90 6/3			125	150	402	157	NR	NR	36.0	2.8	28066	444	200.0	S	-	125	5.00	350	200.0	1250	2.00	1654	2.10	NR	NR	12.60	NR
O90 6/4			125	150	402	157	NR	NR	36.0	2.8	28066	444	200.0	S	-	125	5.00	350	200.0	1250	2.00	1654	2.10	NR	NR	14.20	NR
O90 7/1			120	200	402	157	NR	NR	35.0	2.7	27804	444	200.0	S	-	120	5.00	125	200.0	1250	2.00	1654	1.65	NR	NR	16.80	NR
O90 7/2			120	200	402	157	NR	NR	35.0	2.7	27804	444	200.0	S	-	120	5.00	125	200.0	1250	2.00	1654	1.65	NR	NR	17.60	NR
O90 7/3			120	200	402	157	NR	NR	34.0	2.6	27537	444	200.0	S	-	120	5.00	125	200.0	1250	2.00	1654	1.65	NR	NR	15.40	NR
O90 7/4			120	200	402	157	NR	NR	34.0	2.6	27537	444	200.0	S	-	120	5.00	125	200.0	1250	2.00	1654	1.65	NR	NR	10.30	NR
O90 8/1			120	200	402	157	NR	NR	37.0	2.8	28324	444	200.0	S	-	120	5.00	125	200.0	1250	2.00	1654	1.65	NR	NR	18.00	NR
O90 8/2			120	200	402	157	NR	NR	37.0	2.8	28324	444	200.0	S	-	120	5.00	125	200.0	1250	2.00	1654	1.65	NR	NR	20.70	NR

O90: Oelhers and Moran (1990)

Table A.3. Experimental bending test database (III)

			Geometry of RC beam						Material properties					Plate strengthening								Adhesive		Load configuration				
Specimen (1)	Ext anch (2)	Pr (3)	b mm (4)	h mm (5)	A_s mm^2 (6)	A_s' mm^2 (7)	A_w mm^2 (8)	s_w mm (9)	f_{cm} MPa (10)	f_{ctm} MPa (11)	E_c MPa (12)	f_{ym} MPa (13)	E_s GPa (14)	M (15)	F (16)	b_L mm (17)	t_L mm (18)	a mm (19)	E_L GPa (20)	$\varepsilon_{L,u}$ με (21)	t_a mm (22)	G_a MPa (23)	L m (24)	L_{shear} m (25)	V_{uexp} kN (26)	M_{uexp} kNm (27)	Mode (28)
O90 8/3			120	200	402	157	NR	NR	35.0	2.7	27804	444	200.0	S	-	120	5.00	125	200.0	1250	2.00	1654	1.65	NR	NR	13.40	NR
O90 8/4			120	200	402	157	NR	NR	35.0	2.7	27804	444	200.0	S	-	120	5.00	125	200.0	1250	2.00	1654	1.65	NR	NR	11.30	NR
O90 9/1			125	150	402	157	NR	NR	38.0	2.9	28577	444	200.0	S	-	125	3.00	350	200.0	1250	2.00	1654	2.10	NR	NR	16.70	NR
O90 9/2			125	150	402	157	NR	NR	38.0	2.9	28577	444	200.0	S	-	125	3.00	350	200.0	1250	2.00	1654	2.1	NR	NR	14.00	NR
O90 9/3			125	150	402	157	NR	NR	29.0	2.3	26115	444	200.0	S	-	125	3.00	350	200.0	1250	2.00	1654	2.10	NR	NR	13.50	NR
O90 9/4			125	150	402	157	NR	NR	29.0	2.3	26115	444	200.0	S	-	125	3.00	350	200.0	1250	2.00	1654	2.10	NR	NR	15.30	NR
O90 10/1			120	180	402	157	NR	NR	33.0	2.6	27264	444	200.0	S	-	120	10.00	125	200.0	1250	2.00	1654	1.65	NR	NR	12.30	NR
O90 10/2			120	180	402	157	NR	NR	33.0	2.6	27264	444	200.0	S	-	120	10.00	125	200.0	1250	2.00	1654	1.65	NR	NR	10.80	NR
O90 10/3			120	180	402	157	NR	NR	37.0	2.8	28324	444	200.0	S	-	120	6.50	125	200.0	1250	2.00	1654	1.65	NR	NR	11.20	NR
O90 10/4			120	180	402	157	NR	NR	37.0	2.8	28324	444	200.0	S	-	120	6.50	125	200.0	1250	2.00	1654	1.65	NR	NR	11.70	NR
O90 11/1			120	180	402	157	NR	NR	34.0	2.6	27537	444	200.0	S	-	120	3.00	125	200.0	1250	2.00	1654	1.65	NR	NR	12.30	NR
O90 11/2			120	180	402	157	NR	NR	34.0	2.6	27537	444	200.0	S	-	120	3.00	125	200.0	1250	2.00	1654	1.65	NR	NR	13.10	NR
O90 11/3			120	180	402	157	NR	NR	36.0	2.8	28066	444	200.0	S	-	120	15.00	125	200.0	1250	2.00	1654	1.65	NR	NR	7.90	NR
O90 11/4			120	180	402	157	NR	NR	36.0	2.8	28066	444	200.0	S	-	120	15.00	125	200.0	1250	2.00	1654	1.65	NR	NR	9.20	NR
O90 12/1			120	180	402	157	NR	NR	30.0	2.4	26411	444	200.0	S	-	100	10.00	125	200.0	1250	2.00	1654	1.65	NR	NR	10.40	NR
O90 12/2			120	180	402	157	NR	NR	30.0	2.4	26411	444	200.0	S	-	50	10.00	125	200.0	1250	2.00	1654	1.65	NR	NR	12.70	NR
O90 12/3			120	180	402	157	NR	NR	36.0	2.8	28066	444	200.0	S	-	25	10.00	125	200.0	1250	2.00	1654	1.65	NR	NR	16.40	NR
O90 12/4			120	180	402	157	NR	NR	36.0	2.8	28066	444	200.0	S	-	75	10.00	125	200.0	1250	2.00	1654	1.65	NR	NR	10.60	NR
O90 13/6			120	200	402	157	NR	NR	42.0	3.1	29546	444	200.0	S	-	120	5.00	550	200.0	1250	2.00	1654	2.50	NR	NR	24.40	NR
O90 13/7			120	240	402	157	NR	NR	41.0	3.1	29310	444	200.0	S	-	120	5.00	200	200.0	1250	2.00	1654	1.80	NR	NR	23.90	NR
O90: Oelhers and Moran (1990)																												

Table A.4. Experimental bending test database (IV)

			Geometry of RC beam						Material properties					Plate strengthening								Adhesive		Load configuration				
Specimen (1)	Ext anch (2)	Pr (3)	b mm (4)	h mm (5)	A_s mm^2 (6)	A_s' mm^2 (7)	A_w mm^2 (8)	s_w mm (9)	f_{cm} MPa (10)	f_{ctm} MPa (11)	E_c MPa (12)	f_{ym} MPa (13)	E_s GPa (14)	M (15)	F (16)	b_L mm (17)	t_L mm (18)	a mm (19)	E_L GPa (20)	$\varepsilon_{L,u}$ με (21)	t_a mm (22)	G_a MPa (23)	L m (24)	L_{shear} m (25)	V_{uexp} kN (26)	M_{uexp} kNm (27)	Mode (28)
O90 13/9			120	160	402	157	NR	NR	46.0	3.4	30456	444	200.0	S	-	120	2.00	200	200.0	1250	2.00	1654	1.80	NR	NR	17.60	NR
O9013/10			120	160	402	157	NR	NR	46.0	3.4	30456	444	200.0	S	-	120	2.00	200	200.0	1250	2.00	1654	1.80	NR	NR	16.10	NR
O9013/11			120	160	402	157	NR	NR	35.0	2.7	27804	444	200.0	S	-	120	5.00	200	200.0	1250	2.00	1654	1.80	NR	NR	13.10	NR
O9013/13			120	160	402	157	NR	NR	37.0	2.8	28324	444	200.0	S	-	120	2.00	200	200.0	1250	2.00	1654	1.80	NR	NR	12.60	NR
O9013/14			120	160	402	157	NR	NR	37.0	2.8	28324	444	200.0	S	-	120	5.00	200	200.0	1250	2.00	1654	1.80	NR	NR	9.00	NR
O9013/15			120	160	628	157	NR	NR	33.0	2.6	27264	444	200.0	S	-	120	2.00	200	200.0	1250	2.00	1654	1.80	NR	NR	15.30	NR
O903/16			120	160	628	157	NR	NR	33.0	2.6	27264	444	200.0	S	-	120	5.00	200	200.0	1250	2.00	1654	1.80	NR	NR	11.40	NR
O9013/17			120	160	402	157	NR	NR	43.0	3.2	29779	444	200.0	S	-	120	6.00	200	200.0	1250	2.00	1654	1.80	NR	NR	6.30	NR
O9013/18			120	160	402	157	NR	NR	43.0	3.2	29779	444	200.0	S	-	120	2.00	200	200.0	1250	2.00	1654	1.80	NR	NR	7.90	NR
O9013/19			120	160	226	157	NR	NR	43.0	3.2	29779	444	200.0	S	-	120	2.00	200	200.0	1250	2.00	1654	1.80	NR	NR	10.60	NR
O90 3/20			120	160	226	157	NR	NR	43.0	3.2	29779	444	200.0	S	-	120	5.00	200	200.0	1250	2.00	1654	1.80	NR	NR	10.20	NR
S90 A			89	152	71	0	46	76	36.4	2.8	28170	551	200.0	G	W	75	6.00	0	37.0	10811	0.42	3269	1.52	0.69	NR	NR	P
S90 B	x		89	152	71	0	46	76	36.4	2.8	28170	551	200.0	G	W	75	6.00	0	37.0	10811	0.42	3269	152	0.69	NR	NR	S
S90 C			89	152	71	0	46	76	36.4	2.8	28170	551	200.0	G	W	75	6.00	0	37.0	10811	0.42	3269	152	0.69	NR	NR	P
R91 A			152	305	253	57	97	102	41.4	3.1	29395	414	200.0	-	-	-	-	-	-	-	-	-	2.44	0.91	36.48	33.36	CC
R91 B			152	305	253	57	97	102	41.4	3.1	29395	414	200.0	-	-	-	-	-	-	-	-	-	2.44	0.91	36.26	33.15	CC
R91 C			152	305	253	57	97	102	41.4	3.1	29395	414	200.0	G	W	152	4.76	203	11.7	13706	1.59	3269	2.44	0.91	55.39	50.65	PED
R91 D			152	305	253	57	97	102	41.4	3.1	29395	414	200.0	G	W	151	4.76	203	11.7	13706	1.59	3269	2.44	0.91	59.61	54.51	PED
R91 E	x		152	305	253	57	97	102	41.4	3.1	29395	414	200.0	G	W	154	4.76	229	11.7	13706	1.59	3269	2.44	0.91	62.28	56.95	R
R91 F			152	305	253	57	97	102	41.4	3.1	29395	414	200.0	G	W	154	4.76	381	11.7	13706	1.59	3269	2.44	0.91	66.51	60.82	R

O90: Oelhers and Moran(1990); S90: Saadatmanesh and Ehsani (1990); R91: Ritchie et al. (1991)

Table A.5. Experimental bending test database (V)

			Geometry of RC beam						Material properties					Plate strengthening								Adhesive		Load configuration				
Specimen (1)	Ext anch (2)	Pr (3)	b mm (4)	h mm (5)	A_s mm^2 (6)	A_s' mm^2 (7)	A_w mm^2 (8)	s_w mm (9)	f_{cm} MPa (10)	f_{ctm} MPa (11)	E_c MPa (12)	f_{ym} MPa (13)	E_s GPa (14)	M (15)	F (16)	b_L mm (17)	t_L mm (18)	a mm (19)	E_L GPa (20)	$\varepsilon_{L,u}$ με (21)	t_a mm (22)	G_a MPa (23)	L m (24)	L_{shear} m (25)	V_{uexp} kN (26)	M_{uexp} kNm (27)	Mode (28)
R91 G	x		152	305	253	57	97	102	41.4	3.1	29395	414	200.0	G	W	152	4.19	0	10.3	17800	1.59	3269	2.44	0.91	62.88	57.49	PED
R91 H			152	305	253	57	97	102	41.4	3.1	29395	414	200.0	G	W	152	9.26	203	20.6	11667	1.59	3269	2.44	0.91	55.72	50.95	PED
R91 I			152	305	253	57	97	102	41.4	3.1	29395	414	200.0	H	W	150	4.06	203	27.5	11575	1.59	3269	2.44	0.91	50.61	46.27	PED
R91 J	x		152	305	253	57	97	102	41.4	3.1	29395	414	200.0	G	W	152	3.20	330	30.3	19455	1.59	3269	2.44	0.91	61.50	56.24	PED
R91 K	x		152	305	253	57	97	102	41.4	3.1	29395	414	200.0	G	W	152	3.20	330	30.3	19455	1.59	3269	2.44	0.91	60.06	54.92	PED
R91 L	x		152	305	253	57	97	102	41.4	3.1	29395	414	200.0	C	W	152	1.27	0	54.4	11266	1.59	3269	2.44	0.91	61.38	56.13	R
R91 M	x		152	305	253	57	97	102	41.4	3.1	29395	414	200.0	C	W	152	1.27	0	117.9	12632	1.59	3269	2.44	0.91	72.02	65.86	PED
R91 N	x		152	305	253	57	97	102	41.4	3.1	29395	414	200.0	A	W	154	6.35	305	72.4	16190	1.59	3269	2.44	0.91	54.50	49.83	PED
R91 O			152	305	253	57	97	102	41.4	3.1	29395	414	200.0	S	-	154	2.59	203	199.9	1034	1.59	3269	2.44	0.91	46.71	42.71	PED
R91 P	x		152	305	253	57	97	102	41.4	3.1	29395	414	200.0	S	-	150	2.54	0	199.9	1034	1.59	3269	2.44	0.91	63.21	57.80	CC
S91 A			205	455	1520	253	432	330	35.0	2.7	27804	456	200.0	G	W	152	6.00	158	37.2	10744	1.50	313	4.57	1.98	150.00	297.38	CC
S91 B			205	455	1013	253	1689	150	35.0	2.7	27804	456	200.0	G	W	152	6.00	158	37.2	10744	1.50	313	4.57	1.98	125.00	247.81	PED
S91 C			205	455	253	253	1689	150	35.0	2.7	27804	456	200.0	G	W	152	6.00	158	37.2	10744	1.50	313	4.57	1.98	92.50	183.38	PC
S91 D			205	455	1013	253	1689	150	35.0	2.7	27804	456	200.0	G	W	152	6.00	158	37.2	10744	1.50	313	4.57	1.98	137.50	272.59	PC
S91 E			205	455	0	253	1689	150	35.0	2.7	27804	456	200.0	G	W	152	6.00	158	37.2	10744	1.50	313	4.57	1.98	32.50	64.43	P
D92 1			125	125	200	0	1414	40	22.5	1.8	23996	400	200.0	G	W	100	6.35	0	17.2	12181	0.42	3269	0.95	0.37	NR	NR	CC
D92 2			125	125	200	0	1414	40	22.5	1.8	23996	400	200.0	G	W	100	6.35	0	17.2	12181	0.42	3269	0.95	0.37	NR	NR	S
D92 4			200	300	400	0	1885	120	28.6	2.3	25994	400	200.0	G	W	150	6.35	0	17.2	12181	0.42	3269	4.00	1.50	NR	NR	P
O92 1/1/N			130	175	402	157	0	102	42.0	3.1	29546	444	200.0	S	-	130	5.00	550	200.0	1360	2.00	1658	NR	0.55	41.00	22.55	NR
O92 1/2/S			130	175	402	157	0	102	42.0	3.1	29546	444	200.0	S	-	130	5.00	100	200.0	1360	2.00	1658	NR	0.55	29.70	16.34	PES

R91: Ritchie et al. (1991); S91: Saadatmanesh and Ehsani (1991a); D92: Deblois (1992); O92: Oelhers (1992)

Table A.6. Experimental bending test database (VI)

			Geometry of RC beam						Material properties					Plate strengthening								Adhesive		Load configuration				
Specimen (1)	Ext anch (2)	Pr (3)	b mm (4)	h mm (5)	A_s mm^2 (6)	A_s' mm^2 (7)	A_w mm^2 (8)	s_w mm (9)	f_{cm} MPa (10)	f_{ctm} MPa (11)	E_c MPa (12)	f_{ym} MPa (13)	E_s GPa (14)	M (15)	F (16)	b_L mm (17)	t_L mm (18)	a mm (19)	E_L GPa (20)	ε_{Lu} με (21)	t_a mm (22)	G_a MPa (23)	L m (24)	L_{shear} m (25)	V_{uexp} kN (26)	M_{uexp} kNm (27)	Mode (28)
O92 1/2/N			130	175	402	157	0	102	42.0	3.1	29546	444	200.0	S	-	130	5.00	150	200.0	1360	2.00	1658	NR	0.55	32.50	17.88	PES
O92 1/3/S			130	175	402	157	0	102	42.0	3.1	29546	444	200.0	S	-	130	5.00	250	200.0	1360	2.00	1658	NR	0.55	41.60	22.88	PED
O92 1/3/N			130	175	402	157	0	102	42.0	3.1	22000	444	200.0	S	-	130	5.00	400	200.0	1360	2.00	1658	NR	0.55	34.60	19.03	PED
O92 1/4/S			130	175	402	157	0	102	42.0	3.1	22000	444	200.0	S	-	130	5.00	50	200.0	1360	2.00	1658	NR	0.55	41.00	22.55	PES
O92 2/1/N			130	175	402	157	0	102	47.0	3.5	30675	444	200.0	S	-	130	5.00	300	200.0	1360	2.00	162	NR	0.55	44.00	24.20	PED
O92 2/1/S			130	175	402	157	0	102	47.0	3.5	30675	444	200.0	S	-	130	5.00	75	200.0	1360	2.00	162	NR	0.55	40.10	22.06	PES
O92 2/2/N			130	175	402	157	335	75	47.0	3.5	30675	444	200.0	S	-	130	5.00	300	200.0	1360	2.00	162	NR	550	43.80	24.09	PED
O92 2/2/S			130	175	402	157	335	75	47.0	3.5	30675	444	200.0	S	-	130	5.00	75	200.0	1360	2.00	162	NR	550	43.80	24.09	PES
O92 2/3/N			130	175	402	157	754	75	47.0	3.5	30675	444	200.0	S	-	130	5.00	300	200.0	1360	2.00	162	NR	550	44.90	24.70	PED
O92 2/3/S			130	175	402	157	754	75	47.0	3.5	30675	444	200.0	S	-	130	5.00	75	200.0	1360	2.00	162	NR	550	45.20	24.86	PES
O92 2/4/N			130	175	402	157	1257	45	47.0	3.5	30675	444	200.0	S	-	130	5.00	300	200.0	1360	2.00	162	NR	550	46.10	25.36	PED
O92 2/4/S			130	175	402	157	1257	45	47.0	3.5	30675	444	200.0	S	-	130	5.00	75	200.0	1360	2.00	162	NR	550	44.90	24.70	PES
O92 5/1/N			130	175	402	157	1257	45	49.0	3.6	31104	444	200.0	S	-	130	5.00	400	200.0	1360	2.00	162	NR	550	45.90	25.25	PED
O92 5/1/S			130	175	402	157	1257	45	49.0	3.6	31104	444	200.0	S	-	130	5.00	150	200.0	1360	2.00	162	NR	550	43.90	24.15	PES
O92 6/1			130	175	402	157	NR	102	52.0	3.7	31726	444	200.0	S	-	130	5.00	625	200.0	1360	2.00	162	NR	925	25.00	23.13	PED
O92 6/2			130	175	402	157	NR	102	52.0	3.7	31726	444	200.0	S	-	130	5.00	625	200.0	1360	2.00	162	NR	925	25.50	23.59	PED
O92 6/3			130	175	402	157	NR	102	52.0	3.7	31726	444	200.0	S	-	130	5.00	825	200.0	1360	2.00	162	NR	1125	21.40	24.08	PED
O92 6/4			130	175	402	157	NR	102	52.0	3.7	31726	444	200.0	S	-	130	5.00	825	200.0	1360	2.00	162	NR	1225	21.10	25.85	PED
O92 7/1/N			130	175	402	157	NR	102	51.0	3.7	31522	444	200.0	S	-	130	5.00	1000	200.0	1360	2.00	1658	NR	1400	17.00	23.80	PED
O92 7/1/S			130	175	402	157	NR	102	51.0	3.7	31522	444	200.0	S	-	130	5.00	1000	200.0	1360	2.00	1658	NR	1400	17.50	24.50	PED

O92: Oelhers (1992)

Table A.7. Experimental bending test database (VII)

			Geometry of RC beam						Material properties					Plate strengthening							Adhesive		Load configuration				
Specimen (1)	Ext anch (2)	Pr (3)	b mm (4)	h mm (5)	A_s mm^2 (6)	A_s' mm^2 (7)	A_w mm^2 (8)	s_w mm (9)	f_{cm} MPa (10)	f_{ctm} MPa (11)	E_c MPa (12)	f_{ym} MPa (13)	E_s GPa (14)	M (15)	F (16)	b_L mm (17)	t_L mm (18)	a mm (19)	E_L GPa (20)	ε_{Lu} $\mu\varepsilon$ (21)	t_a mm (22)	G_a MPa (23)	L m (24)	L_{shear} m (25)	V_{uexp} kN (26)	M_{uexp} kNm (27)	Mode (28)
O92 7/2			130	175	402	157	NR	102	51.0	3.7	31522	444	200.0	S	-	130	5.00	1150	200.0	1360	2.00	1658	NR	1000	23.80	23.80	PED
O92 8/1/N			130	175	402	157	NR	102	40.0	3.0	29070	444	200.0	S	-	130	5.00	1300	200.0	1360	2.00	1658	NR	1700	14.70	24.99	PED
O92 8/1/S			130	175	402	157	NR	102	40.0	3.0	29070	444	200.0	S	-	130	5.00	1300	200.0	1360	2.00	1658	NR	1700	14.80	25.16	PED
O92 8/2			130	175	402	157	NR	102	40.0	3.0	29070	444	200.0	S	-	130	5.00	900	200.0	1360	2.00	1658	NR	775	32.00	24.80	PED
T92 2			76	127	33	0	982	40	44.7	3.3	30166	517	200.0	C	W	43	0.20	0	186.0	7796	0.42	3269	1220	458	NR	NR	R
T92 3			76	127	33	0	982	40	44.7	3.3	30166	517	200.0	C	W	61	0.20	0	186.0	7796	0.42	3269	1220	458	NR	NR	R
T92 4			76	127	33	0	982	40	44.7	3.3	30166	517	200.0	C	W	63	0.65	0	186.0	7796	0.42	3269	1.22	0.46	NR	NR	P
T92 5			76	127	33	0	982	40	44.7	3.3	30166	517	200.0	C	W	63	0.65	0	186.0	7796	0.42	3269	1.22	0.46	NR	NR	P
T92 6			76	127	33	0	982	40	44.7	3.3	30166	517	200.0	C	W	63	0.90	0	186.0	7796	0.42	3269	1.22	0.46	NR	NR	P
T92 7			76	127	33	0	982	40	44.7	3.3	30166	517	200.0	C	W	63	0.90	0	186.0	7796	0.42	3269	1.22	0.46	NR	NR	P
T92 8			76	127	33	0	982	40	44.7	3.3	30166	517	200.0	C	W	64	1.90	0	186.0	7796	0.42	3269	1.22	0.46	NR	NR	P
MK93 FL1			150	300	700	200	2381	95	38.9	3.0	28801	517	200.0	C	W	125	0.50	0	82.0	16799	0.42	3269	1.92	0.64	NR	NR	P
MK93 FL1			150	300	700	200	2381	95	38.9	3.0	28801	517	200.0	C	W	125	0.50	0	82.0	16799	0.42	3269	1.92	0.64	NR	NR	R
MK93 FL1			150	300	700	200	2381	95	38.9	3.0	28801	517	200.0	C	W	125	0.50	0	82.0	16799	0.42	3269	1.92	0.64	NR	NR	P
MK93 FL2			150	300	700	200	2381	95	38.9	3.0	28801	517	200.0	C	W	125	1.00	0	82.0	16799	0.42	3269	1.92	0.64	NR	NR	R
MK93 FL2			150	300	700	200	2381	95	38.9	3.0	28801	517	200.0	C	W	125	1.00	0	82.0	16799	0.42	3269	1.92	0.64	NR	NR	P
MK93 FL2			150	300	700	200	2381	95	38.9	3.0	28801	517	200.0	C	W	125	1.00	0	82.0	16799	0.42	3269	1.92	0.64	NR	NR	R
MK93 FL3			150	300	700	200	2381	95	38.9	3.0	28801	517	200.0	C	W	125	1.50	0	82.0	16799	0.42	3269	1.92	0.64	NR	NR	R
MK93 FL3			150	300	700	200	2381	95	38.9	3.0	28801	517	200.0	C	W	125	1.50	0	82.0	16799	0.42	3269	1.92	0.64	NR	NR	R
MK93 FL3			150	300	700	200	2381	95	38.9	3.0	28801	517	200.0	C	W	125	1.50	0	82.0	16799	0.42	3269	1.92	0.64	NR	NR	P

O92: Oelhers (1992); T92: Triantafillou and Plevris. (1992); MK93: Mc Kenna (1993) (referenced by Bonacci and Maalej, 2001)

Table A.8. Experimental bending test database (VIII)

			Geometry of RC beam						Material properties					Plate strengthening								Adhesive		Load configuration				
Specimen (1)	Ext anch (2)	Pr (3)	b mm (4)	h mm (5)	A_s mm^2 (6)	A_s' mm^2 (7)	A_w mm^2 (8)	s_w mm (9)	f_{cm} MPa (10)	f_{ctm} MPa (11)	E_c MPa (12)	f_{ym} MPa (13)	E_s GPa (14)	M (15)	F (16)	b_L mm (17)	t_L mm (18)	a mm (19)	E_L GPa (20)	$\varepsilon_{L,u}$ με (21)	t_a mm (22)	G_a MPa (23)	L m (24)	L_{shear} m (25)	V_{uexp} kN (26)	M_{uexp} kNm (27)	Mode (28)
MK93 F1L			150	300	700	200	2381	95	33.6	2.6	27428	517	200.0	C	W	125	1.00	0	82.0	16799	0.42	3269	1.92	0.64	NR	NR	R
MK93 F2L			150	300	700	200	2381	95	33.6	2.6	27428	517	200.0	C	W	125	1.00	0	82.0	16799	0.42	3269	1.92	0.64	NR	NR	R
MK93 F1L			150	300	700	200	2381	95	33.6	2.6	27428	517	200.0	C	W	125	1.00	0	82.0	16799	0.42	3269	1.92	0.64	NR	NR	R
MK93 F2L			150	300	700	200	2381	95	33.6	2.6	27428	517	200.0	C	W	125	1.00	0	82.0	16799	0.42	3269	1.92	0.64	NR	NR	P
MK93 F4L3			150	300	700	200	2381	95	33.6	2.6	27428	517	200.0	C	W	125	1.50	0	82.0	16799	0.42	3269	1.92	0.64	NR	NR	P
MK93 F1L6			150	300	700	200	2381	95	33.6	2.6	27428	517	200.0	C	W	125	3.00	0	82.0	16799	0.42	3269	1.92	0.64	NR	NR	P
MK93 F2L6			150	300	700	200	2381	95	33.6	2.6	27428	517	200.0	C	W	125	3.00	0	82.0	16799	0.42	3269	1.92	0.64	NR	NR	P
S94 CB			150	150	168	57	105	60	37.7	2.9	28501	450	200.0	-	-	-	-	75	-	-	-	-	1.18	0.39	26.50	10.41	CC
S94 P1			150	150	168	57	105	60	37.7	2.9	28501	450	200.0	C	W	100	1.00	75	15.5	10968	0.42	3269	1.18	0.39	33.50	13.17	R
S94 P2			150	150	168	57	105	60	37.7	2.9	28501	450	200.0	C	W	100	2.00	75	15.5	10968	0.42	3269	1.18	0.39	34.00	13.36	P
S94 P2B	x		150	150	168	57	105	60	37.7	2.9	28501	450	200.0	C	W	100	2.00	75	15.5	10968	0.42	3269	1.18	0.39	32.50	12.77	S
S94 P2bW	x		150	150	168	57	105	60	37.7	2.9	28501	450	200.0	C	W	100	2.00	75	15.5	10968	0.42	3269	1.18	0.39	39.00	15.33	CC
S94 P3			150	150	168	57	105	60	37.7	2.9	28501	450	200.0	C	W	100	3.00	75	15.5	10968	0.42	3269	1.18	0.39	33.00	12.97	P
S94 P3B	x		150	150	168	57	105	60	37.7	2.9	28501	450	200.0	C	W	100	3.00	75	15.5	10968	0.42	3269	1.18	0.39	36.50	14.34	S
S94 P3BW	x		150	150	168	57	105	60	37.7	2.9	28501	450	200.0	C	W	100	3.00	75	15.5	10968	0.42	3269	1.18	0.39	36.00	14.15	P
S94 P3 J	x		150	150	168	57	105	60	37.7	2.9	28501	450	200.0	C	W	100	3.00	75	15.5	10968	0.42	3269	1.18	0.39	41.00	16.11	CC
H95 FRB2			150	150	157	57	942	60	31.0	2.4	26702	414	200.0	S	-	100	1.00	50	200.0	1345	2.00	3269	NR	0.40	34.80	13.92	R
H95 FRB3			150	150	157	57	942	60	31.0	2.4	26702	414	200.0	S	-	100	1.50	50	200.0	1345	2.00	3269	NR	0.40	37.50	15.00	S
H95 FRB5			150	150	157	57	942	60	31.0	2.4	26702	414	200.0	S	-	100	2.00	50	200.0	1345	2.00	3269	NR	0.40	30.00	12.00	P
H95 FRB7			150	150	157	57	942	60	31.0	2.4	26702	414	200.0	S	-	100	3.00	50	200.0	1345	2.00	3269	NR	0.40	29.00	11.60	P

MK93: Mc Kenna (1993) (referenced by Bonacci and Maalej, 2001); S94: Sharif et al. (1994); H95: Hussain (1995)

Table A.9. Experimental bending test database (IX)

			Geometry of RC beam						Material properties					Plate strengthening								Adhesive		Load configuration				
Specimen (1)	Ext anch (2)	Pr (3)	b mm (4)	h mm (5)	A_s mm^2 (6)	A_s' mm^2 (7)	A_w mm^2 (8)	s_w mm (9)	f_{cm} MPa (10)	f_{ctm} MPa (11)	E_c MPa (12)	f_{ym} MPa (13)	E_s GPa (14)	M (15)	F (16)	b_L mm (17)	t_L mm (18)	a mm (19)	E_L GPa (20)	$\varepsilon_{L,u}$ με (21)	t_a mm (22)	G_a MPa (23)	L m (24)	L_{shear} m (25)	V_{uexp} kN (26)	M_{uexp} kNm (27)	Mode (28)
MB95 P113			200	300	200	0	2262	100	44.3	3.3	30076	439	200.0	C	W	167	0.90	500	82.0	16799	0.42	3269	3.00	1.00	NR	NR	P
MB95 P122			200	300	200	0	2262	100	38.5	2.9	28702	439	200.0	C	W	167	0.90	500	82.0	16799	0.42	3269	3.00	1.00	NR	NR	P
MB95 P123	x		200	300	200	0	2262	100	38.5	2.9	28702	439	200.0	C	W	167	0.90	500	82.0	16799	0.42	3269	3.00	1.00	NR	NR	P
C96 B2			914	356	3879	507	1033	152	31.0	2.4	26702	414	200.0	C	W	864	0.17	2115	137.9	14003	0.42	3269	7.53	2.51	NR	NR	CC
C96 B3			914	356	3879	507	1033	152	31.0	2.4	26702	414	200.0	C	W	690	0.17	2115	137.9	14003	0.42	3269	7.53	2.51	NR	NR	CC
H96 1			150	300	600	200	265	95	37.8	2.9	28527	436	200.0	C	W	125	1.19	0	141.0	14000	0.42	3269	2.00	0.67	NR	NR	P
H96 2			300	574	1300	200	101	250	36.9	2.8	28298	453	200.0	C	W	300	0.85	0	141.0	14000	0.42	3269	5.00	0.67		NR	P
Hu96 A			200	150	157	101	377	150	54.0	3.9	32128	575	200.0	-	-	-	-	-	-	-	-	-	2.10	0.75	13.00	9.75	NR
Hu96 A0.78			200	150	157	101	377	150	54.0	3.9	32128	575	200.0	C	P	150	0.78	85	127.0	12063	2.00	1654	2.10	0.75	31.50	23.63	S
Hu96 A0.78b			200	150	157	101	377	150	54.0	3.9	32128	575	200.0	C	P	150	0.78	85	127.0	12063	2.00	1654	2.10	0.75	34.50	25.88	S
Hu96 A1.15			200	150	157	101	377	150	54.0	3.9	32128	575	200.0	C	P	150	1.15	85	127.0	12063	2.00	1654	2.10	0.75	32.50	24.38	NR
Hu96 B			200	150	157	101	754	75	54.0	3.9	32128	575	200.0	-	-	-	-	-	-	-	-	-	2.10	0.75	14.00	10.50	NR
Hu96 B1.80			200	150	157	101	754	75	54.0	3.9	32128	575	200.0	G	P	150	1.80	85	36.0	42556	2.00	1654	2.10	0.75	30.00	22.50	NR
Hu96 B0.40			200	150	157	101	754	75	54.0	3.9	32128	575	200.0	C	P	150	0.40	85	127.0	12063	2.00	1654	2.10	0.75	27.00	20.25	NR
Hu96 B1.15			200	150	157	101	754	75	54.0	3.9	32128	575	200.0	G	P	150	1.15	85	36.0	42556	2.00	1654	2.10	0.75	35.00	26.25	NR
Hu96 C			200	150	402	101	754	75	54.0	3.9	32128	575	200.0	-	-	-	-	-	-	-	-	-	2.10	0.75	28.50	21.38	NR
Hu96 C1.80			200	150	402	101	754	75	54.0	3.9	32128	575	200.0	G	P	150	1.80	85	36.0	29833	2.00	1654	2.10	0.75	43.50	32.63	NR
Hu96 C0.40			200	150	402	101	754	75	54.0	3.9	32128	575	200.0	C	P	150	0.40	85	127.0	12063	2.00	1654	2.10	0.75	38.00	28.50	NR
Hu96 C1.15			200	150	402	101	754	75	54.0	3.9	32128	575	200.0	C	P	150	1.15	85	127.0	12063	2.00	1654	2.10	0.75	51.00	38.25	NR
Q96 A1b			100	100	85	56	14	100	59.5	4.2	33184	350	200.0	C	P	80	1.20	20	49.0	10204	1.00	2692	0.90	0.30	NR	NR	NR

MB95: M'Bazaa (1995) (referenced by Bonacci and Maalej, 2001); C96: Crasto (1996); H96: Hefferman (1996); Hu96: Hutchinson and Rahimi (1996); Quantrill et al. (1996b)

Table A.10. Experimental bending test database (X)

			Geometry of RC beam						Material properties					Plate strengthening								Adhesive		Load configuration				
Specimen (1)	Ext anch (2)	Pr (3)	b mm (4)	h mm (5)	A_s mm^2 (6)	A_s' mm^2 (7)	A_w mm^2 (8)	s_w mm (9)	f_{cm} MPa (10)	f_{ctm} MPa (11)	E_c MPa (12)	f_{ym} MPa (13)	E_s GPa (14)	M (15)	F (16)	b_L mm (17)	t_L mm (18)	a mm (19)	E_L GPa (20)	$\varepsilon_{L,u}$ με (21)	t_a mm (22)	G_a MPa (23)	L m (24)	L_{shear} m (25)	V_{uexp} kN (26)	M_{uexp} kNm (27)	Mode (28)
Q96 A2c			100	100	85	56	14	100	35.7	2.7	27958	350	200.0	C	P	80	1.20	20	49.0	10204	1.00	2692	0.90	0.30	NR	NR	NR
Q96 B2			100	100	85	56	280	50	45.1	3.3	30256	350	215.0	G	P	80	1.20	20	49.0	10204	1.00	2692	0.90	0.30	17.0	5.1	P
Q96 A1c			100	100	85	56	14	100	59.5	4.2	33184	350	200.0	C	P	80	1.20	20	49.0	10204	2.00	2692	0.90	0.30	NR	NR	NR
Q96 A2b			100	100	85	56	14	100	35.7	2.7	27988	350	200.0	C	P	80	1.20	20	49.0	10204	1.00	2692	0.90	0.30	NR	NR	NR
Q96 B3			100	100	85	56	280	50	45.1	3.3	30256	350	215.0	G	P	80	1.20	20	49.0	22000	2.00	2692	0.90	0.30	12.30	3.69	NR
Q96 B4			100	100	85	56	280	50	45.1	3.3	30256	350	215.0	G	P	60	1.60	20	49.0	22000	2.00	2692	0.90	0.30	17.50	5.25	P
Q96 B6			100	100	85	56	280	50	45.1	3.3	30256	350	215.0	C	P	80	1.20	20	118.5	8329	2.00	2692	0.90	0.30	20.40	6.12	P
S96 5STL			203	305	265	21	127	203	29.6	2.3	26307	469	200.0	-	-	-	-	5	-	-	-	-	2.44	1.06	29.90	31.41	CC
S96 5PRE1			203	305	265	21	127	203	29.6	2.3	26307	469	200.0	C	W	203	0.59	5	141.3	19518	0.42	3269	2.44	1.06	33.30	35.53	P
S96 6PRE3			203	305	265	21	127	203	41.4	3.1	29397	469	200.0	C	W	203	1.18	5	141.3	19518	0.42	3269	2.44	1.06	48.96	52.24	P
S96 6PRE5			203	305	265	21	127	203	41.4	3.1	29397	469	200.0	C	W	203	1.77	5	141.3	19518	0.42	3269	2.44	1.07	58.11	60.41	P
V96 P0			150	250	308	57	707	80	40.0	3.0	29070	520	200.0	-	-	-	-	-	-	-	-	-	2.00	0.70	62.50	43.75	CC
V96 P1		x	150	250	308	57	707	80	40.0	3.0	29070	520	200.0	C	P	150	2.50	50	117.0	11538	2.00	3269	2.00	0.70	96.50	67.55	P
V96 P2			150	250	308	57	707	80	40.0	3.0	29070	520	200.0	C	P	150	2.50	50	117.0	11538	2.00	3269	2.00	0.70	97.50	68.25	P
V96 P3		x	150	250	308	57	707	80	40.0	3.0	29070	520	200.0	C	P	150	2.50	50	117.0	11538	2.00	3269	2.00	0.70	77.50	54.25	P
V96 P4			150	250	308	57	707	80	40.0	3.0	29070	520	200.0	C	P	150	2.50	50	117.0	11538	2.00	3269	2.00	0.70	122.50	85.75	P
V96 P5	x	x	150	250	308	57	707	80	40.0	3.0	29070	520	200.0	C	P	150	2.50	50	117.0	11538	2.00	3269	2.00	0.70	82.50	57.75	P
V96 P6	x		150	250	308	57	707	80	40.0	3.0	29070	520	200.0	C	P	150	2.50	50	117.0	11538	2.00	3269	2.00	0.70	105.00	73.50	P
A97 A1			200	200	308	308	377	150	33.0	2.6	27264	540	200.0	-	-	-	-	-	-	-	-	-	2.00	0.70	36.50	25.55	CC
A97 A2			200	200	308	308	377	150	33.0	2.6	27264	540	200.0	-	-	-	-	-	-	-	-	-	2.00	0.70	36.50	25.55	CC

Q96: Quantrill et al. (1996b); S96: Shahawy et al. (1996); V96: Varastehpour and Hamelin (1996); A97: Arduini et al. (1997)

Table A.11. Experimental bending test database (XI)

			Geometry of RC beam						Material properties					Plate strengthening								Adhesive		Load configuration				
Specimen (1)	Ext anch (2)	Pr (3)	b mm (4)	h mm (5)	A_s mm^2 (6)	A_s' mm^2 (7)	A_w mm^2 (8)	s_w mm (9)	f_{cm} MPa (10)	f_{ctm} MPa (11)	E_c MPa (12)	f_{ym} MPa (13)	E_s GPa (14)	M (15)	F (16)	b_L mm (17)	t_L mm (18)	a mm (19)	E_L GPa (20)	ε_{Lu} με (21)	t_a mm (22)	G_a MPa (23)	L m (24)	L_{shear} m (25)	V_{uexp} kN (26)	M_{uexp} kNm (27)	Mode (28)
A97 A3			200	200	308	308	377	150	33.0	2.6	27264	540	200.0	C	P	50	1.30	150	167.0	17401	2.00	4400	2.00	0.70	53.00	37.10	PED
A97 A4			200	200	308	308	377	150	33.0	2.6	27264	540	200.0	C	P	50	1.30	150	167.0	17401	2.00	4400	2.00	0.70	52.00	36.40	PED
A97 A5			200	200	308	308	377	150	33.0	2.6	27264	540	200.0	C	P	50	2.60	150	167.0	17401	2.00	4400	2.00	0.70	42.00	29.40	PED
A97 A6			200	200	308	308	377	150	33.0	2.6	27264	540	200.0	C	P	50	2.60	150	167.0	17401	2.00	4400	2.00	0.70	60.00	42.00	PED
A97 B2			300	400	398	265	1005	100	30.0	2.4	26411	340	200.0	C	W	300	0.59	100	283.3	10589	0.42	4400	2.50	1.10	84.00	92.40	R
A97 B3			300	400	398	265	1005	100	30.0	2.4	26411	340	200.0	C	W	300	1.77	100	283.3	10589	0.42	4400	2.50	1.10	112.50	123.75	PC
A97 B1			300	400	398	265	1005	100	30.0	2.4	26411	340	200.0	-	-	-	-	-	-	-	-	-	2.50	1.10	46.00	50.60	CC
A97 B4	x		300	400	398	265	1005	100	30.0	2.4	26411	340	200.0	C	W	300	1.94	100	283.3	10589	0.42	4400	2.50	1.10	140.00	154.00	O
AN97 S1			320	160	226	226	565	100	36.0	2.8	28066	550	200.0	-	-	-	-	-	-	-	-	-	1.10	0.42	50.00	21.00	CC
AN97 SM2			320	160	226	226	565	100	36.0	2.8	28066	550	200.0	C	W	300	0.54	50	165.1	15000	0.42	725	1.10	0.42	65.00	27.30	PC
AN97 SM3		x	320	160	226	226	565	100	36.0	2.8	28066	550	200.0	C	W	300	0.54	50	165.1	15000	0.42	725	1.10	0.42	55.00	23.10	PC
AN97 SM4			320	160	226	226	565	100	36.0	2.8	28066	550	200.0	C	W	300	0.54	50	165.1	15000	0.42	725	1.10	0.42	39.50	16.59	PC
AN97 SM5			320	160	226	226	565	100	36.0	2.8	28066	550	200.0	C	W	300	0.54	50	165.1	15000	0.42	725	1.10	0.42	72.50	30.45	PC
AN97 SM6		x	320	160	226	226	565	100	36.0	2.8	28066	550	200.0	C	W	300	1.07	100	165.1	15000	0.42	725	1.10	0.42	71.00	29.82	PES
AN97 ST2		x	320	160	226	226	565	100	36.0	2.8	28066	550	200.0	C	W	300	0.54	50	165.1	15000	0.42	741	1.10	0.42	62.50	26.25	P
AN97 ST3			320	160	226	226	565	100	36.0	2.8	28066	550	200.0	C	W	300	0.54	50	266.6	15000	0.42	741	1.10	0.42	79.00	33.18	P
AN97 ST4			320	160	226	226	565	100	36.0	2.8	28066	550	200.0	C	W	300	0.54	50	266.6	15000	0.42	741	1.10	0.42	79.00	33.18	P
AN97 M1			160	320	402	402	565	100	36.0	2.8	28066	550	200.0	-	-	-	-	-	-	-	-	-	2.10	0.95	63.50	60.33	CC
AN97 MM2		x	160	320	402	402	565	100	36.0	2.8	28066	550	200.0	C	W	150	0.54	100	165.1	15000	0.42	725	2.10	0.95	76.00	72.20	PC
AN97 MM3		x	160	320	402	402	565	100	36.0	2.8	28066	550	200.0	C	W	150	0.54	100	165.1	15000	0.42	725	2.10	0.95	67.50	64.13	PC

A97: Arduini et al. (1997); AN97: Arduini and Nanni. (1997)

Table A.12. Experimental bending test database (XII)

			Geometry of RC beam						Material properties					Plate strengthening								Adhesive		Load configuration				
Specimen (1)	Ext anch (2)	Pr (3)	b mm (4)	h mm (5)	A_s mm^2 (6)	A_s' mm^2 (7)	A_w mm^2 (8)	s_w mm (9)	f_{cm} MPa (10)	f_{ctm} MPa (11)	E_c MPa (12)	f_{ym} MPa (13)	E_s GPa (14)	M (15)	F (16)	b_L mm (17)	t_L mm (18)	a mm (19)	E_L GPa (20)	ε_{Lu} με (21)	t_a mm (22)	G_a MPa (23)	L m (24)	L_{shear} m (25)	V_{uexp} kN (26)	M_{uexp} kNm (27)	Mode (28)
AN97 MM4		x	160	320	402	402	565	100	36.0	2.8	28066	550	200.0	C	W	150	0.54	200	165.1	15000	0.42	725	2.10	0.95	86.00	81.70	PES
AN97 MM5	x		160	320	402	402	565	100	36.0	2.8	28066	550	200.0	C	W	150	1.07	200	165.1	15000	0.42	725	2.10	0.95	130.00	123.50	P
AN97 MT2		x	160	320	402	402	565	100	36.0	2.8	28066	550	200.0	C	W	150	0.54	100	165.1	15000	0.42	741	2.10	0.95	75.00	71.25	P
AN97 MT3		x	160	320	402	402	565	100	36.0	2.8	28066	550	200.0	C	W	150	0.54	100	165.1	15000	0.42	741	2.10	0.95	80.00	76.00	P
AN97 MT4		x	160	320	402	402	565	100	36.0	2.8	28066	550	200.0	C	W	150	0.54	100	165.1	15000	0.42	741	2.10	0.95	72.50	68.88	P
AN97 MT5		x	160	320	402	402	565	100	36.0	2.8	28066	550	200.0	C	W	150	0.54	100	165.1	15000	0.42	741	2.10	0.95	75.50	71.73	P
C97 RF1			150	250	400	0	3142	50	35.0	2.7	27804	400	200.0	C	W	150	0.66	0	150.0	16000	0.42	3269	1.20	0.40	NR	NR	P
C97 RF2			150	250	400	0	3142	50	35.0	2.7	27804	400	200.0	C	W	150	0.66	0	150.0	16000	0.42	3269	1.20	0.40	NR	NR	P
G97 1			100	100	85	57	277	51	47.3	3.5	30736	350	215.0	-	-	-	-	-	-	-	-	-	0.90	0.30	8.50	2.55	NR
G97 3			100	100	85	57	277	51	47.3	3.5	30736	350	215.0	-	-	-	-	-	-	-	-	-	0.90	0.40	6.25	2.50	NR
G97 1Au			100	100	85	57	277	51	47.3	3.5	30736	350	215.0	C	W	90	0.50	25	111.0	11468	0.42	4446	0.90	0.30	19.80	5.94	P
G97 1Bu			100	100	85	57	277	51	47.3	3.5	30736	350	215.0	C	W	65	0.70	25	111.0	11468	0.42	4446	0.90	0.30	18.25	5.48	P
G97 1B2u			100	100	85	57	277	51	47.3	3.5	30736	350	215.0	C	W	65	0.70	25	111.0	11468	0.42	4446	0.90	0.30	18.20	5.46	P
G97 1Cu			100	100	85	57	277	51	47.3	3.5	30736	350	215.0	C	W	45	1.00	25	111.0	11468	0.42	4446	0.90	0.30	15.95	4.79	P
G97 2Au			100	100	85	57	277	51	47.3	3.5	30736	350	215.0	C	W	90	0.50	25	111.0	11468	0.42	4446	0.90	0.34	19.25	6.55	PED
G97 2Aa	x		100	100	85	57	277	51	47.3	3.5	30736	350	215.0	C	W	90	0.50	25	111.0	11468	0.42	4446	0.90	0.34	25.33	8.61	P
G97 2A2a	x		100	100	85	57	277	51	47.3	3.5	30736	350	215.0	C	W	90	0.50	25	111.0	11468	0.42	4446	0.90	0.34	19.75	6.72	P
G97 2A3a	x		100	100	85	57	277	51	47.3	3.5	30736	350	215.0	C	W	90	0.50	25	111.0	11468	0.42	4446	0.90	0.34	20.85	7.09	PED
G97 2Bu			100	100	85	57	277	51	47.3	3.5	30736	350	215.0	C	W	65	0.70	25	111.0	11468	0.42	4446	0.90	0.34	17.00	5.78	P
G97 2Ba	x		100	100	85	57	277	51	47.3	3.5	30736	350	215.0	C	W	65	0.70	25	111.0	11468	0.42	4446	0.90	0.34	24.83	8.44	PED

AN97: Arduini and Nanni. (1997); C97: Chaallal et al. (1997); G97: Garden et al. (1997)

Table A.13. Experimental bending test database (XIII)

			Geometry of RC beam						Material properties					Plate strengthening								Adhesive		Load configuration				
Specimen (1)	Ext anch (2)	Pr (3)	b mm (4)	h mm (5)	A_s mm^2 (6)	A_s' mm^2 (7)	A_w mm^2 (8)	s_w mm (9)	f_{cm} MPa (10)	f_{ctm} MPa (11)	E_c MPa (12)	f_{ym} MPa (13)	E_s GPa (14)	M (15)	F (16)	b_L mm (17)	t_L mm (18)	a mm (19)	E_L GPa (20)	ε_{Lu} με (21)	t_a mm (22)	G_a MPa (23)	L m (24)	L_{shear} m (25)	V_{uexp} kN (26)	M_{uexp} kNm (27)	Mode (28)
G97 2B2a	x		100	100	85	57	277	51	47.3	3.5	30736	350	215.0	C	W	65	0.70	25	111.0	11468	0.42	4446	0.90	0.34	17.15	5.83	P
G97 2Cu			100	100	85	57	277	51	47.3	3.5	30736	350	215.0	C	W	45	1.00	25	111.0	11468	0.42	4446	0.90	0.34	17.78	6.04	P
G97 2Ca	x		100	100	85	57	277	51	47.3	3.5	30736	350	215.0	C	W	45	1.00	25	111.0	11468	0.42	4446	0.90	0.34	20.55	6.99	PED
G97 3Au			100	100	85	57	277	51	47.3	3.5	30736	350	215.0	C	W	90	0.50	25	111.0	11468	0.42	4446	0.90	0.40	19.50	7.80	PED
G97 3Bu			100	100	85	57	277	51	47.3	3.5	30736	350	215.0	C	W	65	0.70	25	111.0	11468	0.42	4446	0.90	0.40	17.25	6.90	PED
G97 3Cu			100	100	85	57	277	51	47.3	3.5	30736	350	215.0	C	W	45	1.00	25	111.0	11468	0.42	4446	0.90	0.40	15.35	6.14	PED
N97 C96			127	203	142	142	343	165	36.5	2.8	28196	420	200.0	-	-	-	-	0	-	-	-	-	2.29	0.57	25.50	14.64	NR
N97 C48			127	203	402	142	275	206	36.5	2.8	28196	420	200.0	-	-	-	-	0	-	-	-	-	1.07	0.46	25.50	14.64	NR
N97 IA			127	203	142	142	343	165	36.5	2.8	28196	420	200.0	C	W	127	1.00	0	34.1	11428	0.42	1731	2.29	0.57	69.00	39.61	PED
N97 IB			127	203	142	142	343	165	36.5	2.8	28196	420	200.0	C	W	127	1.00	0	34.1	331	0.42	1731	2.29	0.57	59.00	33.87	P
N97 IBu			127	203	142	142	343	165	36.5	2.8	28196	420	200.0	C	W	127	1.00	0	34.1	331	0.42	1731	2.29	0.57	NR	NR	NR
N97 IBi			127	203	142	142	343	165	36.5	2.8	28196	420	200.0	C	W	127	1.00	0	34.1	331	0.42	1731	2.29	0.57	NR	NR	NR
N97 IC			127	203	142	142	343	165	36.5	2.8	28196	420	200.0	C	W	127	1.00	0	34.1	1988	0.42	1731	2.29	0.57	38.50	22.10	P
N97 ID			127	203	142	142	343	165	36.5	2.8	28196	420	200.0	C	W	127	1.00	0	34.1	1988	0.42	1731	2.29	0.57	32.50	18.66	P
N97 IE	x		127	203	402	142	275	206	36.5	2.8	28196	420	200.0	C	W	127	1.00	0	34.1	331	0.42	1731	1.07	0.46	70.00	32.06	P
N97 IF	x		127	203	402	142	275	206	36.5	2.8	28196	420	200.0	C	W	127	1.00	0	34.1	287	0.42	1731	1.07	0.46	NR	NR	NR
N97 IIA			127	203	142	142	343	165	36.5	2.8	28196	420	200.0	C	W	127	1.00	0	33.4	11835	0.42	1115	2.29	0.57	NR	NR	NR
N97 IIB			127	203	142	142	343	165	36.5	2.8	28196	420	200.0	C	W	127	1.00	0	33.4	413	0.42	1115	2.29	0.57	NR	NR	NR
N97 IIBu			127	203	142	142	343	165	36.5	2.8	28196	420	200.0	C	W	127	1.00	0	33.4	413	0.42	1115	2.29	0.57	NR	NR	NR
N97 IIBi			127	203	142	142	343	165	36.5	2.8	28196	420	200.0	C	W	127	1.00	0	33.4	413	0.42	1115	2.29	0.57	NR	NR	NR

G97: Garden et al. (1997); N97: Norris et al. (1997)

Table A.14. Experimental bending test database (XIV)

			Geometry of RC beam						Material properties					Plate strengthening								Adhesive		Load configuration				
Specimen (1)	Ext anch (2)	Pr (3)	b mm (4)	h mm (5)	A_s mm^2 (6)	A_s' mm^2 (7)	A_w mm^2 (8)	s_w mm (9)	f_{cm} MPa (10)	f_{ctm} MPa (11)	E_c MPa (12)	f_{ym} MPa (13)	E_s GPa (14)	M (15)	F (16)	b_L mm (17)	t_L mm (18)	a mm (19)	E_L GPa (20)	$\varepsilon_{L,u}$ με (21)	t_a mm (22)	G_a MPa (23)	L m (24)	L_{shear} m (25)	V_{uexp} kN (26)	M_{uexp} kNm (27)	Mode (28)
N97 IIIC			127	203	142	142	343	165	36.5	2.8	28196	420	200.0	C	W	127	1.50	0	28.3	3700	0.42	1115	2.29	0.57	NR	NR	NR
N97 IIID			127	203	142	142	343	165	36.5	2.8	28196	420	200.0	C	W	127	1.50	0	28.3	3700	0.42	1115	2.29	0.57	28.00	16.07	NR
N97 IIIE	x		127	203	402	142	275	206	36.5	2.8	28196	420	200.0	C	W	127	1.00	0	33.4	2341	0.42	1115	1.07	0.46	75.00	34.35	NR
N97 IIIF	x		127	203	402	142	275	206	36.5	2.8	28196	420	200.0	C	W	127	1.50	0	28.3	3700	0.42	1115	1.07	0.46	NR	NR	NR
N97 IIIFu	x		127	203	402	142	275	206	36.5	2.8	28196	420	200.0	C	W	127	1.50	0	28.3	3700	0.42	1115	1.07	0.46	100.00	45.80	PES
B98 U			200	260	142	142	1418	100	20.5	1.6	23263	418	210.0	-	-	-	-	-	-	-	-	-	1.80	0.60	24.10	14.46	CC
B98 0.6			200	260	142	142	1418	100	20.5	1.6	23263	418	210.0	C	W	50	1.00	600	155.0	17419	1.00	1038	1.80	0.60	26.15	15.69	P
B98 0.8			200	260	142	142	1418	100	20.5	1.6	23263	418	210.0	C	W	50	1.00	500	155.0	17419	1.00	1038	1.80	0.60	26.90	16.14	P
B98 1.0			200	260	142	142	1418	100	20.5	1.6	23263	418	210.0	C	W	50	1.00	400	155.0	17419	1.00	1038	1.80	0.60	31.05	18.63	P
B98 1.2			200	260	142	142	1418	100	20.5	1.6	23263	418	210.0	C	W	50	1.00	300	155.0	17419	1.00	1038	1.80	0.60	31.60	18.96	P
B98 1.4			200	260	142	142	1418	100	20.5	1.6	23263	418	210.0	C	W	50	1.00	200	155.0	17419	1.00	1038	1.80	0.60	45.30	27.18	P
B98 1.6			200	260	142	142	1418	100	20.5	1.6	23263	418	210.0	C	W	50	1.00	100	155.0	17419	1.00	1038	1.80	0.60	50.20	30.12	P
C98 FS			200	400	942	157	2222	90	33.4	2.6	27374	400	200.0	C	P	50	1.20	0	155.0	15484	1.00	4500	3.00	1.00	138.00	138.00	P
C98 RS	x		200	400	628	157	1000	200	33.4	2.6	27374	400	200.0	C	P	50	1.20	0	155.0	15484	1.00	4500	3.00	1.00	141.00	141.00	P
C98 RS2	x		200	400	628	157	1000	200	33.4	2.6	27374	400	200.0	C	P	50	1.20	0	155.0	15484	1.00	4500	3.00	1.00	143.00	143.00	P
Cl98 LMT1S			150	250	402	101	633	100	35.0	2.7	27804	500	200.0	-	-	-	-	-	-	-	-	-	4.30	2.15	37.00	79.55	CC
Cl98 LMT3S			150	250	402	101	633	100	35.0	2.7	27804	500	200.0	C	W	150	0.80	250	100.0	9000	0.42	3269	4.30	2.15	53.50	115.03	P
Cl98 LMT5S	x		150	250	402	101	633	100	35.0	2.7	27804	500	200.0	C	W	150	0.80	250	100.0	9000	0.42	3269	4.30	2.15	60.50	130.08	R
D98 P1			150	300	308	101	435	130	40.0	3.0	29070	500	200.0	-	-	-	-	-	-	-	-	-	2.80	0.90	45.00	40.50	CC
D98 P2		x	150	300	308	101	435	130	40.0	3.0	29070	500	200.0	G	W	150	3.00	100	11.7	4701	2.00	1654	2.80	0.90	50.50	45.45	R

N97: Norris et al. (1997); B98: Buyukozturk and Hearing (1998); C98: Chaallal et al. (1998c); Cl98: Clement (1998); D98: David et al. (1998)

Table A.15. Experimental bending test database (XV)

			Geometry of RC beam						Material properties					Plate strengthening								Adhesive		Load configuration				
Specimen (1)	Ext anch (2)	Pr (3)	b mm (4)	h mm (5)	A_s mm^2 (6)	A_s' mm^2 (7)	A_w mm^2 (8)	s_w mm (9)	f_{cm} MPa (10)	f_{ctm} MPa (11)	E_c MPa (12)	f_{ym} MPa (13)	E_s GPa (14)	M (15)	F (16)	b_L mm (17)	t_L mm (18)	a mm (19)	E_L GPa (20)	$\varepsilon_{L,u}$ με (21)	t_a mm (22)	G_a MPa (23)	L m (24)	L_{shear} m (25)	V_{uexp} kN (26)	M_{uexp} kNm (27)	Mode (28)
D98 P3		x	150	300	308	101	435	130	40.0	3.0	29070	500	200.0	G	W	150	3.00	100	11.7	4701	2.00	1654	2.80	0.90	50.50	45.45	R
D98 P4		x	150	300	308	101	435	130	40.0	3.0	29070	500	200.0	G	W	150	6.00	100	11.7	4701	2.00	1654	2.80	0.90	57.50	51.75	P
D98 P6			150	300	308	101	435	130	40.0	3.0	29070	500	200.0	G	W	150	6.00	100	11.7	4701	2.00	1654	2.80	0.90	66.00	59.40	P
D98 P7			150	300	308	101	435	130	40.0	3.0	29070	500	200.0	C	P	50	1.20	100	150.0	16000	2.00	1654	2.80	0.90	68.00	61.20	P
D98 P8			150	300	308	101	407	139	40.0	3.0	29070	500	200.0	C	P	50	1.20	100	150.0	16000	2.00	1654	2.80	0.90	71.50	64.35	P
D98 P9			150	300	308	101	404	140	40.0	3.0	29070	500	200.0	C	P	50	2.40	100	150.0	16000	2.00	1654	2.80	0.90	78.00	70.20	P
D98 P10			150	300	308	101	401	141	40.0	3.0	29070	500	200.0	C	P	50	2.40	100	150.0	16000	2.00	1654	2.80	0.90	79.50	71.55	P
G98 1U1.0			100	100	85	57	283	50	44.8	3.3	30189	350	215.0	C	W	67	0.82	20	111.0	12739	2.00	3269	NR	0.30	18.30	5.49	P
G98 2U1.0			100	100	85	57	283	50	44.8	3.3	30189	350	215.0	C	W	67	0.82	20	111.0	12739	2.00	3269	NR	0.30	16.00	4.80	P
G98 3U1.0			100	100	85	57	283	50	44.8	3.3	30189	350	215.0	C	W	67	0.82	40	111.0	12739	2.00	3269	NR	0.34	17.00	5.78	P
G98 4U1.0			100	100	85	57	283	50	44.8	3.3	30189	350	215.0	C	W	67	0.82	20	111.0	12739	2.00	3269	NR	0.40	17.30	6.92	NR
G98 5U1.0			100	100	85	57	283	50	44.8	3.3	30189	350	215.0	C	W	67	0.82	20	111.0	12739	2.00	3269	NR	0.40	17.30	6.92	P
G98 1U2.3			130	230	236	101	377	150	39.0	3.0	28825	556	220.0	C	W	90	1.28	40	115.0	11165	2.00	3269	NR	0.84	50.20	42.42	P
G98 1U4.5			145	230	226	101	377	150	39.0	3.0	28825	556	220.0	C	W	90	1.28	40	115.0	11165	0.42	3269	NR	0.152	30.00	45.75	P
M98 SAB1			150	250	942	101	514	110	53.4	3.8	32001	512	200.0	-	-	-	-	50	-	-	-	-	2.80	0.93	99.95	93.25	CC
M98 FS1	x		150	250	942	101	514	110	42.6	3.2	29696	512	200.0	S	-	150	2.50	50	200.0	1400	2.00	2500	2.80	0.93	105.70	98.62	CC
M98 FS2	x		150	250	942	101	514	110	43.2	3.2	29825	512	200.0	G	P	150	3.50	50	14.3	22897	2.00	2500	2.80	0.93	98.45	91.85	CC
M98 FS3	x		150	250	942	101	514	110	53.2	3.8	31969	512	200.0	G	P	150	3.50	50	14.3	22897	2.00	2500	2.80	0.93	109.90	102.54	R
M98 FS4	x		150	250	942	101	514	110	63.8	4.4	33957	512	200.0	G	P	150	3.50	50	14.3	22897	2.00	2500	2.80	0.93	116.65	108.83	R
M98 FS5	x		150	250	942	101	514	110	53.3	3.8	31985	512	200.0	G	P	150	3.50	50	14.3	22897	2.00	2500	2.80	0.93	115.95	108.18	CC

D98: David et al. (1998); G98: Garden et al. (1998); M98: Mukhopadyaya and Swamy (1998)

Table A.16. Experimental bending test database (XVI)

			Geometry of RC beam						Material properties					Plate strengthening								Adhesive		Load configuration				
Specimen (1)	Ext anch (2)	Pr (3)	b mm (4)	h mm (5)	A_s mm^2 (6)	A_s' mm^2 (7)	A_w mm^2 (8)	s_w mm (9)	f_{cm} MPa (10)	f_{ctm} MPa (11)	E_c MPa (12)	f_{ym} MPa (13)	E_s GPa (14)	M (15)	F (16)	b_L mm (17)	t_L mm (18)	a mm (19)	E_L GPa (20)	ε_{Lu} με (21)	t_a mm (22)	G_a MPa (23)	L m (24)	L_{shear} m (25)	V_{uexp} kN (26)	M_{uexp} kNm (27)	Mode (28)
S98 A1			140	300	402	402	168	150	24.1	1.9	24545	435	200.0	-	-	-	-	-	-	-	-	-	4.80	1.80	27.00	48.60	CC
S98 A11			140	300	402	402	168	150	27.4	2.2	25638	435	200.0	C	P	80	1.20	50	152.0	15100	2.00	3077	4.80	1.80	43.40	78.12	P
S98 A12	x		140	300	402	402	168	150	23.2	1.8	24243	435	200.0	C	P	80	1.20	50	152.0	15100	2.00	3077	4.80	1.80	49.00	88.20	P
S98 A13	x		140	300	402	402	168	150	23.2	1.8	24243	435	200.0	C	P	80	1.20	50	152.0	15100	2.00	3077	4.80	1.80	48.35	87.03	P
S98 A2			140	300	402	402	168	150	27.0	2.1	25487	435	200.0	-	-	-	-	-	-	-	-	-	4.80	1.80	14.60	26.28	CC
S98 A22	x		140	300	402	402	168	150	30.2	2.4	26482	435	200.0	C	P	80	1.20	50	152.0	15100	2.00	3077	4.80	1.80	37.50	67.50	P
S98 A23	x		140	300	402	402	168	150	26.6	2.1	25361	435	200.0	C	P	80	1.20	50	152.0	15100	2.00	3077	4.80	1.80	38.85	69.93	P
S98 A3			140	300	402	402	168	150	23.6	1.9	24381	435	200.0	-	-	-	-	-	-	-	-	-	4.80	1.80	28.60	51.48	CC
S98 A31			140	300	402	402	168	150	28.5	2.2	25958	435	200.0	C	P	80	1.20	50	152.0	15100	2.00	3077	4.80	1.80	37.40	67.32	P
S98 A32	x		140	300	402	402	168	150	23.7	1.9	24409	435	200.0	C	P	80	1.20	50	152.0	15100	2.00	3077	4.80	1.80	49.40	88.92	O
S98 A33	x		140	300	402	402	168	150	24.4	1.9	24654	435	200.0	C	P	80	1.20	50	152.0	15100	2.00	3077	4.80	1.80	49.15	88.47	P
B99 VT1			120	250	157	57	514	110	33.6	2.6	27423	565	200.0	-	-	-	-	-	-	-	-	-	2.35	0.78	23.70	18.57	CC
B99 VT2			120	250	157	57	514	110	33.6	2.6	27423	565	200.0	-	-	-	-	-	-	-	-	-	2.35	0.78	23.50	18.41	CC
B99 VR3			120	250	157	57	514	110	33.6	2.6	27423	565	200.0	C	W	120	0.12	76	163.5	15000	0.42	3269	2.35	0.78	32.60	25.54	CC
B99 VR4			120	250	157	57	514	110	33.6	2.6	27423	565	200.0	C	W	120	0.12	76	163.5	15000	0.42	3269	2.35	0.78	31.00	24.28	R
B99 VR5			120	250	157	57	514	110	33.6	2.6	27423	565	200.0	C	W	120	2.15	76	163.5	15000	0.42	3269	2.35	0.78	51.10	40.03	P
B99 VR6			120	250	157	57	514	110	33.6	2.6	27423	565	200.0	C	W	120	2.15	76	163.5	15000	0.42	3269	2.35	0.78	50.30	39.40	P
B99 VR7			120	250	157	57	514	110	33.6	2.6	27423	565	200.0	C	W	120	3.76	76	163.5	15000	0.42	3269	2.35	0.78	62.10	48.65	P
B99 VR8			120	250	157	57	514	110	33.6	2.6	27423	565	200.0	C	W	120	3.76	76	163.5	15000	0.42	3269	2.35	0.78	62.00	48.57	P
B99 VR9			120	250	157	57	514	110	33.6	2.6	27423	565	200.0	C	W	120	5.37	76	163.5	15000	0.42	3269	2.35	0.78	64.80	50.76	P

S98: Spadea et al. (1998); B99: Beber et al. (1999)

Table A.17. Experimental bending test database (XVII)

			Geometry of RC beam						Material properties					Plate strengthening								Adhesive		Load configuration				
Specimen (1)	Ext anch (2)	Pr (3)	b mm (4)	h mm (5)	A_s mm^2 (6)	A_s' mm^2 (7)	A_w mm^2 (8)	s_w mm (9)	f_{cm} MPa (10)	f_{ctm} MPa (11)	E_c MPa (12)	f_{ym} MPa (13)	E_s GPa (14)	M (15)	F (16)	b_L mm (17)	t_L mm (18)	a mm (19)	E_L GPa (20)	$\varepsilon_{L,u}$ με (21)	t_a mm (22)	G_a MPa (23)	L m (24)	L_{shear} m (25)	V_{uexp} kN (26)	M_{uexp} kNm (27)	Mode (28)
B99 VR10			120	250	157	57	514	110	33.6	2.6	27423	565	200.0	C	W	120	5.37	76	163.5	15000	0.42	3269	2.35	0.78	68.50	53.66	P
R99 1A			200	200	142	142	1392	102	54.8	3.9	32286	410	200.0	-	-	-	-	-	-	-	-	-	2.74	0.91	13.35	12.20	CC
R99 1B			200	200	142	142	1392	102	54.8	3.9	32286	410	200.0	C	W	203	0.45	1	137.9	15997	0.42	3192	2.74	0.91	40.05	36.61	P
R99 1C			200	200	142	142	1392	102	54.8	3.9	32286	410	200.0	C	W	203	0.45	1	137.9	15997	0.42	3192	2.74	0.91	35.60	32.54	P
R99 2A			200	200	259	142	1392	102	54.8	3.9	32286	410	200.0	-	-	-	-	-	-	-	-	-	2.74	0.91	23.35	21.34	CC
R99 2B			200	200	259	142	1392	102	54.8	3.9	32286	410	200.0	C	W	203	0.45	1	137.9	15997	0.42	3192	2.74	0.91	48.95	44.74	P
R99 2C			200	200	259	142	1392	102	54.8	3.9	32286	410	200.0	C	W	203	0.45	1	137.9	15997	0.42	3192	2.74	0.91	35.96	32.87	P
R99 2D			200	200	259	142	1392	102	54.8	3.9	32286	410	200.0	C	W	203	0.45	1	137.9	15997	0.42	3192	2.74	0.91	40.05	36.61	P
R99 3A			200	200	400	142	1392	102	54.8	3.9	32286	410	200.0	-	-	-	-	-	-	-	-	-	2.74	0.91	31.15	28.47	CC
R99 3B			200	200	400	142	1392	102	54.8	3.9	32286	410	200.0	C	W	203	0.45	1	137.9	15997	0.42	3192	2.74	0.91	54.52	49.83	P
R99 3C			200	200	400	142	1392	102	54.8	3.9	32286	410	200.0	C	W	203	0.45	1	137.9	15997	0.42	3192	2.74	0.91	54.07	49.42	P
R99 3D			200	200	400	142	1392	102	54.8	3.9	32286	410	200.0	C	W	203	0.45	1	137.9	15997	0.42	3192	2.74	0.91	54.29	49.62	P
R99 4A			200	200	774	142	1392	102	54.8	3.9	32286	410	200.0	-	-	-	-	-	-	-	-	-	2.74	0.91	35.60	32.54	CC
R99 4B			200	200	774	142	1392	102	54.8	3.9	32286	410	200.0	C	W	203	0.45	1	137.9	15997	0.42	3192	2.74	0.91	53.82	49.19	PC
R99 4C			200	200	774	142	1392	102	54.8	3.9	32286	410	200.0	C	W	203	0.45	1	137.9	15997	0.42	3192	2.74	0.91	52.29	47.79	PC
R99 4D			200	200	774	142	1392	102	54.8	3.9	32286	410	200.0	C	W	203	0.45	1	137.9	15997	0.42	3192	2.74	0.91	55.63	50.84	PC
R99 5A			200	200	612	142	1392	102	54.8	3.9	32286	410	200.0	-	-	-	-	-	-	-	-	-	2.74	0.91	57.85	52.87	CC
R99 5B			200	200	612	142	1392	102	54.8	3.9	32286	410	200.0	C	W	203	0.45	1	137.9	15997	0.42	3192	2.74	0.91	73.43	67.11	PC
R99 5C			200	200	612	142	1392	102	54.8	3.9	32286	410	200.0	C	W	203	0.45	1	137.9	15997	0.42	3192	2.74	0.91	73.43	67.11	PC
R99 5D			200	200	612	142	1392	102	54.8	3.9	32286	410	200.0	C	W	203	0.45	1	137.9	15997	0.42	3192	2.74	0.91	72.76	66.50	PC

B99: Beber et al. (1999); R99: Ross et al. (1999)

Table A.18. Experimental bending test database (XVIII)

			Geometry of RC beam						Material properties					Plate strengthening								Adhesive		Load configuration				
Specimen (1)	Ext anch (2)	Pr (3)	b mm (4)	h mm (5)	A_s mm^2 (6)	A_s' mm^2 (7)	A_w mm^2 (8)	s_w mm (9)	f_{cm} MPa (10)	f_{ctm} MPa (11)	E_c MPa (12)	f_{ym} MPa (13)	E_s GPa (14)	M (15)	F (16)	b_L mm (17)	t_L mm (18)	a mm (19)	E_L GPa (20)	$\varepsilon_{L,u}$ με (21)	t_a mm (22)	G_a MPa (23)	L m (24)	L_{shear} m (25)	V_{uexp} kN (26)	M_{uexp} kNm (27)	Mode (28)
R99 6A			200	200	1019	142	1392	102	54.8	3.9	32286	410	200.0	-	-	-	-	-	-	-	-	-	2.74	0.91	66.75	61.01	CC
R99 6B			200	200	1019	142	1392	102	54.8	3.9	32286	410	200.0	C	W	203	0.45	1	137.9	15997	0.42	3192	2.74	0.91	84.55	77.28	PC
R99 6C			200	200	1019	142	1392	102	54.8	3.9	32286	410	200.0	C	W	203	0.45	1	137.9	15997	0.42	3192	2.74	0.91	76.55	69.97	PC
R99 6D			200	200	1019	142	1392	102	54.8	3.9	32286	410	200.0	C	W	203	0.45	1	137.9	15997	0.42	3192	2.74	0.91	76.55	69.97	PC
J99 A1			100	150	157	402	942	60	28.8	2.5	26055	519	183.7	C	P	50	1.20	175	163.3	19876	2.00	1731	1.50	0.65	20.40	13.26	PC
J99 A4			100	150	157	402	942	60	31.7	2.7	26901	519	183.7	C	P	50	1.20	0	163.3	19876	2.00	1731	1.50	0.65	20.40	13.26	PC
J99 B2			75	150	14	151	236	60	26.7	2.3	25405	192	195.0	-	-	-	-	-	-	-	-	-	1.50	0.65	NR	NR	CC
J99 B4			75	150	151	14	236	60	36.3	3.0	28144	497	174.0	-	-	-	-	-	-	-	-	-	1.50	0.65	NR	NR	CC
J99 B6			75	150	151	14	236	60	33.7	2.8	27455	497	174.0	-	-	-	-	-	-	-	-	-	1.50	0.65	29.80		CC
J99 B7			75	150	14	151	236	60	33.6	2.8	27428	192	195.0	C	P	50	1.20	0	160.0	19375	2.00	1731	1.50	0.65	24.60	15.99	PC
J99 B10			75	150	14	151	236	60	31.3	2.7	26788	192	195.0	-	-	-	-	-	-	-	-	-	1.50	0.65	1.20	0.78	CC
J99 B11			75	150	14	151	236	60	30.0	2.6	26411	192	195.0	C	P	50	1.20	200	160.0	19375	2.00	1731	1.50	0.65	13.40	8.71	PED
J99 B12			75	150	151	14	236	60	30.0	2.6	26411	497	174.0	-	-	-	-		-	-	-	-	1.50	0.65	26.40	17.16	CC
J99 C2			150	150	226	226	565	100	16.5	1.5	21639	507	184.6	-	-	-	-	-	-	-	-	-	1.41	0.60	NR	NR	CC
J99 C3			150	150	226	226	565	100	16.5	1.5	21639	507	184.6	-	-	-	-	-	-	-	-	-	1.41	0.60	50.00	30.25	CC
J99 C5			150	150	226	226	565	100	16.5	1.5	21639	507	184.6	C	P	50	1.20	0	160.0	19375	2.00	1731	1.41	0.60	45.40	27.47	PC
S99 A1			150	250	942	101	514	110	53.4	3.8	32001	503	200.0	-	-	-	-	-	-	-	-	-	2.80	0.93	99.95	93.25	CC
S99 A2	x		150	250	628	101	514	110	53.0	3.8	31920	503	200.0	C	P	150	1.50	50	120.0	13333	1.50	2500	2.80	0.93	89.20	83.22	PC
S99 B1	x		150	250	603	101	377	150	36.0	2.8	28066	475	200.0	C	P	150	1.50	50	120.0	13333	1.50	2500	2.80	0.93	81.15	75.71	CC
S99 B2	x		150	250	603	101	707	80	36.6	2.8	28211	475	200.0	C	P	150	1.50	50	120.0	13333	1.50	2500	2.80	0.93	81.55	76.09	CC

R99: Ross et al. (1999); J99: Juvandes (1999); S99: Swamy and Mukhopadyaya (1999)

Table A.19. Experimental bending test database (IXX)

			Geometry of RC beam						Material properties					Plate strengthening								Adhesive		Load configuration				
Specimen (1)	Ext anch (2)	Pr (3)	b mm (4)	h mm (5)	A_s mm^2 (6)	A_s' mm^2 (7)	A_w mm^2 (8)	s_w mm (9)	f_{cm} MPa (10)	f_{ctm} MPa (11)	E_c MPa (12)	f_{ym} MPa (13)	E_s GPa (14)	M (15)	F (16)	b_L mm (17)	t_L mm (18)	a mm (19)	E_L GPa (20)	ε_{Lu} με (21)	t_a mm (22)	G_a MPa (23)	L m (24)	L_{shear} m (25)	V_{uexp} kN (26)	M_{uexp} kNm (27)	Mode (28)
S99 B3	x		150	250	603	101	377	150	36.2	2.8	28129	475	200.0	C	P	150	1.50	50	120.0	13333	1.50	2500	2.80	0.93	92.90	86.68	PC
S99 B4	x		150	250	402	101	377	150	34.1	2.6	27558	475	200.0	C	P	150	1.50	50	120.0	13333	1.50	2500	2.80	0.93	79.60	74.27	PC
S99 B5	x		150	250	402	101	707	80	34.8	2.7	27751	475	200.0	C	P	150	1.50	50	120.0	13333	1.50	2500	2.80	0.93	74.90	69.88	PC
T99 SB1			200	300	402	402	2094	75	51.2	3.7	31563	527	200.0	C	P	120	1.40	150	155.0	15484	2.10	3269	3.60	1.30	71.40	92.82	PED
T99 SB2			200	300	402	402	2094	75	52.0	3.7	31726	527	200.0	C	P	120	1.40	200	155.0	15484	2.40	3269	3.60	1.30	75.50	98.15	PED
T99 SB3			200	300	402	402	2094	75	52.0	3.7	31726	527	200.0	C	P	120	1.40	250	155.0	15484	3.00	3269	3.60	1.30	73.90	96.07	PED
T99 MB1			200	300	402	402	2094	75	56.0	4.0	32520	527	200.0	C	P	120	1.40	150	210.0	9524	2.40	3269	3.60	1.30	79.60	103.48	PED
T99 HB1			200	300	402	402	2094	75	56.0	4.0	32520	527	200.0	C	P	120	1.40	150	300.0	4667	2.10	3269	3.60	1.30	80.10	104.13	PED
T99 FB1			200	300	402	402	2094	75	51.2	3.7	31563	527	200.0	C	W	150	2.40	150	950.0	18947	0.40	3269	3.60	1.30	74.40	96.72	PED
T99 A1			200	300	603	101	565	100	50.4	3.6	31398	638	200.0	-	-	-	-	-	-.	-	-	-	0.270	1.15	83.50	48.01	CC
T99 A2			200	300	402	101	565	100	51.9	3.7	31706	638	200.0	S	-	160	5.00	100	200.0	1602	3.00	2577	0.270	1.15	94.50	108.68	O
T99 A3			200	300	402	101	565	100	32.2	2.5	27042	638	200.0	S	-	160	5.00	100	200.0	1602	3.00	2885	0.270	1.15	84.50	97.18	O
T99 A4			200	300	402	101	565	100	54.9	3.9	32305	638	200.0	S	-	160	5.00	100	200.0	1602	3.00	2115	0.270	1.15	96.50	110.98	CC
T99 C1			120	150	101	101	1131	50	47.1	3.5	30697	638	200.0	S	-	100	2.00	0	200.0	1505	1.00	2577	0.74	0.37	28.40	10.51	PC
T99 C8			120	150	101	101	1131	50	46.7	3.4	30610	638	200.0	S	-	100	3.00	0	200.0	1550	1.00	2577	0.74	0.37	26.40	9.77	PED
T99 C9			120	150	101	101	1131	50	43.3	3.2	29848	638	200.0	S	-	100	3.00	0	200.0	2075	1.00	2577	0.74	0.37	30.50	11.29	PED
T99 C10			120	150	101	101	1131	50	46.7	3.4	30610	638	200.0	S	-	65	3.00	0	200.0	2075	1.00	2577	0.74	0.37	24.00	8.88	PED
T99 C11			120	150	101	101	1131	50	43.3	3.2	29848	638	200.0	S	-	100	2.00	0	200.0	1505	1.00	1038	0.74	0.37	29.20	10.80	PC
Ta99 A00			100	150	157	57	754	75	28.6	2.3	25994	500	200.0	C	W	100	0.64	0	163.5	15000	0.42	3269	NR	0.60	27.50	16.50	P
Ta99 A15			100	150	157	57	754	75	31.4	2.5	26816	500	200.0	C	W	100	0.64	0	163.5	15000	0.42	3269	NR	0.60	24.70	14.82	P

S99: Swamy and Mukhopadyaya (1999); T99: Täljsten (1999); Ta99: Tan and Mathivoli (1999)

Table A.20. Experimental bending test database (XX)

			Geometry of RC beam						Material properties					Plate strengthening								Adhesive		Load configuration				
Specimen (1)	Ext anch (2)	Pr (3)	b mm (4)	h mm (5)	A_s mm^2 (6)	A_s' mm^2 (7)	A_w mm^2 (8)	s_w mm (9)	f_{cm} MPa (10)	f_{ctm} MPa (11)	E_c MPa (12)	f_{ym} MPa (13)	E_s GPa (14)	M (15)	F (16)	b_L mm (17)	t_L mm (18)	a mm (19)	E_L GPa (20)	$\varepsilon_{L,u}$ με (21)	t_a mm (22)	G_a MPa (23)	L m (24)	L_{shear} m (25)	V_{uexp} kN (26)	M_{uexp} kNm (27)	Mode (28)
Ta99 A25			100	150	157	57	754	75	29.7	2.3	26323	500	200.0	C	W	100	0.64	0	163.5	15000	0.42	3269	NR	0.60	24.30	14.58	P
Ta99 A40			100	150	157	57	754	75	31.4	2.5	26816	500	200.0	C	W	100	0.64	0	163.5	15000	0.42	3269	NR	0.60	24.70	14.82	P
Ta99 A60			100	150	157	57	754	75	28.6	2.3	25994	500	200.0	C	W	100	0.64	0	163.5	15000	0.42	3269	NR	0.60	26.00	15.60	P
Ta99 A75			100	150	157	57	754	75	28.5	2.2	25964	500	200.0	C	W	100	0.64	0	163.5	15000	0.42	3269	NR	0.60	21.90	13.14	P
Ta99 A90			100	150	157	57	754	75	30.1	2.4	26441	500	200.0	C	W	100	0.64	0	163.5	15000	0.42	3269	NR	0.60	19.80	11.88	P
Tu99 A0			150	300	382	382	1110	125	51.7	3.7	31665	428	207.5	-	-	-	-	-	-	-	-	-	2.13	1.06	28.81	30.68	CC
Tu99 A1			150	300	382	382	1110	125	51.7	3.7	31665	428	207.5	C	W	152	0.59	10	142.9	15000	0.42	735	2.13	1.06	18.83	20.06	PC
Tu99 A2			150	300	382	382	1110	125	51.7	3.7	31665	428	207.5	C	W	152	1.17	10	142.9	15000	0.42	735	2.13	1.06	46.19	49.19	PC
Tu99 A3			150	300	382	382	1110	125	51.7	3.7	31665	428	207.5	C	W	152	1.76	10	142.9	15000	0.42	735	2.13	1.06	46.81	49.85	PED
Tu99 A4	x		150	300	382	382	1110	125	51.7	3.7	31665	428	207.5	C	W	152	1.76	10	142.9	15000	0.42	735	2.13	1.06	53.39	56.86	PC
Tu99 A5	x		150	300	382	382	1110	125	51.7	3.7	31665	428	207.5	C	W	152	1.76	10	142.9	15000	0.42	735	2.13	1.06	57.54	61.28	PC
Tu99 A6			150	300	382	382	1110	125	51.7	3.7	31665	428	207.5	C	W	76	0.59	10	142.9	15000	0.42	735	2.13	1.06	38.36	40.86	PC
Tu99 A7			150	300	382	382	1110	125	51.7	3.7	31665	428	207.5	C	W	76	1.17	10	142.9	15000	0.42	735	2.13	1.06	46.81	49.85	PC
Tu99 A8			150	300	382	382	1110	125	51.7	3.7	31665	428	207.5	C	W	76	3.51	10	142.9	15000	0.42	735	2.13	1.06	53.39	56.86	PED
Tu99 B0			150	300	382	382	1110	125	51.7	3.7	31665	428	207.5	-	-	-	-	10	-	-	-	-	3.96	1.98	13.18	26.11	CC
Tu99 B1			150	300	382	382	1110	125	51.7	3.7	31665	428	207.5	C	W	152	0.59	10	142.9	15000	0.42	735	3.96	1.98	22.16	43.88	CC
Tu99 B2			150	300	382	382	1110	125	51.7	3.7	31665	428	207.5	C	W	76	0.59	10	142.9	15000	0.42	735	3.96	1.98	17.95	35.55	R
Tu99 B3			150	300	382	382	1110	125	51.7	3.7	31665	428	207.5	C	W	76	1.17	10	142.9	15000	0.42	735	3.96	1.98	20.37	40.34	CC
Tu99 C0			150	300	382	382	555	250	51.7	3.7	31665	428	207.5	-	-	-	-	10	-	-	-	-	2.13	1.06	33.58	35.77	CC
Tu99 C1			150	300	382	382	555	250	51.7	3.7	31665	428	207.5	C	W	152	0.59	10	142.9	15000	0.42	735	2.13	1.06	41.96	44.69	PC

Ta99: Tan and Mathivoli (1999); Tu99: Tumialan et al. (1999)

Table A.21. Experimental bending test database (XXI)

			Geometry of RC beam						Material properties					Plate strengthening								Adhesive		Load configuration				
Specimen (1)	Ext anch (2)	Pr (3)	b mm (4)	h mm (5)	A_s mm^2 (6)	A_s' mm^2 (7)	A_w mm^2 (8)	s_w mm (9)	f_{cm} MPa (10)	f_{ctm} MPa (11)	E_c MPa (12)	f_{ym} MPa (13)	E_s GPa (14)	M (15)	F (16)	b_L mm (17)	t_L mm (18)	a mm (19)	E_L GPa (20)	$\varepsilon_{L,u}$ με (21)	t_a mm (22)	G_a MPa (23)	L m (24)	L_{shear} m (25)	V_{uexp} kN (26)	M_{uexp} kNm (27)	Mode (28)
Tu99 C2			150	300	382	382	555	250	51.7	3.7	31665	428	207.5	C	W	152	1.76	10	142.9	15000	0.42	735	2.13	1.06	43.14	45.94	PED
D00 V1			120	180	101	101	565	100	36.7	2.8	28247	533	200.0	-	-	-	-	-	-	-	-	-	1.80	0.60	23.87	14.32	CC
D00 V2			120	180	101	101	565	100	36.7	2.8	28247	533	200.0	C	W	70	1.06	30	168.9	15000	0.42	1154	1.80	0.60	37.19	22.31	P
D00 V3	x		120	180	101	101	565	100	36.7	2.8	28247	533	200.0	C	W	70	1.06	30	168.9	15000	0.42	1154	1.80	0.60	39.64	23.78	R
D00 V4			120	180	101	101	565	100	36.7	2.8	28247	533	200.0	C	P	20	1.40	30	200.0	11000	2.00	2692	1.80	0.60	39.22	23.53	P
D00 V5	x		120	180	101	101	565	100	36.7	2.8	28247	533	200.0	C	P	20	1.40	30	200.0	11000	2.00	2692	1.80	0.60	30.33	18.20	P
D00 V6	x		120	180	101	101	565	100	36.7	2.8	28247	533	200.0	C	P	20	1.40	30	200.0	11000	2.00	2692	1.80	0.60	40.81	24.49	P
M00 BF2			200	450	804	0	1000	101	36.5	2.8	28196	590	200.0	C	P	100	1.20	70	159.0	20126	2.00	3269	NR	1.25	185.00	231.25	P
M00 BF3			200	450	804	0	1000	101	34.9	2.7	27778	590	200.0	C	P	100	1.20	70	159.0	20126	2.00	3269	NR	1.25	186.00	232.50	P
M00 BF4			200	450	804	0	1000	101	30.8	2.4	26644	590	200.0	C	P	100	1.20	70	159.0	20126	2.00	3269	NR	1.25	184.20	230.25	P
M00 BF5			200	450	804	0	1000	101	37.4	2.9	28426	590	200.0	C	P	100	1.20	70	159.0	20126	2.00	3269	NR	1.25	177.00	221.25	P
M00 BF8			200	450	402	0	1000	101	39.4	3.0	28924	590	200.0	C	P	100	1.20	70	159.0	20126	2.00	3269	NR	1.25	111.30	139.13	P
M00 BF9			200	450	402	0	1000	101	33.7	2.6	27455	590	200.0	C	-	100	0.22	70	233.0	15021	2.00	3269	NR	1.25	95.80	119.75	P
R00 0.2B			100	100	48	48	190	250	30.0	2.4	26411	267	200.0	-	-	-	-	25	-	-	-	-	0.90	0.30	4.37	1.31	CC
R00 0.52B			100	100	48	48	190	250	30.0	2.4	26411	267	200.0	C	P	10	1.20	25	123.0	11707	2.00	823	0.90	0.30	9.68	2.90	PC
R00 0.89B			100	100	48	48	190	250	30.0	2.4	26411	267	200.0	C	P	20	1.20	25	123.0	11707	2.00	823	0.90	0.30	11.95	3.58	PC
R00 1.42B			100	100	48	48	190	250	30.0	2.4	26411	267	200.0	C	P	40	1.20	25	123.0	11707	2.00	823	0.90	0.30	14.55	4.37	PC
A01 AF0			125	225	101	57	796	71	41.0	3.1	29310	568	185.0	-	-	-	-	-	-	-	-	-	1.50	0.50	27.50	13.75	CC
A01 AF2			125	225	101	57	796	71	41.0	3.1	29310	568	185.0	C	W	75	1.17	200	170.2	15000	0.42	2769	1.50	0.50	41.50	20.75	PES
A01 AF2-1			125	225	101	57	796	71	41.0	3.1	29310	568	185.0	C	W	75	1.17	150	170.2	15000	0.42	2769	1.50	0.50	42.85	21.43	PES

Tu99: Tumialan et al. (1999); D00: Dias et al. (2000a); M00: Matthys (2000) (referenced by Colotti et al., 2004); R00: Ramana et al. (2000); A01: Ahmed et al. (2001)

Table A.22. Experimental bending test database (XXII)

			Geometry of RC beam						Material properties					Plate strengthening								Adhesive		Load configuration				
Specimen (1)	Ext anch (2)	Pr (3)	b mm (4)	h mm (5)	A_s mm^2 (6)	A_s' mm^2 (7)	A_w mm^2 (8)	s_w mm (9)	f_{cm} MPa (10)	f_{ctm} MPa (11)	E_c MPa (12)	f_{ym} MPa (13)	E_s GPa (14)	M (15)	F (16)	b_L mm (17)	t_L mm (18)	a mm (19)	E_L GPa (20)	$\varepsilon_{L,u}$ με (21)	t_a mm (22)	G_a MPa (23)	L m (24)	L_{shear} m (25)	V_{uexp} kN (26)	M_{uexp} kNm (27)	Mode (28)
A01 AF3			125	225	101	57	796	71	41.0	3.1	29310	568	185.0	C	W	75	1.17	100	170.2	15000	0.42	2769	1.50	0.50	48.25	24.13	PES
A01 AF4			125	225	101	57	796	71	41.0	3.1	29310	568	185.0	C	W	75	1.17	50	170.2	15000	0.42	2769	1.50	0.50	55.50	27.75	P
A01 CF3-0			125	225	151	57	796	71	43.0	3.2	29779	568	185.0	-	-	-	-	-	-	-	-	-	1.50	0.50	37.50	18.75	CC
A01 DF1			125	225	151	57	565	100	42.0	3.1	29546	568	185.0	C	W	75	0.59	50	170.2	15000	0.42	2769	1.50	0.50	59.00	29.50	R
A01 DF2			125	225	151	57	565	100	42.0	3.1	29546	568	185.0	C	W	75	1.17	50	170.2	15000	0.42	2769	1.50	0.50	60.00	30.00	P
A01 DF4			125	225	151	57	565	100	40.5	3.1	29190	568	185.0	C	W	75	2.35	50	170.2	15000	0.42	2769	1.50	0.50	62.50	31.25	PES
A01 DF.3			125	225	151	57	565	100	40.5	3.1	29190	568	185.0	C	W	75	0.92	50	170.2	15000	0.42	2769	NR	0.50	60.00	30.00	PES
A01 BF.2.1			125	225	101	57	565	100	41.0	3.1	29310	568	185.0	C	W	75	1.17	50	170.2	15000	0.42	2769	NR	0.50	45.00	22.50	PES
A01 BF.3.1			125	225	101	57	565	100	41.0	3.1	29310	568	185.0	C	W	75	1.17	50	170.2	15000	0.42	2769	NR	0.50	52.00	26.00	P
A01 CF.2.1			125	225	101	57	565	100	43.0	3.2	29779	568	185.0	C	W	75	1.17	100	170.2	15000	0.42	2769	NR	0.50	52.40	26.20	P
A01 CF.3.1			125	225	151	57	565	100	43.0	3.2	29779	568	185.0	C	W	75	1.17	100	170.2	15000	0.42	2769	NR	0.50	59.00	29.50	P
A01 CF.4.1			125	225	201	57	565	100	43.0	3.2	29779	568	185.0	C	W	75	1.17	100	170.2	15000	0.42	2769	NR	0.50	70.00	35.00	P
A01 EF.1.1			125	225	151	57	565	100	46.0	3.4	30456	568	185.0	C	W	75	1.17	50	170.2	15000	0.42	2769	NR	0.50	65.90	32.95	P
A01 EF.3.1			125	225	151	57	565	100	38.0	2.9	28577	568	185.0	C	W	75	1.17	50	170.2	15000	0.42	2769	NR	0.50	59.50	29.75	P
A01 EF.4.1			125	225	151	57	565	100	33.0	2.6	27264	568	185.0	C	W	75	1.17	50	170.2	15000	0.42	2769	NR	0.50	60.30	30.15	P
A01 FF.2.2			125	225	151	57	565	100	39.5	3.0	28948	568	185.0	C	W	75	1.17	70	170.2	15000	0.42	2769	NR	0.70	47.80	33.46	R
A01 FF.2.3			125	225	151	57	565	100	39.5	3.0	28948	568	185.0	C	W	75	1.17	70	170.2	15000	0.42	2769	NR	0.70	53.00	37.10	P
A01 FF.3.2			125	225	151	57	565	100	38.5	2.9	28702	568	185.0	C	W	75	0.92	90	170.2	15000	0.42	2769	NR	0.90	35.60	32.04	R
A01 FF.3.4			125	225	151	57	565	100	38.5	2.9	28702	568	185.0	C	W	75	1.17	90	170.2	15000	0.42	2769	NR	0.90	45.00	40.50	R
Al01 F0			150	200	236	28	1005	100	37.5	2.9	28451	415	200.0	-	-	-	-	-	-	-	-	-	20.5	0.92	17.66	16.33	CC

A01: Ahmed et al. (2001); Al01: Almusallam and Salloum (2001)

Table A.23. Experimental bending test database (XXIII)

			Geometry of RC beam						Material properties					Plate strengthening								Adhesive		Load configuration				
Specimen (1)	Ext anch (2)	Pr (3)	b mm (4)	h mm (5)	A_s mm^2 (6)	A_s' mm^2 (7)	A_w mm^2 (8)	s_w mm (9)	f_{cm} MPa (10)	f_{ctm} MPa (11)	E_c MPa (12)	f_{ym} MPa (13)	E_s GPa (14)	M (15)	F (16)	b_L mm (17)	t_L mm (18)	a mm (19)	E_L GPa (20)	$\varepsilon_{L,u}$ με (21)	t_a mm (22)	G_a MPa (23)	L m (24)	L_{shear} m (25)	V_{uexp} kN (26)	M_{uexp} kNm (27)	Mode (28)
Al01 FG1			150	200	236	28	1005	100	37.5	2.9	28451	415	200.0	C	W	150	1.30	5	27.6	20015	0.42	3269	20.5	0.92	35.20	32.56	CC
Al01 FG2			150	200	236	28	1005	100	37.5	2.9	28451	415	200.0	C	W	150	3.02	5	27.6	20015	0.42	3269	20.5	0.92	41.20	38.11	CC
Al01 FG4			150	200	236	28	1005	100	37.5	2.9	28451	415	200.0	C	W	150	6.46	5	27.6	20015	0.42	3269	20.5	0.92	52.95	48.98	CC
Al01 FC1			150	200	236	28	1005	100	37.5	2.9	28451	415	200.0	C	W	150	1.00	5	68.9	14997	0.42	3269	20.5	0.92	40.95	37.88	CC
Al01 FC2			150	200	236	28	1005	100	37.5	2.9	28451	415	200.0	C	W	150	2.42	5	68.9	14997	0.42	3269	20.5	0.92	51.55	47.68	CC
B01 A0			125	225	101	57	565	100	39.5	3.0	28948	500	200.0	-	-	-	-	-	-	-	-	-	1.50	0.50	27.50	13.75	CC
B01 A1			125	225	101	57	565	100	39.5	3.0	28948	500	200.0	C	W	75	0.73	50	168.7	15000	1.00	2769	1.50	0.50	55.50	27.75	P
B01 B0			125	225	151	57	565	100	39.5	3.0	28948	500	200.0	-	-	-	-	-	-	-	-	-	1.50	0.50	40.00	20.00	CC
B01 B1			125	225	151	57	565	100	39.5	3.0	28948	500	200.0	C	W	75	0.73	50	168.7	15000	1.00	2769	1.50	0.50	65.85	32.93	P
B01 C0			125	225	151	57	565	100	39.5	3.0	28948	500	200.0	-	-	-	-	-	-	-	-	-	1.50	0.50	37.50	18.75	CC
B01 C1			125	225	151	57	565	100	39.5	3.0	28948	500	200.0	C	W	75	0.73	50	168.7	15000	1.00	2769	1.50	0.50	60.25	30.13	P
B01 C2			125	225	151	57	565	100	39.5	3.0	28948	500	200.0	C	W	75	0.73	100	168.7	15000	1.00	2769	1.50	0.50	59.05	29.53	P
B01 D0			125	225	151	57	565	100	39.5	3.0	28948	500	200.0	-	-	-	-	-	-	-	-	-	1.50	0.50	37.50	18.75	CC
B01 D1			125	225	151	57	565	100	39.5	3.0	28948	500	200.0	C	W	75	0.73	50	168.7	15000	1.00	2769	1.50	0.50	59.45	29.73	P
B01 E0			125	225	151	57	565	100	39.5	3.0	28948	500	200.0	-	-	-	-	-	-	-	-	-	1.50	0.50	38.25	19.13	CC
B01 E1			125	225	151	57	565	100	39.5	3.0	28948	500	200.0	C	W	75	0.73	50	168.7	15000	1.00	2769	1.50	0.50	60.30	30.15	P
B01 F0			125	225	129	57	565	100	39.5	3.0	28948	500	200.0	-	-	-	-	-	-	-	-	-	1.50	0.50	32.45	16.23	CC
B01 F1			125	225	129	57	565	100	39.5	3.0	28948	500	200.0	C	W	75	0.73	100	168.7	15000	1.00	2769	1.50	0.50	52.40	26.20	P
B01 G0			125	225	207	57	565	100	39.5	3.0	28948	500	200.0	-	-	-	-	-	-	-	-	-	1.50	0.50	47.75	23.88	CC
B01 G1			125	225	207	57	565	100	39.5	3.0	28948	500	200.0	C	W	75	0.73	100	168.7	15000	1.00	2769	1.50	0.50	70.05	35.03	P
Almusallam and Salloum (2001); B01: Brosens. (2001); C01: Ceroni and Prota (2001)																												

Table A.24. Experimental bending test database (XXIV)

			Geometry of RC beam						Material properties					Plate strengthening								Adhesive		Load configuration				
Specimen (1)	Ext anch (2)	Pr (3)	b mm (4)	h mm (5)	A_s mm^2 (6)	A_s' mm^2 (7)	A_w mm^2 (8)	s_w mm (9)	f_{cm} MPa (10)	f_{ctm} MPa (11)	E_c MPa (12)	f_{ym} MPa (13)	E_s GPa (14)	M (15)	F (16)	b_L mm (17)	t_L mm (18)	a mm (19)	E_L GPa (20)	$\varepsilon_{L,u}$ με (21)	t_a mm (22)	G_a MPa (23)	L m (24)	L_{shear} m (25)	V_{uexp} kN (26)	M_{uexp} kNm (27)	Mode (28)
C01 A1			150	100	101	101	377	150	29.0	2.3	26115	590	200.0	-	-	-	-	-	-	-	-	-	1.80	0.75	4.80	3.60	CC
C01 B1			150	100	157	157	377	150	29.0	2.3	26115	550	200.0	-	-	-	-	-	-	-	-	-	1.80	0.75	10.15	7.61	CC
C01 B2			150	100	157	157	377	150	29.0	2.3	26115	550	200.0	C	W	110	0.59	200	163.5	15000	0.42	3269	1.80	0.75	12.90	9.68	CC
C01 B3			150	100	157	157	377	150	29.0	2.3	26115	550	200.0	C	W	110	0.59	400	163.5	15000	0.42	3269	1.80	0.75	12.90	9.68	CC
C01 C1			100	150	101	101	377	150	29.0	2.3	26115	550	200.0	-	-	-	-	-	-	-	-	-	1.80	0.75	5.90	4.43	O
C01 C2			100	150	101	101	377	150	29.0	2.3	26115	590	200.0	-	-	-	-	-	-	-	-	-	1.80	0.75	5.90	4.43	O
C01 C3			100	150	101	101	377	150	29.0	2.3	26115	590	200.0	C	W	80	0.59	400	163.5	15000	0.42	3269	1.80	0.75	8.95	6.71	PED
C01 C4			100	150	101	101	377	150	29.0	2.3	26115	590	200.0	C	W	80	0.59	500	163.5	15000	0.42	3269	1.80	0.75	8.05	6.04	PED
C01 D1			100	150	157	157	377	150	29.0	2.3	26115	550	200.0	-	-	-	-	-	-	-	-	-	1.40	0.55	14.80	8.14	O
C01 D2			100	150	157	157	377	150	29.0	2.3	26115	550	200.0	C	W	80	0.59	200	163.5	15000	0.42	3269	1.40	0.55	21.05	11.58	R
C01 D3			100	150	157	157	377	150	29.0	2.3	26115	550	200.0	C	W	80	0.59	200	163.5	15000	0.42	3269	1.40	0.55	20.05	11.03	P
F01 F1			155	240	339	226	452	125	80.0	5.2	36625	532	204.0	-	-	-	-	-	-	-	-	-	2.80	1.10	34.15	37.57	CC
F01 F2			155	240	339	226	449	126	80.0	5.2	36625	532	204.0	-	-	-	-	-	-	-	-	-	2.80	1.10	33.95	37.35	CC
F01 F3			155	240	339	226	445	127	80.0	5.2	36625	532	204.0	C	P	120	1.20	0	155.0	15484	2.00	3269	2.80	1.10	55.45	61.00	PC
F01 F4			155	240	339	226	442	128	80.0	5.2	36625	532	204.0	C	P	120	1.20	0	155.0	15484	2.00	3269	2.80	1.10	59.25	65.18	PC
F01 F5			155	240	339	226	438	129	80.0	5.2	36625	532	204.0	C	P	120	1.20	385	155.0	15484	2.00	3269	2.80	1.10	50.00	55.00	PED
F01 F6			155	240	339	226	435	130	80.0	5.2	36625	532	204.0	C	P	120	1.20	385	155.0	15484	2.00	3269	2.80	1.10	51.50	56.65	PED
F01 F7			155	240	339	226	432	131	80.0	5.2	36625	532	204.0	C	P	120	1.20	462	155.0	15484	2.00	3269	2.80	1.10	48.75	53.63	PED
F01 F8			155	240	339	226	428	132	80.0	5.2	36625	532	204.0	C	P	120	1.20	462	155.0	15484	2.00	3269	2.80	1.10	32.00	35.20	PED
F01 F9			155	240	339	226	425	133	80.0	5.2	36625	532	204.0	C	P	120	1.20	550	155.0	15484	2.00	3269	2.80	1.10	31.00	34.10	PED

C01: Ceroni and Prota (2001); F01: Fanning and Kelly (2001)

Table A.25. Experimental bending test database (XXV)

			Geometry of RC beam						Material properties					Plate strengthening								Adhesive		Load configuration				
Specimen (1)	Ext anch (2)	Pr (3)	b mm (4)	h mm (5)	A_s mm^2 (6)	A_s' mm^2 (7)	A_w mm^2 (8)	s_w mm (9)	f_{cm} MPa (10)	f_{ctm} MPa (11)	E_c MPa (12)	f_{ym} MPa (13)	E_s GPa (14)	M (15)	F (16)	b_L mm (17)	t_L mm (18)	a mm (19)	E_L GPa (20)	ε_{Lu} με (21)	t_a mm (22)	G_a MPa (23)	L m (24)	L_{shear} m (25)	V_{uexp} kN (26)	M_{uexp} kNm (27)	Mode (28)
F01 F10			155	240	339	226	422	134	80.0	5.2	36625	532	204.0	C	P	120	1.20	550	155.0	15484	2.00	3269	2.80	1.10	41.00	45.10	PED
K01 A1-R7-1			150	250	253	253	1418	100	28.2	2.2	25872	500	200.0	A	W	130	0.29	100	126.5	19600	0.42	3269	3.40	1.45	NR	NR	P
K01 A1-R5-1			150	250	253	253	1418	100	28.2	2.2	25872	500	200.0	A	W	130	0.29	100	126.5	19600	0.42	3269	2.60	1.05	NR	NR	P
K01 A1-R3-1			150	250	253	253	1418	100	28.2	2.2	25872	500	200.0	A	W	130	0.29	100	126.5	19600	0.42	3269	1.80	0.65	NR	NR	P
K01 A2-R7-1			150	250	397	397	1418	100	28.2	2.2	25872	500	200.0	A	W	130	0.29	100	126.5	19600	0.42	3269	3.40	1.45	NR	NR	CC
K01 A2-R6-1			150	250	397	397	1418	100	28.2	2.2	25872	500	200.0	A	W	130	0.29	100	126.5	19600	0.42	3269	3.02	1.26	NR	NR	CC
K01 A2-R5-1			150	250	397	397	1418	100	28.2	2.2	25872	500	200.0	A	W	130	0.29	100	126.5	19600	0.42	3269	2.60	1.05	NR	NR	CC
K01 A2-R4-1			150	250	397	397	1418	100	28.2	2.2	25872	500	200.0	A	W	130	0.29	100	126.5	19600	0.42	3269	2.18	0.84	NR	NR	CC
K01 A2-R3-1			150	250	397	397	1418	100	28.2	2.2	25872	500	200.0	A	W	130	0.29	100	126.5	19600	0.42	3269	1.80	0.65	NR	NR	CC
K01 A2-R7-2			150	250	397	397	1418	100	28.2	2.2	25872	500	200.0	A	W	130	0.57	100	126.5	19600	0.42	3269	3.40	1.45	NR	NR	P
K01 A2-R6-2			150	250	397	397	1418	100	28.2	2.2	25872	500	200.0	A	W	130	0.57	100	126.5	19600	0.42	3269	3.02	1.26	NR	NR	P
K01 A2-R5-2			150	250	397	397	1418	100	28.2	2.2	25872	500	200.0	A	W	130	0.57	100	126.5	19600	0.42	3269	2.60	1.05	NR	NR	P
K01 A2-R4-2			150	250	397	397	1418	100	28.2	2.2	25872	500	200.0	A	W	130	0.57	100	126.5	19600	0.42	3269	2.18	0.84	NR	NR	P
K01 A2-R3-2			150	250	397	397	1418	100	28.2	2.2	25872	500	200.0	A	W	130	0.57	100	126.5	19600	0.42	3269	1.80	0.65	NR	NR	P
K01 A3-R7-1			150	250	573	573	1418	100	28.2	2.2	25872	500	200.0	A	W	130	0.29	100	126.5	19600	0.42	3269	3.40	1.45	NR	NR	CC
K01 A3-R5-1			150	250	573	573	1418	100	28.2	2.2	25872	500	200.0	A	W	130	0.29	100	126.5	19600	0.42	3269	2.60	1.05	NR	NR	CC
K01 A3-R3-1			150	250	573	573	1418	100	28.2	3.3	25872	500	200.0	A	W	130	0.29	100	126.5	19600	0.42	3269	1.80	0.65	NR	NR	CC
L01 C-21			153	153	253	143	1092	58	20.9	1.7	23429	414	200.0	-	-	-	-	-	-	-	-	-	1.07	0.43	23.61	10.20	CC
L01 F21S102-1			153	153	253	143	1092	58	20.9	1.7	23429	414	200.0	G	W	102	3.20	51	13.8	16790	2.00	823	1.07	0.43	27.55	11.90	CC
L01 F21E102-1			153	153	253	143	1092	58	20.9	1.7	23429	414	200.0	G	W	102	3.20	51	17.0	20647	2.00	823	1.07	0.43	28.70	12.40	CC

F01: Fanning and Kelly (2001); K01; Kishi et al. (2001); L01: Lamanna et al. (2001)

Table A.26. Experimental bending test database (XXVI)

			Geometry of RC beam						Material properties					Plate strengthening								Adhesive		Load configuration				
Specimen (1)	Ext anch (2)	Pr (3)	b mm (4)	h mm (5)	A_s mm^2 (6)	A_s' mm^2 (7)	A_w mm^2 (8)	s_w mm (9)	f_{cm} MPa (10)	f_{ctm} MPa (11)	E_c MPa (12)	f_{ym} MPa (13)	E_s GPa (14)	M (15)	F (16)	b_L mm (17)	t_L mm (18)	a mm (19)	E_L GPa (20)	ε_{Lu} με (21)	t_a mm (22)	G_a MPa (23)	L m (24)	L_{shear} m (25)	V_{uexp} kN (26)	M_{uexp} kNm (27)	Mode (28)
L01 F21D102-1			153	153	253	143	1092	58	20.9	1.7	23429	414	200.0	G	W	102	6.40	51	15.5	13194	2.00	823	1.07	0.43	28.01	12.10	CC
L01 F21H102-1			153	153	253	143	1092	58	20.9	1.7	23429	414	200.0	G	W	102	3.20	51	27.3	20538	2.00	823	1.07	0.43	30.79	13.30	CC
L01 F21S102-2			153	153	253	143	1092	58	20.9	1.7	23429	414	200.0	G	W	102	3.20	51	13.8	16790	2.00	823	1.07	0.43	30.79	13.30	CC
L01 F21S102-2R			153	153	253	143	1092	58	20.9	1.7	23429	414	200.0	G	W	102	3.20	51	13.8	16790	2.00	823	1.07	0.43	29.40	12.70	CC
L01 F21S511			153	153	253	143	1092	58	20.9	1.7	23429	414	200.0	G	W	51	3.20	51	13.8	16790	2.00	823	1.07	0.43	27.55	11.90	CC
L01 B21S102			153	153	253	143	1092	58	20.9	1.7	23429	414	200.0	G	W	102	3.20	51	13.8	16790	2.00	823	1.07	0.43	32.41	14.00	PED
L01 B21S51			153	153	253	143	1092	58	20.9	1.7	23429	414	200.0	G	W	51	3.20	51	13.8	16790	2.00	823	1.07	0.43	29.86	12.90	PED
L01 C42			153	153	253	143	1092	58	42.5	3.2	29658	414	200.0	-	-	-	-	-	-	-	-	-	1.07	0.43	27.78	12.00	CC
L01 F42S102L			153	153	253	143	1092	58	42.5	3.2	29658	414	200.0	G	W	102	3.20	51	13.8	16790	2.00	823	1.07	0.43	27.78	12.00	CC
L01 F42S1021			153	153	253	143	1092	58	42.5	3.2	29658	414	200.0	G	W	102	3.20	51	13.8	16790	2.00	823	1.07	0.43	31.02	13.40	CC
L01 F42S1021R			153	153	253	143	1092	58	42.5	3.2	29658	414	200.0	G	W	102	3.20	51	13.8	16790	2.00	823	1.07	0.43	33.33	14.40	CC
L01 F42S1021RR			153	153	253	143	1092	58	42.5	3.2	29658	414	200.0	G	W	102	3.20	51	13.8	16790	2.00	823	1.07	0.43	30.56	13.20	CC
L01 B42S102			153	153	253	143	1092	58	42.5	3.2	29658	414	200.0	G	W	102	3.20	51	13.8	16790	2.00	823	1.07	0.43	43.98	19.00	PC
Li01 A			130	200	101	101	377	150	37.0	2.8	28324	550	200.0	C	W	120	1.30	30	120.0	8000	0.42	1154	1.10	0.40	45.50	18.20	P
Li01 B	x		130	200	101	101	377	150	37.0	2.8	28324	550	200.0	C	W	120	1.30	30	120.0	8000	0.42	1154	1.10	0.40	46.50	18.60	P
Li01 C	x		130	200	101	101	377	150	37.0	2.8	28324	550	200.0	C	W	120	1.30	30	120.0	8000	0.42	1154	1.10	0.40	46.50	18.60	P
Li01 D	x		130	200	101	101	377	150	37.0	2.8	28324	550	200.0	C	W	120	1.30	30	120.0	8000	0.42	1154	1.10	0.40	47.50	19.00	P
Li01 E	x		130	200	101	101	377	150	37.0	2.8	28324	550	200.0	C	W	120	1.30	30	120.0	8000	0.42	1154	1.10	0.40	51.50	20.60	S
M01 B1			115	150	236	157	942	60	30.3	2.4	26499	534	183.6	-	-	-	-	-	-	-	-	-	1.35	0.50	29.50	14.75	CC
M01 B2			115	150	236	157	942	60	30.3	2.4	26499	534	183.6	C	W	115	0.11	10	161.4	15000	0.64	565	1.35	0.50	36.00	18.00	R

L01: Lamanna et al. (2001); Li01: Li (2001); M01: Maalej and Bian (2001)

Table A.27. Experimental bending test database (XXVII)

			Geometry of RC beam						Material properties					Plate strengthening								Adhesive		Load configuration				
Specimen (1)	Ext anch (2)	Pr (3)	b mm (4)	h mm (5)	A_s mm^2 (6)	A_s' mm^2 (7)	A_w mm^2 (8)	s_w mm (9)	f_{cm} MPa (10)	f_{ctm} MPa (11)	E_c MPa (12)	f_{ym} MPa (13)	E_s GPa (14)	M (15)	F (16)	b_L mm (17)	t_L mm (18)	a mm (19)	E_L GPa (20)	$\varepsilon_{L,u}$ με (21)	t_a mm (22)	G_a MPa (23)	L m (24)	L_{shear} m (25)	V_{uexp} kN (26)	M_{uexp} kNm (27)	Mode (28)
M01 B3			115	150	236	157	942	60	30.3	2.4	26499	534	183.6	C	W	115	0.22	10	161.4	15000	0.64	565	1.35	0.50	43.00	21.50	PED
M01 B4			115	150	236	157	942	60	30.3	2.4	26499	534	183.6	C	W	115	0.33	10	161.4	15000	0.64	565	1.35	0.50	41.00	20.50	PED
M01 B5			115	150	236	157	942	60	30.3	2.4	26499	534	183.6	C	W	115	0.44	10	161.4	15000	0.64	565	1.35	0.50	39.50	19.75	PED
N01 CB1			120	150	236	57	1131	50	32.1	2.5	27014	384	200.0	-	-	-	-	-	-	-	-	-	1.33	0.44	21.05	9.26	CC
N01 A950			120	150	236	57	1131	50	32.1	2.5	27014	384	200.0	C	P	80	1.20	190	181.0	1685	1.50	4923	1.33	0.44	28.10	12.36	PED
N01 A1100			120	150	236	57	1131	50	32.1	2.5	27014	384	200.0	C	P	80	1.20	115	181.0	1848	1.50	4923	1.33	0.44	28.65	12.61	PED
N01 A1150			120	150	236	57	1131	50	32.1	2.5	27014	384	200.0	C	P	80	1.20	90	181.0	1622	1.50	4923	1.33	0.44	29.45	12.96	PED
N01 A1500			120	150	236	57	1131	50	44.6	3.3	30144	384	200.0	C	P	80	1.20	0	181.0	1622	1.50	4923	1.33	0.44	59.00	25.96	CC
N01 B1			120	150	57	57	1131	50	44.6	3.3	30144	400	200.0	C	P	80	1.20	115	181.0	2400	1.50	4923	1.33	0.44	24.60	10.82	PES
N01 B2			120	150	628	57	1131	50	44.6	3.3	30144	466	200.0	C	P	80	1.20	115	181.0	2250	1.50	4923	1.33	0.44	65.05	28.62	PED
N01 C5			120	150	236	57	1131	50	25.1	2.0	24887	384	200.0	C	P	80	1.20	115	181.0	2116	1.50	4923	1.33	0.44	35.50	15.62	PED
N01 C10			120	150	236	57	1131	50	25.1	2.0	24887	384	200.0	C	P	80	1.20	115	181.0	1750	1.50	4923	1.33	0.44	34.00	14.96	PED
N01 C20			120	150	236	57	1131	50	25.1	2.0	24887	384	200.0	C	P	80	1.20	115	181.0	1755	1.50	4923	1.33	0.44	31.50	13.86	PED
O01 1E			300	200	402	101	1508	150	35.2	2.7	27857	580	210.0	-	-	-	-	-	-	-	-	-	2.00	1.00	41.00	41.00	CC
O01 1D		x	300	200	402	101	1508	150	35.2	2.7	27857	580	210.0	C	P	100	1.40	250	150.0	16000	3.00	3692	2.00	1.00	40.00	40.00	PED
O01 1D2		x	300	200	402	101	1508	150	35.2	2.7	27857	580	210.0	C	P	50	1.40	100	150.0	16000	3.00	3692	2.00	1.00	55.50	55.50	PC
O01 1C		x	300	200	402	101	1508	150	35.2	2.7	27857	580	210.0	C	P	100	1.40	100	150.0	16000	3.00	3692	2.00	1.00	52.00	52.00	PC
O01 1C2		x	300	200	402	101	1508	150	35.2	2.7	27857	580	210.0	C	P	100	1.40	100	150.0	16000	3.00	3692	2.00	1.00	60.50	60.50	PC
O01 1B		x	300	200	402	101	1508	150	35.2	2.7	27857	580	210.0	C	P	100	1.40	100	150.0	16000	3.00	3692	2.00	1.00	50.20	50.20	PC
O01 1B2		x	300	200	402	101	1508	150	35.2	2.7	27857	580	210.0	C	P	10	1.40	100	150.0	16000	2.00	3692	2.00	1.00	45.85	45.85	PC

M01: Maalej and Bian. (2001); N01: Nguyen et al. (2001); O01:Oller (2001, 2002, 2004)

Table A.28. Experimental bending test database (XXVIII)

			Geometry of RC beam						Material properties					Plate strengthening								Adhesive		Load configuration				
Specimen (1)	Ext anch (2)	Pr (3)	b mm (4)	h mm (5)	A_s mm^2 (6)	A_s' mm^2 (7)	A_w mm^2 (8)	s_w mm (9)	f_{cm} MPa (10)	f_{ctm} MPa (11)	E_c MPa (12)	f_{ym} MPa (13)	E_s GPa (14)	M (15)	F (16)	b_L mm (17)	t_L mm (18)	a mm (19)	E_L GPa (20)	$\varepsilon_{L,u}$ με (21)	t_a mm (22)	G_a MPa (23)	L m (24)	L_{shear} m (25)	V_{uexp} kN (26)	M_{uexp} kNm (27)	Mode (28)
O01 1A			300	200	402	101	1508	150	35.2	2.7	27857	580	210.0	C	P	100	1.40	100	150.0	16000	3.00	3692	2.00	1.00	54.50	54.50	PC
O01 2E			300	200	628	101	2262	100	35.2	2.7	27857	580	210.0	-	-	-	-	-	-	-	-	-	2.00	1.00	56.85	56.85	CC
O01 2D		x	300	200	628	101	2262	100	35.2	2.7	27857	580	210.0	C	P	100	1.40	100	150.0	16000	3.00	3692	2.00	1.00	64.00	64.00	PC
O01 2D2		x	300	200	628	101	2262	100	35.2	2.7	27857	580	210.0	C	P	100	1.40	100	150.0	16000	3.00	3692	2.00	1.00	81.50	81.50	PC
O01 2C		x	300	200	628	101	2262	100	35.2	2.7	27857	580	210.0	C	P	50	1.40	100	150.0	16000	3.00	3692	2.00	1.00	71.40	71.40	PC
O01 2B	x	x	300	200	628	101	2262	100	35.2	2.7	27857	580	210.0	C	P	50	1.40	100	150.0	16000	3.00	3692	2.00	1.00	76.50	76.50	PC
O01 2A	x	x	300	200	628	101	2262	100	35.2	2.7	27857	580	210.0	C	P	100	1.40	100	150.0	16000	3.00	3692	2.00	0.100	77.30	77.30	PC
P01 A			120	180	157	101	565	100	58.0	4.1	32902	400	200.0	C	P	50	1.20	25	155.0	15484	2.00	4923	2.85	0.95	61.70	58.62	PED
P01 C	x		120	180	157	101	113	500	58.0	4.1	32902	400	200.0	C	P	50	1.20	25	155.0	15484	2.00	4923	2.85	0.95	62.00	58.90	PED
R01 A1			200	150	157	101	377	150	49.2	3.6	31146	575	210.0	-	-	-	-	-	-	-	-	-	2.10	0.75	13.10	9.83	CC
R01 A2			200	150	157	101	377	150	49.2	3.6	31146	575	210.0	-	-	-	-	-	-	-	-	-	2.10	0.75	13.10	9.83	CC
R01 A3			200	150	157	101	377	150	49.2	3.6	31146	575	210.0	-	-	-	-	-	-	-	-	-	2.10	0.75	13.30	9.98	CC
R01 A4			200	150	157	101	377	150	49.2	3.6	31146	575	210.0	C	W	150	0.80	85	127.0	12063	2.00	2692	2.10	0.75	30.95	23.21	P
R01 A5			200	150	157	101	377	150	49.2	3.6	31146	575	210.0	C	W	150	0.80	85	127.0	12063	2.00	2692	2.10	0.75	31.60	23.70	P
R01 A6			200	150	157	101	377	150	49.2	3.6	31146	575	210.0	C	W	150	1.20	85	127.0	12063	2.00	2692	2.10	0.75	29.70	22.28	P
R01 A7			200	150	157	101	377	150	49.2	3.6	31146	575	210.0	C	W	150	1.20	85	127.0	12063	2.00	2692	2.10	0.75	35.30	26.48	P
R01 A8		x	200	150	157	101	377	150	49.2	3.6	31146	575	210.0	C	W	150	0.80	85	127.0	12063	2.00	2692	2.10	0.75	32.60	24.45	P
R01 A9		x	200	150	157	101	377	150	49.2	3.6	31146	575	210.0	C	W	150	0.80	85	127.0	12063	2.00	2692	2..10	0.75	31.95	23.96	P
R01 A10			200	150	157	101	377	150	49.2	3.6	31146	575	210.0	C	W	150	0.80	85	127.0	12063	2.00	2692	2.10	0.75	33.75	25.31	P
R01 A11			200	150	157	101	377	150	49.2	3.6	31146	575	210.0	C	W	150	0.80	85	127.0	12063	2.00	2692	2.10	0.75	34.70	26.03	P

O01: Oller (2001, 2002, 2004); P01: Podolka (2001); R01: Rahimi and Hutchinson (2001)

Table A.29. Experimental bending test database (IXXX)

			Geometry of RC beam						Material properties					Plate strengthening								Adhesive		Load configuration				
Specimen (1)	Ext anch (2)	Pr (3)	b mm (4)	h mm (5)	A_s mm^2 (6)	A_s' mm^2 (7)	A_w mm^2 (8)	s_w mm (9)	f_{cm} MPa (10)	f_{ctm} MPa (11)	E_c MPa (12)	f_{ym} MPa (13)	E_s GPa (14)	M (15)	F (16)	b_L mm (17)	t_L mm (18)	a mm (19)	E_L GPa (20)	$\varepsilon_{L,u}$ με (21)	t_a mm (22)	G_a MPa (23)	L m (24)	L_{shear} m (25)	V_{uexp} kN (26)	M_{uexp} kNm (27)	Mode (28)
R01 B1			200	150	157	101	754	75	49.2	3.6	31146	575	210.0	-	-	-	-	-	-	-	-	-	2.10	0.75	14.60	10.95	CC
R01 B2			200	150	157	101	754	75	49.2	3.6	31146	575	210.0	-	-	-	-	-	-	-	-	-	2.10	0.75	14.20	10.65	CC
R01 B3			200	150	157	101	754	75	49.2	3.6	31146	575	210.0	C	W	150	0.40	85	127.0	12063	2.00	2692	2.10	0.75	27.60	20.70	P
R01 B4			200	150	157	101	754	75	49.2	3.6	31146	575	210.0	C	W	150	0.40	85	127.0	12063	2.00	2692	2.10	0.75	26.25	19.69	P
R01 B5			200	150	157	101	754	75	49.2	3.6	31146	575	210.0	C	W	150	1.20	85	127.0	12063	2.00	2692	2.10	0.75	34.85	26.14	P
R01 B6			200	150	157	101	754	75	49.2	3.6	31146	575	210.0	C	W	150	1.20	85	127.0	12063	2.00	2692	2.10	0.75	34.80	26.10	P
R01 B7			200	150	157	101	754	75	49.2	3.6	31146	575	210.0	G	W	150	1.80	85	36.0	29833	2.00	2692	2.10	0.75	29.55	22.16	P
R01 B8			200	150	157	101	754	75	49.2	3.6	31146	575	210.0	G	W	150	1.80	85	36.0	29833	2.00	2692	2.10	0.75	30.80	23.10	P
R01 B9			200	150	157	101	754	75	49.2	3.6	31146	575	210.0	S	-	150	3.00	85	210.0	200000	2.00	2692	2.10	0.75	31.35	23.51	CC
R01 B10			200	150	157	101	754	75	49.2	3.6	31146	575	210.0	S	-	150	3.00	85	210.0	200000	2.00	2692	2.10	0.75	31.10	23.33	CC
R01 C1			200	150	402	101	754	75	49.2	3.6	31146	575	210.0	-	-	-	-	-	-	-	-	-	2.10	0.75	29.25	21.94	CC
R01 C2			200	150	402	101	754	75	49.2	3.6	31146	575	210.0	-	-	-	-	-	-	-	-	-	2.10	0.75	28.15	21.11	CC
R01 C3			200	150	402	101	754	75	49.2	3.6	31146	575	210.0	C	W	150	0.40	85	127.0	12063	2.00	2692	2.10	0.75	37.45	28.09	P
R01 C4			200	150	402	101	754	75	49.2	3.6	31146	575	210.0	C	W	150	0.40	85	127.0	12063	2.00	2692	2.10	0.75	38.60	28.95	P
R01 C5			200	150	402	101	754	75	49.2	3.6	31146	575	210.0	C	W	150	1.20	85	127.0	12063	2.00	2692	2.10	0.75	51.55	38.66	P
R01 C6			200	150	402	101	754	75	49.2	3.6	31146	575	210.0	C	W	150	1.20	85	127.0	12063	2.00	2692	2.10	0.75	50.70	38.03	P
R01 C7			200	150	402	101	754	75	49.2	3.6	31146	575	210.0	G	W	150	1.80	85	36.0	29833	2.00	2692	2.10	0.75	43.55	32.66	P
R01 C8			200	150	402	101	754	75	49.2	3.6	31146	575	210.0	G	W	150	1.80	85	36.0	29833	2.00	2692	2.10	0.75	43.35	32.51	P
R01 C9			200	150	402	101	754	75	49.2	3.6	31146	575	210.0	S		150	3.00	85	210.0	200000	2.00	2692	2.10	0.75	42.70	32.03	PED
R01C10			200	150	402	101	754	75	49.2	3.6	31146	575	210.0	S		150	3.00	85	210.0	200000	2.00	2692	2.10	0.75	41.20	30.90	PED
R01: Rahimi and Hutchinson (2001)																												

Table A.30. Experimental bending test database (XXX)

			Geometry of RC beam						Material properties					Plate strengthening								Adhesive		Load configuration				
Specimen (1)	Ext anch (2)	Pr (3)	b mm (4)	h mm (5)	A_s mm^2 (6)	A_s' mm^2 (7)	A_w mm^2 (8)	s_w mm (9)	f_{cm} MPa (10)	f_{ctm} MPa (11)	E_c MPa (12)	f_{ym} MPa (13)	E_s GPa (14)	M (15)	F (16)	b_L mm (17)	t_L mm (18)	a mm (19)	E_L GPa (20)	ε_{Lu} με (21)	t_a mm (22)	G_a MPa (23)	L m (24)	L_{shear} m (25)	V_{uexp} kN (26)	M_{uexp} kNm (27)	Mode (28)
W01 C-B			150	300	698	201	2006	100	45.6	3.4	30367	400	200.0	-	-	-	-	-	-	-	-	-	2.80	1.10	67.62	74.38	CC
W01 S-A			150	300	698	201	2006	100	45.6	3.4	30367	400	200.0	C	P	50	1.20	0	155.0	15484	2.00	3269	2.80	1.10	90.91	100.00	P
W01 S-B			150	300	698	201	2006	100	45.6	3.4	30367	400	200.0	C	P	50	1.20	0	155.0	15484	2.00	3269	2.80	1.10	100.04	110.04	P
W01 S-C			150	300	698	201	2006	100	45.6	3.4	30367	400	200.0	C	P	50	1.20	0	155.0	15484	2.00	3269	2.80	1.10	98.37	108.21	P
W01 S-D			150	300	698	201	2006	100	45.6	3.4	30367	400	200.0	C	P	50	1.20	0	155.0	15484	2.00	3269	2.80	1.10	100.15	110.16	P
W01 R-A			150	300	698	201	2006	100	45.6	3.4	30367	400	200.0	C	W	135	0.53	0	114.5	15000	0.42	3269	2.80	1.10	82.52	90.77	P
W01 R-A			150	300	698	201	2006	100	45.6	3.4	30367	400	200.0	C	W	135	0.53	0	114.5	15000	0.42	3269	2.80	1.10	85.92	94.51	P
W01 R-C			150	300	698	201	2006	100	45.6	3.4	30367	400	200.0	C	W	135	0.53	0	114.5	15000	0.42	3269	2.80	1.10	89.27	98.20	P
W01 R-D			150	300	698	201	2006	100	45.6	3.4	30367	400	200.0	C	W	135	0.53	0	114.5	15000	0.42	3269	2.80	1.10	97.26	106.99	P
G02 C			152	254	402	142	1390	102	55.2	3.9	32364	415	200.0	-	-	-	-	-	-	-	-	-	2.44	0.84	47.85	40.15	CC
G02 C1			152	254	402	142	1390	102	55.2	3.9	32364	415	200.0	C	W	152	0.55	102	217.9	12000	0.42	1325	2.44	0.84	50.95	42.75	R
G02 C2			152	254	402	142	1390	102	55.2	3.9	32364	415	200.0	C	P	152	1.30	102	153.8	14000	2.00	1325	2.44	0.84	66.30	55.63	P
G02 C3			152	254	402	142	1390	102	55.2	3.9	32364	415	200.0	C	W	152	2.32	102	49.2	14000	0.42	1325	2.44	0.84	67.20	56.38	P
G02 H-50-1			152	254	402	142	1390	102	55.2	3.9	32364	415	200.0	H	W	152	1.00	102	22.4	17400	0.42	580	2.44	0.84	NR	NR	NR
G02 H-50-2			152	254	402	142	1390	102	55.2	3.9	32364	415	200.0	H	W	152	1.00	102	22.4	17400	0.42	580	2.44	0.84	57.40	48.16	R
G02 H-75-1			152	254	402	142	1390	102	55.2	3.9	32364	415	200.0	H	W	152	1.50	102	22.6	17400	0.42	580	2.44	0.84	NR	NR	NR
G02 H-75-2			152	254	402	142	1390	102	55.2	3.9	32364	415	200.0	H	W	152	1.50	102	22.6	17400	0.42	580	2.44	0.84	65.40	54.87	P
G02 CS			152	254	402	142	1390	102	55.2	3.9	32364	415	200.0	C	W	152	0.13	102	217.9	12000	0.42	1325	2.44	0.84	NR	NR	NR
G02 H-S50-1			152	254	402	142	1390	102	55.2	3.9	32364	415	200.0	H	W	152	1.00	102	22.4	17400	0.42	580	2.44	0.84	NR	NR	NR
G02 H-S50-2			152	254	402	142	1390	102	55.2	3.9	32364	415	200.0	H	W	152	1.00	102	22.4	17400	0.42	580	2.44	0.84	NR	NR	NR

W01: White and Soudki (2001); G02: Grace et al. (2002)

Table A.31. Experimental bending test database (XXXI)

			Geometry of RC beam						Material properties					Plate strengthening								Adhesive		Load configuration				
Specimen (1)	Ext anch (2)	Pr (3)	b mm (4)	h mm (5)	A_s mm^2 (6)	A_s' mm^2 (7)	A_w mm^2 (8)	s_w mm (9)	f_{cm} MPa (10)	f_{ctm} MPa (11)	E_c MPa (12)	f_{ym} MPa (13)	E_s GPa (14)	M (15)	F (16)	b_L mm (17)	t_L mm (18)	a mm (19)	E_L GPa (20)	ε_{Lu} με (21)	t_a mm (22)	G_a MPa (23)	L m (24)	L_{shear} m (25)	V_{uexp} kN (26)	M_{uexp} kNm (27)	Mode (28)
G02 H-S75-1			152	254	402	142	1390	102	55.2	3.9	32364	415	200.0	H	W	152	1.50	102	22.6	17400	0.42	580	2.44	0.84	NR	NR	NR
G02 H-S75-2			152	254	402	142	1390	102	55.2	3.9	32364	415	200.0	H	W	152	1.50	102	22.6	17400	0.42	580	2.44	0.84	NR	NR	NR
H02 2			150	250	157	157	1571	100	35.4	2.7	27910	537	231.0	C	W	150	1.32	350	19.7	13132	0.42	3269	1.50	0.50	53.00	26.50	P
H02 4			150	250	393	157	1571	100	36.2	2.8	28118	537	231.0	C	W	150	1.32	200	19.7	13132	0.42	3269	1.50	0.50	65.40	32.70	P
H02 5			150	250	393	157	1571	100	40.6	3.1	29214	537	231.0	C	W	150	2.64	50	19.7	13132	0.42	3269	1.50	0.50	79.40	39.70	P
H02 6			150	250	393	157	1571	100	39.9	3.0	29045	537	231.0	C	W	150	1.32	200	19.7	13132	0.42	3269	1.50	0.50	63.10	31.55	P
H02 7			150	250	393	157	1571	100	37.6	2.9	28476	537	231.0	C	W	150	1.32	350	19.7	13132	0.42	3269	1.50	0.50	53.90	26.95	P
K02 B1			240	350	452	101	628	90	40.0	3.0	29070	504	200.0	C	P	80	1.40	70	182.0	15385	3.00	902	4.35	1.45	214.00	310.30	PC
K02 B2			240	350	452	101	628	90	40.0	3.0	29070	504	200.0	C	P	80	1.40	70	182.0	15385	3.00	902	4.35	1.45	170.00	246.50	PC
K02 B3			240	350	452	101	628	90	40.0	3.0	29070	504	200.0	C	P	80	1.50	70	107.0	12150	3.00	902	4.35	1.45	104.00	150.80	PC
K02 B4			240	350	452	101	628	90	40.0	3.0	29070	504	200.0	C	P	80	1.50	70	107.0	12150	3.00	902	4.35	1.45	190.00	275.50	PC
K02 B5			200	350	452	101	628	90	40.0	3.0	29070	504	200.0	C	P	100	1.20	70	180.0	17778	2.00	902	4.35	1.45	142.00	205.90	PC
K02 B6			200	350	452	101	628	90	40.0	3.0	29070	504	200.0	C	P	100	1.20	70	180.0	17778	6.00	902	4.35	1.45	149.00	216.05	PC
Lu02 LB1			300	800	2262	157	565	100	30.0	2.4	26411	400	200.0	C	W	300	0.88	0	167.0	15000	0.42	3269	7.20	2.40	NR	NR	NR
Lu02 LB2			300	800	2262	157	565	100	30.0	2.4	26411	400	200.0	C	W	300	0.88	0	167.0	15000	0.42	3269	7.20	2.40	NR	NR	NR
Lu02 MB1			150	400	628	157	565	100	30.0	2.4	26411	400	200.0	C	W	150	0.44	0	167.0	15000	0.42	3269	3.60	1.20	NR	NR	NR
Lu02 MB2			150	400	628	157	565	100	30.0	2.4	26411	400	200.0	C	W	150	0.44	0	167.0	15000	0.42	3269	3.60	1.20	137.20	164.64	NR
Lu02 SB1			75	200	157	157	565	100	30.0	2.4	26411	400	200.0	C	W	75	0.22	0	167.0	15000	0.42	3269	1.80	0.60	NR	NR	NR
Lu02 SB2			75	200	157	157	565	100	30.0	2.4	26411	400	200.0	C	W	75	0.22	0	167.0	15000	0.42	3269	1.80	0.60	NR	NR	NR
Lu02 SB3			75	200	157	157	565	100	30.0	2.4	26411	400	200.0	C	W	75	0.22	0	167.0	15000	0.42	3269	1.80	0.60	37.85	22.71	NR

G02: Grace et al. (2002); H02: Hau (2002) (referenced by Smith and Teng, 2002); K02: Kim and Sebastian (2002); Lu02: Luk and Leung (2002)

Table A.32. Experimental bending test database (XXXII)

			Geometry of RC beam						Material properties					Plate strengthening								Adhesive		Load configuration				
Specimen (1)	Ext anch (2)	Pr (3)	b mm (4)	h mm (5)	A_s mm^2 (6)	A_s' mm^2 (7)	A_w mm^2 (8)	s_w mm (9)	f_{cm} MPa (10)	f_{ctm} MPa (11)	E_c MPa (12)	f_{ym} MPa (13)	E_s GPa (14)	M (15)	F (16)	b_L mm (17)	t_L mm (18)	a mm (19)	E_L GPa (20)	$\varepsilon_{L,u}$ με (21)	t_a mm (22)	G_a MPa (23)	L m (24)	L_{shear} m (25)	V_{uexp} kN (26)	M_{uexp} kNm (27)	Mode (28)
B03 CA/B			203	356	396	143	1397	102	35.1	2.7	27831	440	210.0	-	-	-	-	-	-	-	-	-	2.69	1.06	130.80	139.30	CC
B03 A1			203	356	396	143	1397	102	35.1	2.7	27831	440	210.0	C	W	50	1.17	811	163.5	15000	0.42	3269	2.69	1.06	119.70	127.48	P
B03 A2			203	356	396	143	1397	102	35.1	2.7	27831	440	210.0	C	W	50	1.17	709	163.5	15000	0.42	3269	2.69	1.06	125.90	134.08	P
B03 A3			203	356	396	143	1397	102	35.1	2.7	27831	440	210.0	C	W	50	1.17	303	163.5	15000	0.42	3269	2.69	1.06	138.30	147.29	P
B03 A4			203	356	396	143	1397	102	37.2	2.8	28375	440	210.0	C	W	100	0.59	684	163.5	15000	0.42	3269	2.69	1.06	129.00	137.39	P
B03 B1			203	356	396	143	1397	102	37.2	2.8	28375	440	210.0	C	W	75	1.18	176	163.5	15000	0.42	3269	2.69	1.06	132.60	141.22	P
B03 B2	x		203	356	396	143	1397	102	37.2	2.8	28375	440	210.0	C	W	50	1.18	176	163.5	15000	0.42	3269	2.69	1.06	141.90	151.12	R
B03 B3			203	356	396	143	1397	102	37.2	2.8	28375	440	210.0	C	W	50	1.18	176	163.5	15000	0.42	3269	2.69	1.06	137.00	145.91	R
B03 B4	x		203	356	396	143	1397	102	34.3	2.7	27617	438	210.0	C	W	50	1.18	176	163.5	15000	0.42	3269	2.69	1.06	132.60	141.22	R
B03 B5	x		203	356	396	143	1397	102	34.3	2.7	27617	438	210.0	C	W	50	1.18	455	163.5	15000	0.42	3269	2.69	1.06	129.90	138.34	P
B03 CC/D			203	406	396	143	1397	102	35.1	2.7	27831	440	210.0	-	-	-	-		-	-	-	-	3.00	1.22	125.90	153.60	CC
B03 C1			203	406	396	143	1397	102	35.1	2.7	27831	440	210.0	C	W	50	1.04	128	62.0	12258	0.42	3269	3.00	1.22	143.70	175.31	P
B03 C2			203	406	396	143	1397	102	35.1	2.7	27831	440	210.0	C	W	50	1.04	128	62.0	12258	0.42	3269	3.00	1.22	125.90	153.60	P
B03 C3	x		203	406	396	143	1397	102	35.1	2.7	27831	440	210.0	C	W	50	1.04	128	62.0	12258	0.42	3269	3.00	1.22	149.00	181.78	R
B03 C4			203	406	396	143	1397	102	37.2	2.8	28375	440	210.0	C	W	50	1.04	128	62.0	12258	0.42	3269	3.00	1.22	132.60	161.77	P
B03 D1			203	406	396	143	1397	102	37.2	2.8	28375	440	210.0	C	P	50	1.19	128	155.0	15484	2.00	3269	3.00	1.22	128.10	156.28	P
B03 D2			203	406	396	143	1397	102	37.2	2.8	28375	440	210.0	C	P	50	1.19	128	155.0	15484	2.00	3269	3.00	1.22	133.90	163.36	P
H03 H1			152	229	253	253	613	102	34.5	2.7	27671	400	210.0	-	-	-	-	-	-	-	-	-	2.13	0.96	65.83	63.54	CC
H03 H2			152	229	253	253	613	102	34.5	2.7	27671	400	210.0	C	W	127	1.65	102	159.3	15000	0.05	69	2.13	0.96	65.83	63.54	P
H03 H3			152	229	253	253	613	102	34.5	2.7	27671	400	210.0	C	P	89	0.64	153	124.1	15000	0.39	7	2.13	0.96	90.74	87.58	P

B03: Breña et al. (2003); H03: Harmon et al. (2003)

Table A.33. Experimental bending test database (XXXIII)

			Geometry of RC beam						Material properties					Plate strengthening								Adhesive		Load configuration				
Specimen (1)	Ext anch (2)	Pr (3)	b mm (4)	h mm (5)	A_s mm^2 (6)	A_s' mm^2 (7)	A_w mm^2 (8)	s_w mm (9)	f_{cm} MPa (10)	f_{ctm} MPa (11)	E_c MPa (12)	f_{ym} MPa (13)	E_s GPa (14)	M (15)	F (16)	b_L mm (17)	t_L mm (18)	a mm (19)	E_L GPa (20)	$\varepsilon_{L,u}$ με (21)	t_a mm (22)	G_a MPa (23)	L m (24)	L_{shear} m (25)	V_{uexp} kN (26)	M_{uexp} kNm (27)	Mode (28)
H03 H4			152	229	253	253	613	102	34.5	2.7	27671	400	210.0	C	P	51	1.27	330	124.1	15000	1.02	7	2.13	0.96	85.18	82.22	P
H03 H5			152	229	253	253	613	102	34.5	2.7	27671	400	210.0	C	P	51	1.27	330	124.1	15000	1.02	7	2.13	0.96	75.84	73.20	P
R03 A1			200	200	339	101	2011	50	50.0	3.6	31314	390	200.0	-	-	-	-	-	-	-	-	-	2.10	0.70	NR	NR	NR
R03 A1*		x	200	200	339	101	2011	50	50.0	3.6	31314	390	200.0	C	P	120	1.20	100	165.0	16970	2.50	1462	2.10	0.70	69.00	48.30	P
R03 A2			200	200	339	101	2011	50	50.0	3.6	31314	390	200.0	C	P	120	1.20	100	165.0	16970	2.50	1462	2.10	0.70	78.30	54.81	PED
R03 A3	x		200	200	339	101	2011	50	50.0	3.6	31314	390	200.0	C	P	120	1.20	100	165.0	16970	2.50	1462	2.10	0.70	89.00	62.30	P
R03 B1			200	200	462	101	1005	100	50.0	3.6	31314	390	200.0	-	-	-	-		-	-	-	-	2.10	0.70	NR	NR	NR
R03 B1*		x	200	200	462	101	1005	100	50.0	3.6	31314	390	200.0	C	W	100	1.10	100	162.1	15000	1.00	1462	2.10	0.70	75.90	53.13	P
R03 B2	x		200	200	462	101	1005	100	50.0	3.6	31314	390	200.0	C	W	100	1.10	100	162.1	15000	1.00	1462	2.10	0.70	93.70	65.59	PC
K B1			178	235	253	0	1870	76	37.9	2.9	28557	414	193.0	-	-	-	-	-	-	-	-	-	2.08	0.69	42.93	29.80	CC
K B2		x	178	235	253	0	1870	76	37.9	2.9	28557	414	193.0	C	W	127	0.54	25	58.5	16044	0.42	875	2.08	0.69	NR	NR	NR
K B3		x	178	235	253	0	1870	76	37.9	2.9	28557	414	193.0	C	W	25	0.54	25	58.5	16044	0.42	875	2.08	0.69	NR	NR	NR
K B4		x	178	235	253	0	1870	76	37.9	2.9	28557	414	193.0	C	W	25	0.54	25	71.4	17451	0.42	928	2.08	0.69	NR	NR	NR
K B5		x	178	235	253	0	1870	76	37.9	2.9	28557	414	193.0	C	W	127	0.54	25	71.4	17451	0.42	928	2.08	0.69	NR	NR	NR
K B6		x	178	235	253	0	1870	76	37.9	2.9	28557	414	193.0	C	W	25	0.54	25	58.5	16044	0.42	875	2.08	0.69	NR	NR	NR
K B7		x	178	235	253	0	1870	76	37.9	2.9	28557	414	193.0	C	W	127	0.54	25	58.5	16044	0.42	875	2.08	0.69	NR	NR	NR
K B8		x	178	235	253	0	1870	76	37.9	2.9	28557	414	193.0	C	W	127	0.54	25	58.5	16044	0.42	875	2.08	0.69	58.47	40.59	R
K B9		x	178	235	253	0	1870	76	37.9	2.9	28557	414	193.0	C	W	127	0.54	25	71.4	17451	0.42	928	2.08	0.69	53.07	36.84	R
K B10		x	178	235	776	0	1870	76	37.9	2.9	28557	414	193.0	C	W	127	0.54	25	58.5	16044	0.42	875	2.08	0.69	NR	NR	NR
K B11		x	178	235	776	0	1870	76	37.9	2.9	28557	414	193.0	C	W	127	0.54	25	71.4	17451	0.42	928	2.08	0.69	NR	NR	NR

H03: Harmon et al. (2003); R03: Ravinovitch and Frostig (2003); K: Kuriger et al.

Table A.34. Experimental bending test database (XXXIV)

			Geometry of RC beam						Material properties					Plate strengthening								Adhesive		Load configuration				
Specimen (1)	Ext anch (2)	Pr (3)	b mm (4)	h mm (5)	A_s mm^2 (6)	A_s' mm^2 (7)	A_w mm^2 (8)	s_w mm (9)	f_{cm} MPa (10)	f_{ctm} MPa (11)	E_c MPa (12)	f_{ym} MPa (13)	E_s GPa (14)	M (15)	F (16)	b_L mm (17)	t_L mm (18)	a mm (19)	E_L GPa (20)	ε_{Lu} με (21)	t_a mm (22)	G_a MPa (23)	L m (24)	L_{shear} m (25)	V_{uexp} kN (26)	M_{uexp} kNm (27)	Mode (28)
K B12		x	178	235	776	0	1870	76	37.9	2.9	28557	414	193.0	C	W	127	0.54	25	71.4	17451	0.42	928	2.08	0.69	NR	NR	NR
K B13		x	178	235	253	0	1870	76	37.9	2.9	28557	414	193.0	C	W	127	0.54	25	71.4	17451	0.42	928	2.08	0.69	NR	NR	NR
K B2b		x	178	235	253	0	1870	76	37.9	2.9	28557	414	193.0	C	W	127	2.69	25	58.5	16044	0.42	875	2.08	0.69	71.28	49.48	PES
K B3b		x	178	235	253	0	1870	76	37.9	2.9	28557	414	193.0	C	W	25	2.69	25	58.5	16044	0.42	875	2.08	0.69	42.23	29.31	P
K B4b		x	178	235	253	0	1870	76	37.9	2.9	28557	414	193.0	C	W	25	2.69	25	71.4	17451	0.42	928	2.08	0.69	43.13	29.94	P
K B5b		x	178	235	253	0	1870	76	37.9	2.9	28557	414	193.0	C	W	127	2.69	25	71.4	17451	0.42	928	2.08	0.69	66.43	46.12	PES
K B6b		x	178	235	253	0	1870	76	37.9	2.9	28557	414	193.0	C	W	25	2.69	25	58.5	16044	0.42	875	2.08	0.69	44.34	30.78	P
K B7b		x	178	235	253	0	1870	76	37.9	2.9	28557	414	193.0	C	W	127	2.69	25	58.5	16044	0.42	875	2.08	0.69	70.68	49.06	PES
K B10b		x	178	235	776	0	1870	76	37.9	2.9	28557	414	193.0	C	W	127	2.69	25	58.5	16044	0.42	875	2.08	0.69	NR	NR	NR
K B11b		x	178	235	776	0	1870	76	37.9	2.9	28557	414	193.0	C	W	127	2.69	25	71.4	17451	0.42	928	2.08	0.69	NR	NR	NR
K B12b		x	178	235	776	0	1870	76	37.9	2.9	28557	414	193.0	C	W	127	2.69	25	71.4	17451	0.42	928	2.08	0.69	NR	NR	NR
K B13b		x	178	235	253	0	1870	76	37.9	2.9	28557	414	193.0	C	W	127	2.69	25	71.4	17451	0.42	928	2.08	0.69	66.63	46.26	PES

K: Kuriger et al.

APPENDIX B

EXPERIMENTAL DATABASE OF SHEAR TESTS

B.1. Introduction

Appendix B summarizes the experimental data collected from the literature regarding specimens subjected to pure shear. The assembled data have been used to evaluate the reliability of the formulation derived in Chapter 3 through the comparison of the theoretical transferred force to the ultimate value obtained experimentally.

B.2. Shear test database

B.2.1. Selection criteria for the database

From the existing set-ups to evaluate the bond strength, only shear tests have been included in the database. Beam bending tests have been removed because the original purpose of the database is to check the validity of the formulation developed for pure shear specimens in Chapter 3.

For the inclusion on the database, specimens should consist of one or two concrete prisms blocks externally strengthened by bonded plates in one (single shear test) or two opposite sides of the concrete block (double shear test). These specimens are loaded by an axial load that introduces a shear state in the bonded connection.

As shown in the database, the double shear test method has been the most popular up to date. When performing a single shear test, special care should be taken because a bending moment can be introduced at the plate end due to a possible eccentricity on the applied load. This bending moment affects test results.

Despite the slight differences between the compiled tests regarding the test set-up, the loading mechanism is very similar. In a pulling test, the tensile forces in each laminate are balanced by a pulling force applied in the concrete by steel plates bonded on the remaining sides of the beam or through a steel rebar embedded in the concrete block. In a pushing test, the force is applied through a supporting wedge.

Specimens for which geometry, material properties, failure mode or failure load were not reported have been excluded from the analysis of this database.

B.2.2. Compiled data

Following a chronological order, Tables B.1 to B.10 summarize the details of the assembled specimens in terms of geometry, material properties, and loading configuration. Units are specified in each column.

Specimens have been named in column 1 as the first author initial followed by the publication year of the source describing the test and by the specimen name according to this publication. Column 2 indicates the type of shear test, denoting: *S* for single shear tests and *D* for double shear tests.

The geometry of the block prism is given by columns 3 to 8, where b, h, A_s, A_s', A_w, and s_w denote the width and depth of the prism, the internal tensile steel reinforcement area, the internal compressive steel reinforcement area, the shear reinforcement area and stirrups spacing, respectively. As observed in Tables B.1 to B10, most of the compiled shear tests were performed by using concrete prisms without internal reinforcement. Hence, in those cases, the transference of stresses between concrete and the external reinforcement is developed without the interference of the internal steel.

Concrete properties, such as the mean cylinder compressive strength (f_{cm}), the tensile strength (f_{ctm}) and the modulus of elasticity (E_c), are summarized in columns 9 to 11. Columns 12 and 13 list the internal steel properties, that is, the yield strength (f_{ym}) and the modulus of elasticity (E_s).

The geometry and mechanical properties of the externally bonded plates are given by b_L, t_L, L_L, E_L, ε_{Lu}, being the plate width, thickness, length, modulus of elasticity and ultimate strain of the bonded plate (columns 16 to 20). The material, denoted as *M*, is listed in column (14) where: *A* Aramid Fiber Reinforced Polymer (AFRP) laminate, *C* Carbon Fiber Reinforced Polymer (CFRP) laminate, *G* Glass Fiber Reinforced Polymer (GFRP) laminate, and *S* steel plate. For FRP laminates, the fabrication procedure (wet lay-up (*W*) or pultruded (*P*)) is given by column 15, as *F*.

The thickness (t_a) and the shear modulus (G_a) of the adhesive are listed in columns 21 and 22.

Regarding the test set-up and the applied load: L, P_{exp}, $\varepsilon_{L,max}$, τ_{max} (columns 23 to 26) represent, the specimen length, the maximum applied force at failure, the laminate strain at the load application point at failure and finally, the maximum shear stress average between the strain gauges affixed close to the application point. This average bond stress was calculated as the difference of tensile force by the surface area of the laminate.

Column 27 reports the mode of failure given by the following nomenclature: *CC* as concrete crushing, *R* as plate rupture, *P* as premature failure beneath the interface between concrete and adhesive, *O* as other failure modes like adhesive failure or plate-to-adhesive interfacial failure.

It should be mentioned that the initials *NR* denote data not clearly reported in the published references.

The last row of Tables A.1 to A.34 gives the reference source of the data shown in each table.

B.2.3. Assumptions for geometry and material properties

In general, all geometry and material properties were reported in the existing references. However, some cases showed some missing data. In these cases, if the basic properties, the failure mode and the ultimate load are available, the remaining missing data will have been assumed following the criteria described below.

1) For concrete properties, in case no split cylinder test was performed to obtain the tensile strength and no information about the modulus of elasticity was available, both values have been calculated by using the Spanish Structural Concrete Code (EHE, 1999)
2) Regarding the strengthening material, only the thickness of the sheet was reported for some of the wet lay-up laminates. In this case, when the number of plies employed on the plate manufacturing is known, the plate thickness has been calculated as the sheet thickness plus the adhesive between sheets by the total number of plies, as shown by equation (B.1). It should be noted that The reported value in column 17 of Tables B.1 to B.10 is the plate thickness and not the sheet thickness.

$$t_L = n\left(t_{sheet} + t_{adh,sheets}\right) \tag{B.1}$$

3) The adhesive properties are the most common missing data, especially the thickness which is difficult to control on site. To be consistent with the bending test database described in Appendix A, the missing adhesive thickness has been assumed as 2.00 *mm* for pultruded plates and 0.42 *mm* for wet lay-up laminates.
4) For the adhesive modulus of elasticity, a value of 8500 *MPa* has been assumed according to Smith and Teng (2002) and the compiled bending database of Appendix A. However, the average value for the 104 shear tests well-documented is much lower (3917 *MPa*).

All these assumptions do not significantly affect the results of the statistical analysis performed in Chapter 3.

Table B.1. Experimental shear test database (I)

		Geometry of RC beam						Material properties					Plate strengthening							Adhesive		Load configuration				
Specimen (1)	Test (2)	b mm (3)	h mm (4)	A_s mm^2 (5)	A_s' mm^2 (6)	A_w mm^2 (7)	s_w mm (8)	f_{cm} MPa (9)	f_{ctm} MPa (10)	E_c MPa (11)	f_{ym} MPa (12)	E_s GPa (13)	M (14)	F (15)	b_L mm (16)	t_L mm (17)	L_L mm (18)	E_L GPa (19)	ε_{Lu} $\mu\varepsilon$ (20)	t_a mm (21)	G_a MPa (22)	L mm (23)	P_{exp} kN (24)	$\varepsilon_{L,max}$ $\mu\varepsilon$ (25)	τ_{max} MPa (26)	Mode (27)
S86 1		60	60	-	-	-	-	19.8	1.6	18789	-	-	S	-	60	3.00	150	200.0	1825	1.00	467	150	19.53	543	NR	P
S86 2		60	60	-	-	-	-	35.5	2.7	25342	-	-	S	-	60	3.00	150	200.0	1825	1.00	467	150	22.68	630	NR	P
S86 3		60	60	-	-	-	-	47.6	3.5	28726	-	-	S	-	60	3.00	150	200.0	1825	1.00	467	150	24.93	693	NR	P
S86 4		60	60	-	-	-	-	56.3	4.0	30740	-	-	S	-	60	3.00	150	200.0	1825	1.00	467	150	29.97	833	NR	P
S86 5		60	60	-	-	-	-	35.6	2.7	25373	-	-	S	-	60	3.00	150	200.0	1825	1.00	467	150	21.78	605	NR	P
S86 6		60	60	-	-	-	-	35.6	2.7	25373	-	-	S	-	60	3.00	150	200.0	1825	1.00	467	150	21.42	595	NR	P
S86 7		60	60	-	-	-	-	35.6	2.7	25373	-	-	S	-	60	3.00	150	200.0	1825	1.00	467	150	25.47	708	NR	P
T94 G100 40	S	60	200	-	-	-	-	41.2	3.1	27042	-	-	S	-	40	2.90	100	200.0	NR	3.00	2577	1200	21.70	935	NR	NR
T94 G200 40	S	60	200	-	-	-	-	41.2	3.1	27042	-	-	S	-	40	2.90	200	200.0	NR	3.00	2577	1200	39.50	1703	NR	NR
T94 G400 40	S	60	200	-	-	-	-	41.2	3.1	27042	-	-	S	-	40	2.90	400	200.0	NR	3.00	2577	1200	41.10	1772	NR	NR
T94 G50 60	S	60	200	-	-	-	-	41.2	3.1	27042	-	-	S	-	60	2.90	50	200.0	NR	3.00	2577	1200	12.70	365	NR	NR
T94 G100 60	S	60	200	-	-	-	-	41.2	3.1	27042	-	-	S	-	60	2.90	100	200.0	NR	3.00	2577	1200	20.00	575	NR	NR
T94 G150 60	S	60	200	-	-	-	-	41.2	3.1	27042	-	-	S	-	60	2.90	150	200.0	NR	3.00	2577	1200	46.30	1330	NR	NR
T94 G200 60	S	60	200	-	-	-	-	41.2	3.1	27042	-	-	S	-	60	2.90	200	200.0	NR	3.00	2577	1200	48.80	1402	NR	NR
T94 G400 60	S	60	200	-	-	-	-	41.2	3.1	27042	-	-	S	-	60	2.90	400	200.0	NR	3.00	2577	1200	58.40	1678	NR	NR
T94 G400 60	S	60	200	-	-	-	-	41.2	3.1	27042	-	-	S	-	60	2.90	400	200.0	NR	3.00	2577	1200	53.00	1523	NR	NR
T94 G100 80	S	60	200	-	-	-	-	41.2	3.1	27042	-	-	S	-	80	2.90	100	200.0	NR	3.00	2577	1200	39.60	853	NR	NR
T94 G150 80	S	60	200	-	-	-	-	41.2	3.1	27042	-	-	S	-	80	2.90	150	200.0	NR	3.00	2577	1200	50.90	1097	NR	NR
T94 G200 80	S	60	200	-	-	-	-	41.2	3.1	27042	-	-	S	-	80	2.90	200	200.0	NR	3.00	2577	1200	67.30	1450	NR	NR
T94 G300 80	S	60	200	-	-	-	-	41.2	3.1	27042	-	-	S	-	80	2.90	300	200.0	NR	3.00	2577	1200	68.00	1466	NR	NR

S86: Swamy et al. (1986); T94: Täljsten (1994)

Table B.2. Experimental shear test database (II)

		Geometry of RC beam						Material properties					Plate strengthening							Adhesive		Load configuration				
Specimen (1)	Test (2)	b mm (3)	h mm (4)	A_s mm^2 (5)	A_s' mm^2 (6)	A_w mm^2 (7)	s_w mm (8)	f_{cm} MPa (9)	f_{ctm} MPa (10)	E_c MPa (11)	f_{ym} MPa (12)	E_s GPa (13)	M (14)	F (15)	b_L mm (16)	t_L mm (17)	L_L mm (18)	E_L GPa (19)	ε_{Lu} με (20)	t_a mm (21)	G_a MPa (22)	L mm (23)	P_{exp} kN (24)	$\varepsilon_{L,max}$ με (25)	τ_{max} MPa (26)	Mode (27)
T94 G500 80	S	200	200	-	-	-	-	41.2	3.1	27042	-	-	S	-	80	2.90	500	200.0	NR	3.00	2577	1200	67.30	1450	NR	NR
T94 G600 80	S	200	200	-	-	-	-	41.2	3.1	27042	-	-	S	-	80	2.90	600	200.0	NR	3.00	2577	1200	71.40	1539	NR	NR
T94 G800 80	S	200	200	-	-	-	-	41.2	3.1	27042	-	-	S	-	80	2.90	800	200.0	NR	3.00	2577	1200	61.60	1328	NR	NR
T94 I100 80	S	200	200	-	-	-	-	41.2	3.1	27042	-	-	G	NR	80	1.00	100	20.4	NR	3.00	2577	1200	20.70	12662	NR	NR
T94 I200 80	S	200	200	-	-	-	-	41.2	3.1	27042	-	-	G	NR	80	1.00	200	20.4	NR	3.00	2577	1200	21.90	13396	NR	NR
T94 I500 80	S	200	200	-	-	-	-	41.2	3.1	27042	-	-	G	NR	80	1.00	500	20.4	NR	3.00	2577	1200	24.10	14742	NR	NR
T94 J100 50	S	200	200	-	-	-	-	41.2	3.1	27042	-	-	C	NR	50	1.20	100	162.0	NR	3.00	2577	1200	17.30	1780	NR	NR
T94 J200 50	S	200	200	-	-	-	-	41.2	3.1	27042	-	-	C	NR	50	1.20	200	162.0	NR	3.00	2577	1200	27.50	2829	NR	NR
T94 J300 50	S	200	200	-	-	-	-	41.2	3.1	27042	-	-	C	NR	50	1.20	300	162.0	NR	3.00	2577	1200	35.10	3611	NR	NR
T94 J400 50	S	200	200	-	-	-	-	41.2	3.1	27042	-	-	C	NR	50	1.20	400	162.0	NR	3.00	2577	1200	26.90	2767	NR	NR
C96 1	S	229	152	-	-	-	-	36.1	2.8	25531	-	-	G	W	25	1.02	76	108.5	15242	1.00	1989	76	8.46	3023	NR	P
C96 2	S	229	152	-	-	-	-	47.1	3.5	28602	-	-	G	W	25	1.02	76	108.5	15242	1.00	1989	76	9.93	3548	NR	P
C96 3	S	229	152	-	-	-	-	47.1	3.5	28602	-	-	G	W	25	1.02	76	108.5	15242	1.00	1989	76	10.63	3800	NR	P
C96 4	S	229	152	-	-	-	-	47.1	3.5	28602	-	-	G	W	25	1.02	76	108.5	15242	1.00	1989	76	10.63	3800	NR	P
C96 5	S	229	152	-	-	-	-	43.6	3.2	27698	-	-	G	W	25	1.02	76	108.5	15242	1.00	849	76	10.53	3762	NR	P
C96 6	S	229	152	-	-	-	-	43.6	3.2	27698	-	-	G	W	25	1.02	76	108.5	15242	1.00	90	76	8.95	3199	NR	O
C96 7	S	229	152	-	-	-	-	43.6	3.2	27698	-	-	G	W	25	1.02	76	108.5	15242	1.00	90	76	9.61	3433	NR	P
C96 8	S	229	152	-	-	-	-	43.6	3.2	27698	-	-	G	W	25	1.02	76	108.5	15242	1.00	609	76	10.51	3757	NR	P
C96 9	S	229	152	-	-	-	-	43.6	3.2	27698	-	-	G	W	25	1.02	76	108.5	15242	1.00	609	76	11.19	4000	NR	P
C96 10	S	229	152	-	-	-	-	24.0	1.9	20963	-	-	G	W	25	1.02	76	108.5	15242	1.00	609	76	9.86	3525	NR	P

T94: Täljsten (1994); C96: Chajes et al. (1996b)

Table B.3. Experimental shear test database (III)

		Geometry of RC beam						Material properties					Plate strengthening							Adhesive		Load configuration				
Specimen (1)	Test (2)	b mm (3)	h mm (4)	A_s mm^2 (5)	A_s' mm^2 (6)	A_w mm^2 (7)	s_w mm (8)	f_{cm} MPa (9)	f_{ctm} MPa (10)	E_c MPa (11)	f_{ym} MPa (12)	E_s GPa (13)	M (14)	F (15)	b_L mm (16)	t_L mm (17)	L_L mm (18)	E_L GPa (19)	ε_{Lu} με (20)	t_a mm (21)	G_a MPa (22)	L mm (23)	P_{exp} kN (24)	$\varepsilon_{L,max}$ με (25)	τ_{max} MPa (26)	Mode (27)
C96 11	S	229	152	-	-	-	-	28.9	2.3	23034	-	-	G	W	25	1.02	76	108.5	15242	1.00	609	76	9.34	3337	NR	P
C96 12	S	229	152	-	-	-	-	43.7	3.3	27724	-	-	G	W	25	1.02	76	108.5	15242	1.00	609	76	11.20	4002	NR	P
C96 13	S	229	152	-	-	-	-	36.4	2.8	25625	-	-	G	W	25	1.02	51	108.5	15242	1.00	609	51	8.09	2891	NR	P
C96 14	S	229	152	-	-	-	-	36.4	2.8	25625	-	-	G	W	25	1.02	102	108.5	15242	1.00	609	102	12.81	4576	NR	P
C96 15	S	152	152	-	-	-	-	36.4	2.8	25625	-	-	G	W	25	1.02	152	108.5	15242	1.00	609	152	11.91	4257	NR	P
C96 16	S	152	152	-	-	-	-	36.4	2.8	25625	-	-	G	W	25	1.02	203	108.5	15242	1.00	609	203	11.57	4133	NR	P
M97 1	D	100	100	-	-	-	-	40.8	3.1	26929	-	-	C	W	50	0.53	75	162.0	NR	0.42	3269	75	11.60	2702	1.67	P
M97 2	D	100	100	-	-	-	-	40.8	3.1	26929	-	-	C	W	50	0.53	150	162.0	NR	0.42	3269	150	18.40	4287	1.23	P
M97 3	D	100	100	-	-	-	-	43.3	3.2	27617	-	-	C	W	50	0.53	300	162.0	NR	0.42	3269	300	23.90	5568	0.80	P
M97 4	D	100	100	-	-	-	-	42.4	3.2	27374	-	-	C	W	50	0.53	75	267.0	NR	0.42	3269	75	20.00	2827	2.67	P
M97 5	D	100	100	-	-	-	-	42.4	3.2	27374	-	-	C	W	50	0.53	150	267.0	NR	0.42	3269	150	14.60	2064	0.97	R
M97 6	D	100	100	-	-	-	-	42.7	3.2	27455	-	-	C	W	50	0.59	65	162.0	NR	0.42	3269	65	19.10	4031	2.94	P
M97 7	D	100	100	-	-	-	-	42.7	3.2	27455	-	-	C	W	50	0.59	150	162.0	NR	0.42	3269	150	32.50	6860	2.17	P
M97 8	D	100	100	-	-	-	-	44.7	3.3	27988	-	-	C	W	50	0.53	700	162.0	NR	0.42	3269	700	20.00	4659	0.31	P
BN99 1	S	150	150	-	-	-	-	42.5	3.2	27401	-	-	G	W	25	1.00	180	29.2	16164	1.00	1271	180	11.41	15384	NR	R
BN99 2	S	150	150	-	-	-	-	42.5	3.2	27401	-	-	G	W	25	2.00	320	29.2	16164	1.00	1271	320	21.40	14427	NR	R
BN99 3	S	150	150	-	-	-	-	42.5	3.2	27401	-	-	C	W	25	0.33	160	75.7	34726	1.00	1253	160	8.50	34729	NR	R
BN99 4	S	150	150	-	-	-	-	42.5	3.2	27401	-	-	C	W	25	0.66	320	75.7	34726	1.00	1253	320	15.10	30847	NR	R
N00 1	D	150	150	-	-	-	-	25.0	2.0	21419	-	-	C	P	50	1.27	75	175.0	16100	2.00	1654	700	12.67	1152	NR	NR
N00 2	D	150	150	-	-	-	-	55.0	3.9	30456	-	-	C	P	50	1.27	75	175.0	16100	2.00	1654	700	14.01	1273	NR	NR

C96: Chajes et al. (1996b); M97: Maeda et al. (1997); BN99: Bizindavyi and Neale (1999); N00: Neubauer (2000)

Table B.4. Experimental shear test database (IV)

		Geometry of RC beam						Material properties					Plate strengthening							Adhesive		Load configuration				
Specimen (1)	Test (2)	b mm (3)	h mm (4)	A_s mm^2 (5)	A_s' mm^2 (6)	A_w mm^2 (7)	s_w mm (8)	f_{cm} MPa (9)	f_{ctm} MPa (10)	E_c MPa (11)	f_{ym} MPa (12)	E_s GPa (13)	M (14)	F (15)	b_L mm (16)	t_L mm (17)	L_L mm (18)	E_L GPa (19)	ε_{Lu} $\mu\varepsilon$ (20)	t_a mm (21)	G_a MPa (22)	L mm (23)	P_{exp} kN (24)	$\varepsilon_{L,max}$ $\mu\varepsilon$ (25)	τ_{max} MPa (26)	Mode (27)
N00 3	D	150	150	-	-	-	-	25.0	2.0	21419	-	-	C	P	50	1.27	150	175.0	16100	2.00	1654	700	20.69	1881	NR	NR
N00 4	D	150	150	-	-	-	-	25.0	2.0	21419	-	-	C	P	50	1.27	150	175.0	16100	2.00	1654	700	18.66	1696	NR	NR
N00 5	D	150	150	-	-	-	-	55.0	3.9	30456	-	-	C	P	50	1.27	150	175.0	16100	2.00	1654	700	33.36	3033	NR	NR
N00 6	D	150	150	-	-	-	-	25.0	2.0	21419	-	-	C	P	50	1.44	150	150.6	13300	2.00	1654	700	23.99	2204	NR	NR
N00 7	D	150	150	-	-	-	-	55.0	3.9	30456	-	-	C	P	50	1.44	150	150.6	13300	2.00	1654	700	28.36	2605	NR	NR
N00 8	D	150	150	-	-	-	-	25.0	2.0	21419	-	-	C	P	50	1.42	150	205.5	13000	2.00	1654	700	25.49	1751	NR	NR
N00 9	D	150	150	-	-	-	-	55.0	3.9	30456	-	-	C	P	50	1.42	150	205.5	13000	2.00	1654	700	27.99	1922	NR	NR
N00 10	D	150	150	-	-	-	-	25.0	2.0	21419	-	-	C	P	50	1.27	225	175.0	16100	2.00	1654	700	29.00	2637	NR	NR
N00 11	D	150	150	-	-	-	-	25.0	2.0	21419	-	-	C	P	50	1.27	300	175.0	16100	2.00	1654	700	24.75	2250	NR	NR
N00 12	D	150	150	-	-	-	-	25.0	2.0	21419	-	-	C	P	50	1.27	300	175.0	16100	2.00	1654	700	30.88	2808	NR	NR
N00 13	D	150	150	-	-	-	-	25.0	2.0	21419	-	-	C	P	50	1.27	300	175.0	16100	2.00	1654	700	25.19	2290	NR	NR
N00 14	D	150	150	-	-	-	-	55.0	3.9	30456	-	-	C	P	50	1.27	300	175.0	16100	2.00	1654	700	31.58	2871	NR	NR
N00 15	D	150	150	-	-	-	-	55.0	3.9	30456	-	-	C	P	50	1.44	300	150.6	13300	2.00	1654	700	43.57	4002	NR	NR
N00 16	D	150	150	-	-	-	-	25.0	2.0	21419	-	-	C	P	50	1.44	300	150.6	13300	2.00	1654	700	25.10	2305	NR	NR
N00 17	D	150	150	-	-	-	-	25.0	2.0	21419	-	-	C	P	50	1.44	300	150.6	13300	2.00	1654	700	27.35	2513	NR	NR
N00 18	D	150	150	-	-	-	-	55.0	3.9	30456	-	-	C	P	50	1.42	300	205.5	13000	2.00	1654	700	27.34	1878	NR	NR
N00 19	D	150	150	-	-	-	-	55.0	3.9	30456	-	-	C	P	50	1.42	300	205.5	13000	2.00	1654	700	28.14	1933	NR	NR
N00 20	D	150	150	-	-	-	-	25.0	2.0	21419	-	-	C	P	50	1.42	300	205.5	13000	2.00	1654	700	23.60	1621	NR	NR
N00 21	D	150	150	-	-	-	-	55.0	3.9	30456	-	-	C	P	50	1.27	300	175.0	16100	2.00	1654	700	31.68	2880	NR	NR
N00 22	D	150	150	-	-	-	-	25.0	2.0	21419	-	-	C	P	50	1.27	550	175.0	16100	2.00	1654	700	25.93	2358	NR	NR

N00: Neubauer (2000)

Table B.5. Experimental shear test database (V)

		Geometry of RC beam						Material properties					Plate strengthening							Adhesive		Load configuration				
Specimen (1)	Test (2)	b mm (3)	h mm (4)	A_s mm^2 (5)	A_s' mm^2 (6)	A_w mm^2 (7)	s_w mm (8)	f_{cm} MPa (9)	f_{ctm} MPa (10)	E_c MPa (11)	f_{ym} MPa (12)	E_s GPa (13)	M (14)	F (15)	b_L mm (16)	t_L mm (17)	L_L mm (18)	E_L GPa (19)	ε_{Lu} με (20)	t_a mm (21)	G_a MPa (22)	L mm (23)	P_{exp} kN (24)	$\varepsilon_{L,max}$ με (25)	τ_{max} MPa (26)	Mode (27)
N00 23	D	150	150	-	-	-	-	25.0	2.0	21419	-	-	C	P	50	1.27	550	175.0	16100	2.00	1654	700	23.16	2106	NR	NR
N00 24	D	150	150	-	-	-	-	55.0	3.9	30456	-	-	C	P	50	1.27	550	175.0	16100	2.00	1654	700	33.76	3069	NR	NR
T00 CL-1	D	27	27	-	-	-	-	35.9	2.8	25468	-	-	C	W	27	0.30	171	163.4	NR	0.13	962	228	8.45	6493	NR	NR
T00 CL-2	D	27	27	-	-	-	-	35.9	2.8	25468	-	-	C	W	27	0.46	171	163.4	NR	0.29	962	228	8.45	4210	NR	NR
T00 CL-3	D	27	27	-	-	-	-	35.9	2.8	25468	-	-	C	W	27	0.72	171	163.4	NR	0.55	962	228	8.45	2679	NR	NR
T00 CH-1	D	27	27	-	-	-	-	35.9	2.8	25468	-	-	C	W	27	0.30	171	263.5	NR	0.13	962	228	8.45	4026	NR	NR
T00 CH-2	D	27	27	-	-	-	-	35.9	2.8	25468	-	-	C	W	27	0.46	171	263.5	NR	0.29	962	228	8.45	2610	NR	NR
T00 CH-3	D	27	27	-	-	-	-	35.9	2.8	25468	-	-	C	W	27	0.72	171	263.5	NR	0.55	962	228	8.45	1661	NR	NR
B01 L50W80N1(a)	D	150	150	-	-	-	-	44.9	3.3	28040	-	-	C	W	80	0.37	50	103.9	NR	0.20	929	200	13.35	4375	NR	P
B01 L50W80N2(a)	D	150	150	-	-	-	-	44.9	3.3	28040	-	-	C	W	80	0.73	50	103.9	NR	0.20	929	200	14.58	2389	NR	P
B01 L50W120N1(a)	D	150	150	-	-	-	-	44.9	3.3	28040	-	-	C	W	120	0.37	50	103.9	NR	0.20	929	200	17.36	3793	NR	P
B01 L50W120N2(a)	D	150	150	-	-	-	-	44.9	3.3	28040	-	-	C	W	120	0.73	50	103.9	NR	0.20	929	200	18.87	2062	NR	P
B01 L80W80N1(a)	D	150	150	-	-	-	-	44.9	3.3	28040	-	-	C	W	80	0.37	80	103.9	NR	0.20	929	200	18.03	5909	NR	P
B01 L80W80N2(a)	D	150	150	-	-	-	-	44.9	3.3	28040	-	-	C	W	80	0.73	80	103.9	NR	0.20	929	200	19.93	3266	NR	P
B01 L80W120N1(a)	D	150	150	-	-	-	-	44.9	3.3	28040	-	-	C	W	120	0.37	80	103.9	NR	0.20	929	200	22.90	5004	NR	P
B01 L80W120N2(a)	D	150	150	-	-	-	-	44.9	3.3	28040	-	-	C	W	120	0.73	80	103.9	NR	0.20	929	200	26.86	2934	NR	P
B01 L120W80N1(a)	D	150	150	-	-	-	-	44.9	3.3	28040	-	-	C	W	80	0.37	120	103.9	NR	0.20	929	200	19.68	6450	NR	P
B01 L120W80N2(a)	D	150	150	-	-	-	-	44.9	3.3	28040	-	-	C	W	80	0.73	120	103.9	NR	0.20	929	200	24.40	3999	NR	P
B01 L120W120N1(a)	D	150	150	-	-	-	-	44.9	3.3	28040	-	-	C	W	120	0.37	120	103.9	NR	0.20	929	200	28.42	6210	NR	P
B01 L120W120N2(a)	D	150	150	-	-	-	-	44.9	3.3	28040	-	-	C	W	120	0.73	120	103.9	NR	0.20	929	200	34.31	3748	NR	P

N00: Neubauer (2000); T00: Tripi et al. (2000); B01: Brosens (2001)

Table B.6. Experimental shear test database (VI)

		Geometry of RC beam						Material properties					Plate strengthening							Adhesive		Load configuration				
Specimen (1)	Test (2)	b mm (3)	h mm (4)	A_s mm^2 (5)	A_s' mm^2 (6)	A_w mm^2 (7)	s_w mm (8)	f_{cm} MPa (9)	f_{ctm} MPa (10)	E_c MPa (11)	f_{ym} MPa (12)	E_s GPa (13)	M (14)	F (15)	b_L mm (16)	t_L mm (17)	L_L mm (18)	E_L GPa (19)	ε_{Lu} με (20)	t_a mm (21)	G_a MPa (22)	L mm (23)	P_{exp} kN (24)	$\varepsilon_{L,max}$ με (25)	τ_{max} MPa (26)	Mode (27)
B01 L150W80N1(a)	D	150	150	-	-	-	-	44.9	3.3	28040	-	-	C	W	80	0.37	150	103.9	NR	0.20	929	200	22.64	7420	NR	P
B01 L150W80N2(a)	D	150	150	-	-	-	-	44.9	3.3	28040	-	-	C	W	80	0.73	150	103.9	NR	0.20	929	200	32.74	5365	NR	P
B01 L150W80N3(a)	D	150	150	-	-	-	-	44.9	3.3	28040	-	-	C	W	80	1.10	150	103.9	NR	0.20	929	200	35.51	3879	NR	P
B01 L150W120N1(a)	D	150	150	-	-	-	-	44.9	3.3	28040	-	-	C	W	120	0.37	150	103.9	NR	0.20	929	200	31.76	6940	NR	P
B01 L150W120N2(a)	D	150	150	-	-	-	-	44.9	3.3	28040	-	-	C	W	120	0.73	150	103.9	NR	0.20	929	200	41.86	4573	NR	P
B01 L150W120N3(a)	D	150	150	-	-	-	-	44.9	3.3	28040	-	-	C	W	120	1.10	150	103.9	NR	0.20	929	200	45.32	3301	NR	P
B01 L200W80N1(a)	D	150	150	-	-	-	-	44.9	3.3	28040	-	-	C	W	80	0.37	200	103.9	NR	0.20	929	200	21.50	7047	NR	P
B01 L200W80N2(a)	D	150	150	-	-	-	-	44.9	3.3	28040	-	-	C	W	80	0.73	200	103.9	NR	0.20	929	200	33.41	5475	NR	P
B01 L200W80N3(a)	D	150	150	-	-	-	-	44.9	3.3	28040	-	-	C	W	80	1.10	200	103.9	NR	0.20	929	200	38.27	4181	NR	P
B01 L200W120N1(a)	D	150	150	-	-	-	-	44.9	3.3	28040	-	-	C	W	120	0.37	200	103.9	NR	0.20	929	200	35.82	7827	NR	P
B01 L200W120N2(a)	D	150	150	-	-	-	-	44.9	3.3	28040	-	-	C	W	120	0.73	200	103.9	NR	0.20	929	200	47.34	5172	NR	P
B01 L200W120N3(a)	D	150	150	-	-	-	-	44.9	3.3	28040	-	-	C	W	120	1.10	200	103.9	NR	0.20	929	200	51.16	3726	NR	P
K01 S1-1	D	100	100	-	-	-	-	34.9	2.7	25149	-	-	C	W	10	0.53	145	152.6	NR	0.42	3269	300	6.25	7711	NR	R
K01 S1-2	D	100	100	-	-	-	-	36.3	2.8	25594	-	-	C	W	10	0.53	250	152.0	NR	0.42	3269	300	57.8	7161	NR	R
K01 S1-3	D	100	100	-	-	-	-	36.3	2.8	25594	-	-	C	W	20	0.53	145	151.7	NR	0.42	3269	300	98.4	6105	NR	R
K01 S1-4	D	100	100	-	-	-	-	36.3	2.8	25594	-	-	C	W	20	0.53	175	151.6	NR	0.42	3269	300	8.78	5452	NR	P
K01 S1-5	D	100	100	-	-	-	-	34.9	2.7	25149	-	-	C	W	30	0.53	100	151.5	NR	0.42	3269	300	12.89	5339	NR	P
K01 S1-6	D	100	100	-	-	-	-	34.9	2.7	25149	-	-	C	W	30	0.53	175	151.4	NR	0.42	3269	300	14.71	6095	NR	R
K01 S1-7	D	100	100	-	-	-	-	38.8	2.9	26353	-	-	C	W	30	0.53	250	151.4	NR	0.42	3269	300	12.83	5318	NR	P
K01 S1-8	D	100	100	-	-	-	-	36.3	2.8	25594	-	-	C	W	50	0.53	250	151.4	NR	0.42	3269	300	22.52	5602	NR	NR

B01: Brosens (2001); K01: Kamiharako et al. (2001)

Table B.7. Experimental shear test database (VII)

		Geometry of RC beam						Material properties					Plate strengthening							Adhesive		Load configuration				
Specimen (1)	Test (2)	b mm (3)	h mm (4)	A_s mm^2 (5)	A_s' mm^2 (6)	A_w mm^2 (7)	s_w mm (8)	f_{cm} MPa (9)	f_{ctm} MPa (10)	E_c MPa (11)	f_{ym} MPa (12)	E_s GPa (13)	M (14)	F (15)	b_L mm (16)	t_L mm (17)	L_L mm (18)	E_L GPa (19)	ε_{Lu} $\mu\varepsilon$ (20)	t_a mm (21)	G_a MPa (22)	L mm (23)	P_{exp} kN (24)	$\varepsilon_{L,max}$ $\mu\varepsilon$ (25)	τ_{max} MPa (26)	Mode (27)
K01 S1-9	D	100	100	-	-	-	-	41.5	3.1	27126	-	-	C	W	70	0.53	175	151.4	NR	0.42	3269	300	29.84	5302	NR	P
K01 S1-10	D	100	100	-	-	-	-	41.5	3.1	27126	-	-	C	W	90	0.53	175	151.4	NR	0.42	3269	300	29.38	4061	NR	P
N01 C5SCFH(1)	D	100	100	-	-	-	-	57.6	4.0	31019	-	-	C	W	50	0.59	300	147.7	NR	0.42	3269	300	25.63	5914	6.79	P
N01 C5SCFH(2)	D	100	100	-	-	-	-	57.6	4.0	31019	-	-	C	W	50	0.59	300	147.7	NR	0.42	3269	300	25.32	5844	6.79	P
N01 C5SCFH(3)	D	100	100	-	-	-	-	57.6	4.0	31019	-	-	C	W	50	0.59	300	147.7	NR	0.42	3269	300	27.24	6286	6.79	P
N01 C5 SCF(1)	D	100	100	-	-	-	-	57.6	4.0	31019	-	-	C	W	50	0.59	300	72.9	NR	0.42	3269	300	18.90	8838	7.49	R
N01 C5 SCF(2)	D	100	100	-	-	-	-	57.6	4.0	31019	-	-	C	W	50	0.59	300	72.9	NR	0.42	3269	300	16.96	7928	7.49	P
N01 C5 SCF(3)	D	100	100	-	-	-	-	57.6	4.0	31019	-	-	C	W	50	0.59	300	72.9	NR	0.42	3269	300	16.63	7777	7.49	P
N01 C5SCFL(1)	D	100	100	-	-	-	-	57.6	4.0	31019	-	-	C	W	50	0.59	300	32.9	NR	0.42	3269	300	12.19	12622	7.33	P
N01 C5SCFL(2)	D	100	100	-	-	-	-	57.6	4.0	31019	-	-	C	W	50	0.59	300	32.9	NR	0.42	3269	300	11.79	12208	7.33	P
N01 C5SCFL(3)	D	100	100	-	-	-	-	57.6	4.0	31019	-	-	C	W	50	0.59	300	32.9	NR	0.42	3269	300	12.22	12653	7.33	P
N01 C5HCF(1)	D	100	100	-	-	-	-	57.6	4.0	31019	-	-	C	W	50	0.59	300	117.2	NR	0.42	3269	300	19.99	5833	9.13	R
N01 C5HCF(2)	D	100	100	-	-	-	-	57.6	4.0	31019	-	-	C	W	50	0.59	300	117.2	NR	0.42	3269	300	19.47	5683	9.13	P
N01 C5HCF(3)	D	100	100	-	-	-	-	57.6	4.0	31019	-	-	C	W	50	0.59	300	117.2	NR	0.42	3269	300	16.24	4740	9.13	R
N01 C5ARF(1)	D	100	100	-	-	-	-	57.6	4.0	31019	-	-	A	W	50	0.61	300	36.0	NR	0.42	3269	300	12.76	11564	7.17	P
N01 C5ARF(2)	D	100	100	-	-	-	-	57.6	4.0	31019	-	-	A	W	50	0.61	300	36.0	NR	0.42	3269	300	12.85	11650	7.17	P
N01 C5ARF(3)	D	100	100	-	-	-	-	57.6	4.0	31019	-	-	A	W	50	0.61	300	36.0	NR	0.42	3269	300	11.88	10766	7.17	P
N01 M5SCFH(1)	D	100	100	-	-	-	-	50.9	3.7	29523	-	-	C	W	50	0.59	300	147.7	NR	0.42	3269	300	20.64	4763	6.83	P
N01 M5SCFH(2)	D	100	100	-	-	-	-	50.9	3.7	29523	-	-	C	W	50	0.59	300	147.7	NR	0.42	3269	300	22.28	5142	6.83	P
N01 M5SCFH(3)	D	100	100	-	-	-	-	50.9	3.7	29523	-	-	C	W	50	0.59	300	147.7	NR	0.42	3269	300	23.57	5439	6.83	P

K01: Kamiharako et al. (2001); N01: Nakaba et al. (2001)

Table B.8. Experimental shear test database (VIII)

		Geometry of RC beam						Material properties					Plate strengthening							Adhesive		Load configuration				
Specimen (1)	Test (2)	b mm (3)	h mm (4)	A_s mm^2 (5)	A_s' mm^2 (6)	A_w mm^2 (7)	s_w mm (8)	f_{cm} MPa (9)	f_{ctm} MPa (10)	E_c MPa (11)	f_{ym} MPa (12)	E_s GPa (13)	M (14)	F (15)	b_L mm (16)	t_L mm (17)	L_L mm (18)	E_L GPa (19)	ε_{Lu} με (20)	t_a mm (21)	G_a MPa (22)	L mm (23)	P_{exp} kN (24)	$\varepsilon_{L,max}$ με (25)	τ_{max} MPa (26)	Mode (27)
N01 M5SCF(1)	D	100	100	-	-	-	-	50.9	3.7	29523	-	-	C	W	50	0.59	300	72.9	NR	0.42	3269	300	15.35	7176	6.25	P
N01 M5SCF(2)	D	100	100	-	-	-	-	50.9	3.7	29523	-	-	C	W	50	0.59	300	72.9	NR	0.42	3269	300	16.86	7882	6.25	P
N01 M5SCF(3)	D	100	100	-	-	-	-	50.9	3.7	29523	-	-	C	W	50	0.59	300	72.9	NR	0.42	3269	300	16.29	7615	6.25	P
N01 M5SCFL(1)	D	100	100	-	-	-	-	50.9	3.7	29523	-	-	C	W	50	0.59	300	32.9	NR	0.42	3269	300	8.75	9061	7.44	P
N01 M5SCFL(2)	D	100	100	-	-	-	-	50.9	3.7	29523	-	-	C	W	50	0.59	300	32.9	NR	0.42	3269	300	8.73	9035	7.44	P
N01 M5SCFL(3)	D	100	100	-	-	-	-	50.9	3.7	29523	-	-	C	W	50	0.59	300	32.9	NR	0.42	3269	300	10.02	10371	7.44	P
N01 M5HCF(1)	D	100	100	-	-	-	-	50.9	3.7	29523	-	-	C	W	50	0.59	300	117.2	NR	0.42	3269	300	16.56	4832	7.71	P
N01 M5HCF(2)	D	100	100	-	-	-	-	50.9	3.7	29523	-	-	C	W	50	0.59	300	117.2	NR	0.42	3269	300	16.25	4742	7.71	P
N01 M5HCF(3)	D	100	100	-	-	-	-	50.9	3.7	29523	-	-	C	W	50	0.59	300	117.2	NR	0.42	3269	300	14.64	4272	7.71	P
N01 M5ARF(1)	D	100	100	-	-	-	-	50.9	3.7	29523	-	-	A	W	50	0.61	300	36.0	NR	0.42	3269	300	12.85	11650	6.50	P
N01 M5ARF(2)	D	100	100	-	-	-	-	50.9	3.7	29523	-	-	A	W	50	0.61	300	36.0	NR	0.42	3269	300	12.17	11034	6.50	P
N01 M5ARF(3)	D	100	100	-	-	-	-	50.9	3.7	29523	-	-	A	W	50	0.61	300	36.0	NR	0.42	3269	300	12.71	11518	6.50	P
N01 C2SCF(1)	D	100	100	-	-	-	-	23.8	1.9	20869	-	-	C	W	50	0.59	300	72.9	NR	0.42	3269	300	14.09	6587	6.99	P
N01 C2SCF(2)	D	100	100	-	-	-	-	23.8	1.9	20869	-	-	C	W	50	0.59	300	72.9	NR	0.42	3269	300	13.87	6484	6.99	P
N01 C2SCF(3)	D	100	100	-	-	-	-	23.8	1.9	20869	-	-	C	W	50	0.59	300	72.9	NR	0.42	3269	300	15.08	7052	6.99	P
N01 C2PSCF(1)	D	100	100	-	-	-	-	23.8	1.9	20869	-	-	C	W	50	0.59	300	72.9	NR	0.42	3269	300	14.54	6797	5.60	P
N01 C2PSCF(2)	D	100	100	-	-	-	-	23.8	1.9	20869	-	-	C	W	50	0.59	300	72.9	NR	0.42	3269	300	15.14	7078	5.60	P
N01 C2PSCF(3)	D	100	100	-	-	-	-	23.8	1.9	20869	-	-	C	W	50	0.59	300	72.9	NR	0.42	3269	300	15.29	7148	5.60	P
S01 P1	D	200	200	48	48	589	40	33.0	2.6	24518	-	-	C	W	100	0.43	200	105.0	13333	0.42	3269	300	35.00	7752	1.14	NR
S01 P2	D	200	200	48	48	589	40	33.0	2.6	24518	-	-	C	W	100	0.43	200	105.0	13333	0.42	3269	300	35.00	7752	1.14	NR

N01: Nakaba et al. (2001); S01: Souza and Apleton (2001)

Table B.9. Experimental shear test database (IX)

		Geometry of RC beam						Material properties					Plate strengthening							Adhesive		Load configuration				
Specimen (1)	Test (2)	b mm (3)	h mm (4)	A_s mm^2 (5)	A_s' mm^2 (6)	A_w mm^2 (7)	s_w mm (8)	f_{cm} MPa (9)	f_{ctm} MPa (10)	E_c MPa (11)	f_{ym} MPa (12)	E_s GPa (13)	M (14)	F (15)	b_L mm (16)	t_L mm (17)	L_L mm (18)	E_L GPa (19)	ε_{Lu} με (20)	t_a mm (21)	G_a MPa (22)	L mm (23)	P_{exp} kN (24)	$\varepsilon_{L,max}$ με (25)	τ_{max} MPa (26)	Mode (27)
S01 P3	D	200	200	48	48	589	40	33.0	2.6	24518	-	-	C	W	100	0.43	150	105.0	13333	0.42	3269	300	29.00	6423	1.21	NR
S01 P4	D	200	200	48	48	589	40	33.0	2.6	24518	-	-	C	W	100	0.43	150	105.0	13333	0.42	3269	300	29.00	6423	1.21	NR
F02 A	D	140	140	-	-	-	-	38.0	2.9	26115	-	-	C	W	50	0.80	190	62.5	8000	0.20	3269	200	NR	NR	NR	NR
F02 B	D	140	140	-	-	-	-	38.0	2.9	26115	-	-	C	W	50	0.80	190	50.0	11000	0.20	3269	200	NR	NR	NR	NR
F02 C	D	140	140	-	-	-	-	38.0	2.9	26115	-	-	C	W	50	0.80	190	53.7	8000	0.20	3269	200	NR	NR	NR	NR
U02 AS1-1	D	200	200	63	-	-	-	NR	NR	NR	NR	177.0	C	W	120	0.11	600	230.0	15126	0.42	3269	640	NR	NR	NR	NR
U02 AS1-2	D	200	200	63	-	-	-	NR	NR	NR	NR	177.0	C	W	120	0.11	601	230.0	15126	0.42	3269	640	NR	NR	NR	NR
U02 AS1-3	D	200	200	63	-	-	-	NR	NR	NR	NR	177.0	C	W	120	0.11	602	230.0	15126	0.42	3269	640	NR	NR	NR	NR
U02 AS2-0	D	150	150	63	-	-	-	NR	NR	NR	NR	177.0	C	W	120	0.11	603	230.0	15126	0.42	3269	640	NR	NR	NR	NR
U02 AS2-3	D	150	150	63	-	-	-	NR	NR	NR	NR	177.0	C	W	120	0.11	604	230.0	15126	0.42	3269	640	NR	NR	NR	NR
U02 AS3-0	D	150	150	91	-	-	-	NR	NR	NR	NR	170.0	C	W	120	0.11	605	230.0	15126	0.42	3269	640	NR	NR	NR	NR
U02 AS3-1	D	150	150	91	-	-	-	NR	NR	NR	NR	170.0	C	W	120	0.11	606	230.0	15126	0.42	3269	640	NR	NR	NR	NR
U02 AS3-2	D	150	150	91	-	-	-	NR	NR	NR	NR	170.0	C	W	120	0.11	607	230.0	15126	0.42	3269	640	NR	NR	NR	NR
U02 BS4-1	D	150	150	23	-	-	-	NR	NR	NR	NR	188.0	C	W	150	0.11	608	230.0	15126	0.42	3269	640	NR	NR	NR	NR
U02 BS4-2	D	150	150	23	-	-	-	NR	NR	NR	NR	188.0	C	W	150	0.11	609	230.0	15126	0.42	3269	640	NR	NR	NR	NR
U02 BS4-3	D	150	150	23	-	-	-	NR	NR	NR	NR	188.0	C	W	150	0.11	610	230.0	15126	0.42	3269	640	NR	NR	NR	NR
U02 BS2-2	D	150	150	63	-	-	-	NR	NR	NR	NR	177.0	C	W	150	0.11	611	230.0	15126	0.42	3269	640	NR	NR	NR	NR
U02BS5-0	D	150	150	123	-	-	-	NR	NR	NR	NR	178.0	C	W	150	0.11	612	230.0	15126	0.42	3269	640	NR	NR	NR	NR
U02 BS5-2	D	150	150	123	-	-	-	NR	NR	NR	NR	178.0	C	W	150	0.11	613	230.0	15126	0.42	3269	640	NR	NR	NR	NR
Sa03 T1-1	D	100	100	-	-	-	-	31.9	2.5	24138	-	-	C	W	50	0.84	50	99.5	10955	0.42	3269	400	15.80	3781	NR	P

S01: Souza and Appleton (2001); F02: Ferrier and Hamelin (2002); U02: Ueda et al. (2002); S03: Sato and Vecchio (2003)

Table B.10. Experimental shear test database (X)

		Geometry of RC beam						Material properties					Plate strengthening							Adhesive		Load configuration				
Specimen (1)	Test (2)	b mm (3)	h mm (4)	A_s mm^2 (5)	A_s' mm^2 (6)	A_w mm^2 (7)	s_w mm (8)	f_{cm} MPa (9)	f_{ctm} MPa (10)	E_c MPa (11)	f_{ym} MPa (12)	E_s GPa (13)	M (14)	F (15)	b_L mm (16)	t_L mm (17)	L_L mm (18)	E_L GPa (19)	ε_{Lu} με (20)	t_a mm (21)	G_a MPa (22)	L mm (23)	P_{exp} kN (24)	$\varepsilon_{L,max}$ με (25)	τ_{max} MPa (26)	Mode (27)
Sa03 T1 2	D	100	100	-	-	-	-	31.9	2.5	24138	-	-	C	W	50	0.84	50	99.5	10955	0.42	3269	400	19.40	4642	NR	P
Sa03 T2 1	D	100	100	-	-	-	-	31.9	2.5	24138	-	-	C	W	50	0.84	100	99.5	10955	0.42	3269	400	21.70	5193	NR	P
Sa03 T2 2	D	100	100	-	-	-	-	31.9	2.5	24138	-	-	C	W	50	0.84	100	99.5	10955	0.42	3269	400	26.40	6317	NR	P
Sa03 T4 1	D	100	100	-	-	-	-	31.9	2.5	24138	-	-	C	W	50	0.84	200	99.5	10955	0.42	3269	400	26.30	6293	NR	P
Sa03 T4 2	D	100	100	-	-	-	-	31.9	2.5	24138	-	-	C	W	50	0.84	200	99.5	10955	0.42	3269	400	23.30	5575	NR	P
S03: Sato and Vecchio (2003)																										

APPENDIX C

EXPERIMENTAL PROGRAM

C.1. Introduction

To contribute to the better understanding of the flexural behavior of RC structures externally strengthened with bonded FRP laminates, ten strengthened beams were tested by the author at the Structural Technology Laboratory of the Department of Construction Engineering at the School of Civil Engineering of Barcelona.

The following sections describe, with more detail than Chapter 2, the geometry, material properties and casting of the beam specimens, the instrumentation affixed to the beams, the testing procedure, some results and a discussion about them, and finally a comparison between the experimental and numerical results obtained by a moment-curvature analysis of the strengthened section.

C.2. Test set-up

C.2.1. Specimen details: geometry, materials and fabrication

Geometry

Ten simply supported beams reinforced with CFRP laminates were tested during this experimental program. The beam dimensions were 2400 x 300 x 200 *mm*.

In view of its internal tensile reinforcement identified in Table C.1, the beams were divided into two groups: Beam group 1 and Beam group 2. To avoid the possibility of shear failure, the beams were also provided with enough shear reinforcement.

Table C.1. Internal reinforcement of tested beams.

Beam	Bottom longitudinal rebars	Top longitudinal rebars	Transverse stirrups
1	$2\phi 16\ mm$ ($\rho_s = 0.67\%$)	$2\phi 8\ mm$ ($\rho_{s'} = 0.16\%$)	$\phi 12\ mm$ / $0.15\ m$ ($\rho_w = 0.50\%$)
2	$2\phi 20\ mm$ ($\rho_s = 1.40\%$)	$2\phi 8\ mm$ ($\rho_{s'} = 0.16\%$)	$\phi 12\ mm$ / $0.10\ m$ ($\rho_w = 0.50\%$)

Materials

Cylinder compression tests and splitting tensile tests were performed to obtain the concrete's mechanical properties (Figure C.1). The average 28-day compressive strength was 35.2 *MPa* and the tensile strength obtained from the test and reduced according to the CEB FIB Model Code 90 was 2.76 *MPa*. Since no strain gauges were affixed to the concrete cylinder, information about the concrete modulus of elasticity is unavailable.

The nominal yield strength of internal steel reinforcement was 500 *MPa*. According to the data of the manufacturer, the average yield strength should be 550 *MPa*. Results of 450 *mm* long rebars tested in tension (Figure C.1) suggested a slightly higher value (580 *MPa*).

Prefabricated laminates (CFRP) from S&P Clever Reinforcement Company supplied by courtesy of Bettor MBT and Fosroc Euco were bonded as an external reinforcement with different arrangements as explained in Chapter 2. These arrangements are repeated here, in Table C.2 and Table C.3, for the sake of completeness. According to the manufacturer, laminates should have a nominal elastic modulus of 150 *GPa*, and a nominal tensile stress at failure of 2500 *MPa* (at 1.6% strain). Tests conducted at the Structural Technology Laboratory (see Figure C.1) according to the ASTM D3039 Standard Test Method for tensile properties of Fiber-Resin Composites (ASTM D3039, 1989) gave a mean value of 147 *GPa* for the elastic modulus.

Additionally, in some tests, a ply of S&P C Sheet 240 was applied as an external anchorage. The nominal thickness of the carbon fiber lamina should be 0.117 *mm* with an elastic modulus of 240 *GPa* and a ultimate strength of 3500 *MPa*. The mechanical properties of the resulting wet lay-up composite were obtained by the tensile test according to the ASTM D3039 of some specimens composed by some carbon fiber laminas embedded on a resin matrix. The mean value of the experimental elastic modulus of the carbon-resin system was 169 *GPa*, and the mean value of the experimental ultimate tensile stress was 1740 *MPa*.

Table C.2. External reinforcement of Beam group 1.

Beam	Test #	External reinforcement	ρ_L/ρ_s (%)
1/E	1	Control Beam	-
1/D	1	1 laminate S&P 150/2000, 100 *mm* x 1.4 *mm*, length = 1500 *mm* (Euxit 220)	0.34
	2	2 laminates S&P 150/2000, 50 *mm* x 1.4 *mm*, length = 1800 *mm* (MBrace adhesive)	0.34
1/C	1	1 laminate S&P 150/2000, 100 *mm* x 1.4 *mm*, length = 1800 *mm* (Euxit 220)	0.34
	2	1 laminate S&P 150/2000, 100 *mm* x 1.4 *mm*, length = 1800 *mm* (MBrace adhesive) and S&P C Sheet 240 (MBrace saturant)	0.43
1/B	1	1 laminate S&P 150/2000, 100 *mm* x 1.4 *mm*, length = 1800 *mm* (Euxit 220)	0.34
	2	2 slot-applied laminates S&P 150/2000, 10 *mm* x 1.4 *mm*, length = 1800 *mm* (MBrace adhesive)	0.07
1/A	1	1 laminate S&P 150/2000, 100 *mm* x 1.4 *mm*, length = 1800 *mm* (Euxit 220)	0.34

Table C.3. External reinforcement of Beam group 2.

Beam	Test #	External reinforcement	ρ_L/ρ_s (%)
2/E	1	Control Beam	-
2/D	1	1 laminate S&P 150/2000, 100 *mm* x 1.4 *mm*, length = 1800 *mm* (Euxit 220)	0.22
	2	2 laminates S&P 150/2000, 100 *mm* x 1.4 *mm*, length = 1800 *mm* (Euxit 220)	0.44
2/C	1	2 laminates S&P 150/2000, 50 *mm* x 1.4 *mm*, length = 1800 *mm* (MBrace adhesive)	0.22
2/B	1	2 laminates S&P 150/2000, 50 *mm* x 1.4 *mm*, length = 1800 *mm* (MBrace adhesive) and S&P C Sheet 240 (MBrace saturant)	0.22
2/A	1	1 laminate S&P 150/2000, 100 *mm* x 1.4 *mm*, length = 1800 *mm* (MBrace adhesive) and S&P C Sheet 240 (MBrace Saturant)	0.22

Pultruded laminates were bonded to the bottom side of the beam by using two types of epoxy resin. Euxit 220, supplied by FOSROC EUCO, was employed in Beams 1/A, 1/B, 1/C, 1/D and 2/D. According to the manufacturer, its elastic modulus at 20º*C* was 9600 *MPa*. MBrace adhesive, supplied by BETTOR MBT, was applied in the remaining beams. According to the technical sheet, the elastic modulus of the adhesive obtained by testing dumb-bell specimens at 23º*C* was 10700 *MPa*. The wet lay-up anchorages were bonded to the concrete by MBrace Saturant which is an epoxy resin with a nominal elastic modulus at 23º*C* of 7300 *MPa*.

Figure C.1. Tests to characterize concrete, internal steel and CFRP properties.

Fabrication of test specimens

Beams were cast by courtesy of GALA S.A., in a building construction of Montcada i Reixac on April of 2001 (Figure C.2). Ten beams and twenty concrete cylinders of 150 x 300 *mm* were stored in the construction for seven days. It should be mentioned that some cracks appeared on the top side of the beams due to a plastic settlement of the concrete during the curing process. These cracks of 2 *mm* width were placed on the top of the shear stirrups.

Figure C.2. Casting of the beam specimens.

Bonding of laminates

To ensure the load transfer from the external reinforcement to the substrate, the concrete surface was roughened by grinding. After roughening, the surface was blown with clean air to remove dust. Laminates were cleaned with acetone before bonding. The Euxit 220 epoxy was applied by hand with an approximate thickness of 3 - 4 *mm* in Beams 1/A, 1/B, 1/C, 1/D and 2/D. Due to the work conditions during this process (beams were turned upside down), the adhesive was applied only to the concrete surface by using a metal spatula, as shown in Figure C.3. In the remaining beams, the external reinforcement was bonded by using another epoxy trademark, MBrace adhesive. By following the BETTOR MBT guidelines, the concrete surface was previously treated with a primer to improve bonding.

In Beams 2/A and 2/B, CFRP wet lay-up laminates were additionally used as external anchorages. In this case, the surface was sandpapered and primed. A first coat of MBrace saturant was extended on both the CFRP sheet and the concrete support by using a roller. Then, the fiber anchorage was bonded to the concrete and a second adhesive coat was applied. By using the same roller, the excess of adhesive was removed.

Figure C.3. Bonding application procedure.

C.2.2. Instrumentation and testing procedure

Electrical resistance strain gauges were affixed in different locations along the external surface of the CFRP laminates to measure the strain along the bonded reinforcement. Two strain gauges were affixed in the concrete at midspan: one in the compression zone and the other one at the mid-depth of the section.

The beam deflection was monitored throughout the test with three displacement transducers: one of them placed at midspan and the other two close to the supports.

The simply supported beams with an effective span of 2.0 *m* were tested in a three-point bending configuration by using deflection control. The test set-up is shown in Figure C.4.

Load was applied monotonically by means of a computer-controlled MTS hydraulic actuator with a maximum load capacity of 1000 *kN* and a maximum stroke of 250 *mm*. The data acquisition system was an analog-to-digital converter, which contained an analog multiplexing module with 16 channels (DBK54), and five modules of eight channels to connect the strain gauges (DBK43A).

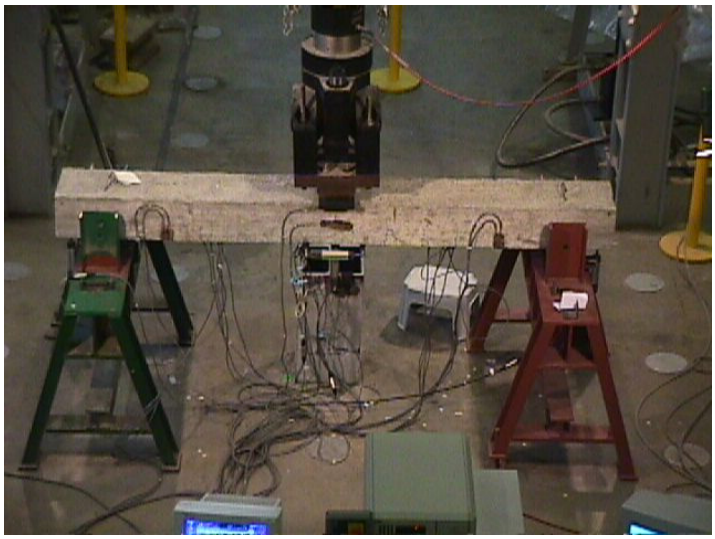

Figure C.4. View of the test set-up.

C.3. Test results

For each specimen, a summary of test observations and test results are given in this section. All beams, with the exception of Beam 1/A, were loaded up to a theoretical service load before bonding the external reinforcement to simulate a stress state similar to a real strengthening situation. Therefore, all beams except Beam 1/A were precracked before plate strengthening. After applying the external reinforcement, beams were tested up to failure. Figure C.6, Figure C.10, Figure C.16, Figure C.22, Figure C.28, Figure C.34, Figure C.38, Figure C.44, Figure C.52, Figure C.59, Figure C.66, Figure C.70, Figure C.77, and Figure C.83 show the test set-up for each specimen. Table C.4, Table C.6, Table C.8, Table C.10, Table C.12, Table C.14, Table C.16, Table C.18, Table C.20, Table C.22, Table C.24, Table C.25, Table C.27, and Table C.29 summarize for service load tests: the cracking load (F_{cr}), the service load (F_s), the yielding load (F_y), the failure load (F_u), and the displacements at midspan associated to both load levels ($\delta(x = L/2)$); and for failure tests: the service load (F_s), the yielding load (F_y), the failure load (F_u), and the deflections at midspan ($\delta(x = L/2)$) and the laminatestrain at midspan (ε_L $(x = L/2)$) under these different load levels. The maximum laminate strain was obtained as the average of the strain gauges placed on the laminate at midspan. The crack pattern under both service and failure load and the instrumentation affixed are presented in Figure C.7, Figure C.11, Figure C.17, Figure C.23, Figure C.29, Figure C.35, Figure C.39, Figure C.45, Figure C.53, Figure C.60, Figure C.71, Figure C.78 and Figure C.84. A more detailed description of the location of the strain gauges is given by Table C.5, Table C.7, Table C.9, Table C.11, Table C.13, Table C.15, Table C.17, Table C.19, Table C.21, Table C.23, Table C.26, Table C.28 and Table C.30. First row of these tables indicates the name of the strain gauge. Second row indicates the surface where the strain gauge was affixed, being "C" concrete and "L" laminate. The coordinate system used in these tables has the origin at midspan as shown in Figure C.5.

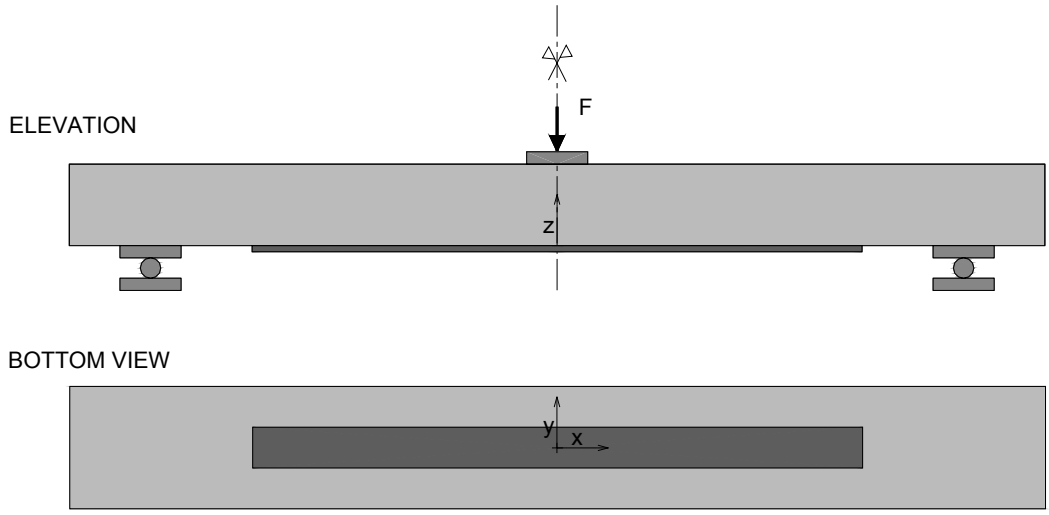

Figure C.5. Origin of coordinates.

Figure C.9, Figure C.13, Figure C.19, Figure C.25, Figure C.37, Figure C.41, Figure C.49, Figure C.56, Figure C.63, Figure C.69, Figure C.74, Figure C.80 and Figure C.87 show the applied load against deflection at midspan, and the applied load against the laminate strain at midspan for the strengthened beams. In addition, the strain evolution along the laminate length is given for some load levels of the failure test by Figure C.14, Figure C.20, Figure C.26, Figure C.32, Figure C.42, Figure C.50, Figure C.57, Figure C.64, Figure C.75, Figure C.81, and Figure C.88. Finally, the mean shear stress between two strain gauges is obtained as the increment in the tensile force divided by the distance between the strain gauges. The shear stress distribution is plotted for different load levels of each strengthened beam in Figure C.15, Figure C.21, Figure C.27, Figure C.43, Figure C.51, Figure C.58, Figure C.65, Figure C.76, and Figure C.82.

In case, two laminates were applied to strengthen the reinforced concrete beam, the laminate close to the data acquisition system in the test set-up was named laminate 1, the other one was known as laminate 2.

C.3.1. Beam 1/E (Control Beam)

Test observations

The control beam showed a ductile flexural response typical of reinforced concrete beams. First cracking occurred at a load of 12.3 *kN*. Thereafter, the crack pattern extended along the beam and crack widths increased steadily. The average crack distance was 150 *mm*. As shown in Figure C.9, the initial stiffness changed with the steel yielding at a load of 75.0 *kN*. Failure took place due to concrete crushing (see Figure C.7) within the compression zone at a load of 80.0 *kN*.

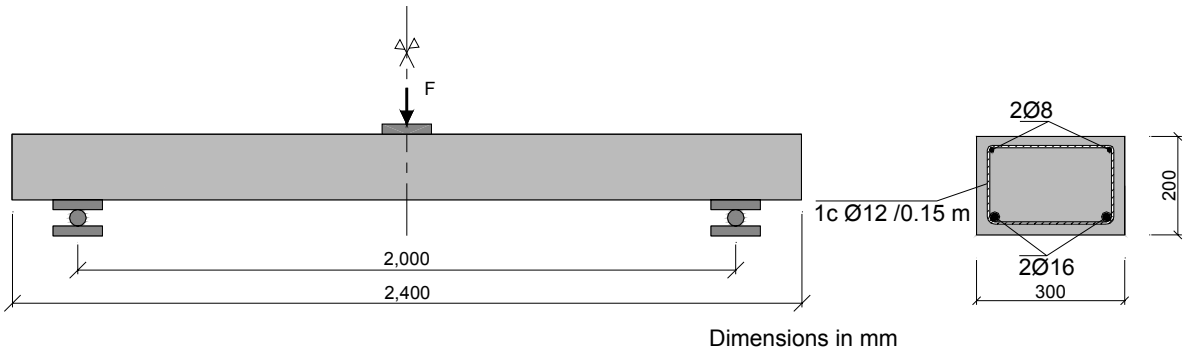

Figure C.6. Test set-up of Beam 1/E.

Table C.4. Summary of test results.

	Service test		Failure test		
	F_{cr} (*kN*)	F_s (*kN*)	F_s (*kN*)	F_v (*kN*)	F_u (*kN*)
	12.3	49.5	50.3	75.0	80.0
$\delta(x = L/2)$ (*mm*)	0.9	7.3	7.6	12.6	40.5

Table C.5. Strain gauge distribution.

Gauge	1	2	3	4	5	6	7	8	9	10	11	12
Surface	C	C	C	-	C	C	C	C	C	C	C	-
x (*mm*)	-703	-700	-699	-	-20	0	0	0	657	674	700	-
y (*mm*)	0	0	30	-	0	0	-15	15	0	0	0	-
z (*mm*)	170	102	0	-	100	165	0	0	97	170	0	-

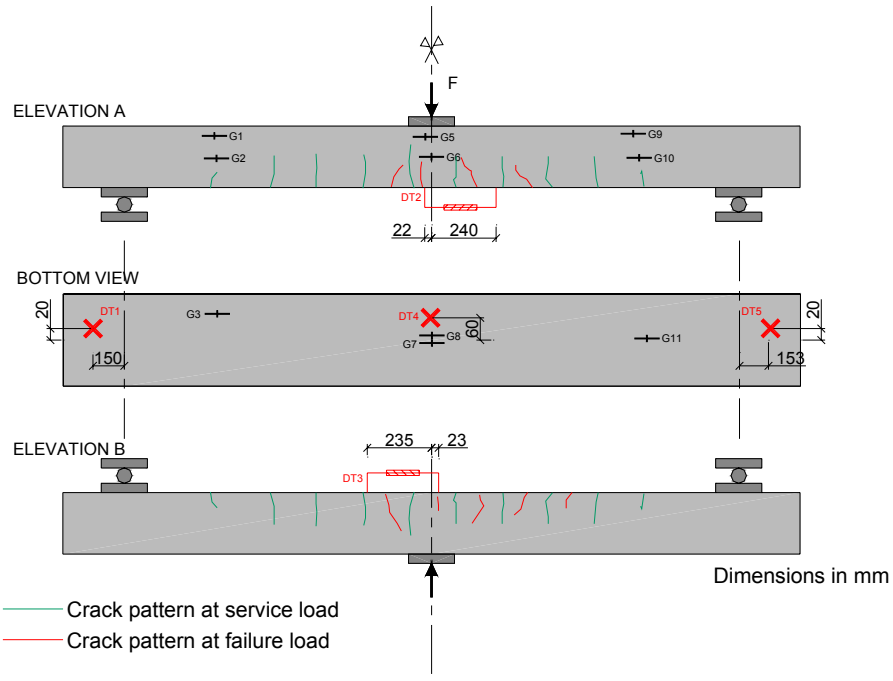

Figure C.7. Crack Pattern at service and at failure load, and instrumentation affixed to Beam 1/E.

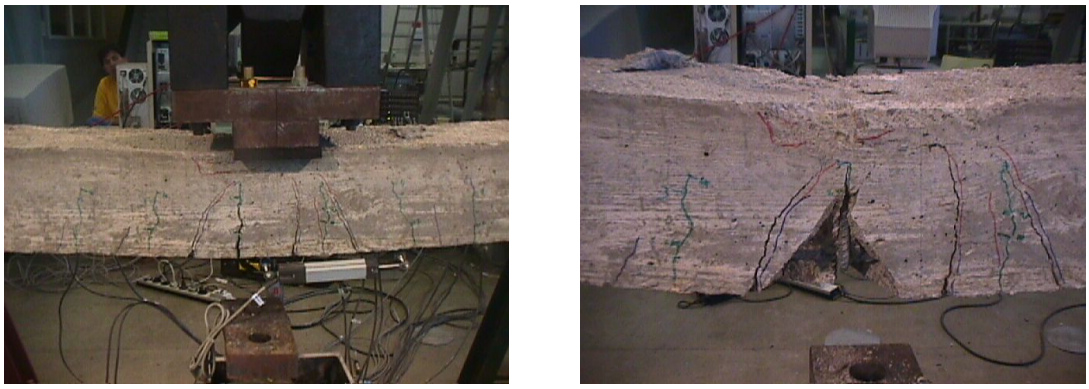

Figure C.8. Concrete crushing failure in Beam 1/E.

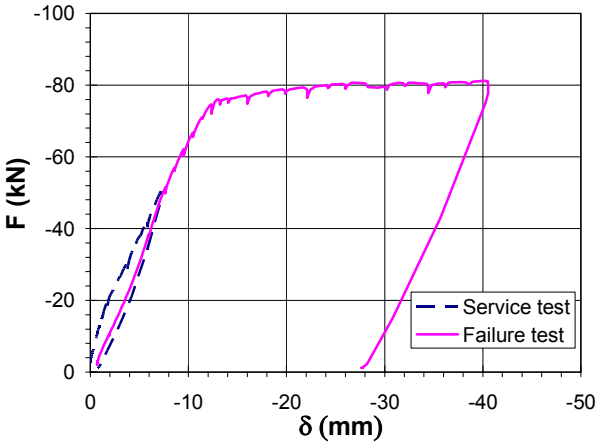

Figure C.9. Midspan displacement of Beam 1/E.

C.3.2. Beam 1/D

Test observations

Beam 1/D was tested in two stages. During the first stage, the unstrengthened beam was tested up to a load of 50.0 *kN* to simulate a stress state similar to real service conditions. Due to the applied preload, cracks grew within the same average distance (150 *mm*) as the control beam. After removing the beam from the test location, it was strengthened by means of a pultruded laminate 1500 *mm* long with a cross-section of 100 *mm* x 1.4 *mm* (Figure C.10). During the second stage, the failure test of the strengthened beam was performed in two cycles: the first one up to service load (50.0 *kN*) and the second up to failure (80.0 *kN*). As shown in Figure C.11, some intermediate cracks formed in Beam 1/D between the existing flexural cracks after reaching the service load. When the applied load reached 80.0 *kN*, the laminate peeled-off in a sudden and brittle manner before the yielding of the internal steel. A thin layer in the concrete cover near the bonded zone was also detached as shown in Figure C.12. Failure might have initiate at the plate end as shown by the high shear stress concentration near one of the laminate ends (see Figure C.15). The failure load (80.0 *kN*) did not increase in relation to the control beam. By comparing Figure C.13 to Figure C.9, and as will be shown in §C.4, the externally strengthened beam 1/D showed a reduction on the midspan displacements

in relation to control Beam 1/E due to the increase in stiffness. The maximum laminate strain of 2801 $\mu\varepsilon$ was obtained near midspan as shown in Figure C.14. In Figure C.15, the average value of shear stresses between strain gauges is plotted. Since the greater number of strain gauges was located at the laminate end, the average value near midspan is not reliable.

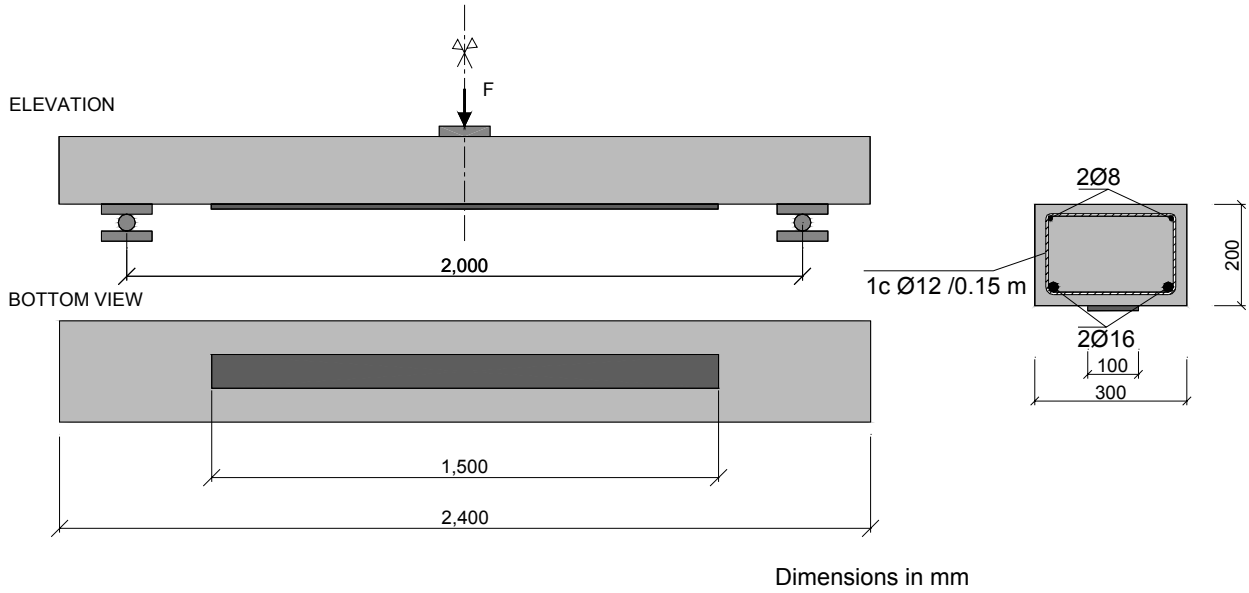

Figure C.10. Test set-up for Beam 1/D.

Table C.6. Summary of test results.

	Service test		Failure test		
	F_{cr} (kN)	F_s (kN)	F_s (kN)	F_y (kN)	F_u (kN)
	11.2	55.0	49.7	-	80.0
$\delta(x = L/2)$ (mm)	1.41	8.15	6.24	-	10.09
ε_L ($x = L/2$) ($\mu\varepsilon$)	-	-	1801	-	2801

Table C.7. Strain gauge distribution in Beam 1/D.

Gauge	1	2	3	4	5	6	7	8	9	10	11	12
Surface	C	C	L	C	C	C	C	-	C	C	C	C
x (mm)	-717	-712	-712	-740	0	0	0	-	708	696	700	700
y (mm)	0	96	-95	0	0	0	100	-	0	0	96	-85
z (mm)	23	0	0	23	82	-2	0	-	25	25	0	0

Gauge	13	14	15	16	17	18	19	20	21	22	23	24
Surface	L	L	L	L	L	L	L	L	L	L	L	L
x (mm)	-584	-707	-709	662	-6	0	0	86	706	706	660	582
y (mm)	0	-10	8	0	0	8	-8	0	-12	-29	0	0
z (mm)	0	0	0	0	0	0	0	0	0	0	0	0

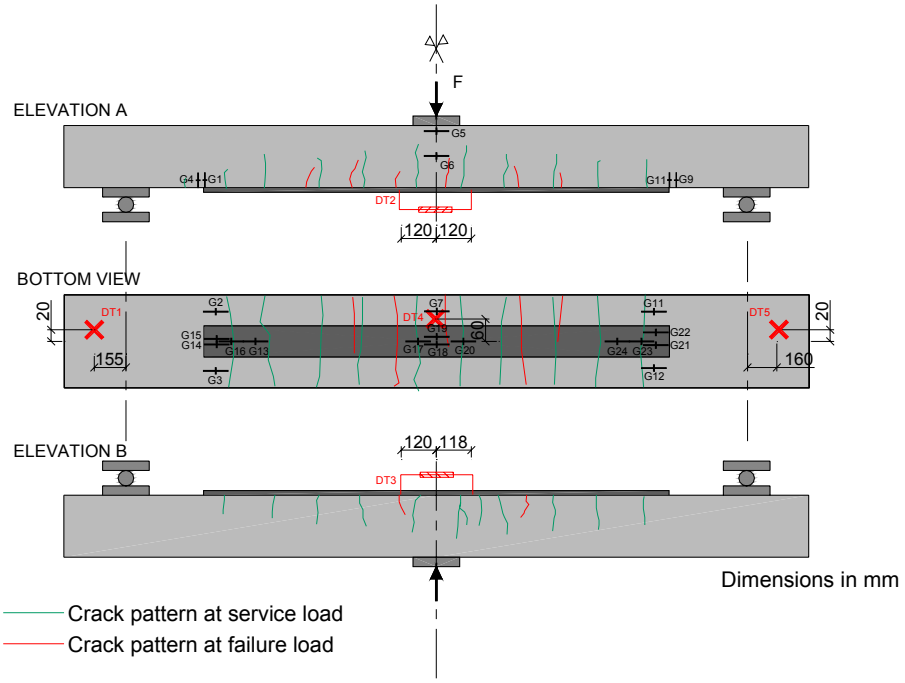

Figure C.11. Crack pattern at service and at failure load, and instrumentation affixed to Beam 1/D.

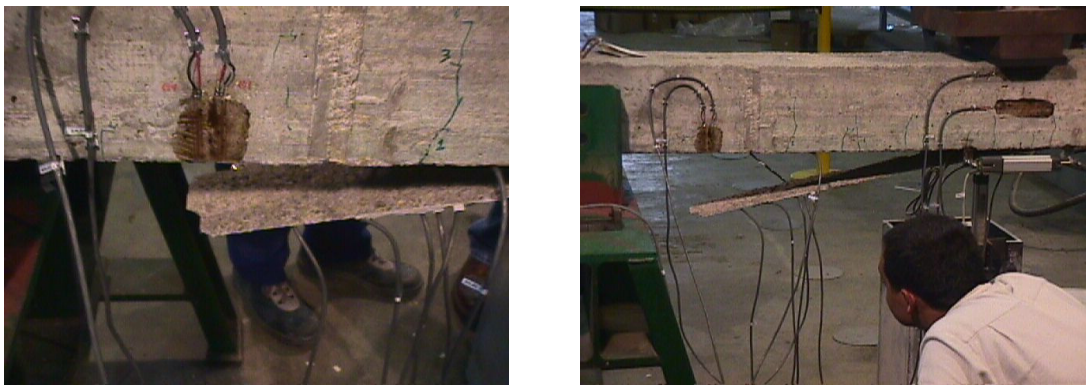

Figure C.12. Peeling failure in Beam 1/D due to a lack of anchorage.

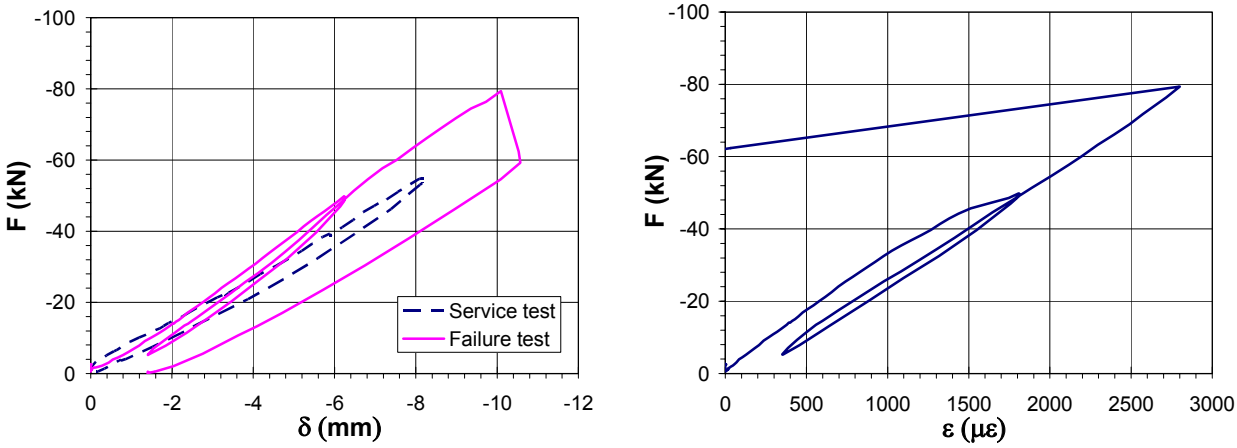

Figure C.13. Midspan displacement. Strain profile in the laminate center of Beam 1/D.

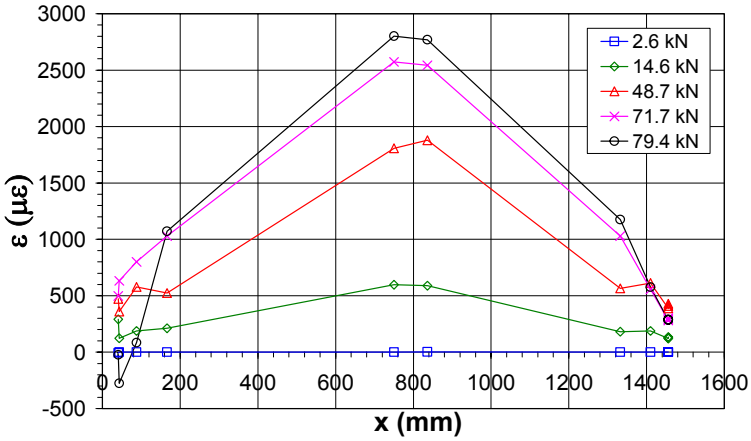

Figure C.14. Laminate strain distribution along Beam 1/D.

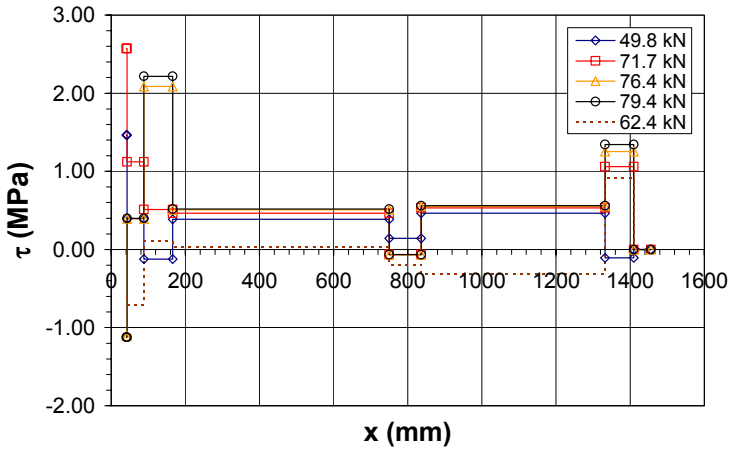

Figure C.15. Shear stress distribution along Beam 1/D.

C.3.3. Beam 1/C

Test observations

To reduce the high stress concentration observed at the laminate end in Beam 1/D, the bonded laminate was extended up to the supports in Beam 1/C and in the following tests, as shown in Figure C.16. Similar to Beam 1/D, Beam 1/C was preloaded to 47.8 *kN* before plate bonding. During the service test of the unstrengthened beam, the crack spacing showed an average of 150 *mm* (Figure C.17). After strengthening, the beam was tested to failure in two cycles: first to a service load state (50.2 *kN*) and second to load failure (104.0 *kN*). An increase of 26.9 % in the failure load was observed in relation to the control beam. During the failure test and after reaching the service load, some intermediate cracks with an inclination between 45º and 60º formed and propagated between the flexural cracks that opened in the service test of the unstrengthened beam. Although the extension of the laminate up to the supports did not change the mode of failure, the peeling initiation point moved towards midspan. Thus, in this case, the brittle laminate debonding was due to the effects of flexural or shear cracks and was probably initiated near the red intermediate crack shown in Figure C.18 (right). Since

strain gauges were not affixed to the internal steel, the analysis of the laminate strain distribution, given by Figure C.19, does not clearly show if the internal steel was yielded or not before failure. The maximum laminate strain was 3942 $\mu\varepsilon$. Since the majority of strain gauges were affixed at midspan or at the laminate end, the laminate strain distribution between both locations was not available. As shown in Figure C.20, the laminate strain has been approached in a linear manner between the strain gauge locations. Therefore, like in Beam 1/D, the average stress between these locations is not reliable.

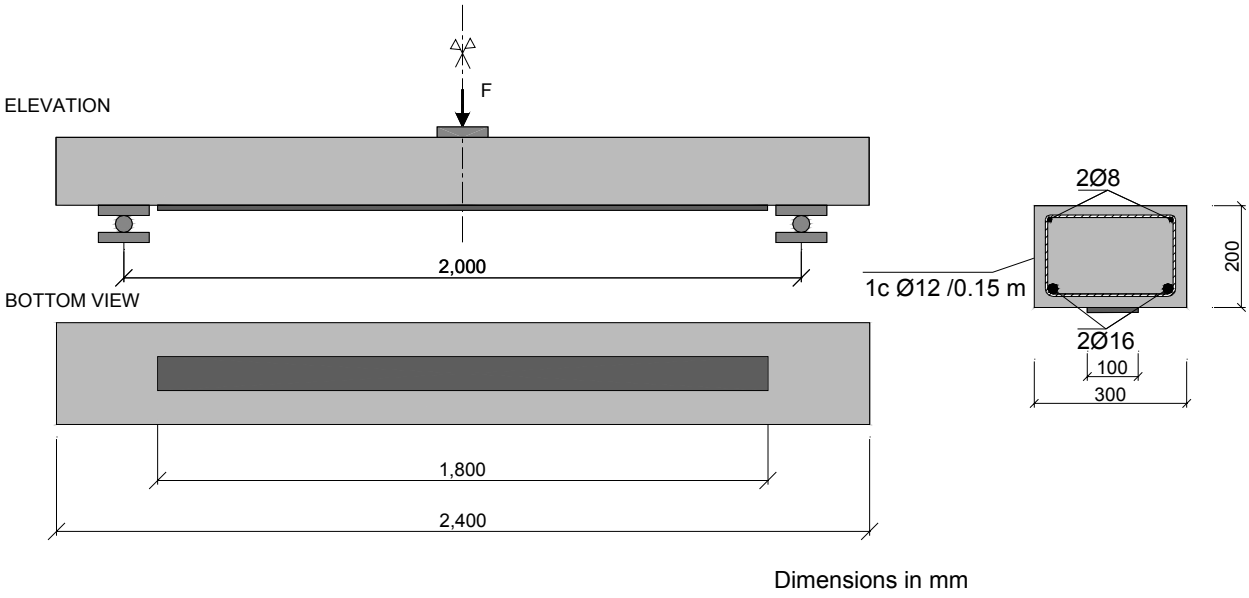

Figure C.16. Test set-up for Beam 1/C.

Table C.8. Summary of test results.

	Service test		Failure test		
	F_{cr} (*kN*)	F_s (*kN*)	F_s (*kN*)	F_y (*kN*)	F_u (*kN*)
	13.3	47.8	50.26	-	104.0
$\delta(x = L/2)$ (*mm*)	1.11	7.82	5.95	-	14.32
ε_L $(x = L/2)$ ($\mu\varepsilon$)	-	-	1697	-	3942

Table C.9. Strain gauge distribution in Beam 1/C.

Gauge	1	2	3	4	5	6	7	8	9	10	11	12
Surface	C	C	C	-	C	C	C	-	C	C	-	C
x (*mm*)	-855	-860	-860	-	3	4	0	-	89	860	-	850
y (*mm*)	0	95	-100	-	0	0	100	-	0	100	-	-101
z (*mm*)	29	0	0	-	21.3	11.8	0	-	34	0	-	0

Gauge	13	14	15	16	17	18	19	20	21	22	23	24
Surface	L	L	L	L	L	L	L	L	L	L	L	L
x (*mm*)	-860	-860	-810	-735	-11	0	0	56	860	860	810	735
y (*mm*)	13	0	0	0	2	-2	-11	2	12	-13	0	0
z (*mm*)	0	0	0	0	0	0	0	0	0	0	0	0

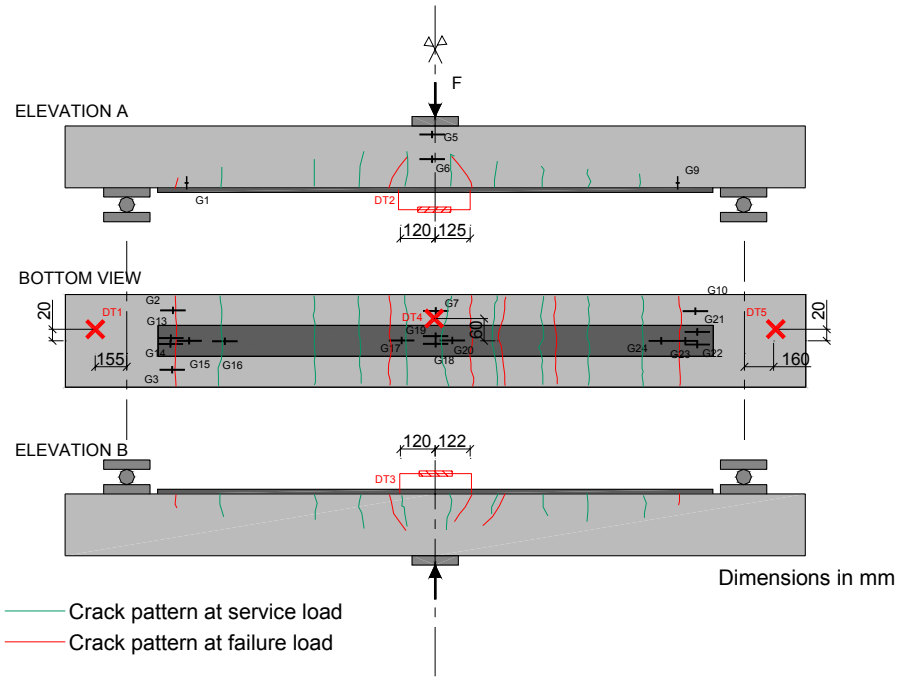

Figure C.17. Crack pattern at service and at failure, together with the instrumentation affixed to Beam 1/C.

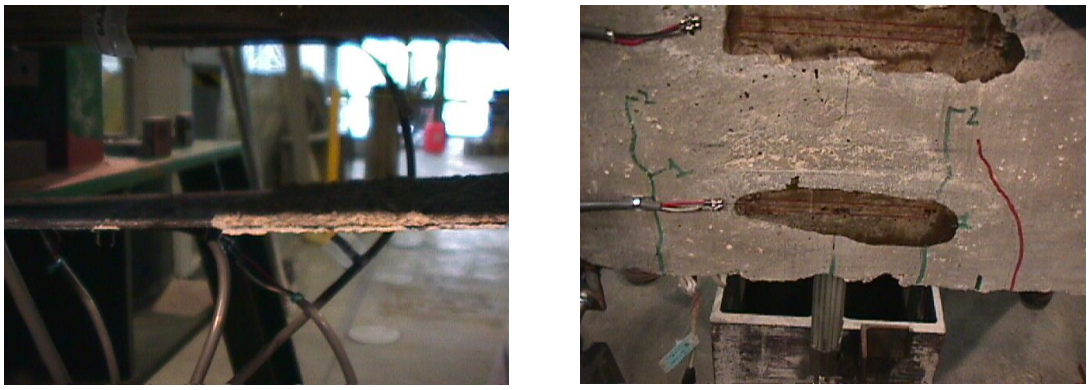

Figure C.18. Peeling failure in Beam 1/C initiated around flexural or shear cracks.

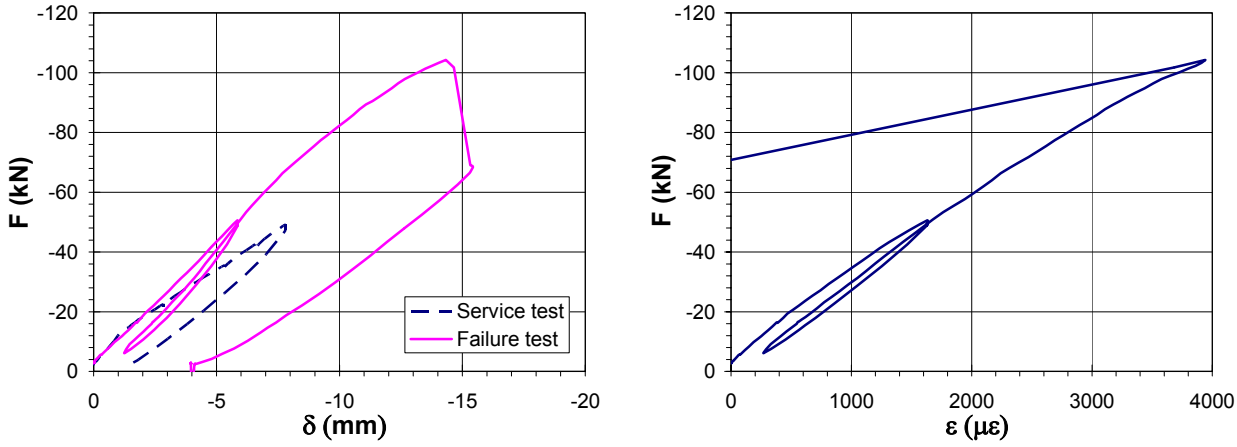

Figure C.19. Midspan displacement. Strain profile in the laminate center of Beam 1/C.

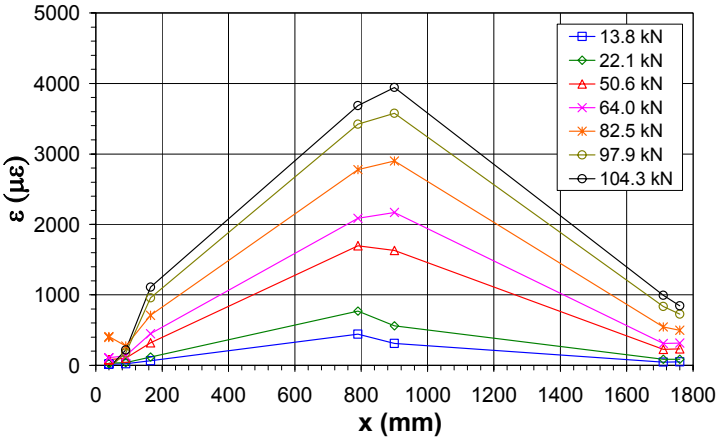

Figure C.20. Laminate strain distribution along Beam 1/C.

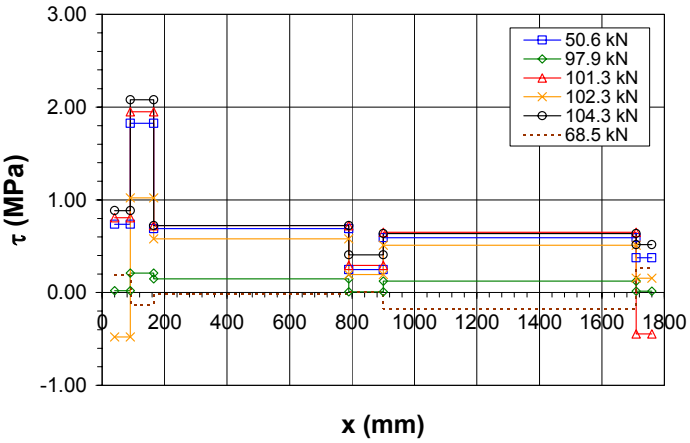

Figure C.21. Shear stress distribution along Beam 1/C.

C.3.4. Beam 1/B

Test observations

Beam 1/B was tested with the same configuration of Beam 1/C to corroborate the results obtained previously (Figure C.22). The main difference was the location of strain gauges which were distributed along the laminate length in Beam 1/B. A preload of 50.1 *kN* was applied before laminate bonding. The strengthened beam was tested to failure in three cycles: the first cycle was up to the service load (50.7 *kN*), the second cycle was up to the control beam failure load (80.0 *kN*), and during the third cycle the laminate peeled-off at an applied load of 100.4 *kN*. The laminate peeling-off was initiated near midspan and propagated to the end of the laminate. The same observations of Beam 1/C can be applied here because no significant differences were observed. The maximum laminate strain of 3647 $\mu\varepsilon$ was obtained at midspan under failure load (Figure C.25 and Figure C.26). Due to the strain gauge distribution, the shear stresses are mean values within a distance around 250 *mm* in this case.

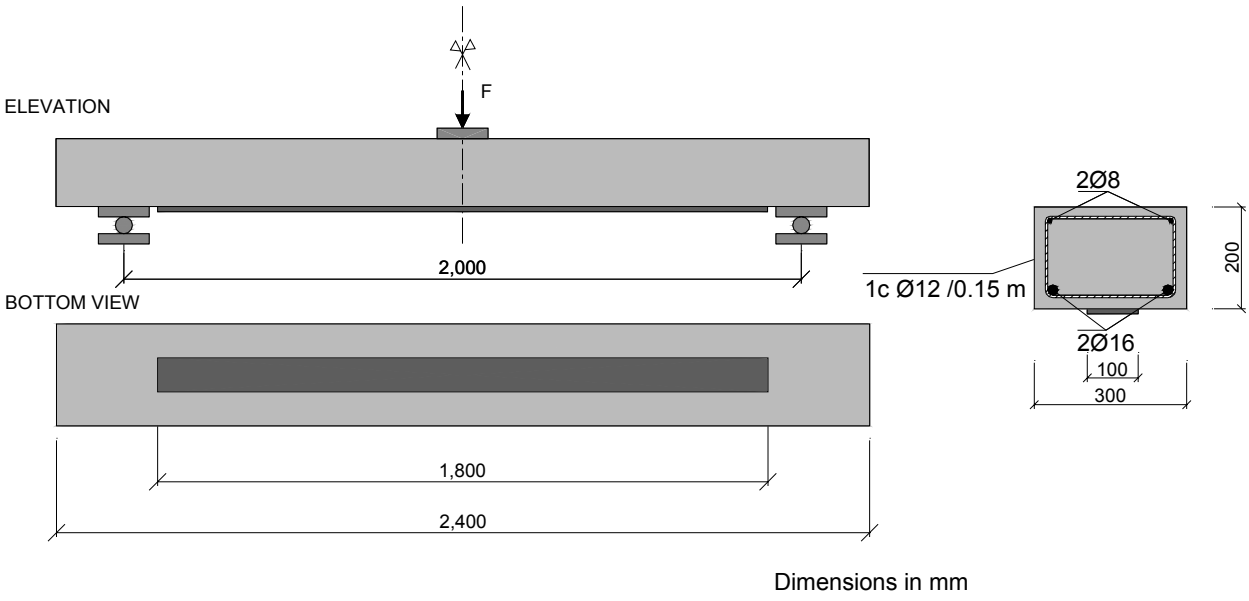

Figure C.22. Test set-up for Beam 1/B.

Table C.10. Summary of test results.

	Service test		Failure test		
	F_{cr} (kN)	F_s (kN)	F_s (kN)	F_y (kN)	F_u (kN)
	12.73	49.2	50.7	-	100.4
$\delta(x = L/2)$ (mm)	0.82	7.54	5.70	-	13.5
ε_L $(x = L/2)$ $(\mu\varepsilon)$	-	-	1710	-	3647

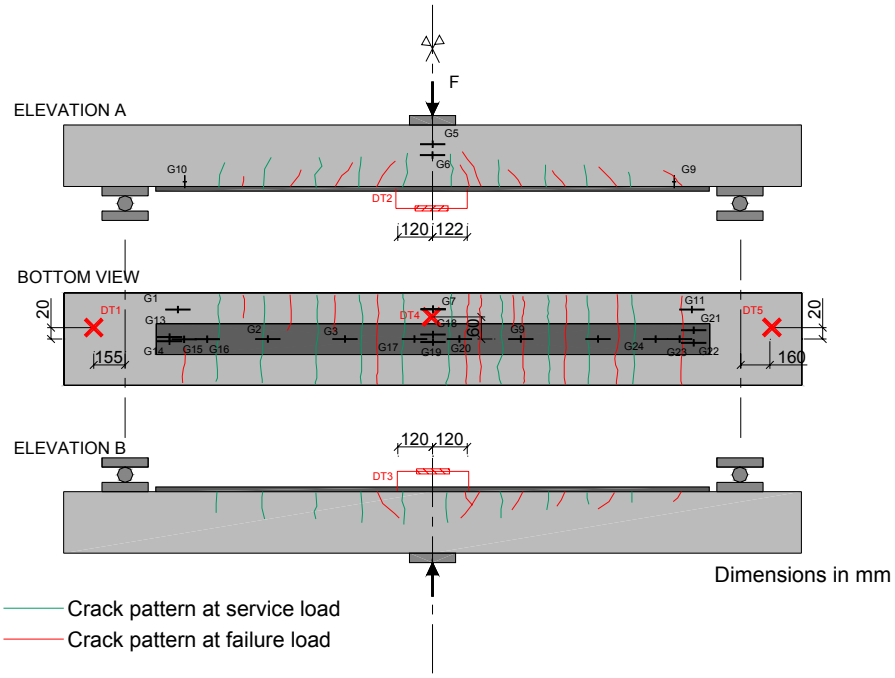

Figure C.23. Crack pattern at service and at failure load, and instrumentation affixed to Beam 1/B.

Table C.11. Strain gauge distribution.

Gauge	1	2	3	4	5	6	7	8	9	10	11	12
Surface	-	L	L	-	C	C	C	-	L	L	-	-
x (*mm*)	-	-537	-286	-	0	0	-5	-	281	528	-	-
y (*mm*)	-	0	0	-	0	0	105	-	0	0	-	-
z (*mm*)	-	0	0	-	137	132	0	-	0	0	-	-

Gauge	13	14	15	16	17	18	19	20	21	22	23	24
Surface	L	L	L	L	L	L	L	L	L	L	L	L
x (*mm*)	-860	-860	-810	-735	-87	0	0	90	857	857	809	732
y (*mm*)	10	-8	0	0	0	0	-10	0	10	-8	0	0
z (*mm*)	0	0	0	0	0	0	0	0	0	0	0	0

Figure C.24. Peeling failure in Beam 1/B initiated around flexural or shear cracks.

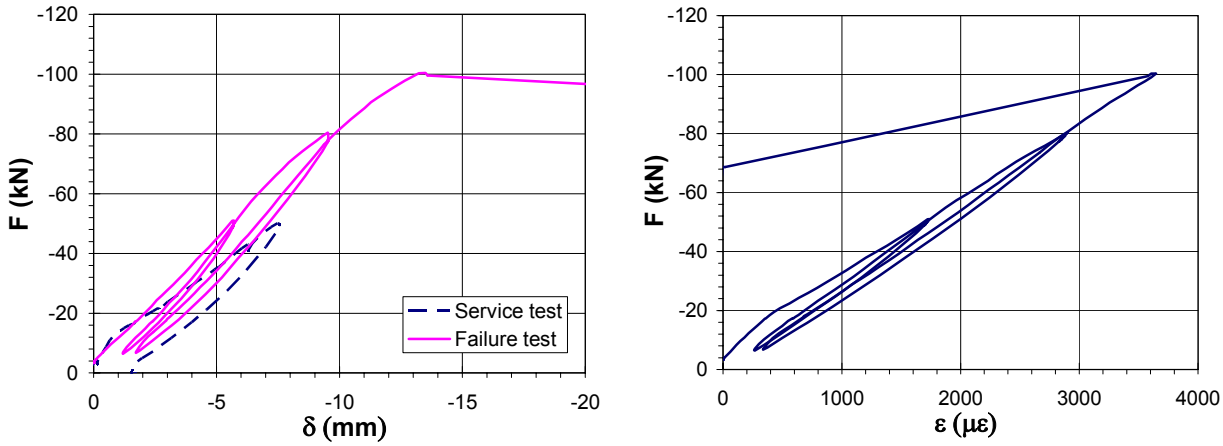

Figure C.25. Midspan displacement. Strain profile in the laminate center of Beam 1/B.

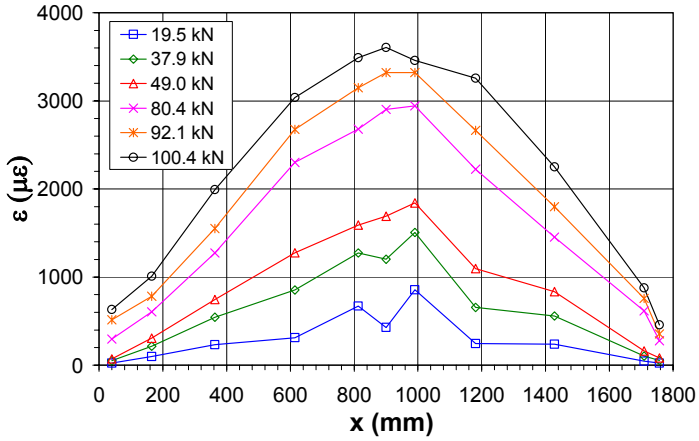

Figure C.26. Laminate strain distribution along Beam 1/B.

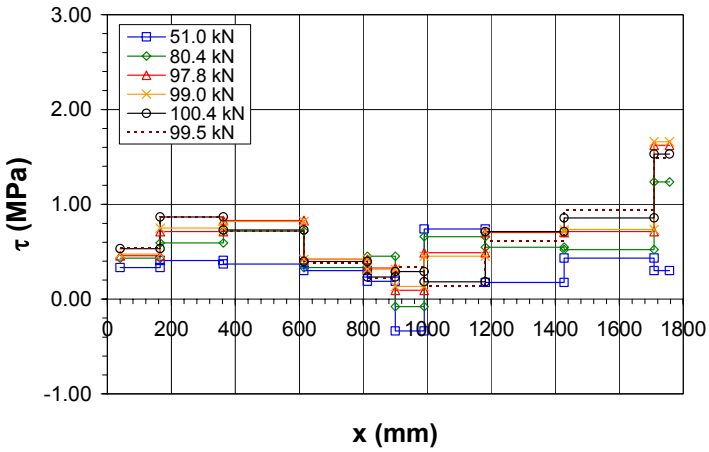

Figure C.27. Shear stress distribution along Beam 1/B.

C.3.5. Beam 1/A

Test observations

Beam 1/A was strengthened without any prior load application to study the influence of existing cracks. Like Beam 1/B, Beam 1/A was tested in three cycles up to failure (at a load of 109.0 *kN*). As shown in Figure C.29 and Figure C.30 (right), the crack pattern of the non-precracked beam was very similar to the rest of the specimens. Before service load was reached, some flexural cracks formed within a distance of 150 *mm* on average between them, that is, with the same spacing obtained in the service test of the preloaded beams. First cracking was observed under a slightly higher value of the applied load in comparison to the precracked beams because of the external laminate. Afterwards, as long as the applied load increased, some intermediate cracks appeared in between the existing ones. The sudden and brittle laminate debonding, shown in Figure C.30, probably initiated near midspan, around one of the cracks shown in Figure C.31 (left), and then propagated towards one of the laminate ends. In some locations, the laminate debonding process pulled out a concrete layer between the external reinforcement and the internal steel rebars leaving some visible stirrups (Figure C.31 right).

Due to an error committed during the data acquisition, the load history is not available. Therefore, graphs of load vs. midspan displacement, load vs. maximum laminate strain are not given in this section. Figure C.32 and Figure C.33 show the laminate strain and shear stress distribution along the bonded length only for failure load.

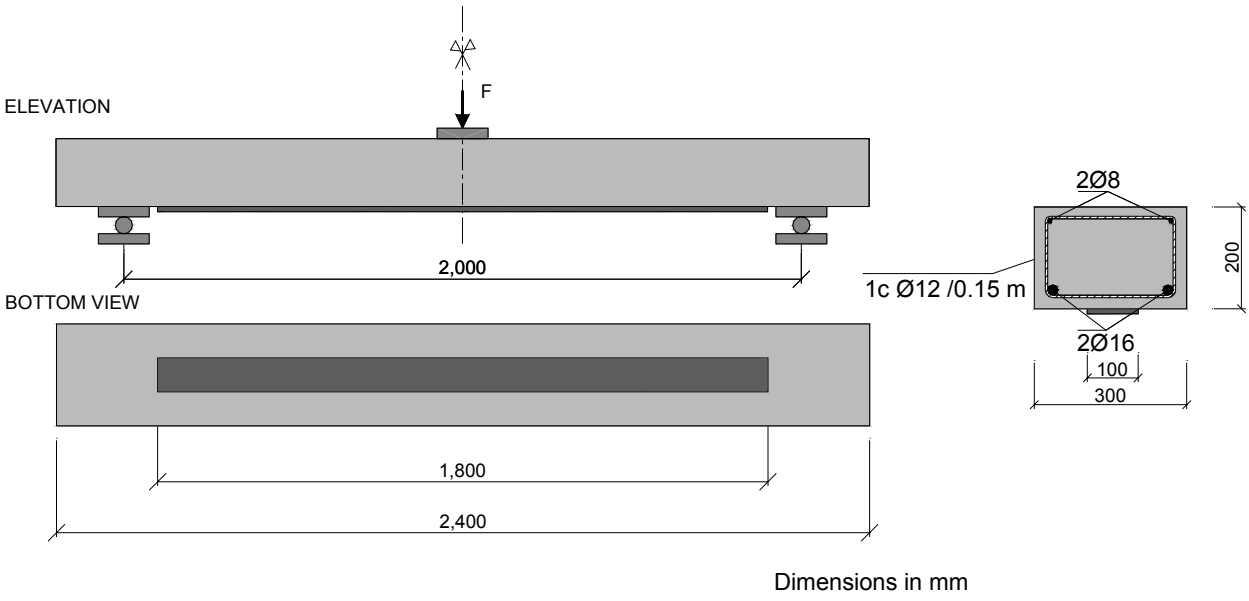

Figure C.28. Test set-up for Beam 1/A.

Table C.12. Summary of test results.

	Service test		Failure test		
	F_{cr} (*kN*)	F_s (*kN*)	F_s (*kN*)	F_y (*kN*)	F_u (*kN*)
	-	-	50.0		109.0
$\delta(x = L/2)$ (*mm*)	-	-	-	-	-
ε_L $(x = L/2)$ ($\mu\varepsilon$)	-	-	1861	-	4437

Table C.13. Strain gauge distribution.

Gauge	1	2	3	4	5	6	7	8	9	10	11	12
Surface	C	L	L	L	C	C	C	L	L	L	L	-
x (*mm*)	-854	-400	-250	-152	0	0	0	149	253	400	815	-
y (*mm*)	105	30	0	2	0	0	98	0	-2	0	97	-
z (*mm*)	0	0	0	0	175	102	0	0	0	0	0	-

Gauge	13	14	15	16	17	18	19	20	21	22	23	24
Surface	L	L	L	L	L	L	L	L	L	L	L	L
x (*mm*)	-855	-855	-778	-726	-60	0	0	61	872	872	821	746
y (*mm*)	15	0	8	5	-2	5	-10	-2	2	-16	-3	-4
z (*mm*)	0	0	0	0	0	0	0	0	0	0	0	0

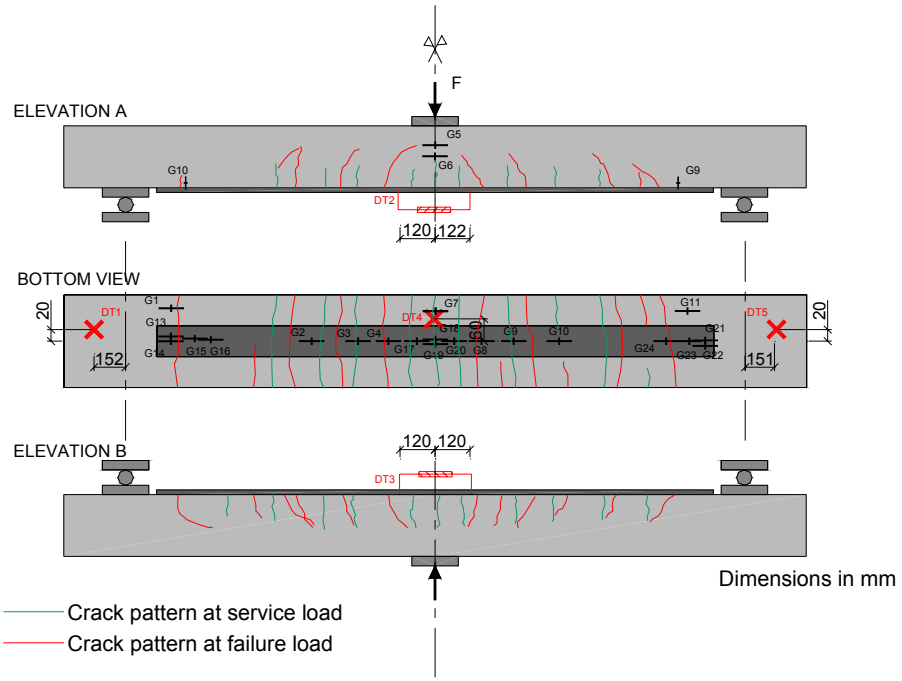

Figure C.29. Crack pattern at service and at failure load, and instrumentation affixed to Beam 1/A.

Figure C.30. Peeling failure in Beam 1/A initiated near midspan.

Figure C.31. Possible crack location of the debonding initiation. Visible stirrup after failure in Beam 1/A.

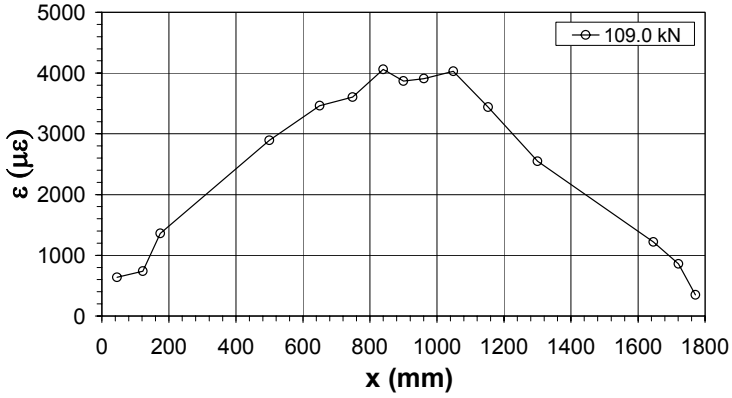

Figure C.32. Laminate strain distribution along Beam 1/A at failure.

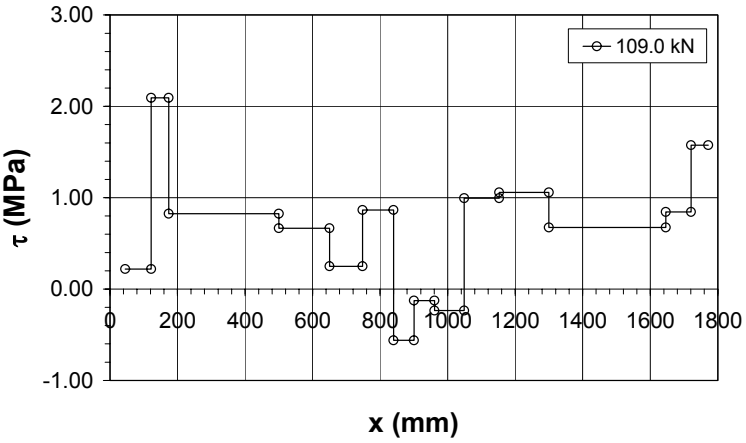

Figure C.33. Shear stress distribution along Beam 1/A at failure.

C.3.6. Beam 2/E (Control Beam)

Test observations

Control Beam 2/E was tested in two cycles. During the first cycle up to service load (72.3 *kN*), some flexural cracks formed and grew within a distance of 100 *mm*. A maximum crack width of 0.20 *mm* was observed in this first cycle. During the second cycle, some intermediate cracks appeared with an inclination between 45º and 60º. Failure due to concrete crushing occurred when the applied load was 113.7 *kN*. The width of the cracks placed near midspan reached 6.0 *mm* at failure, as shown in Figure C.36.

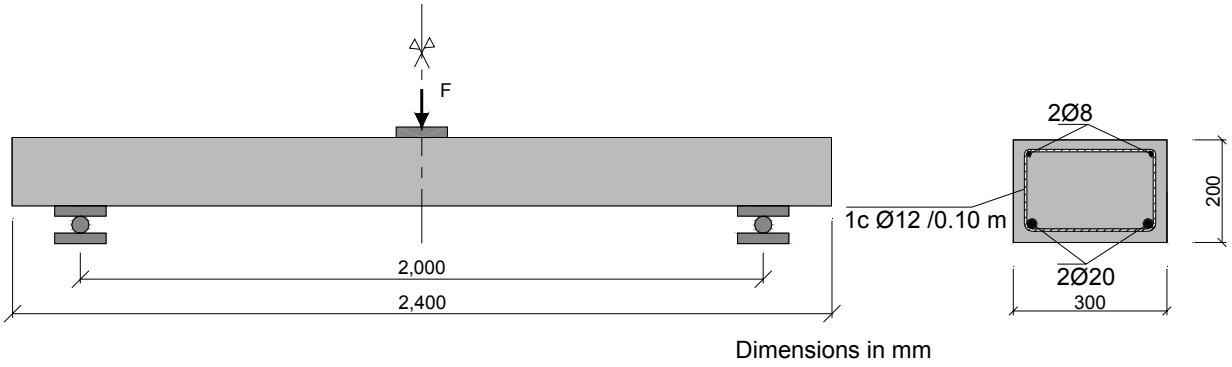

Figure C.34. Test set-up for Beam 2/E.

Table C.14. Summary of test results.

	Failure test			
	F_{cr} (kN)	F_s (kN)	F_y (kN)	F_u (kN)
	-	72.3	104.3	113.7
$\delta(x = L/2)$ (mm)	-	9.1	14.2	71.3

Table C.15. Strain gauge distribution.

Gauge	1	2	3	4	5	6	7	8	9	10	11	12
Surface	-	-	-	-	C	C	-	-	-	-	-	-
x (mm)	-	-	-	-	0	0	-	-	-	-	-	-
y (mm)	-	-	-	-	0	0	-	-	-	-	-	-
z (mm)	-	-	-	-	170	90	-	-	-	-	-	-

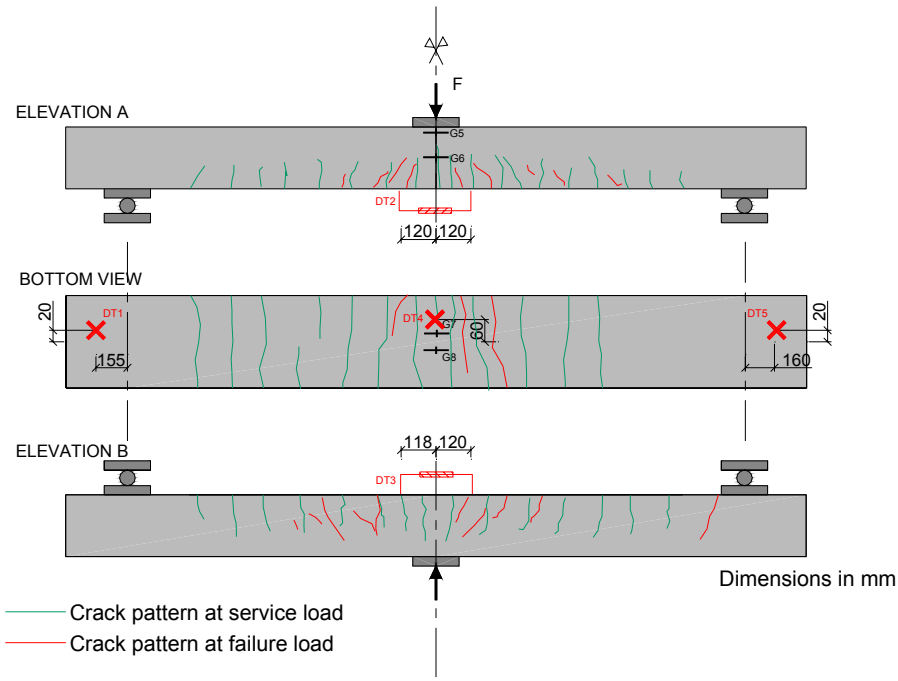

Figure C.35. Crack pattern at service and at failure load, and instrumentation affixed to Beam 2/E.

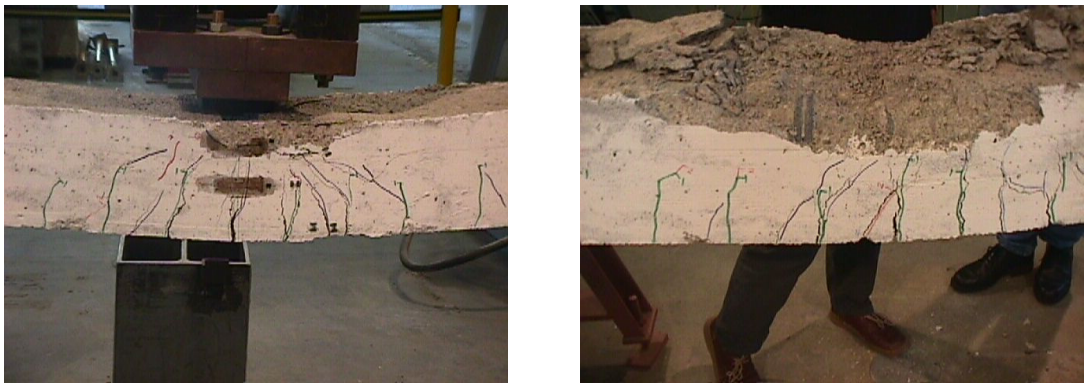

Figure C.36. Concrete crushing in Beam 2/E.

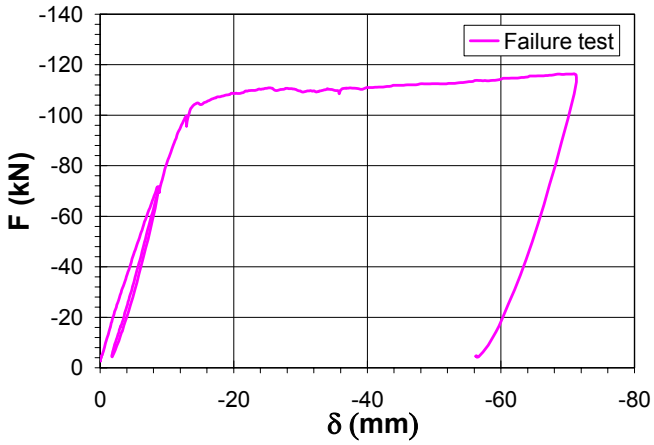

Figure C.37. Midspan displacement of Beam 2/E.

C.3.7. Beam 2/D

Test observations

The dimensions and properties of the bonded laminate in Beam 2/D were the same as Beam 1/C and 1/B. As shown in Figure C.38, the only difference between them was the diameter of the internal rebars and the stirrups spacing. For the same amount of external reinforcement, Beam group 2 showed a lower ratio between external and internal reinforcement in comparison to Beam group 1. All Beam group 2 was preloaded to a load level similar to service, and hence precracked before plate bonding. The failure test was performed in three cycles: first to the service load (73.4 *kN*), second to the control beam failure load, and finally to failure (128.0 *kN*). Due to the higher amount of internal reinforcement, an increase in the failure load was observed in Beam 2/D (128.0 *kN*) compared to Beams 1/B (100.4 *kN*) and 1/C (104.0 *kN*). However, the percentage of increase in relation to the control beam was lower for Beam 2/D (12.6 %) than for Beams 1/B, (22.4 %), and 1/C, (26.8 %). A layer in the concrete cover failed in tension near midspan involving the laminate debonding which propagated to one of the laminate ends (Figure C.40). When peeling failure initiated, the maximum laminate strain was 3905 $\mu\varepsilon$. Once the applied load reaches 74.4 *kN*, a peak in the left hand side of the laminate strain distribution is observed (see Figure C.42). This peak can be

explained by the existence of a flexural crack in the vertical of the G17 strain gauge location. Since the strain distribution felt down at x=1005 *mm* (G20) an instant after failure, the peeling initiation point can be inferred near this location. As shown in Figure C.40, the debonding process propagated towards the right hand side of the laminate.

The crack width measured at the end of the service test for the unstrengthened section was 0.25 *mm*. For safety reasons, during the failure test, the crack width was only measured at the end of the first and second cycle. The crack width of the strengthened section under failure load was 0.15 *mm*, lower than for the unstrengthened section due to the laminate existence. The measured crack width was 0.30 *mm* at the end of the second load cycle (105.3 *kN*).

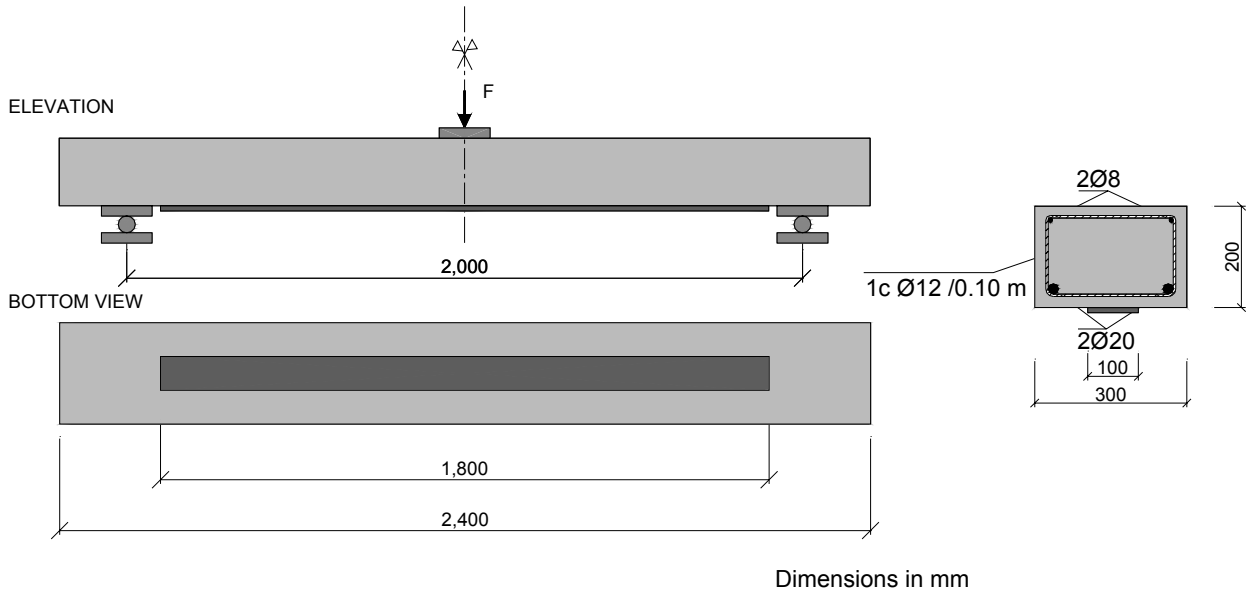

Figure C.38. Test set-up for Beam 2/D.

Table C.16. Summary of test results.

	Service test		Failure test		
	F_{cr} (*kN*)	F_s (*kN*)	F_s (*kN*)	F_y (*kN*)	F_u (*kN*)
	17.3	74.1	74.3	115.9	128.0
$\delta(x = L/2)$ (*mm*)	0.90	8.7	7.5	12.9	15.1
ε_L $(x = L/2)$ ($\mu\varepsilon$)	-	-		3540	3910

Table C.17. Strain gauge distribution.

Gauge	1	2	3	4	5	6	7	8	9	10	11	12
Surface	C	L	L	L	C	C	C	L	L	L	C	-
x (*mm*)	-850	-402	-237	-115	-2	0	0	249	390	567	850	-
y (*mm*)	110	4	6	3	0	0	112	0	0	0	112	-
z (*mm*)	0	0	0	0	165	112	0	0	0	0	0	-

Gauge	13	14	15	16	17	18	19	20	21	22	23	24
Surface	L	L	L	L	L	-	L	L	L	-	L	L
x (*mm*)	-856	-805	-732	-560	-63	-	0	105	860	-	810	738
y (*mm*)	2	0	2	2	4	-	-8	2	-2	-	-2	0
z (*mm*)	0	0	0	0	0	-	0	0	0	-	0	0

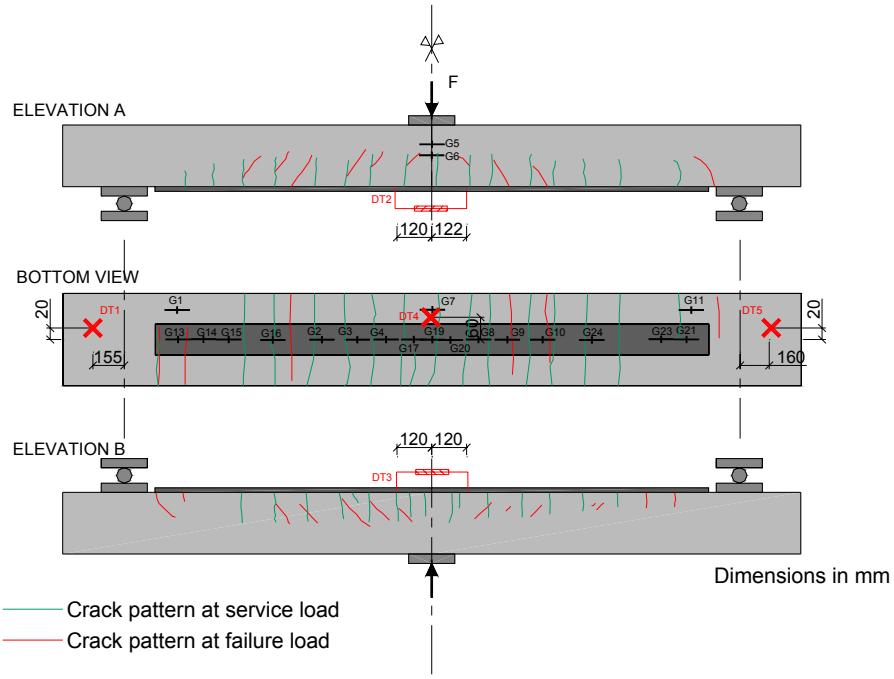

Figure C.39. Crack pattern at service and at failure load, and instrumentation affixed to Beam 2/D.

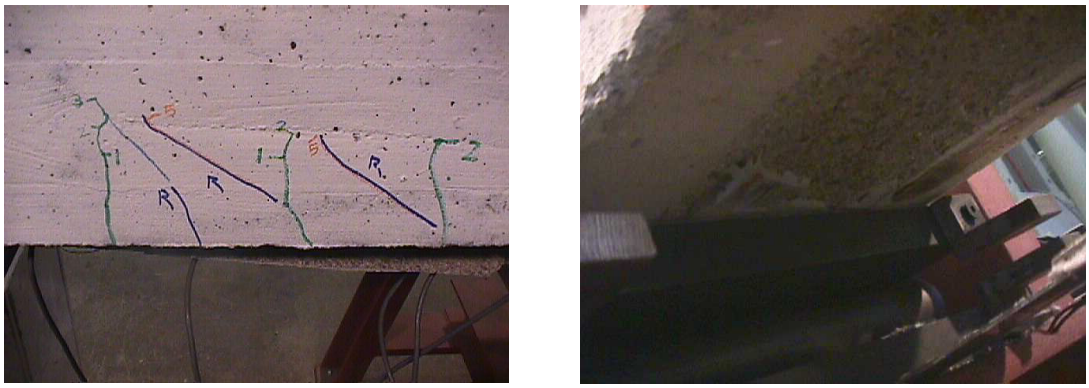

Figure C.40. Peeling failure in Beam 2/D. Concrete at the plate end after debonding.

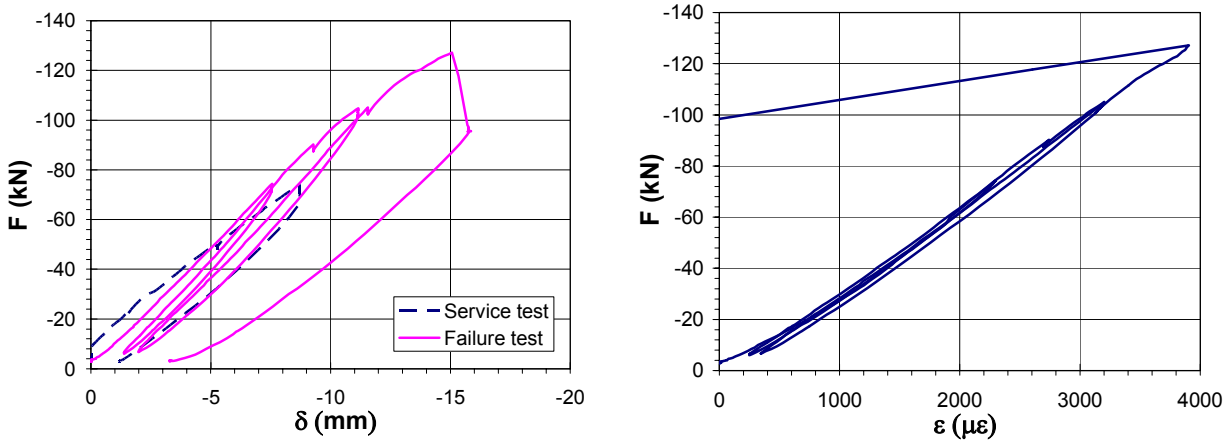

Figure C.41. Midspan displacement. Strain profile in the laminate center of Beam 2/D.

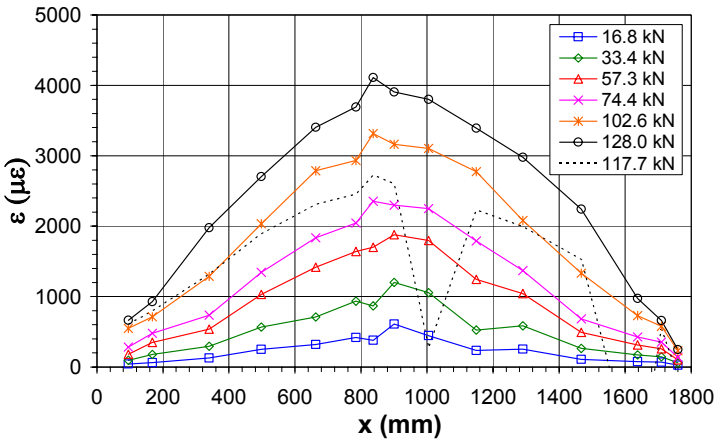

Figure C.42. Laminate strain distribution along Beam 2/D.

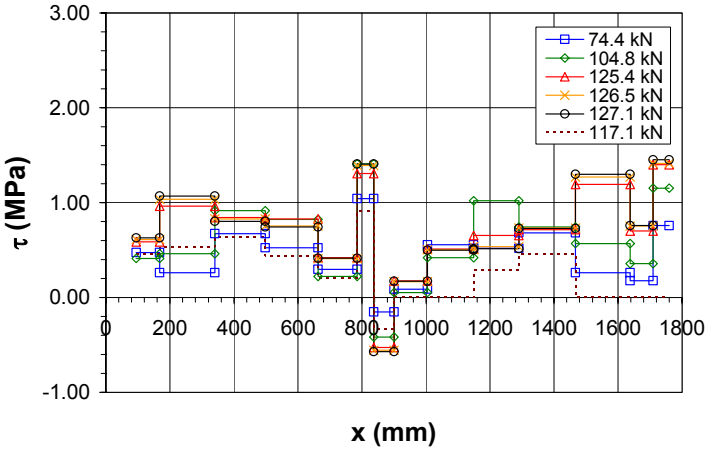

Figure C.43. Shear stress distribution along Beam 2/D.

C.3.8. Beam 2/C

Test observations

The same amount of external reinforcement as in Beam 2/D was applied in this case but distributed in two laminates of 50 *mm* width aligned with the vertical shear stirrups (see Figure C.44). By using this layout, the transmission of the vertical component of the laminate tensile force to the internal steel stirrups seemed to be enhanced. The failure test was performed in three cycles: to the service load (75.5 *kN*), then to the control beam load failure, and finally to failure. When the applied load reached 142.8 *kN*, laminate 1 peeled-off and the applied load decreased in a brittle manner. Afterwards, the applied load recovered, and when it reached 118.8 *kN*, the detachment of laminate 2 occurred. As shown in Figure C.47, laminate 1 pulled out a thin layer of the concrete cover during its debonding. In addition, part of laminate 2 peeled-off at the interface between the concrete and the adhesive. At a load level close to failure, concrete crushed in the compression zone near the load application point (Figure C.48).

As observed, by adopting a different laminate configuration, the failure load, 142.8 *kN*, increased significantly compared to Beam 2/D. The percentage of strengthening in relation to the control beam was 25.6 %, which represents an increase of 13.0 % with respect to Beam 2/D (12.6 %). In addition, the maximum laminate strain at failure of 5619 $\mu\varepsilon$ was significantly higher.

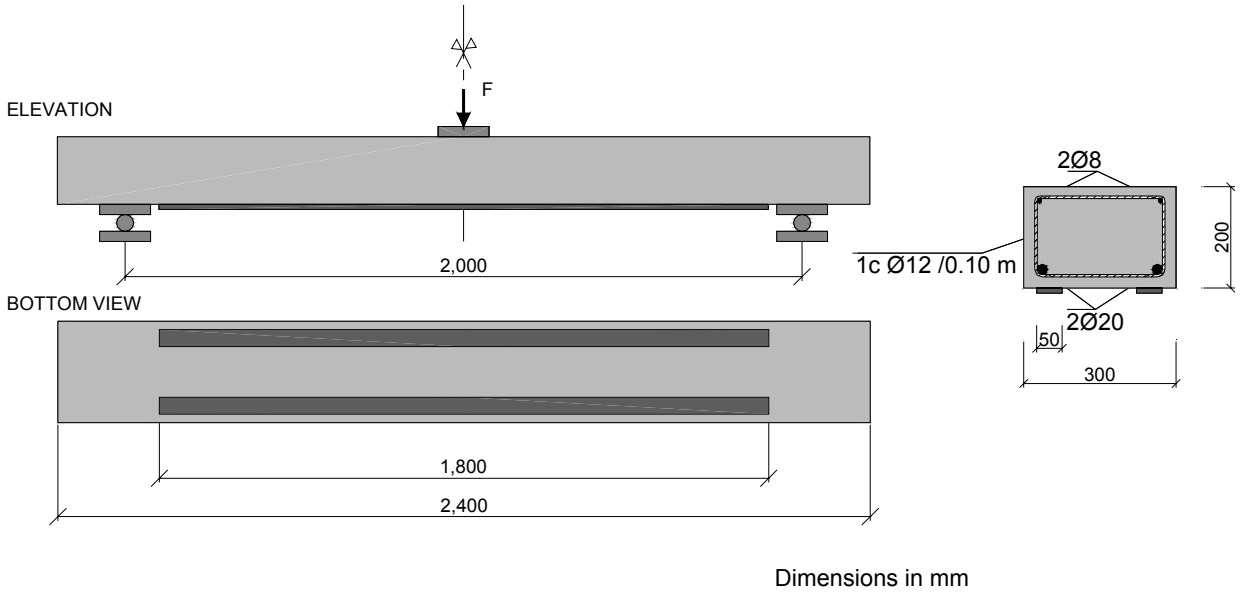

Figure C.44. Test set-up for Beam 2/C.

Table C.18. Summary of test results.

	Service test		Failure test		
	F_{cr} (*kN*)	F_s (*kN*)	F_s (*kN*)	F_y (*kN*)	F_u (*kN*)
	11.2	70.2	75.7	116.6	142.8
$\delta(x = L/2)$ (*mm*)	0.63	9.4	8.1	12.9	19.6
ε_L $(x = L/2)$ ($\mu\varepsilon$)	-	-	2239	3549	5619

Table C.19. Strain gauge distribution.

Gauge	1	2	3	4	5	6	7	8	9	10	11	12
Surface	L1	L2	L1	L2	C	C	-	-	L1	L2	L1	L2
x (*mm*)	-436	-420	-232	-220	0	12	-	-	250	272	445	440
y (*mm*)	-1	3	-1	0	0	0	-	-	2	2	0	0
z (*mm*)	0	0	0	0	170	99.4	-	-	0	0	0	0

Gauge	13	14	15	16	17	18	19	20	21	22	23	24
Surface	L1	L2	L1	L2	L1	L2	L1	L2	L1	L2	L1	L2
x (*mm*)	-890	-890	-654	-653	-116	-116	0	0	0	0	158	172
y (*mm*)	10	0	0	1	-1	0	6	10	-5	-1	-1	0
z (*mm*)	0	0	0	0	0	0	0	0	0	0	0	0

Gauge	25	26	27	28	29	30	31
Surface	L1	-	L1	-	L2	-	L2
x (*mm*)	636	-	885	-	617	-	890
y (*mm*)	0	-	0	-	0	-	-2
z (*mm*)	0	-	0	-	0	-	0

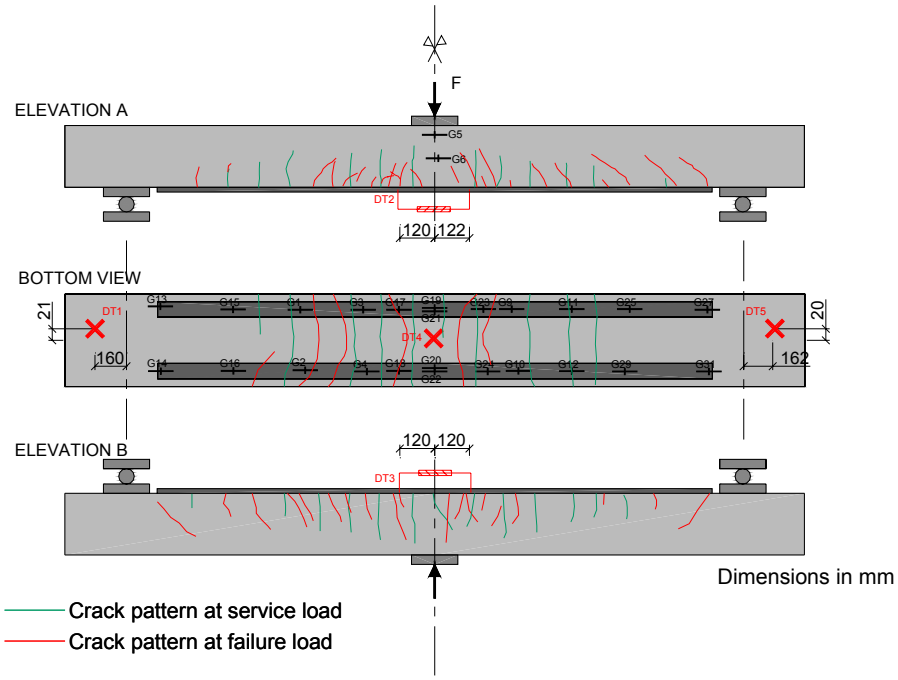

Figure C.45. Crack Pattern at service and at failure load, together with the instrumentation affixed to Beam 2/C.

Figure C.46. Peeling failure in Beam 2/C. Concrete at the plate end after debonding.

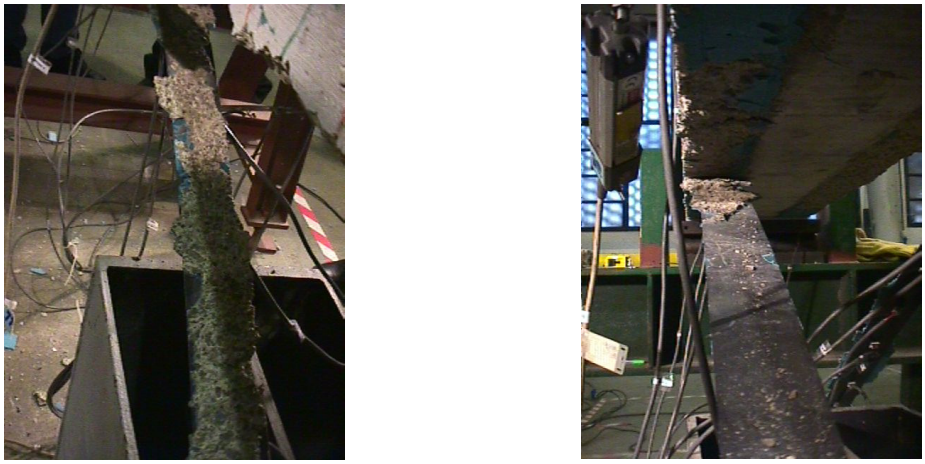

Figure C.47. Laminate 1 pulled out a thin layer of concrete during its dettachment. Part of laminate 2 debonded at the interface between concrete and adhesive.

Figure C.48. Concrete crushed near the load application point for a load level close to failure.

Figure C.49. Midspan displacement. Strain profile in the laminate center of Beam 2/C.

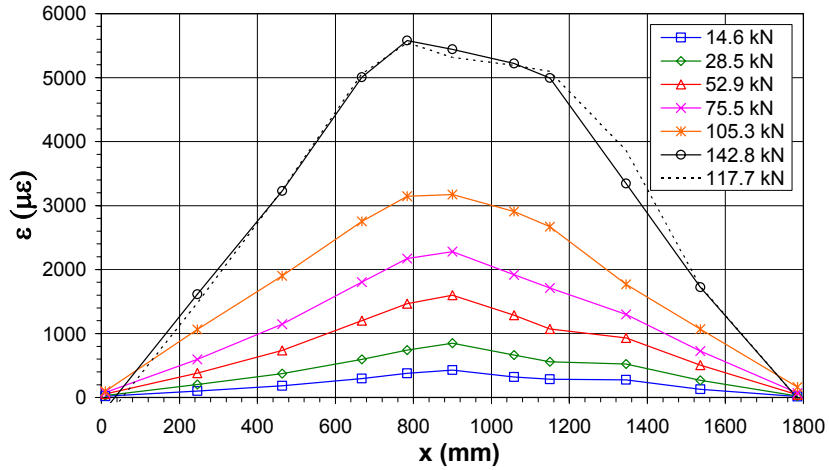

Figure C.50. Laminate strain distribution along one of the laminates in Beam 2/C.

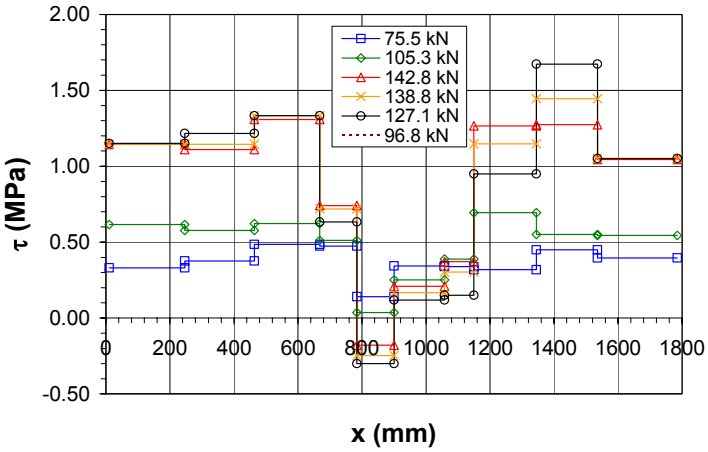

Figure C.51. Shear stress distribution along one of the laminates in Beam 2/C.

C.3.9. Beam 2/B

Test observations

In order to delay the laminate peeling-off caused by the effect of cracks, an external anchorage was applied in Beam 2/B by bonding full-height laminas of carbon fibers with a U shape, in four locations along the beam span: two anchorages were applied at the laminate end and the remaining two were bonded symmetrically at 175 *mm* from midspan (Figure C.52 and Figure C.54). The external anchorages consisted of a unidirectional wet lay-up CFRP laminate made of C-sheet 240 supplied by Bettor MBT. In this occasion, the laminas were anchored in the compression zone. Two laminates of 50 *mm* x 1.4 *mm* were employed to strengthen the concrete beam in the same configuration as Beam 2/C. Failure was slightly delayed by the use of the bonded anchorages. The failure load was 153.1 *kN*. As shown in Figure C.56, the midspan deflection at failure was slightly reduced compared to the rest of beams that belong to Beam group 2. In addition, the laminate strain at midspan reached 5156 $\mu\varepsilon$, a slightly higher value than the beams without external anchorages. The laminate peeled-off due to the effects of existing flexural cracks or due to the effects of intermediate shear cracks that appeared along the span. However, in this case, the external anchorages held the laminate during its sliding towards the rupture of the fibers of the CFRP lamina (Figure C.54 and Figure C.55). Since the anchorage fibers were placed in the direction perpendicular to the pultruded laminate, there was not strength in the longitudinal direction. Therefore, if a bidirectional anchorage with a lamina sequence of 0/90º, was employed, the peeling phenomena would have been delayed in a more noticeable manner.

As shown in Figure C.57, once the applied load reached 106.3 *kN*, the laminate strain at gauge 20 of laminate 1 was higher than at any other location, with a maximum value of 6170 $\mu\varepsilon$. In addition, it increased more rapidly than in the nearest gauges 18 and 22. Meanwhile, in the homologues gauges of laminate 2, the strain did not increase by following the same progression. A possible explanation is given if laminate 2 have already initiated its debonding. Therefore, laminate 1 should assume alone the tensile force increment due to the following load increments. For this reason, the average shear

stress between gauge 20 and the following gauge 22 were higher than in the rest of the laminate 1.

As shown in Figure C.55 (right), concrete crushed at failure in the compression zone under the load application point, probably due to a non-plane contact through the elastomeric bearing between the load cell and the concrete.

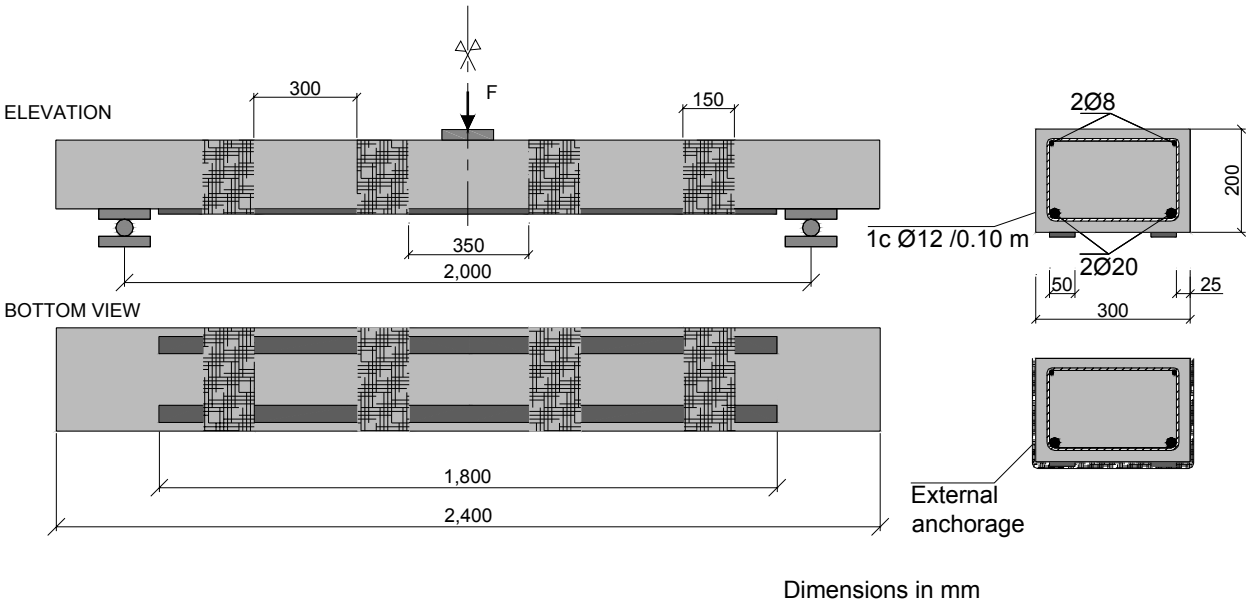

Figure C.52. Test set-up for Beam 2/B.

Table C.20. Summary of test results.

	Service test		Failure test		
	F_{cr} (*kN*)	F_s (*kN*)	F_s (*kN*)	F_v (*kN*)	F_u (*kN*)
	-	70.4	76.4	138.8	153.1
$\delta(x = L/2)$ (*mm*)	-	9.4	7.3	14.6	17.9
ε_L $(x = L/2)$ $(\mu\varepsilon)$	-	-	2940	3920	5160

Table C.21. Strain gauge distribution.

Gauge	1	2	3	4	5	6	7	8	9	10	11	12
Surface	L2	L1	L2	L2	C	C	-	-	L2	L1	L2	L1
x (*mm*)	-850	-850	-563	-560	0	0	-	-	-383	-380	-100	-100
y (*mm*)	0	0	0	0	0	0	-	-	2	-3	1	0
z (*mm*)	0	0	0	0	175	105	-	-	0	0	0	0

Gauge	13	14	15	16	17	18	19	20	21	22	23	24
Surface	L2	L1	L2	L1	L2	L1	L2	L1	L2	L1	L2	L1
x (*mm*)	0	0	0	0	147	152	370	374	572	580	851	853
y (*mm*)	5	-3	-5	3	-1	0	0	0	0	0	0	0
z (*mm*)	0	0	0	0	0	0	0	0	0	0	0	0

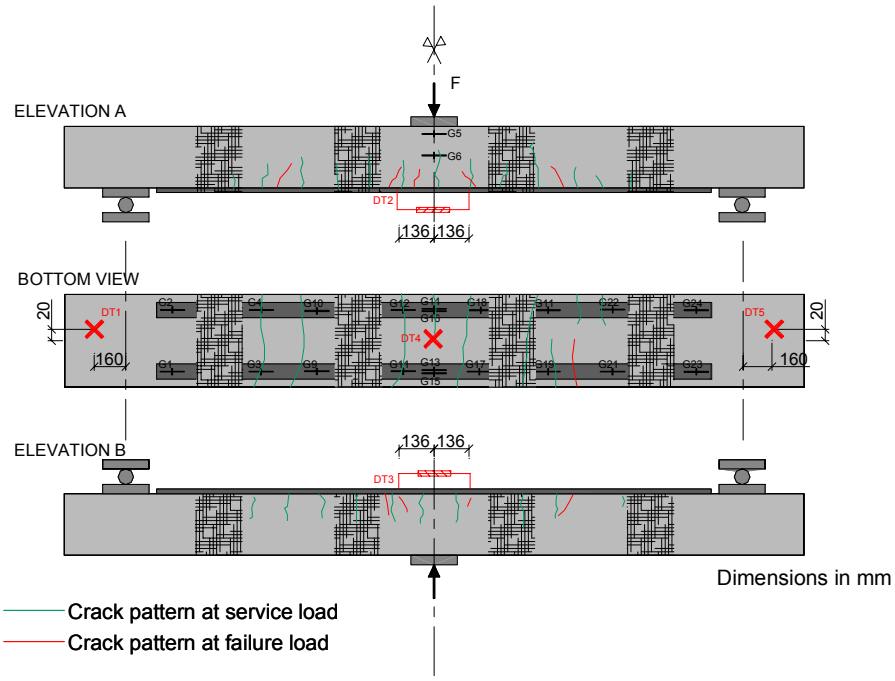

Figure C.53. Crack pattern at service and at failure load, and instrumentation affixed to Beam 2/B.

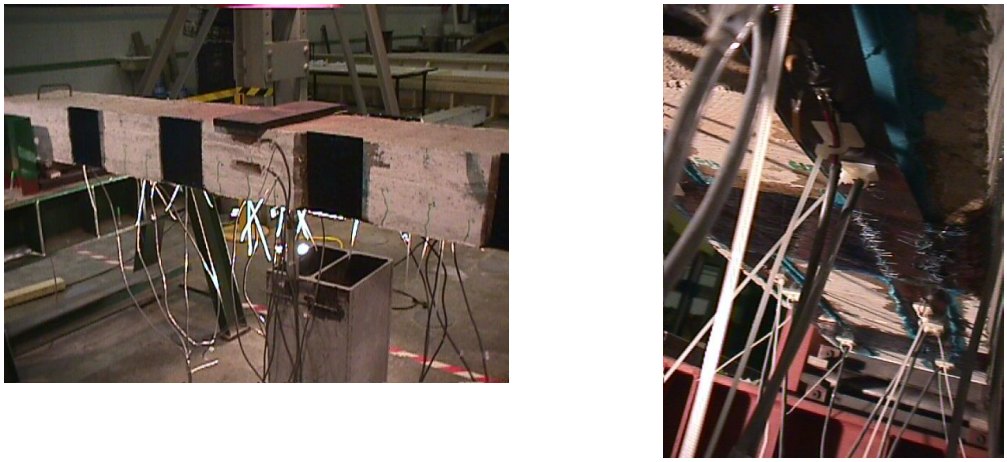

Figure C.54. External anchorages applied on Beam 2/B. Laminate debonding followed by the slip of the laminate up to the rupture of the external anchorage nearest to midspan.

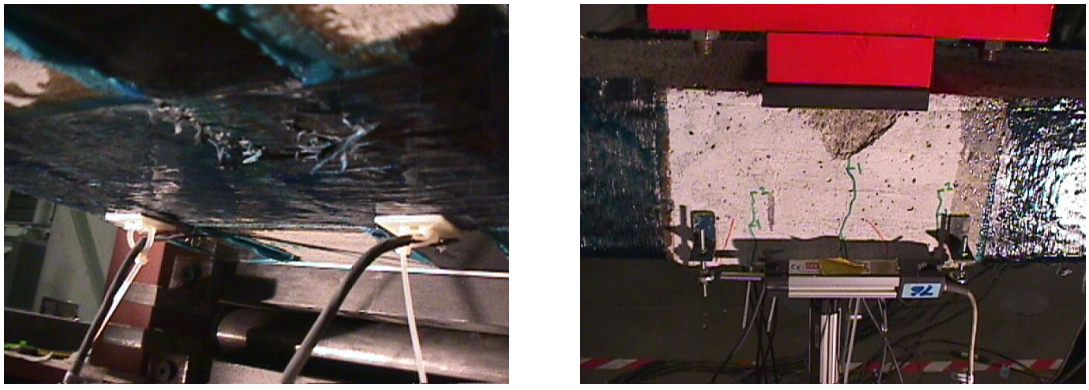

Figure C.55. Rupture of the fibers on the external anchorage at the plate end. Concrete crushing under the load application point.

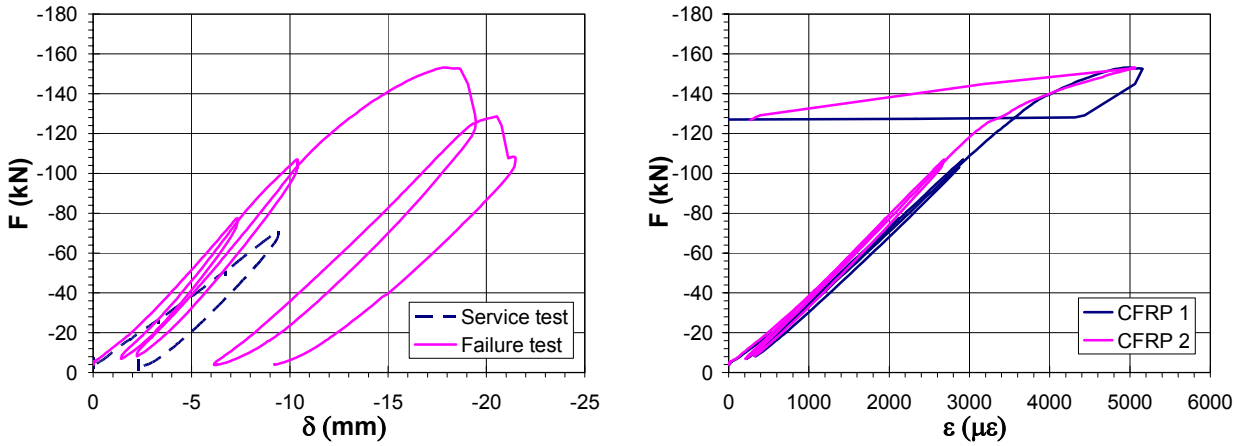

Figure C.56. Midspan displacement. Strain profile in the laminate center of Beam 2/B.

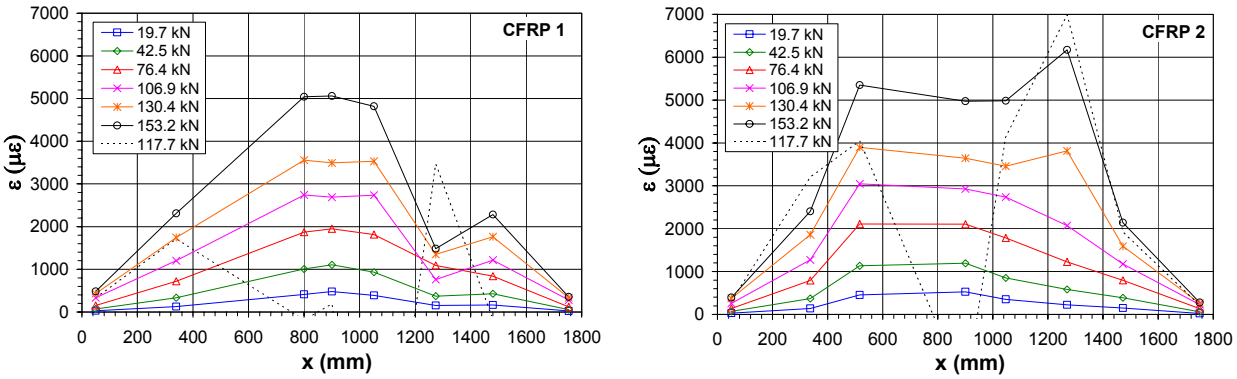

Figure C.57. Strain distribution along Beam 2/B Laminate 1. Strain distribution for Laminate 2.

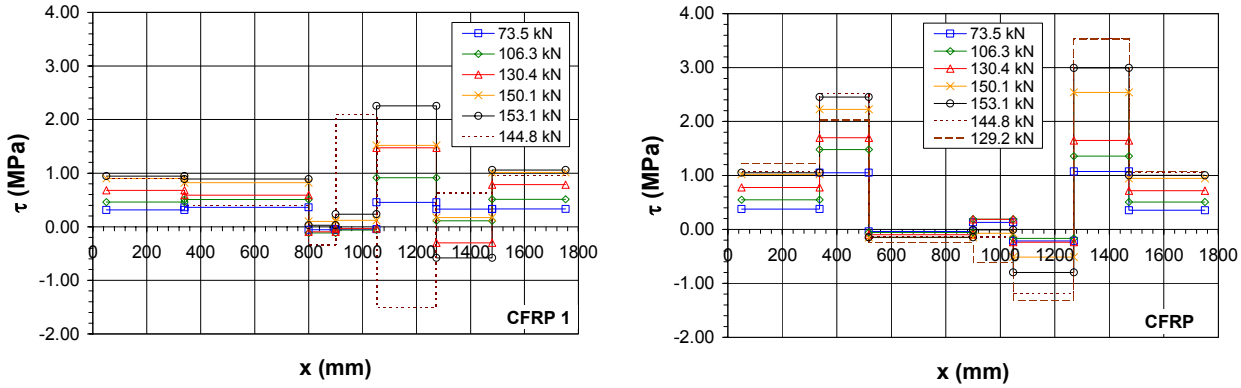

Figure C.58. Shear stress distribution along Beam 2/B Laminate 1. Shear stress distribution for Laminate 2.

C.3.10. Beam 2/A

Test observations

One pultruded laminate of 100 *mm* x 1.4 *mm* was bonded to the concrete tensile face of Beam 2/A. The need of lateral external anchorages affixed to the webs was studied in this case by bonding the CFRP laminas only to the bottom side of the concrete beam (see Figure C.61). Beam 2/A's failure load, 154.6 *kN*, was similar to that of Beam 2/B (153.1 *kN*), showing that at least in this case, the anchorage of the CFRP wet lay-up laminas in the concrete compression zone does not seem necessary. However, the author believes that more research in this topic should be performed to confirm the results of Beam 2/A. In general, the behavior of Beam 2/A was very similar to Beam 2/B. Since the bonding of the longitudinal laminate was better performed, the peeling of the laminate was not initiated in the laminate-adhesive interface (Figure C.62). The laminate peeling-off involved the detachment of a layer in the concrete cover. The maximum laminate strain at failure 5642 $\mu\varepsilon$ was observed at midspan, as shown in Figure C.64. The laminate strain registered by the gauge G17, which was placed on the top of one of the external anchorages, increased before failure more than the neighboring gauges. This fact can be explained by the development of an intermediate crack between the existing flexural cracks after service load.

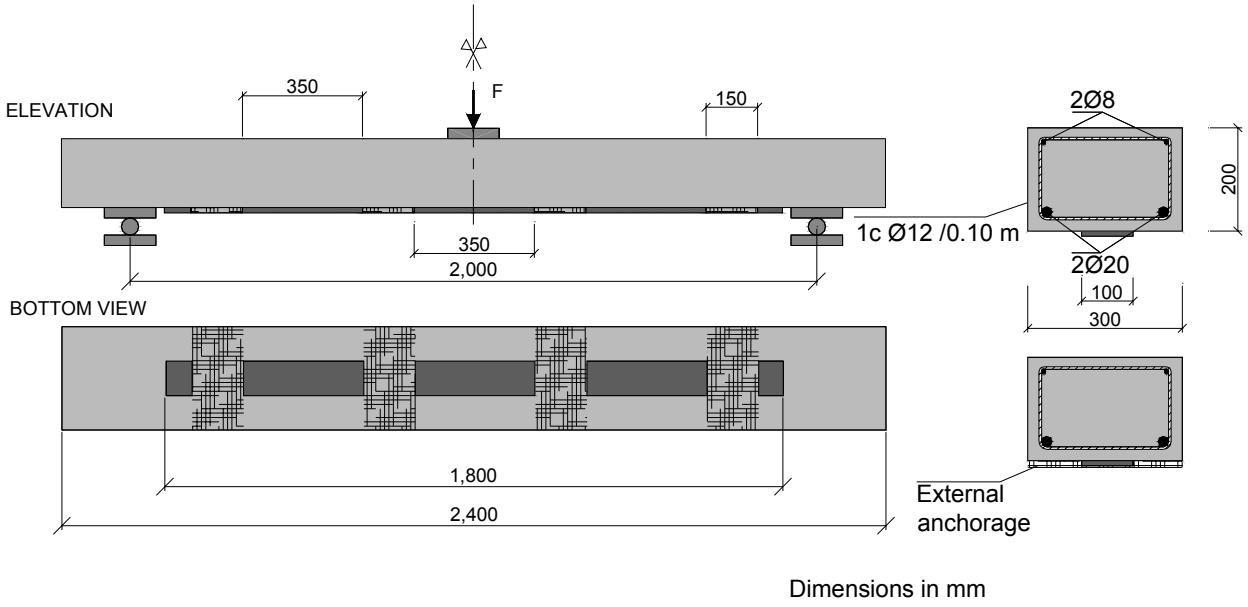

Figure C.59. Test set-up for Beam 2/A.

Table C.22. Summary of test results.

	Service test		Failure test		
	F_{cr} (*kN*)	F_s (*kN*)	F_s (*kN*)	F_y (*kN*)	F_u (*kN*)
	18.8	72.8	74.8	140.4	154.6
$\delta(x = L/2)$ (*mm*)	1.1	7.5	6.9	14.5	19.6
ε_L $(x = L/2)$ ($\mu\varepsilon$)	-	-	1960	4090	5640

Table C.23. Strain gauge distribution.

Gauge	1	2	3	4	5	6	7	8	9	10	11	12
Surface	L	L	L	L	C	C	-	-	-	L	L	L
x (*mm*)	-843	-695	-617	-378	0	0	-	-	-	-197	-172	-132
y (*mm*)	0	2	0	1	0	0	-	-	-	2	0	0
z (*mm*)	0	0	0	0	154	105	-	-	-	0	0	0

Gauge	13	14	15	16	17	18	19	20	21	22	23	24
Surface	L	L	L	L	L	L	L	L	L	L	-	-
x (*mm*)	0	0	67	139	182	183	374	521	643	833	-	-
y (*mm*)	-2	2	0	0	6	100	0	0	0	0	-	-
z (*mm*)	0	0	0	0	0	0	0	0	0	0	-	-

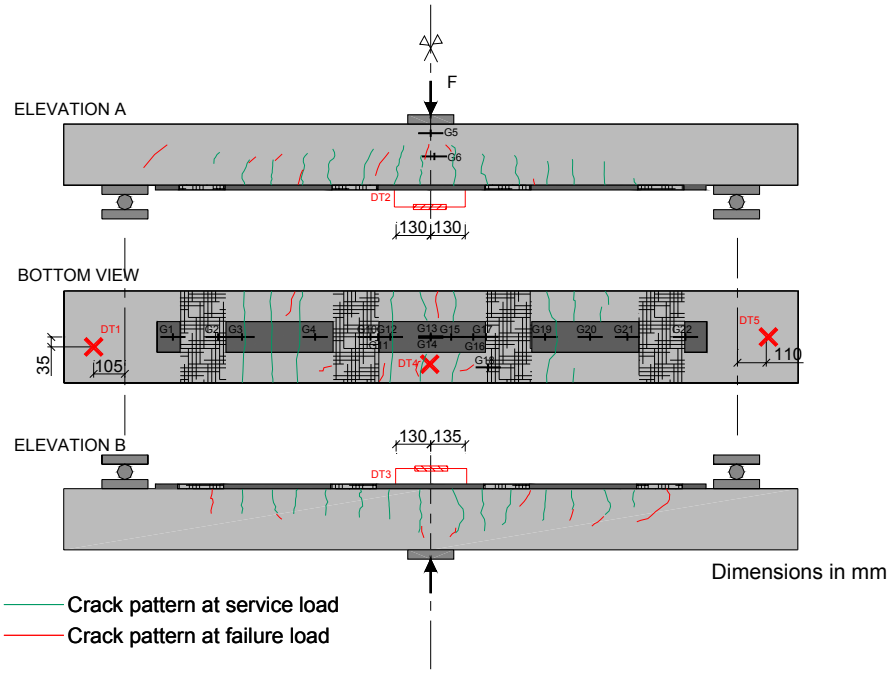

Figure C.60. Crack pattern at service and at failure load, and instrumentation affixed to Beam 2/A.

Figure C.61. External anchorages applied only on the bottom side of Beam 2/A.

Figure C.62. Peeling of the laminate between two cracks in the concrete interface. Rupture of the external anchorage at the plate end.

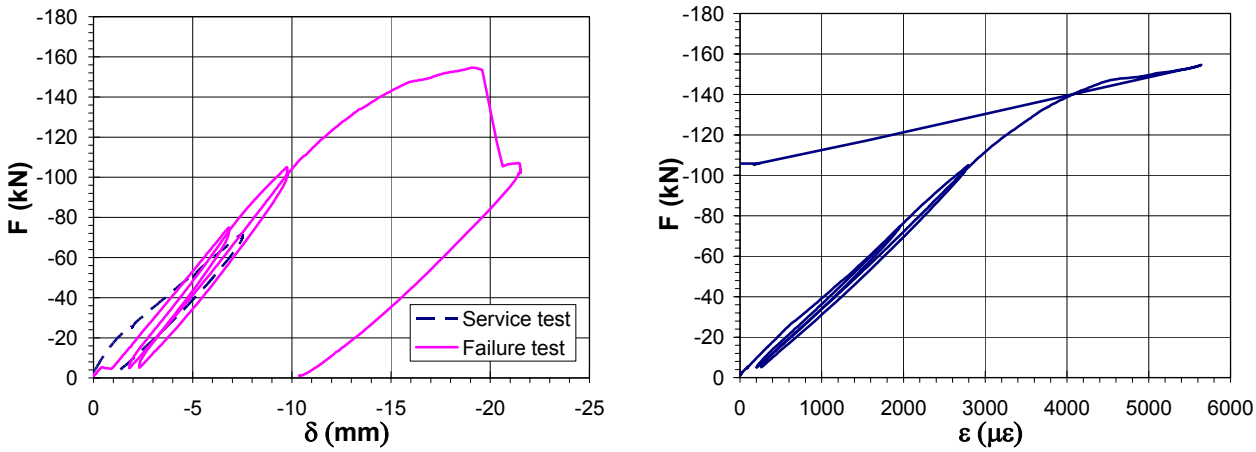

Figure C.63. Midspan displacement. Strain profile in the laminate center of Beam 2/A.

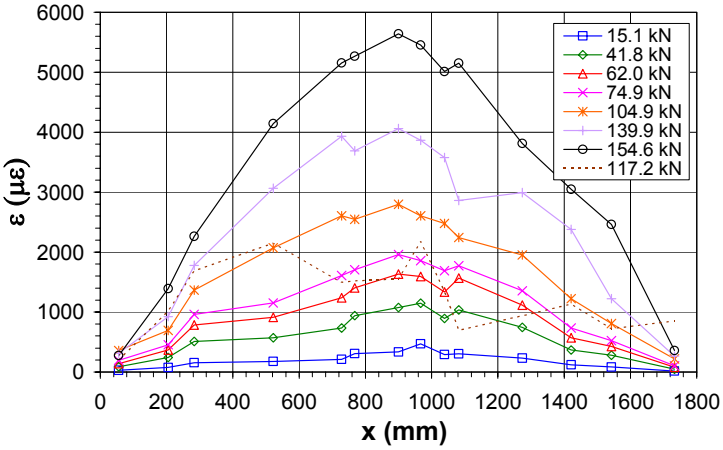

Figure C.64. Laminate strain distribution along Beam 2/A.

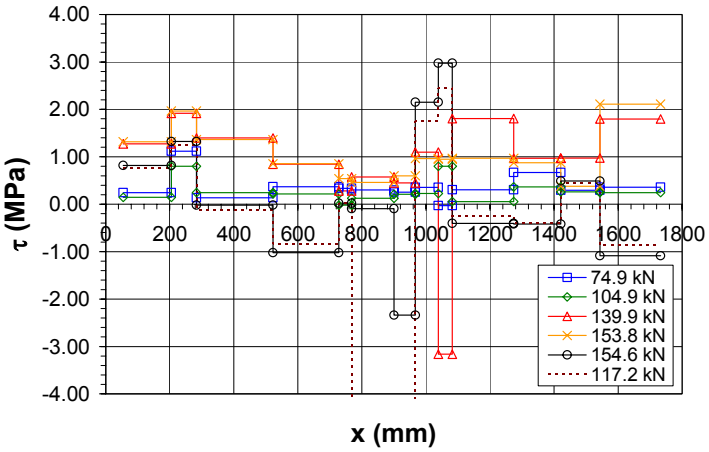

Figure C.65. Shear stress distribution along Beam 2/A.

Beams 1/D, 1/B, 1/C, and 2/D were not damaged after the premature laminate peeling-off. Therefore, all of them were strengthened and tested to failure again as described in the following sections.

C.3.11. Beam 1/D (#2)

Test observations

Like in Beam 2/C, two laminates of 50 *mm* x 1.4 *mm* were bonded in the vertical of the shear stirrups of Beam 1/D (#2) (Figure C.66). The three-point bending test was performed in three cycles, as shown in Figure C.69. In the last one, when the applied load reached 112.0 *kN* and the laminate strain was 4112 $\mu\varepsilon$, one of the laminates peeled-off. Then, the applied load decreased in a brittle manner to 74.9 *kN*. Later on, the applied load recovered up to 100.7 *kN*, when the second laminate debonded. The maximum strain registered in laminate 2 after the debonding of the first laminate was of 4982 $\mu\varepsilon$. The insignificant increase in both the failure load and the maximum laminate strain in relation to the previous tests may be due to an insufficient bonding generated by an incorrect application of the external reinforcement.

As shown in both Figure C.67 and Figure C.68, the laminate peeling failure was initiated near midspan and propagated towards the laminate end. Since the bond between the support and the external reinforcement was imperfect, the laminate peeled-off along the interface between adhesive and concrete, without observing a concrete dettachment in more than half of the debonded length.

Due to an error committed at the end of the test during the unload process, the beam crushed. Thus, the position of the affixed instrumentation was not registered and the plots of the distribution of laminate strain and shear stress are not available.

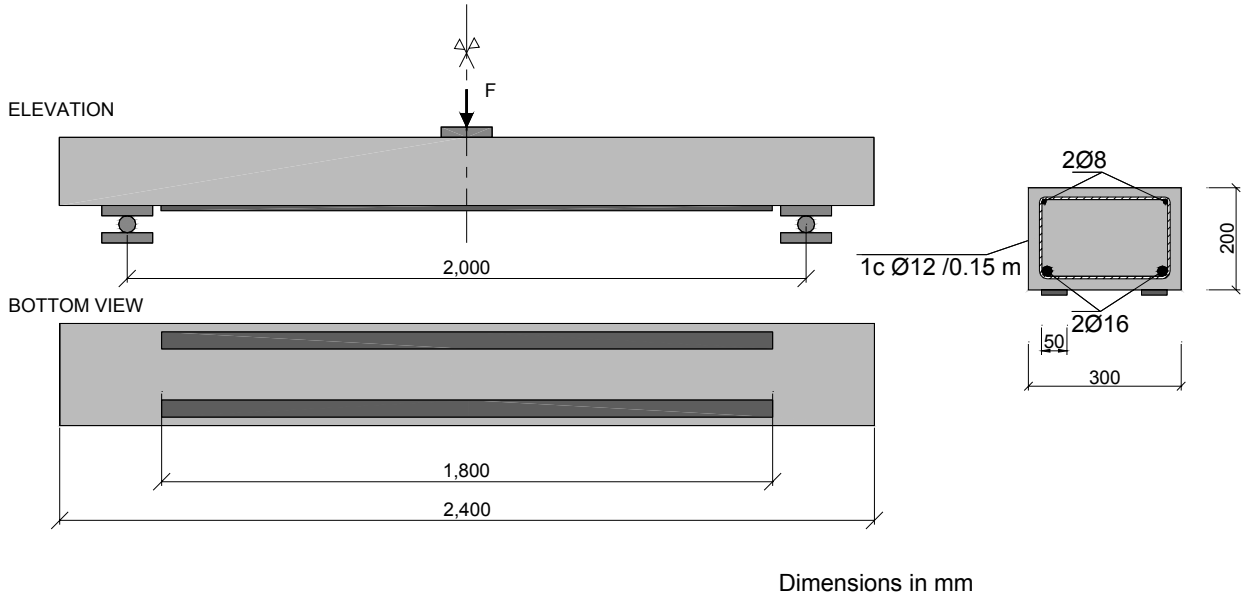

Figure C.66. Test set-up for Beam 1/D (#2).

Table C.24. Summary of test results.

	Service test		Failure test		
	F_{cr} (*kN*)	F_s (*kN*)	F_s (*kN*)	F_v (*kN*)	F_u (*kN*)
	11.2	55.0	49.8	-	112.0
$\delta(x = L/2)$ (*mm*)	1.41	8.15	6.7	-	15.7
ε_L $(x = L/2)$ $(\mu\varepsilon)$	-	-	1504	-	3992

Figure C.67. Debonding of both laminates at the end of the test. Peeling may have initiated due to an intermediate existing crack that appeared during the first failure test of Beam 1/D.

Figure C.68. Laminate 1 peeled-off without the detachment of a concrete cover layer in more than half of the debonded laminate.

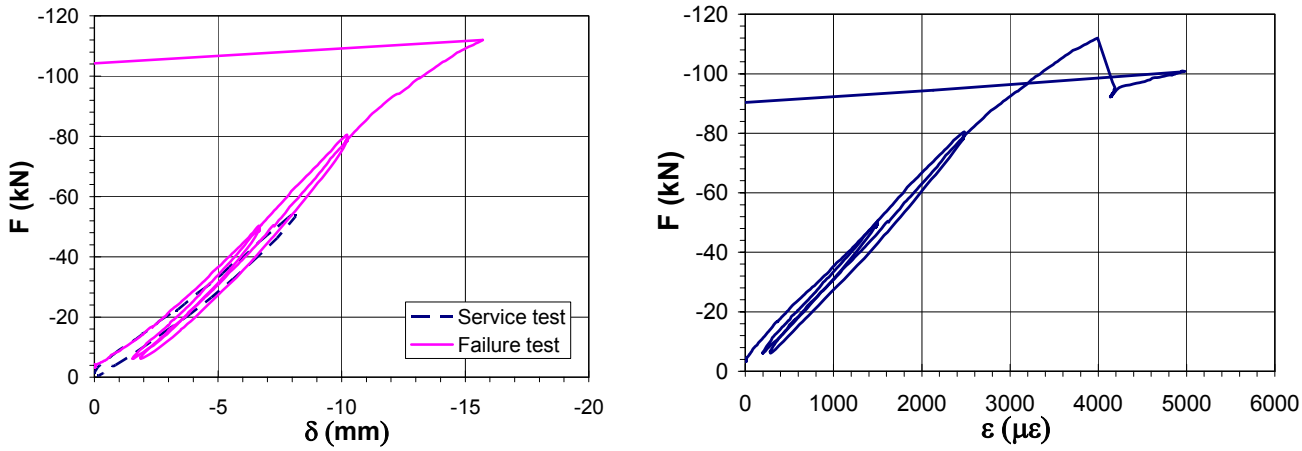

Figure C.69. Midspan displacement. Strain profile in the laminate center of Beam 1/D (#2).

C.3.12. Beam 2/D (#2)

Test observations

Since no significant damage was caused during the previous failure test, Beam 2/D was strengthened in this occassion by two laminates of 100 *mm* x 1.4 *mm*, and was tested again (Figure C.70). The amount of external reinforcement was twice the area applied on the remaining beams of group 2. Both laminates were placed at 20 *mm* from the wedges with the purpose of being as close as possible to the vertical stirrups. The load was applied in three cycles: to service load, to the control beam failure load, and finally, to failure. In the last cycle, when the load was 163.0 *kN*, one of the laminates initiated its debonding near midspan and propagated up to the nearest laminate end. A few seconds later, the remaining laminate peeled-off towards the same side. Both Figure C.72 and Figure C.73 show the evidence of a concrete failure in tension that caused laminate debonding and left some stirrups within sight. As shown in Figure C.73 and in Figure C.75, the maximum laminate strain at failure was 4121 $\mu\varepsilon$, similar to the value reached in Beam 2/D with half of the external reinforcement area (3910 $\mu\varepsilon$).

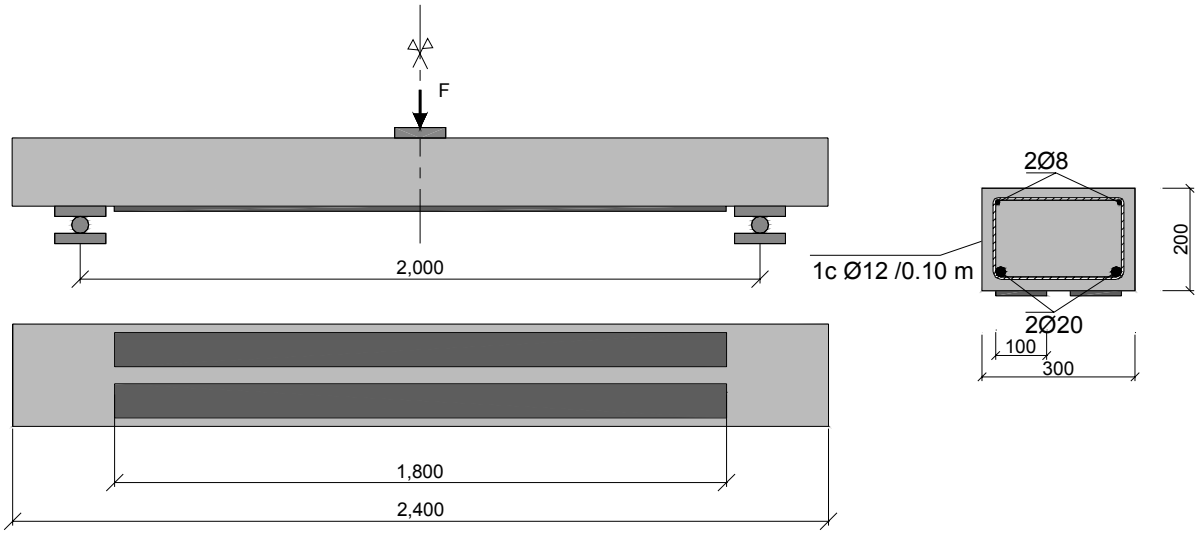

Figure C.70. Test set-up for Beam 2/D (#2).

Table C.25. Summary of test results.

	Service test		Failure test		
	F_{cr} (*kN*)	F_s (*kN*)	F_s (*kN*)	F_y (*kN*)	F_u (*kN*)
	17.3	74.1	77.54	-	163.0
$\delta(x = L/2)$ (*mm*)	0.90	8.7	8.4	-	17.8
ε_L $(x = L/2)$ ($\mu\varepsilon$)	-	-	2139	-	4121

Table C.26. Strain gauge distribution.

Gauge	1	2	3	4	5	6	7	8	9	10	11	12
Surface	L1	L2	L1	L2	L1	L2	L1	L2	L1	L2	L1	L2
x (*mm*)	-857	-863	-601	-603	-397	-403	-239	-248	-119	-117	0	0
y (*mm*)	1	0	0	-2	0	0	0	3	0	5	3	8
z (*mm*)	0	0	0	0	0	0	0	0	0	0	0	0

Gauge	13	14	15	16	17	18	19	20	21	22	23	24
Surface	L1	L2	L1	L2	L1	L2	L1	L2	L1	L2	L1	L2
x (*mm*)	0	0	84	77	288	297	445	446	610	605	860	858
y (*mm*)	-20	-2	0	0	0	5	-4	5	2	0	0	0
z (*mm*)	0	0	0	0	0	0	0	0	0	0	0	0

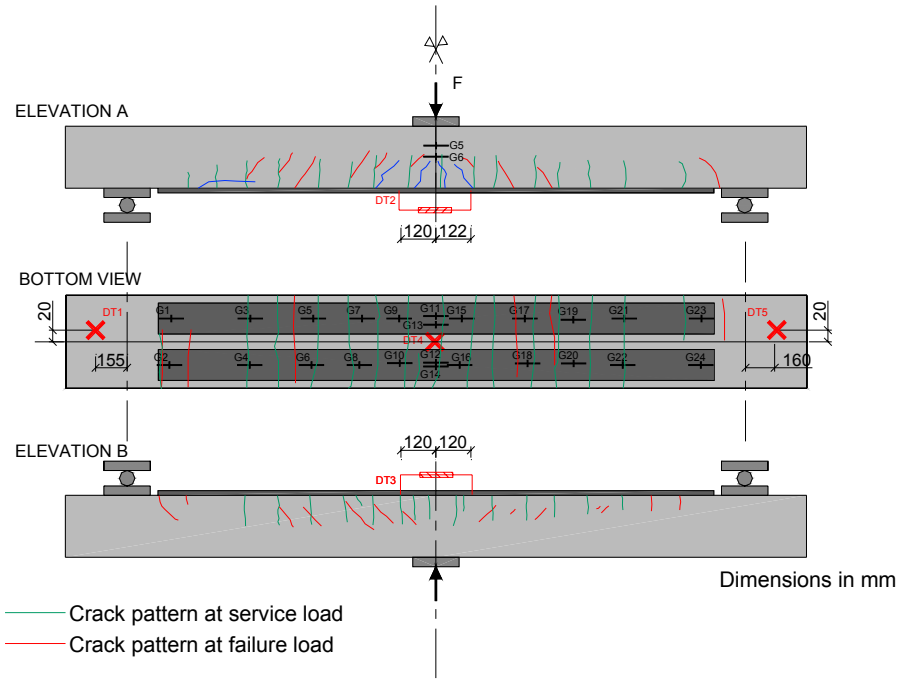

Figure C.71. Crack pattern at service and at failure load, together with the instrumentation affixed to Beam 2/D (#2).

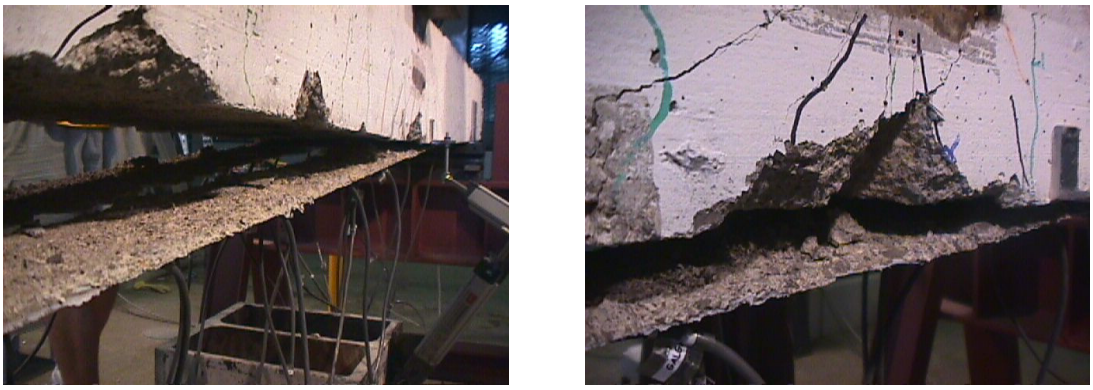

Figure C.72. Debonding of both laminates at the end of the test. Peeling may have been initiated due to an intermediate crack, and propagated in the same direction for both laminates.

Figure C.73. Both laminates peeled-off with the detachment of the concrete cover, leaving some visible stirrups.

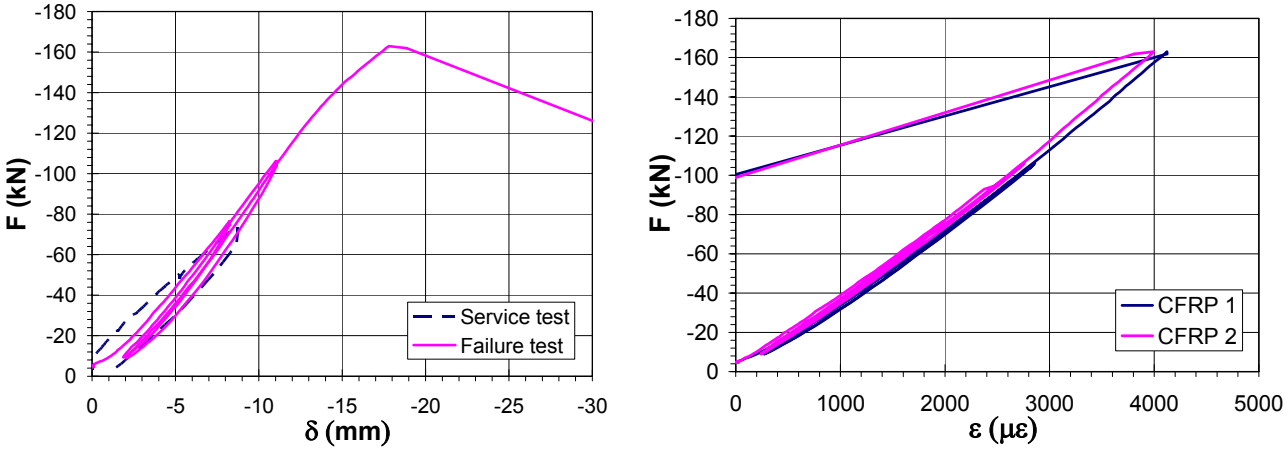

Figure C.74. Midspan deflection. Strain profile in the laminate center of Beam 2/D (#2).

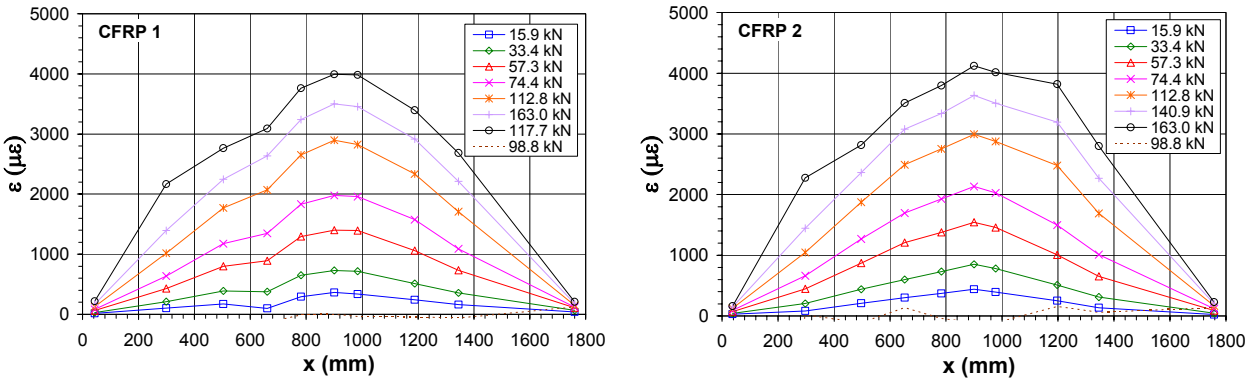

Figure C.75. Strain distribution along both laminates in Beam 2/D (#2).

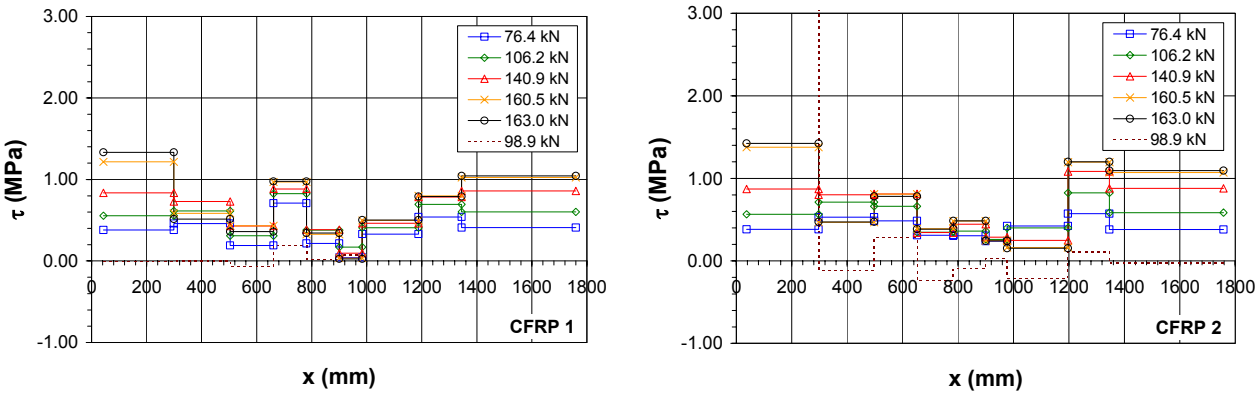

Figure C.76. Shear stress distribution along both laminates in Beam 2/D (#2).

C.3.13. Beam 1/C (#2)

Test observations

In the second test of Beam 1/C, the beam was strengthened by means of a wet lay-up unidirectional lamina of CFRP and a pultruded laminate of 100 *mm* x 1.4 *mm* (see Figure C.77) on top of it. A tensile failure in the concrete generated the pultruded

laminate debonding and the rupture of fibers in the unidirectional lamina, because there was not strength available in the direction perpendicular to the laminate (Figure C.79). The higher external-to-internal reinforcement ratio (0.43 %) in comparison to the rest of the beams of group 1 (0.34 %) implied an increase in the failure load (121.0 *kN*) as shown by Figure C.80. The maximum strain reached on the laminate at midspan was 4181 $\mu\varepsilon$. However, the laminate strain profile along the bonded length (Figure C.81) showed that the maximum recorded strain, 4528 $\mu\varepsilon$, was not located at midspan but in the vertical of one existing cracks.

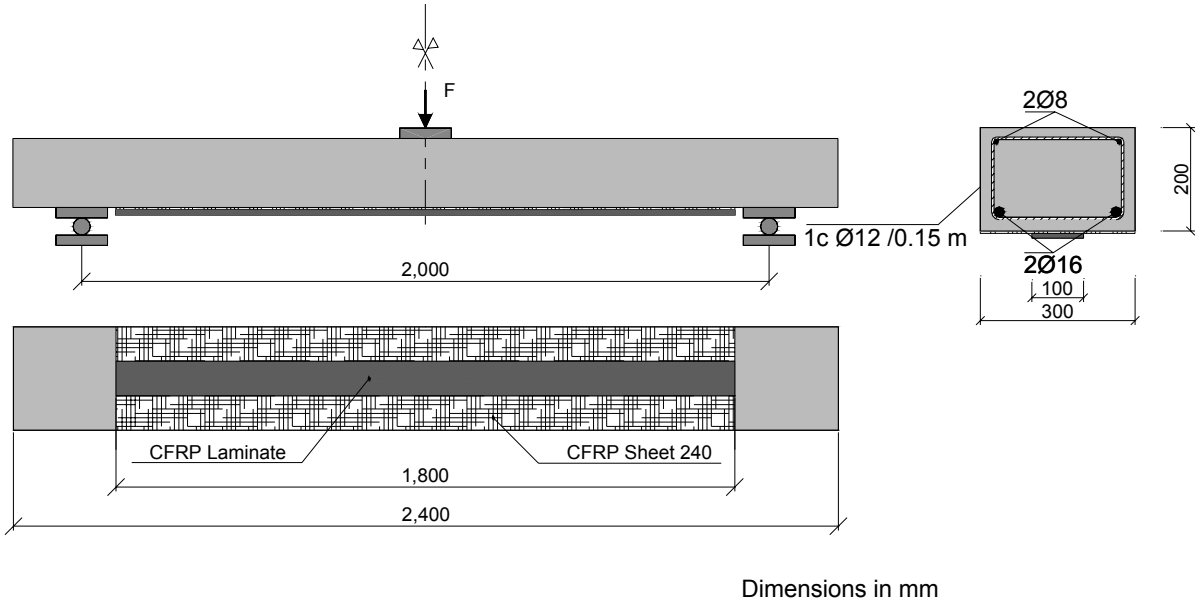

Figure C.77. Test set-up for Beam 1/C (#2).

Table C.27. Summary of test results.

	Service test		Failure test		
	F_{cr} (*kN*)	F_s (*kN*)	F_s (*kN*)	F_v (*kN*)	F_u (*kN*)
	13.3	47.8	51.2	117.9	122.0
$\delta(x = L/2)$ (*mm*)	1.11	7.82	7.1	16.1	17.8
$\varepsilon_L(x = L/2)$ ($\mu\varepsilon$)	-	-	1320	3460	4181

Table C.28. Strain gauge distribution.

Gauge	1	2	3	4	5	6	7	8	9	10	11	12
Surface	-	-	-	-	-	-	-	-	L	L	L	-
x (*mm*)	-	-	-	-	-	-	-	-	711	884	187	-
y (*mm*)	-	-	-	-	-	-	-	-	2	0	0	-
z (*mm*)	-	-	-	-	-	-	-	-	0	0	0	-

Gauge	13	14	15	16	17	18	19	20	21	22	23	24
Surface	L	L	L	L	-	-	-	L	L	L	L	L
x (*mm*)	-850	-674	-506	-260	-	-	-	-96	0	0	332	489
y (*mm*)	1	0	0	-1	-	-	-	0	3	-5	-2	0
z (*mm*)	0	0	0	0	-	-	-	0	0	0	0	0

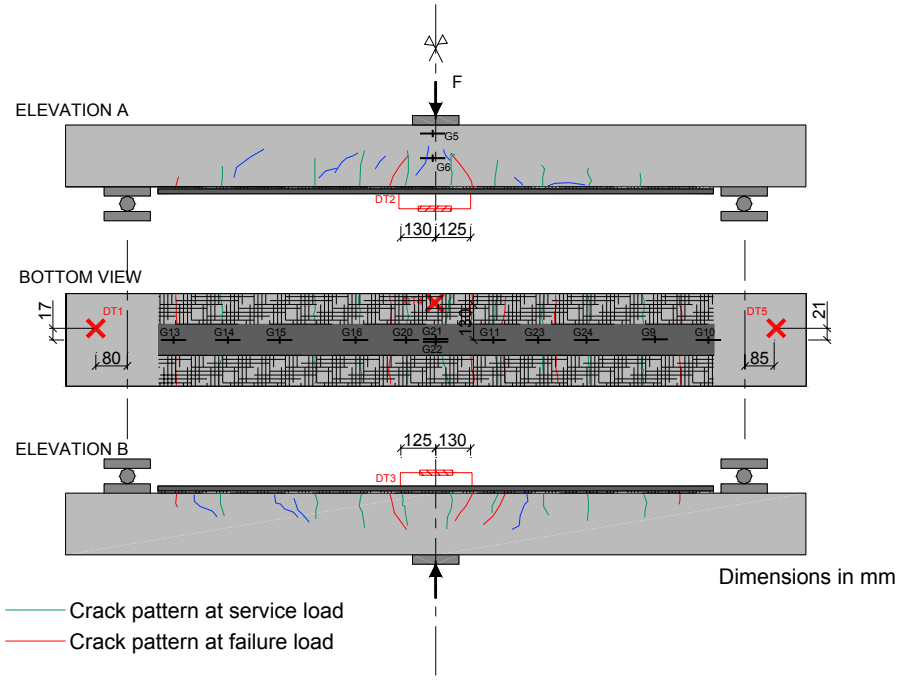

Figure C.78. Crack pattern at service and at failure load, together with the instrumentation affixed to Beam 1/C (#2).

Figure C.79. Pultruded laminate bonded on the top of a wet lay-up lamina. Laminate peeling of both pultruded and wet lay-up laminates.

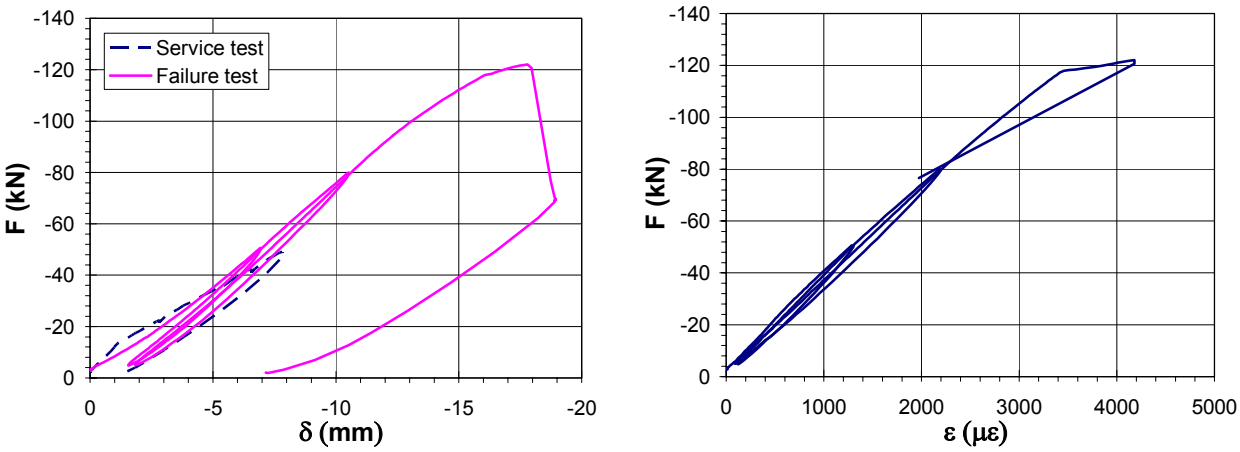

Figure C.80. Midspan displacement. Strain profile in the laminate center of Beam 1/C (#2).

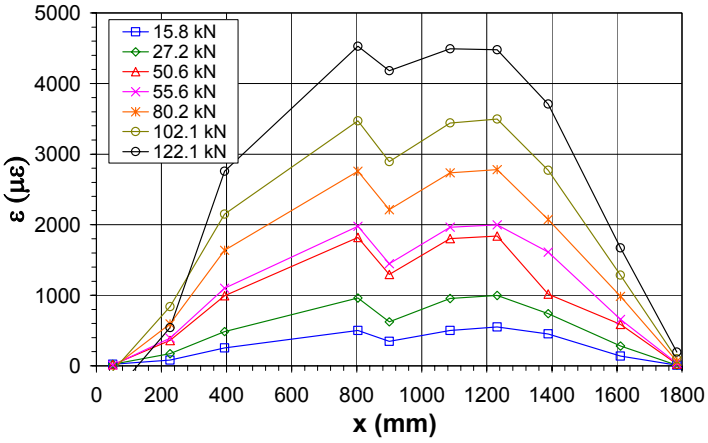

Figure C.81. Laminate strain distribution along Beam 1/C (#2).

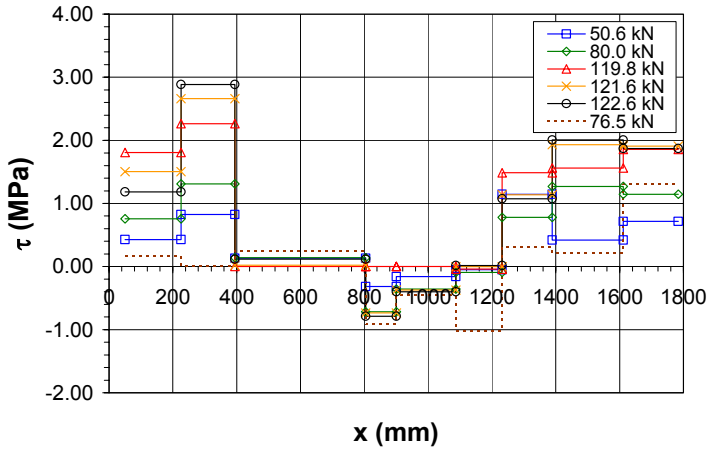

Figure C.82. Shear stress distribution along Beam 1/C (#2).

C.3.14. Beam 1/B (#2)

Test observations

The application of laminates in special saw-cuts slots in the concrete shows several advantages such as increase of the ductility, prevention or delay of the peeling phenomenon, extra protection against fire, mechanical and environmental damaging effects, and easier and faster installation. However, the area of near surface mounted laminates is lower compared to the externally bonded reinforcement because the saw-cuts slots are made in the concrete cover.

To evaluate the efficiency of this technique Beam 1/B was then strengthened by two laminates of 10 *mm* x 1.4 *mm* applied in slots of 15 *mm* depth (Figure C.83). The strengthening procedure is shown in Figure C.85.

In spite of the lower ratio of reinforcement applied, an increase in the load capacity of 11.8 % was observed in relation to the control beam. Due to an error of the acquisition system, the maximum measured strain was 7000 $\mu\varepsilon$ under a load of 85.0 *kN*. However,

the maximum strain was probably higher at failure when the applied load was 92.5 *kN*. The results proved that this technique was more effective than the externally bonded reinforcing technique because of the improvement in bond strength. Hence, higher stresses were mobilized at failure, larger deformations were attained, and a higher resistance to peeling phenomenon was observed. The debonding of the laminate was initiated in the bond line between adhesive and laminate. Failure occurred after the sliding of the laminate (Figure C.86). The drops observed in Figure C.87 at the end of the test correspond to the bonding loose and the initiation of sliding.

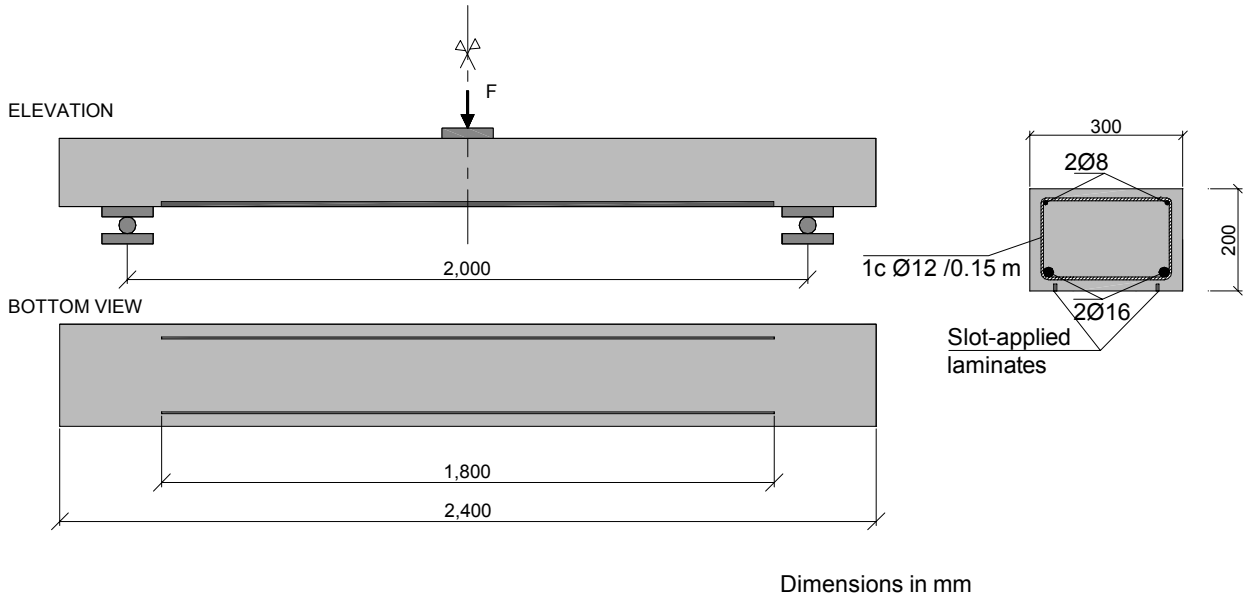

Figure C.83. Test set-up for Beam 1/B (#2).

Table C.29. Summary of test results.

	Service test		Failure test		
	F_{cr} (*kN*)	F_s (*kN*)	F_s (*kN*)	F_y (*kN*)	F_u (*kN*)
	13.3	47.8	51.4	78.2	92.5
$\delta(x = L/2)$ (*mm*)	1.11	7.82	8.9	12.9	37.9
ε_L $(x = L/2)$ ($\mu\varepsilon$)	-	-	2450	3730	>7000

Table C.30. Strain gauge distribution.

Gauge	1	2	3	4	5	6	7	8	9	10	11	12
Surface	-	-	-	-	C	C	-	-	-	-	-	-
x (*mm*)	-	-	-	-	0	0	-	-	-	-	-	-
y (*mm*)	-	-	-	-	0	0	-	-	-	-	-	-
z (*mm*)	-	-	-	-	137	132	-	-	-	-	-	-

Gauge	13	14	15	16	17	18	19	20	21	22	23	24
Surface	L1	L2	L1	L2	L1	L2	L1	L2	L1	L2	-	-
x (*mm*)	-803	-800	-400	-400	-1	2	500	495	97	100		
y (*mm*)	0	0	0	0	0	0	0	0	0	0		
z (*mm*)	0	0	0	0	0	0	0	0	0	0		

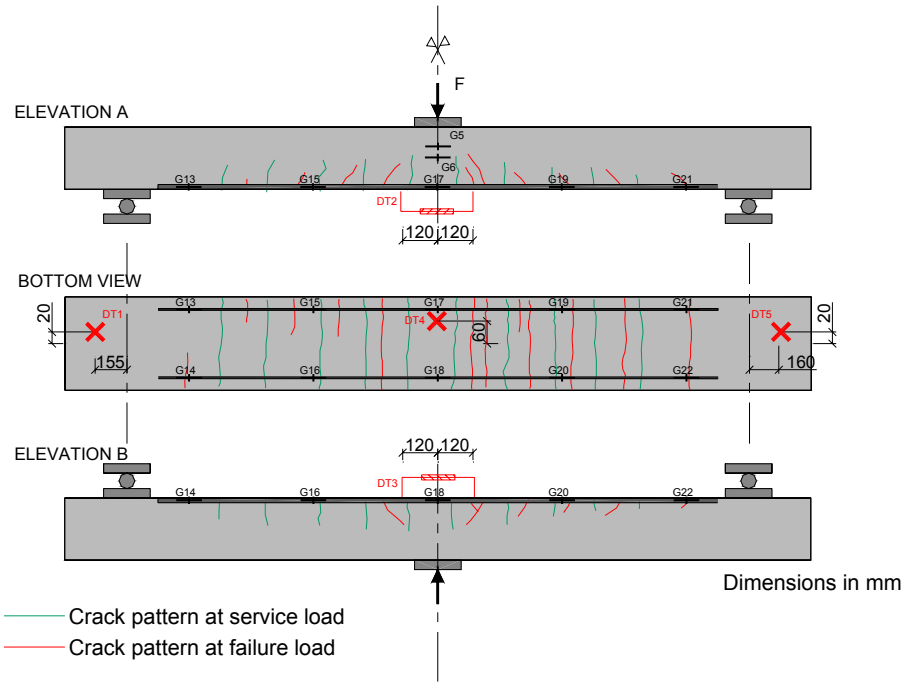

Figure C.84. Crack Crack pattern at service and at failure load, together with the instrumentation affixed to Beam 1/B (#2).

Figure C.85. Two slot-applied laminates were bonded in Beam 1/B (#2).

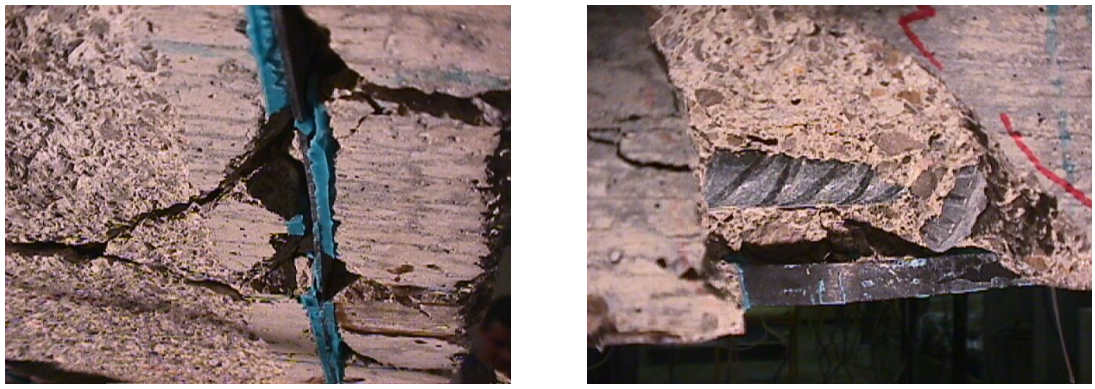

Figure C.86. Peeling failure in Beam 1/B (#2) due to the effect of cracks.

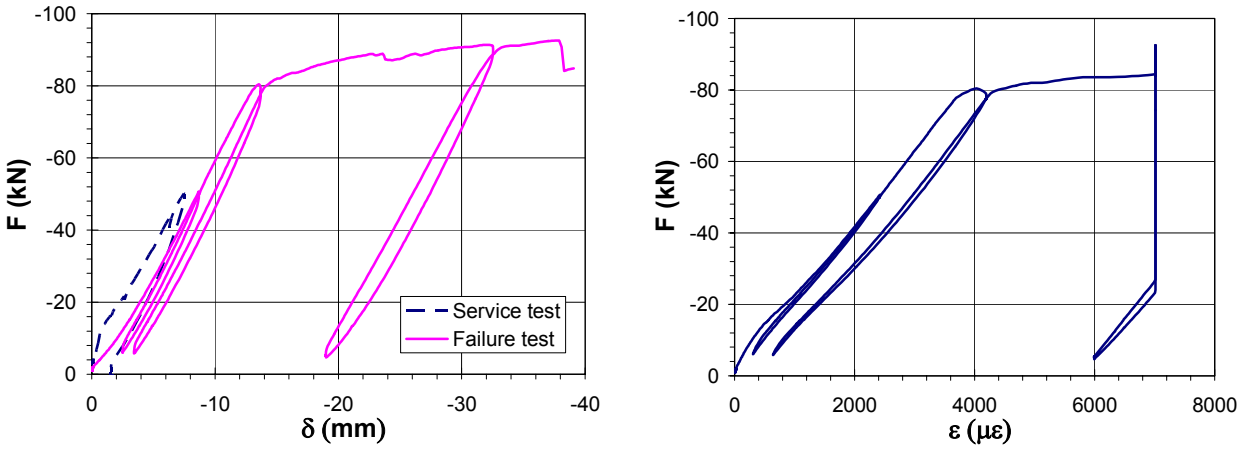

Figure C.87. Midspan displacement. Strain profile in the laminate center of Beam 1/B (#2).

Figure C.88 shows the laminate strain evolution along the laminate for different load levels. As observed, the strain gauges exceeded their capacity once they reached 7000 $\mu\varepsilon$.

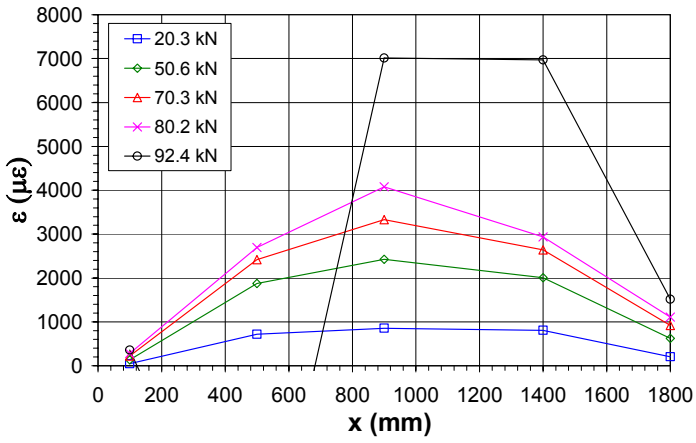

Figure C.88. Laminate strain distribution along Beam 1/B (#2).

C.4. Discussion of results

After the description of test results given by §C.3, a short discussion about them is presented in this section.

First of all, the midspan deflection of an externally strengthened beam of each group is compared to the control beam. As observed in Figure C.89, the existence of a bonded laminate increased the stiffness of the original concrete beam. However, this increase was more considerable for low external-to-internal reinforcement ratios, in other words, for Beam group 1 rather than for Beam group 2.

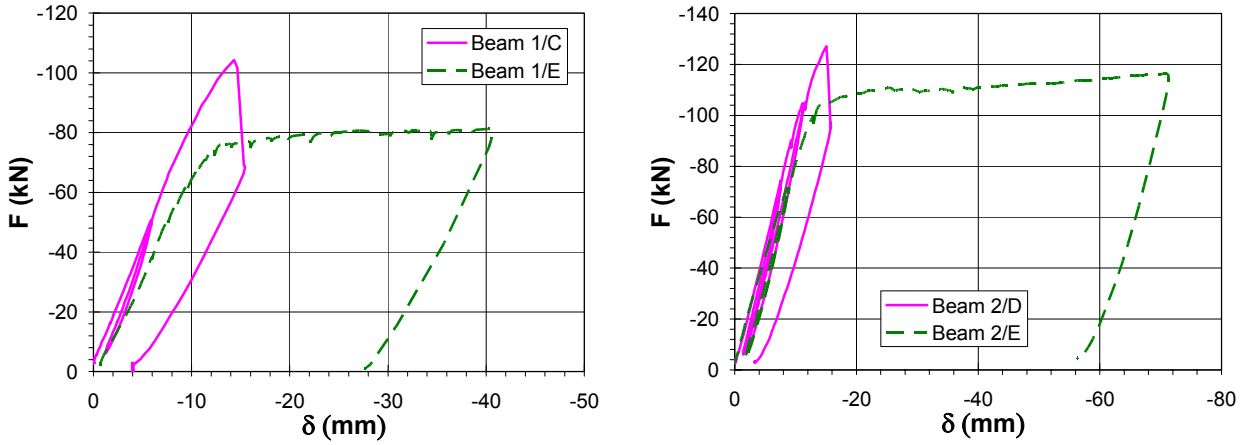

Figure C.89. Comparison of midspan deflection between Beams 1/E and 1/C and between Beams 2/D and 2/E.

When studying the Beam 1 group alone, the response of Beam 1/D up to failure was very similar to Beam 1/C. By extending the laminate to the supports in Beam 1/C, a significant increase in the failure load and in the maximum strain (2801 $\mu\varepsilon$ vs. 3942 $\mu\varepsilon$) was observed (see Figure C.90).

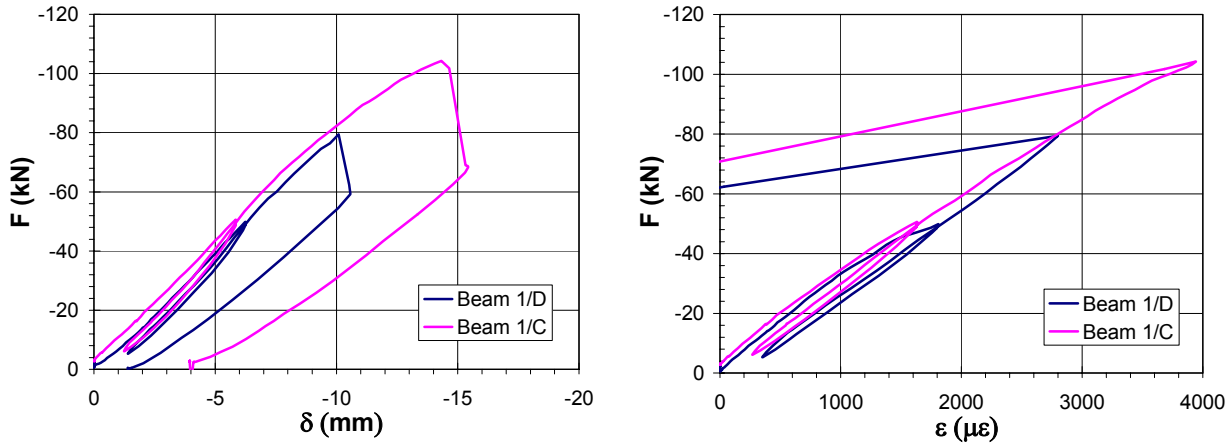

Figure C.90. Comparison between Beams 1/D and 1/C in terms of midspan deflection and midspan laminate strain.

Since both Beams 1/C and 1/B were strengthened and tested with the same configuration, test results were almost identical in terms of midspan deflection and midspan laminate strain (Figure C.91).

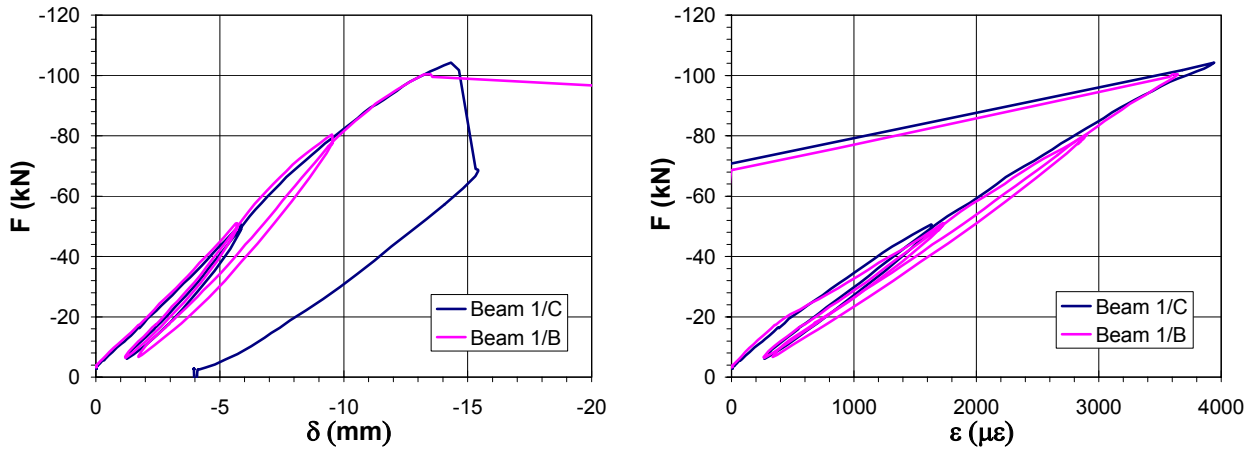

Figure C.91. Midspan deflection and maximum strain between Beams 1/C and 1/B

Beam 2/D was externally strengthened as Beam 1/C and 1/B. The only difference between them was the higher internal steel ratio that generated a higher bending stiffness. The same value of deflection and laminate strain was reached in Beam 2/D for a higher applied load (Figure C.92).

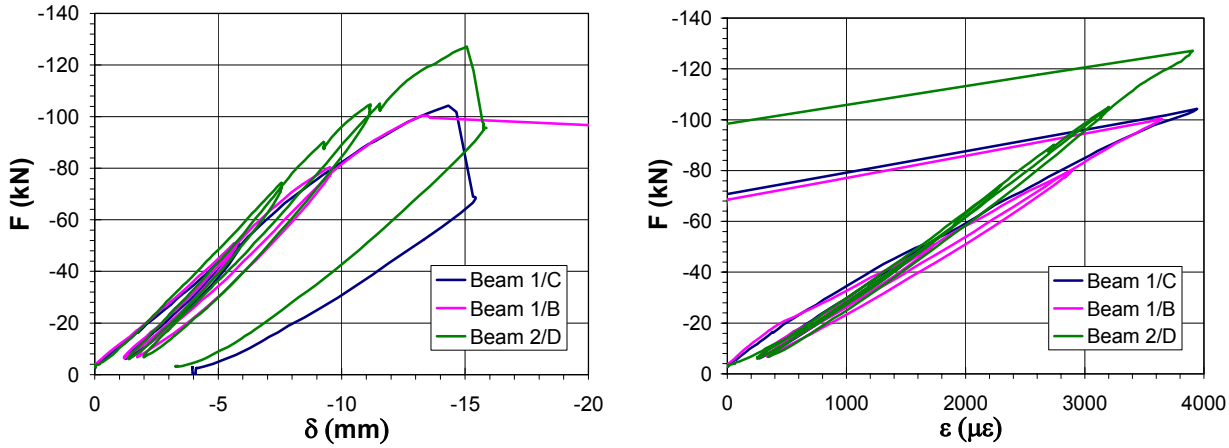

Figure C.92. Comparison between Beam 2/D and Beams 1/B and 1/C with the same amount of external reinforcement.

When analyzing the Beam group 2, the effect of bonding the same reinforcement area but divided into two laminates placed in the vertical of the shear stirrups (Beam 2/C) instead of in the center of the beam soffit (Beam 2/D) did not increase the stiffness because of the same amount of strengthened area, but implied an increase of the failure load and the maximum laminate strain. (Figure C.93)

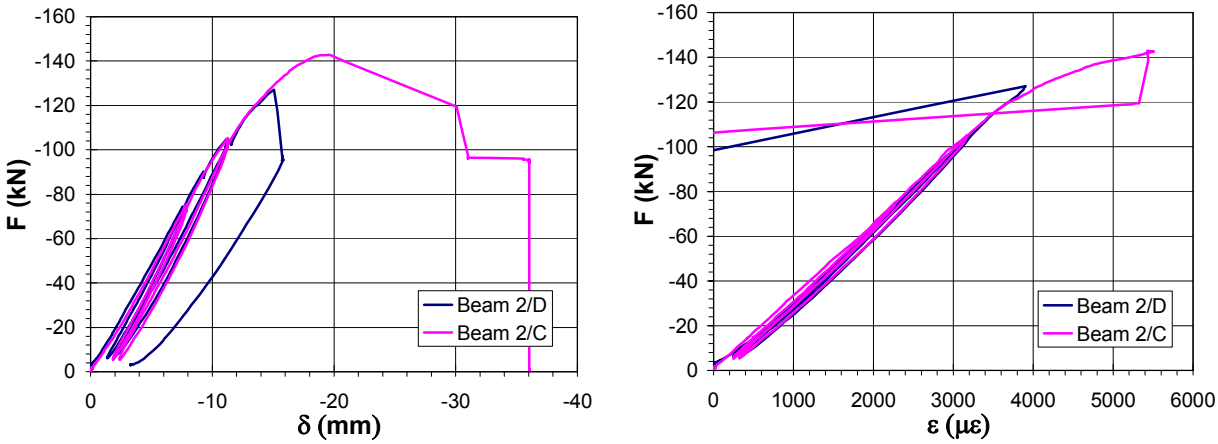

Figure C.93. Midspan deflection and laminate strain for Beams 2/D and 2/C with the same amount of external reinforcement but in a different distribution.

Figure C.94 and Figure C.95 compare the results in terms of deflection and laminate strain for beams with the same amount of external reinforcement bonded in the vertical of the stirrups or in the center of the tension concrete face, with or without external anchorages (Beams 2/C and 2/B; and Beams 2/D and 2/A, respectively). The application of external anchorages along the bonded laminate generated an increase in the stiffness of the strengthened beam. The beam with external anchorages and two laminates in the vertical of the stirrups reached a slightly higher failure load and showed a decrease of the maximum strain at failure (Figure C.94). When the laminate was bonded to the center of the soffit, the external anchorage implied an increase of 17.2 % in the failure load and a significant increment in the maximum strain reached at failure (Figure C.95).

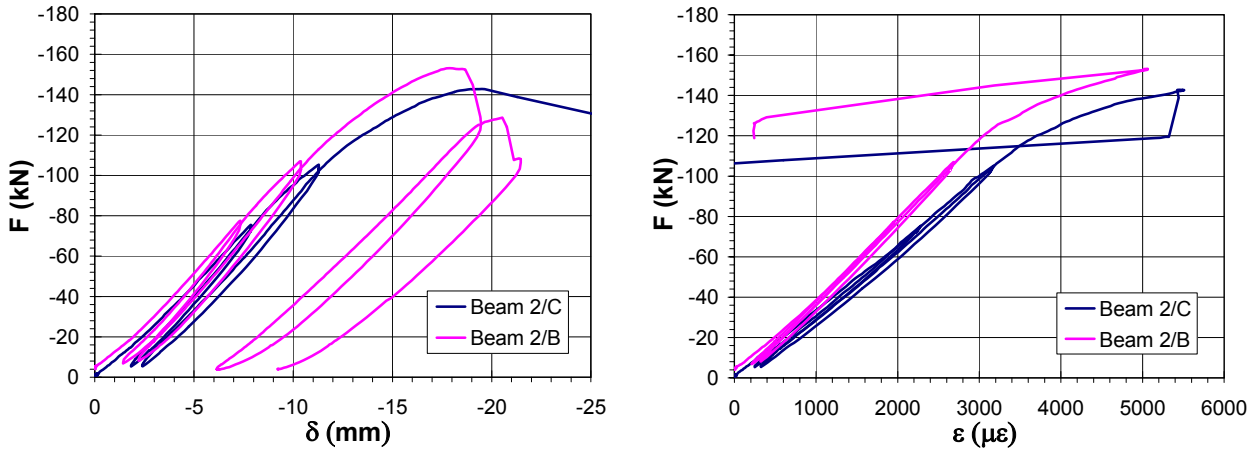

Figure C.94. Comparison in terms of deflection and laminate strain at midspan between Beams 2/C and 2/B, without and with external anchorage respectively, both with two pultruded laminates bonded on the vertical of the shear stirrups.

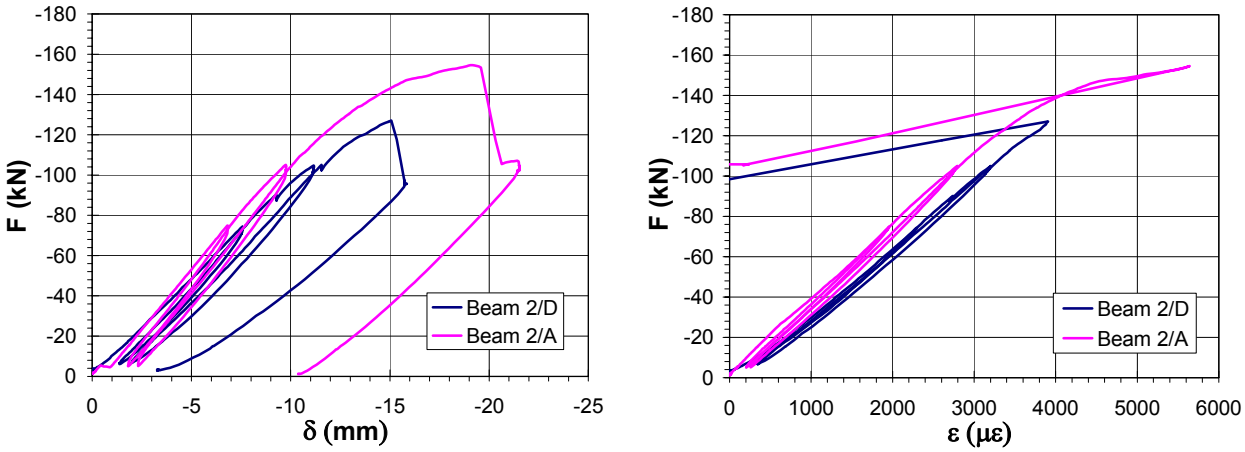

Figure C.95. Comparison in terms of deflection and laminate strain at midspan between Beams 2/D and 2/A, without and with external anchorage respectively, both with a pultruded laminate bonded on the center of the beam soffit.

In Beam 2/B, the external anchorages had a U-shape and were spread up to the compression zone of the concrete beam. In Beam 2/A, the efficiency of the lateral webs of the anchorage was studied, by bonding the external anchorage only to the beam soffit. In both cases a unidirectional wet lay-up lamina was employed as an external anchorage with the fibers placed perpendicular to the pultruded laminate. As shown in Figure C.96, the behavior of both Beam 2/B and 2/A was very similar in terms of failure load, deflection and laminate strain at midspan.

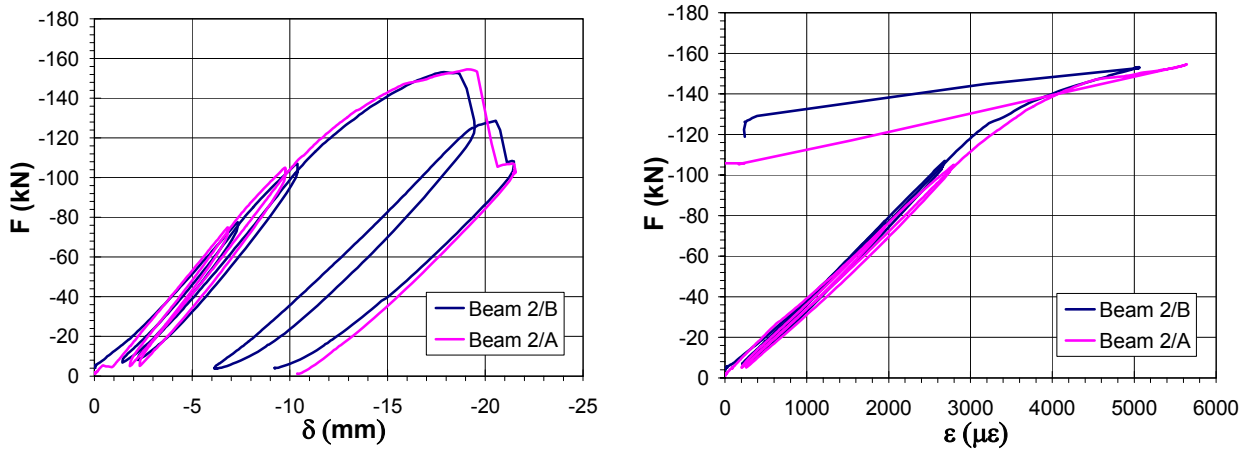

Figure C.96. Comparison between Beam 2/B with external anchorages spread to the webs and Beam 2/A with external anchorages only bonded to the beam soffit.

During its second test after failure, Beam 2/D (#2) was strengthened by two laminates of 100 *mm* x 1.4 *mm*, doubling the amount of external reinforcement area in comparison to the first test of Beam 2/D. As a result, Beam 2/D (#2) reached a higher failure load, 163.0 *kN*. However, this reported value was lower than twice the failure load of Beam 2/D (128.0 *kN*). In addition, the increase of stiffness can only be appreciate in Figure C.97, where the maximum laminate strain at failure was very similar for both beams, but the failure load was significantly higher for the second test of Beam 2/D.

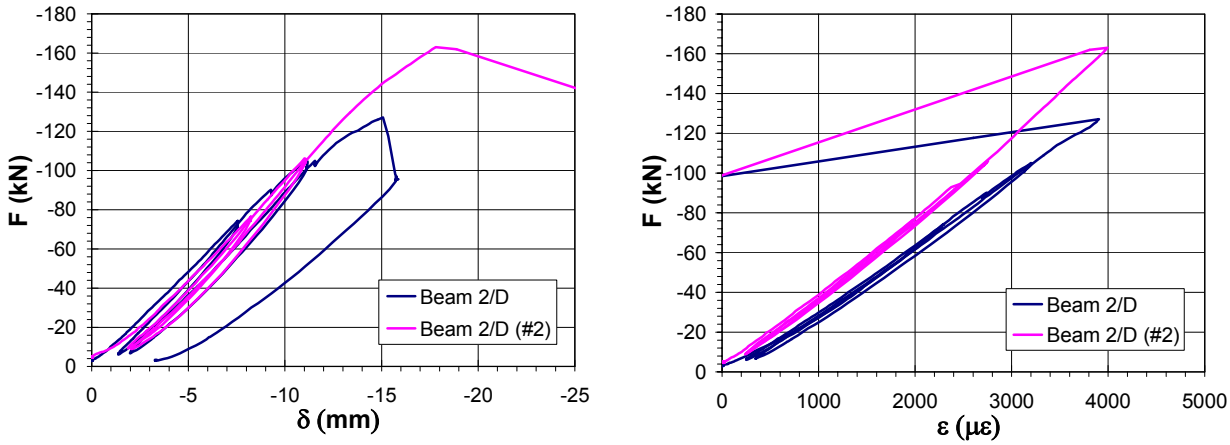

Figure C.97. Midspan deflection and laminate strain for Beam 2/D and Beam 2/D (#2) which was strengthened with the double amount of external reinforcement.

An improvement in the ductility was obtained by bonding two slot-applied laminates in the second test of Beam 1/B. As shown by Figure C.98, the maximum deflection of Beam 1/B (#2) (37.9 *mm*) with two slot-applied laminates was almost three times the maximum deflection of Beam 1/B (13.5 *mm*). In addition, the improvement in the laminate bond allowed an increase in the laminate strain and the development of higher stresses. The maximum laminate strain was at least twice the maximum value reached in the rest of the Beam group 1. The strain increment is only around twice because the data acquisition system stopped registering strain values at 92.7 % of the failure load.

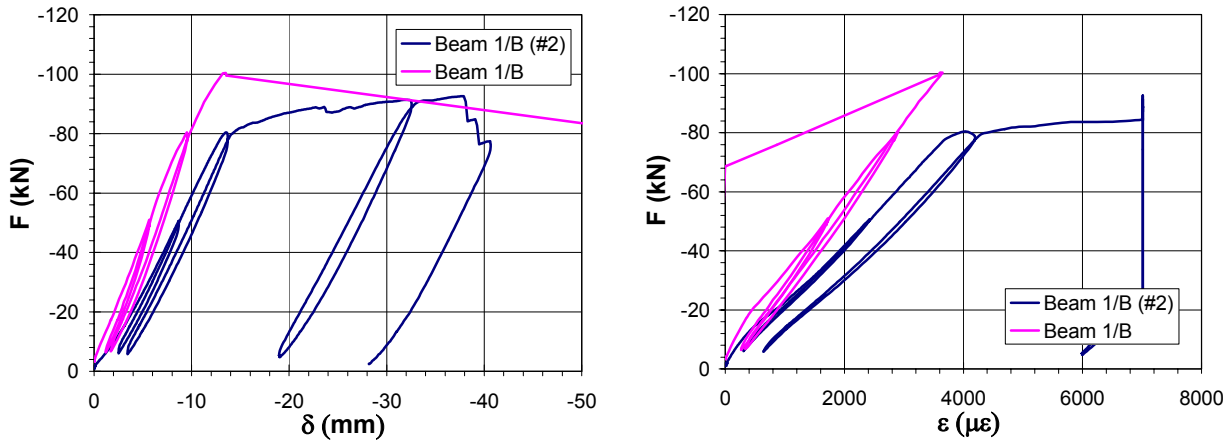

Figure C.98. Comparison between Beams 1/B (#2) strengthened by slot-applied laminates and 1/B strengthened by an externally bonded reinforcement.

C.4.1. Comparison of test and numerical results

A moment-curvature analysis was performed to obtain the theoretical predictions in failure load for both Beam group 1 and Beam group 2. As shown in Figure C.99 and Figure C.100, the theoretical prediction of the failure load was always higher than the experimental value. The expected mode of failure in the moment-curvature analysis was due to concrete crushing in the compression zone because the ultimate laminate strain of

16000 $\mu\varepsilon$ was never reached. However, as explained in §C.3, all tests failed in a brittle and sudden manner that involved the laminate peeling-off before reaching the theoretical prediction, that is before the development of a classical failure mode.

All beams that were represented in both plots of Figure C.99 were strengthened by one or two pultruded laminates and with the same resulting strengthening area. As shown in Figure C.99, Beam 1/D, with a short laminate length (1500 *mm*) compared to the rest of beams (1800 *mm*), failed before the yielding of the internal rebars. The bonded laminate peeled-off in both Beams 1/C and 1/B just after the initiation of steel yielding. This might be explained by the fact that once the steel yields, the tensile stress in the laminate increases at a much faster rate, and the plate alone resists further increments of the tensile component of the bending moment. Hence, the shear stresses on the interface between concrete and the external reinforcement should increase significantly. If the interfacial shear stresses reach the concrete tensile strength, a tensile failure in concrete will occur and the laminate will peel-off. It is not clear enough if the laminate of Beam 2/D debonded before or after steel yielding. By observing Figure C.99, the experimental stiffness was somewhat higher than the predicted value for the Beam group 1 and slightly lower for the Beam group 2.

The location of the laminate in the vertical of the shear stirrups delayed the laminate debonding as shown in Beam 2/C and Beam 1/D (#2) (Figure C.99 and Figure C.101 respectively).

For Beams 2/B and 2/A with external anchorages, Figure C.100 compares the experimental laminate strain at midspan against the applied load, to the theoretical laminate strain obtained by a moment-curvature analysis performed without taking into account the effect of the anchorages. As observed, the addition of external anchorages along the bonded length not only delayed the peeling failure, but also increased the experimental beam stiffness.

As observed in Figure C.100, the laminate strain reduced significantly in Beam 2/D (#2) with twice the amount of external reinforcement. Therefore, a curvature reduction is observed with a higher degree of strengthening.

The laminate strain at midspan in Beam 1/B (#2), which was strengthened by two slot-applied laminates, was very similar to the moment-curvature analysis prediction. The strain at failure was not recorded due to an error of the acquisition system but it is clearly observed that it happened after steel yielding. In Figure C.101, the experimental failure load was plotted. By comparing it to the predicted value, the concrete in the compression zone had almost crushed, while the laminates debonded and slid along the saw-cut slots.

As a general conclusion, for all tested beams, the measured and predicted curves for the laminate strain were reasonably close. The main difference was on the predicted failure load because the bonded laminate peeled-off before concrete crushed or the laminate fibers ruptured.

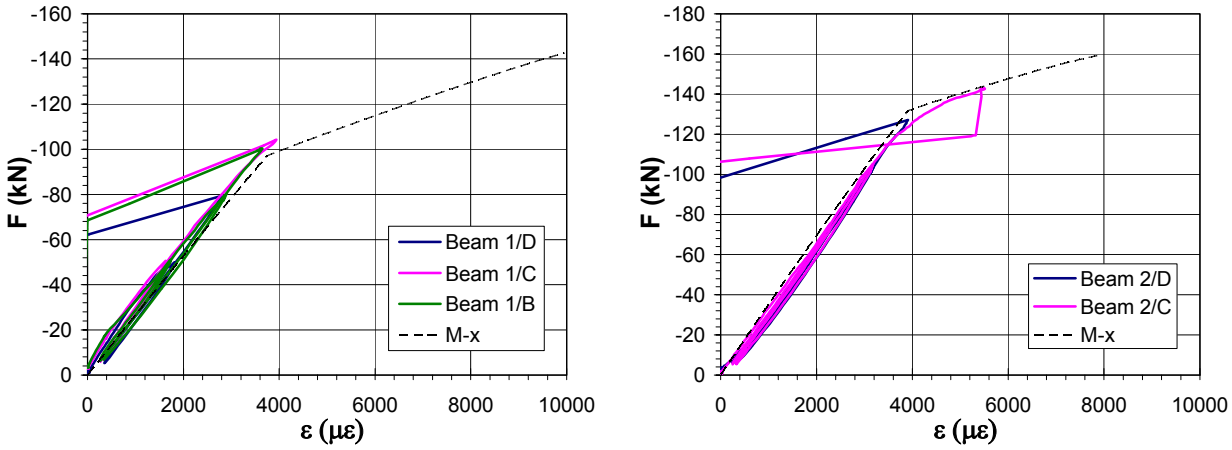

Figure C.99. Experimental and theoretical load vs. laminate strain in Beams 1/D, 1/C, 1/B and 2/D and 2/C.

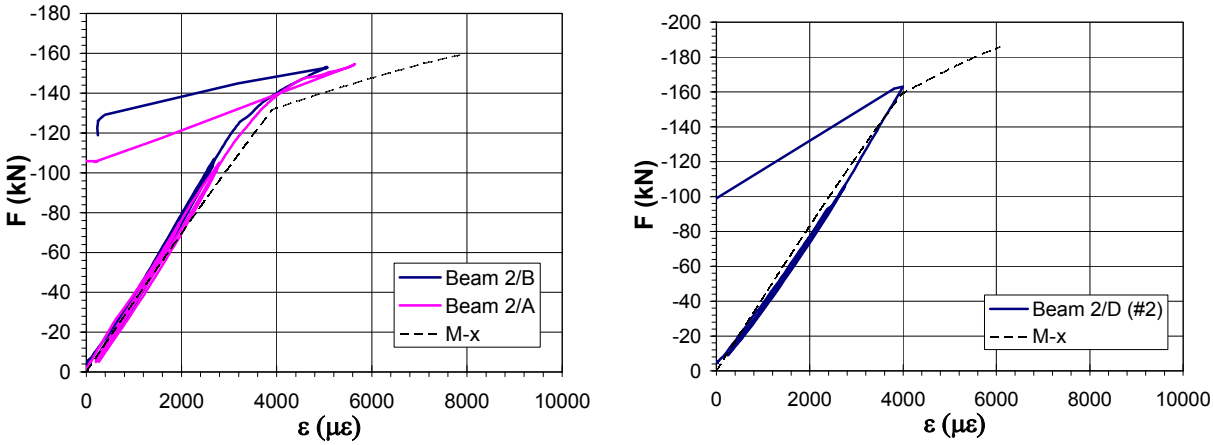

Figure C.100. Experimental and theoretical load vs. laminate strain in Beam 2/A, 2/B and 2/D (#2).

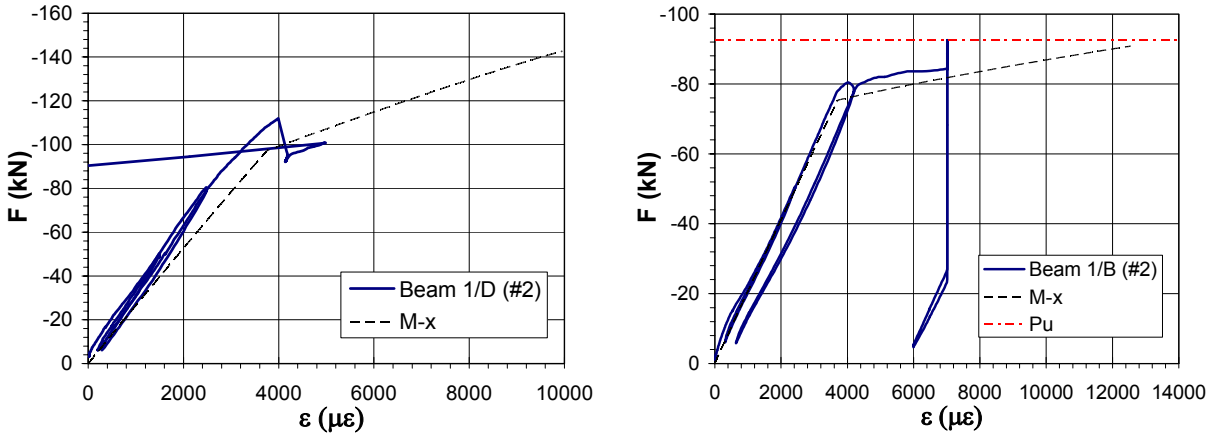

Figure C.101. Experimental and theoretical load vs. laminate strain in Beam 1/D (#2) and 1/B (#2).

Table C.31 summarizes for Beam group 1, Beam group 2, Beam 2/D (#2) and Beam 1/B (#2), the theoretical applied load and the associated laminate strain at yielding and at failure.

Table C.31. Summary of predicted results by the moment-curvature analysis.

	Laminate cross-section	F_y (kN)	ε_{Ly} ($\mu\varepsilon$)	F_u (kN)	ε_{Lu} ($\mu\varepsilon$)
Beam 1	1 x 100 *mm* x 1.4 *mm*	97.7	3817	142.6	9956
Beam 2	1 x 100 *mm* x 1.4 *mm*	132.2	3968	159.1	7857
Beam 2/D (#2)	2 x 100 *mm* x 1.4 *mm*	160.0	4050	185.8	6091
Beam 1/B (#2)	2 x 10 *mm* x 1.4 *mm*	75.5	3792	90.8	12550

In Table C.32 the experimental failure load is compared to predicted failure load given by Table C.31. In addition, the maximum experimental strain (column 3) is compared in column 5 of Table C.32 to the laminate strain obtained by the moment curvature analysis for the experimental failure load (column 4). For Beam group 1, the experimental values are close and, in some extent, lower than 1.00. On the contrary, for Beam group 2, the experimental strains are close but vaguely higher than 1.00. The predicted laminate strains for Beams 2/B and 2/A were significantly higher than the experimental values. Note that the possible increase in the stiffness derived from the external anchorages was not taken into account in the moment-curvature analysis. As mentioned in Chapter 2, except for Beam 1/B (#2), the experimental laminate strains were always lower than the recommended strain to prevent peeling failure (8000 $\mu\varepsilon$). Finally, column 6 compares the experimental maximum laminate strain with the ultimate laminate strain given by the manufacturer. The maximum experimental laminate strain is at maximum 0.35 its ultimate strain indicating the under-utilization of the CFRP material.

Table C.32. Summary of test results.

	$F_{u,\exp}$ (kN)	$F_{u,\exp}/F_{u,M\text{-}\chi}$	$\varepsilon_{Lu,\exp}$ ($\mu\varepsilon$)	$\varepsilon_{Lu,\ M\text{-}\chi(Pu)}$ ($\mu\varepsilon$)	$\varepsilon_{Lu,\exp}/\varepsilon_{Lu,M\text{-}\chi(Pu)}$	$\varepsilon_{Lu,\exp}/\varepsilon_{Lu}$
	(1)	(2)	(3)	(4)	(5)	(6)
Beam 1/D	80.0	0.56	2801	3065	0.91	0.18
Beam 1/C	104.0	0.73	3942	4599	0.86	0.25
Beam 1/B	100.4	0.70	3647	4149	0.88	0.23
Beam 1/A	109.0	0.76	4437	5239	0.85	0.28
Beam 2/D	128.0	0.80	3910	3790	1.03	0.24
Beam 2/C	142.8	0.90	5619	5340	1.05	0.35
Beam 2/B	153.1	0.96	5160	6823*	0.76*	0.32*
Beam 2/A	154.6	0.97	5640	7061*	0.80*	0.35*
Beam 1/D (#2)	112.0	0.79	3992	5628	0.71	0.25
Beam 1/B (#2)	92.5	1.02	>7000	-	-	-
Beam 2/D (#2)	163.0	0.88	4121	4261	0.97	0.26

* Moment-curvature analysis for Beams 2/B and 2/A did not take into account the external anchorages.

APPENDIX D

ASSUMPTIONS AND BOUNDARY CONDITIONS EMPLOYED IN THE DERIVATION OF THE STRESS GOVERNING EQUATIONS

D.1. Introduction

To clarify the formulation given in Chapter 3 and Chapter 4, this appendix compiles the different assumptions and contour conditions, considered in the derivation of the governing equations for the interfacial shear stresses in a pure shear specimen and in a beam element subjected to transverse loads. In the last case, equations have been derived for both an element between two cracks and an element between the plate end and its nearest crack.

D.2. Pure shear specimen

When studying a joint loaded in pure shear, the application of equilibrium and strain compatibility provides the governing equation for the interfacial shear stresses along the bonded length. In the derivation of the formulae presented in this section and in Chapter 3, the following assumptions have been made: the adhesive is only exposed to shear forces; the thickness and width of the adherents and adhesive are constant along the bonded length; since the concrete axial stiffness is much higher than the laminate axial stiffness, the concrete axial strain is neglected; and finally, the normal stresses are uniformly distributed along the laminate.

By applying equilibrium to a differential element, equation (D.1) that relates the laminate tensile stress and the interfacial shear stress can be derived.

$$\frac{d\sigma_L}{dx}(x) = \frac{1}{t_L}\tau(x) \tag{D.1}$$

As explained in Chapter 3, a bilinear bond-slip relationship is assumed. Therefore, the slip between concrete and laminate is related to the interfacial shear stress by equation (D.2).

$$s(x) = \begin{cases} \dfrac{s_{LM}}{\tau_{LM}}\tau(x) & (Zone\ I) \\ s_{LM} + \dfrac{s_{L0} - s_{LM}}{\tau_{LM}}(\tau_{LM} - \tau(x)) & (Zone\ II) \end{cases} \tag{D.2}$$

Following the assumptions described above and when no transverse loads are acting, the governing equation for the interfacial shear stress can be derived by incorporating equation (D.2) into the differential of equation (D.1), as shown by equation (D.3).

$$\begin{aligned} &\frac{d^2\sigma_L}{dx^2}(x) = \frac{1}{t_L}\frac{d\tau(x)}{dx} = \frac{1}{t_L}\frac{\tau_{LM}}{s_i}\frac{ds(x)}{dx} = \frac{1}{t_L}\frac{\tau_{LM}}{s_i}\left(\frac{du_L}{dx}(x) - \frac{du_c}{dx}(x)\right) = \\ &= \frac{1}{t_L}\frac{\tau_{LM}}{s_i}\varepsilon_L(x) = \frac{1}{E_L t_L}\frac{\tau_{LM}}{s_i}\sigma_L(x) \end{aligned} \tag{D.3}$$

where:

$$s_i = \begin{cases} s_{LM} & (Zone\ I) \\ s_{L0} - s_{LM} & (Zone\ II) \end{cases} \tag{D.4}$$

Therefore, the governing equation for the interfacial shear stress related to the upward branch of the bond-slip relationship (Zone I) can be rewritten as equation (D.5).

$$\frac{d^2\sigma_L^I}{dx^2}(x) - \Omega_1^2\sigma_L^I(x) = 0 \tag{D.5}$$

where:

$$\Omega_1^2 = \frac{1}{E_L t_L}\frac{\tau_{LM}}{s_{LM}} \tag{D.6}$$

Similarly, equation (D.7) gives the governing differential equation for the downward branch of the bilinear bond-slip relationship (Zone II).

$$\frac{d^2\sigma_L^{II}}{dx^2}(x) + \Omega_2^2\sigma_L^{II}(x) = 0 \tag{D.7}$$

where:

$$\Omega_2^2 = \frac{1}{E_L t_L} \frac{\tau_{LM}}{s_{L0} - s_{LM}} \tag{D.8}$$

The shear stress distribution for the different stages related to the crack propagation process, described in Chapter 3, can be derived by applying the appropriate boundary conditions to the general solutions of equations (D.5) and (D.7) of Zone I and Zone II, respectively given by equations (D.9) and (D.10).

$$\sigma_L^I(x) = C_1 \cosh(\Omega_1 x) + C_2 \sinh(\Omega_1 x) \tag{D.9}$$

$$\sigma_L^{II}(x) = C_3 \cos(\Omega_2 x) + C_4 \sin(\Omega_2 x) \tag{D.10}$$

Table D.1. Contour conditions for the different stages of a pure shear specimen.

Stage	Unknown variables	# contour conditions	Contour conditions
Stage 1	$C_1;\ C_2$	2	$\sigma_L^I(x=0) = \frac{P}{b_L t_L}$ $\sigma_L^I(x=L) = 0$
Stage 2a	$C_1;\ C_2;\ C_3;$ $C_4;\ x_{LM}$	5	$\sigma_L^{II}(x=0) = \frac{P}{b_L t_L}$ $\sigma_L^I(x=x_{LM}) = \sigma_L^{II}(x=x_{LM})$ $\tau^I(x=x_{LM}) = \tau^{II}(x=x_{LM}) = \tau_{LM}$ $\sigma_L^I(x=L) = 0$
Stage 2b	$C_3;\ C_4$	2	$\sigma_L^{II}(x=0) = \frac{P}{b_L t_L}$ $\sigma_L^{II}(x=L) = 0$
Stage 3a	$C_1;\ C_2;\ C_3;$ $C_4;\ x_{LM};\ x_{L0}$	6	$\sigma_L^{II}(x=x_{L0}) = \frac{P}{b_L t_L}$ $\sigma_L^I(x=x_{LM}) = \sigma_L^{II}(x=x_{LM})$ $\tau^I(x=x_{LM}) = \tau^{II}(x=x_{LM}) = \tau_{LM}$ $\sigma_L^I(x=L) = 0$ $\tau^{II}(x=x_{L0}) = 0$
Stage 3b	$C_3;\ C_4;\ x_{L0}$	3	$\sigma_L^{II}(x=x_{L0}) = \frac{P}{b_L t_L}$ $\sigma_L^I(x=L) = 0$ $\tau^{II}(x=x_{L0}) = 0$

Table D.1 summarizes the contour conditions that should be applied to find the integration constants for each stage described in Chapter 3. During Stage 2a, the downward branch of the bond-slip relationship is initiated at some locations named Zone II. To find the shear stress distribution in this stage, the limit between both Zone I

and Zone II, which is the maximum shear stress location x_{LM}, should be defined. Therefore, another unknown variable should be solved with an additional contour condition. During Stage 2b, that initiates when the maximum shear stress reaches the laminate end, the complete interface is in Zone II of the bond-slip relationship, and only two contour conditions are required. A macrocrack opens and propagates during Stage 3a. The macrocrack tip, given by x_{L0}, is obtained by assuming a zero shear stress value at this location. Stage 3b is similar to Stage 2b. However, the existence of a macrocrack implies the necessity of an additional contour condition.

D.3. Specimen subjected to transverse loads

When a beam element is subjected to transverse loads, the governing equations for the shear stresses can be derived by applying equilibrium and compatibility relations to a differential element *dx* as shown in Chapter 4. Before doing it, the following assumptions should be made: the shear deformation is neglected to uncouple the shear and normal peeling stresses; the thickness and width of the adherents and adhesive are assumed constant along the bonded length; and finally, the laminate bending stiffness is neglected.

By applying equilibrium and assuming a bilinear bond-slip relationship, equations (D.1) and (D.2) are also obtained. However, in this case, when equation (D.2) is incorporated to the differential of equation (D.1), the concrete strain on the bottom fiber can not be neglected, as shown by equation (D.11). As a consequence, the main difference with the previous case of a pure shear specimen will be the non-homogeneity of the governing equations.

$$\begin{aligned}&\frac{d^2\sigma_L}{dx^2}(x)=\frac{1}{t_L}\frac{d\tau(x)}{dx}=\frac{1}{t_L}\frac{\tau_{LM}}{s_i}\frac{ds(x)}{dx}=\frac{1}{t_L}\frac{\tau_{LM}}{s_i}\left(\frac{du_L}{dx}(x)-\frac{du_{c,b}}{dx}(x)\right)=\\&=\frac{1}{t_L}\frac{\tau_{LM}}{s_{L_M}}\left(\varepsilon_L(x)-\varepsilon_{c,b}(x)\right)=\frac{1}{E_L t_L}\frac{\tau_{LM}}{s_i}\sigma_L(x)-\frac{1}{E_C t_L}\frac{\tau_{LM}}{s_i}\sigma_{c,b}(x)\end{aligned} \tag{D.11}$$

The governing equation (D.11) can be rewritten for both Zones I and II as shown by equations (D.12) and (D.13).

$$\frac{d^2\sigma_L^I}{dx^2}(x)-\Omega_1^2\sigma_L^I(x)=-\Omega_1^2\frac{E_L}{E_c}\sigma_{c,b}(x) \tag{D.12}$$

$$\frac{d^2\sigma_L^{II}}{dx^2}(x)+\Omega_2^2\sigma_L^{II}(x)=\Omega_2^2\frac{E_L}{E_c}\sigma_{c,b}(x) \tag{D.13}$$

Both differential equations will be solved in §D.3.1 and in §D.3.2 for an element between two cracks and for an element at the plate end respectively.

D.3.1. Beam element between two cracks

First of all, to solve both equations (D.12) and (D.13), the concrete stress distribution in the bottom concrete fiber is assumed as a parabolic function along the crack distance (s_{cr}) (see Chapter 4). This parabolic function, given by equation (D.14), is obtained by knowing that the concrete tensile stress in the crack tips (crack I and crack J) is zero, and assuming a certain value depending on the tensile strength (βf_{ctm}) at half of the crack distance.

$$\sigma_{c,b}(x) = -\frac{4}{s_{cr}^2}\beta f_{ctm}\left((x-x_I)^2 - s_{cr}(x-x_I)\right) \tag{D.14}$$

After incorporating equation (D.14) into equations (D.12) and (D.13), the general expression for shear stresses in an element between two cracks for the upward (Zone I) and downward (Zone II) branch of the bond-slip relationship is given by equations (D.15) and (D.16).

$$\sigma_L^I(x) = C_1\cosh(\Omega_1 x) + C_2\sinh(\Omega_1 x) + \frac{2\mu}{\Omega_1^2} + \mu\left((x-x_I)^2 - s_{cr}(x-x_I)\right) \tag{D.15}$$

$$\sigma_L^{II}(x) = C_3\cos(\Omega_2 x) + C_4\sin(\Omega_2 x) - \frac{2\mu}{\Omega_2^2} + \mu\left((x-x_I)^2 - s_{cr}(x-x_I)\right) \tag{D.16}$$

where

$$\mu = -\frac{4}{s_{cr}^2}\beta f_{ctm}\frac{E_L}{E_c} \tag{D.17}$$

Some contour conditions related to each stage of the crack propagation process, described in Chapter 4, should be applied to obtain the integration constants. Table D.2 summarizes them, indicating the unknown variables in each stage. Since the shear stress distribution near each crack is opposite to the laminate tensile force, two interfacial problems of Zone I develop along the crack distance from the early stages (Stage 1). Later on, Zone II appears near crack J (Stage 2a.1). When the maximum shear stress reaches the less loaded crack (crack I), Zone II will also develop near this crack tip (Stage 2a.2). Then, two Zone I's and Zone II's stress distributions are found along the crack distance. Note that the limit between the four zones will be: $x_{LM,left}$, which is the maximum shear stress location nearest to the less loaded crack (crack I); $x_{LM,right}$ which is the maximum shear stress location nearest to crack J; and finally, x_K which is the zero shear stress location. Thus, to find the location of these limit points, some additional contour conditions to those defined for the integration constants should be applied. During Stage 3a, a horizontal macrocrack will open near crack J. The tensile stress along the debonded length is assumed to be constant and equal to the tensile stress on the crack tip. The macrocrack tip location will be obtained by imposing that the shear stress at this location is zero. The same happens in Stage 3c, where the macrocrack has initiated near both crack tips.

Table D.2. Contour conditions for the different stages of an element between two cracks.

Stage	Unknown variables	# contour conditions	Contour conditions
Stage 1	C_1^{IK} ; C_2^{IK} ; C_1^{KJ} ; C_2^{KJ} ; x_K	5	$\sigma_{L,IK}^{I}(x=x_I)=\sigma_{L,I}$ $\sigma_{L,KJ}^{II}(x=x_J)=\sigma_{L,J}$ $\tau_{IK}^{I}(x=x_K)=\tau_{KJ}^{I}(x=x_K)=0$ $\sigma_{L,IK}^{I}(x=x_K)=\sigma_{L,KJ}^{I}(x=x_K)$
Stage 2a.1	C_1^{IK} ; C_2^{IK} ; C_1^{KJ} ; C_2^{KJ} ; C_3^{KJ} ; C_4^{KJ} ; $x_{LM,right}$; x_K	8	$\sigma_{L,IK}^{I}(x=x_I)=\sigma_{L,I}$ $\sigma_{L,KJ}^{II}(x=x_J)=\sigma_{L,J}$ $\sigma_{L,KJ}^{I}(x=x_{LM,right})=\sigma_{L,IK}^{II}(x=x_{LM,right})$ $\tau_{KJ}^{I}(x=x_{LM,right})=\tau_{KJ}^{II}(x=x_{LM,right})=\tau_{LM}$ $\tau_{IK}^{I}(x=x_K)=\tau_{KJ}^{I}(x=x_K)=0$ $\sigma_{L,IK}^{I}(x=x_K)=\sigma_{L,KJ}^{I}(x=x_K)$
Stage 2a.2	C_1^{IK} ; C_2^{IK} ; C_3^{IK} ; C_4^{IK} ; C_1^{KJ} ; C_2^{KJ} ; C_3^{KJ} ; C_4^{KJ} ; $x_{LM,left}$; $x_{LM,right}$; x_K	11	$\sigma_{L,IK}^{II}(x=x_I)=\sigma_{L,I}$ $\sigma_{L,IK}^{I}(x=x_{LM,left})=\sigma_{L,IK}^{II}(x=x_{LM,left})$ $\tau_{IK}^{I}(x=x_{LM,left})=\tau_{IK}^{II}(x=x_{LM,left})=\tau_{LM}$ $\sigma_{L,KJ}^{II}(x=x_J)=\sigma_{L,J}$ $\sigma_{L,KJ}^{I}(x=x_{LM,right})=\sigma_{L,IK}^{II}(x=x_{LM,right})$ $\tau_{KJ}^{I}(x=x_{LM,right})=\tau_{KJ}^{II}(x=x_{LM,right})=\tau_{LM}$ $\tau_{IK}^{I}(x=x_K)=\tau_{KJ}^{I}(x=x_K)=0$ $\sigma_{L,IK}^{I}(x=x_K)=\sigma_{L,KJ}^{I}(x=x_K)$
Stage 2b	C_3^{KJ} ; C_4^{KJ}	2	$\sigma_{L,IJ}^{II}(x=x_I)=\sigma_{L,I}$ $\sigma_{L,IJ}^{II}(x=x_J)=\sigma_{L,J}$
Stage 3a	C_1^{IK} ; C_2^{IK} ; C_3^{IK} ; C_4^{IK} ; C_1^{KJ} ; C_2^{KJ} ; C_3^{KJ} ; C_4^{KJ} ; $x_{LM,left}$; $x_{LM,right}$; x_K ; x_{L0}	12	$\sigma_{L,IK}^{II}(x=x_I)=\sigma_{L,I}$ $\sigma_{L,IK}^{I}(x=x_{LM,left})=\sigma_{L,IK}^{II}(x=x_{LM,left})$ $\tau_{IK}^{I}(x=x_{LM,left})=\tau_{IK}^{II}(x=x_{LM,left})=\tau_{LM}$ $\sigma_{L,KJ}^{II}(x=x_{L0,right})=\sigma_{L,J}$ $\sigma_{L,KJ}^{I}(x=x_{L0,right})=\sigma_{L,IK}^{II}(x=x_{L0,right})$ $\tau_{KJ}^{I}(x=x_{LM,right})=\tau_{KJ}^{II}(x=x_{LM,right})=\tau_{LM}$ $\tau_{IK}^{I}(x=x_K)=\tau_{KJ}^{I}(x=x_K)=0$ $\sigma_{L,IK}^{I}(x=x_K)=\sigma_{L,KJ}^{I}(x=x_K)$ $\tau_{KJ}^{II}(x=x_{L0})=0$
Stage 3b	C_3^{KJ} ; C_4^{KJ} ; x_{L0}	3	$\sigma_{L,IJ}^{II}(x=x_I)=\sigma_{L,I}$ $\sigma_{L,IJ}^{II}(x=x_{L0})=\sigma_{L,J}$ $\tau_{IJ}^{II}(x=x_{L0})=0$

Table D.3. Contour conditions for the different stages of an element between two cracks.

Stage	Unknown variables	# contour conditions	Contour conditions
Stage 3c	C_1^{IK} ; C_2^{IK} ; C_3^{IK} ; C_4^{IK} ; C_1^{KJ} ; C_2^{KJ} ; C_3^{KJ} ; C_4^{KJ} ; $x_{LM,left}$; $x_{LM,right}$; x_K ; $x_{L0,left}$; $x_{L0,right}$	13	$\sigma_{L,IK}^{II}\left(x=x_{L0,left}\right)=\sigma_{L,I}$ $\sigma_{L,IK}^{I}\left(x=x_{LM,left}\right)=\sigma_{L,IK}^{II}\left(x=x_{LM,left}\right)$ $\tau_{IK}^{I}\left(x=x_{LM,left}\right)=\tau_{IK}^{II}\left(x=x_{LM,left}\right)=\tau_{LM}$ $\sigma_{L,KJ}^{II}\left(x=x_{L0,right}\right)=\sigma_{L,J}$ $\sigma_{L,KJ}^{I}\left(x=x_{LM,right}\right)=\sigma_{L,IK}^{II}\left(x=x_{LM,right}\right)$ $\tau_{KJ}^{I}\left(x=x_{LM,right}\right)=\tau_{KJ}^{II}\left(x=x_{LM,right}\right)=\tau_{LM}$ $\tau_{IK}^{I}\left(x=x_K\right)=\tau_{KJ}^{I}\left(x=x_K\right)=0$ $\sigma_{L,IK}^{I}\left(x=x_K\right)=\sigma_{L,KJ}^{I}\left(x=x_K\right)$ $\tau_{IK}^{II}\left(x=x_{L0,left}\right)=0$ $\tau_{KJ}^{II}\left(x=x_{L0,right}\right)=0$

D.3.2. Beam element at the laminate end

The case of a beam element between the laminate end and the nearest crack is very similar to a beam element between two cracks. The main difference is the laminate tensile force at the laminate end which is zero. At maximum, the three zones of the bond-slip relationship can be developed along the interface. Therefore, three stages will be distinguished as explained in Chapter 4.

The concrete tensile stress distribution on the concrete bottom fiber is defined as a parabolic function with a zero value on the crack tip, and its maximum value at the laminate end and depending on the concrete tensile strength.

$$\sigma_{c,b}(x)=-\frac{1}{s_{cr}^2}\beta f_{ctm}\left(x^2-s_{cr}^2\right) \tag{D.18}$$

By incorporating equation (D.18) into equations (D.12) and (D.13), the general solution of both differential equations for Zone I and II are found to be equations (D.19) and (D.20). The integration constants are calculated by applying some contour conditions summarized in Table D.4.

$$\sigma_L^I(x)=C_1\cosh(\Omega_1 x)+C_2\sinh(\Omega_1 x)+\frac{2\mu}{\Omega_1^2}+\mu\left(x^2-s_{cr}^2\right) \tag{D.19}$$

$$\sigma_L^{II}(x)=C_3\cos(\Omega_2 x)+C_4\sin(\Omega_2 x)-\frac{2\mu}{\Omega_2^2}+\mu\left(x^2-s_{cr}^2\right) \tag{D.20}$$

From Stage 2a, part of the interface is considered as Zone I and the rest as Zone II. The transition point between both Zone I and II, which is the maximum shear stress location,

x_{LM}, should be obtained. For this purpose, an additional boundary condition should be applied.

At the beginning of Stage 3a, a horizontal macrocrack opens near crack J. As in the previous cases, the macrocrack tip location is calculated by assuming a zero shear stress at this location.

Table D.4. Contour conditions for the different stages of an element between two cracks.

Stage	Unknown variables	# contour conditions	Contour conditions
Stage 1	$C_1;\ C_2$	2	$\sigma_L^I(x=0)=0$ $\sigma_L^{II}(x=x_J)=\sigma_{L,J}$
Stage 2a	$C_1;\ C_2;\ C_3;$ $C_4;\ x_{LM}$	5	$\sigma_L^I(x=0)=0$ $\sigma_L^{II}(x=x_J)=\sigma_{L,J}$ $\sigma_L^I(x=x_{LM})=\sigma_L^{II}(x=x_{LM})$ $\tau^I(x=x_{LM})=\tau^{II}(x=x_{LM})=\tau_{LM}$
Stage 2b	$C_3;\ C_4$	2	$\sigma_L^I(x=0)=0$ $\sigma_L^{II}(x=x_J)=\sigma_{L,J}$
Stage 3a	$C_1;\ C_2;\ C_3;$ $C_4;\ x_{LM}$	5	$\sigma_L^I(x=0)=0$ $\sigma_L^{II}(x=x_{L0})=\sigma_{L,J}$ $\sigma_L^I(x=x_{LM})=\sigma_L^{II}(x=x_{LM})$ $\tau^I(x=x_{LM})=\tau^{II}(x=x_{LM})=\tau_{LM}$
Stage 3b	$C_3;\ C_4;\ x_{L0}$	3	$\sigma_L^I(x=0)=0$ $\sigma_L^{II}(x=x_{L0})=\sigma_{L,J}$ $\tau^{II}(x=x_{L0})=0$

In conclusion, by applying the boundary conditions of Table D.2, Table D.3 and Table D.4 to the respective governing equations between two cracks or at the plate end, the interfacial shear stress distribution, the laminate tensile stress distribution, and the relative sliding between concrete and laminate can be obtained along the span of a beam subjected to transverse loads as shown in Chapter 4.